Rolando Barbucci *Ed.*

Hydrogels

Biological Properties and Applications

Springer

To Enrica,
my wife and irreplaceable coworker

Rolando Barbucci (Editor)

Hydrogels

Biological Properties and Applications

Springer

Rolando Barbucci
Department of Chemical and Biosystem Sciences and Technologies
and Interuniversity Research Center for Advanced Medical Systems
(C.R.I.S.M.A.)
University of Siena, Italy

Library of Congress Control Number: 2008941152

ISBN 978-88-470-1103-8 Springer Milan Berlin Heidelberg New York
e-ISBN 978-88-470-1104-5 Springer Milan Berlin Heidelberg New York

Springer is a part of Springer Science+Business Media
springer.com

Printed in Italy

Cover-Design: Francesca Tonon, Milan
Typesetting with Latex: PTP-Berlin, Protago-TEX-Production GmbH, Germany
Printing and Binding: Signum, Bollate (MI)

Springer-Verlag Italia Srl, Via Decembrio 28
20137 Milan

Preface

Hydrogels are a particular class of compounds of which the major constituent is water. In fact, water is present in the hydrogel up to 90% and is contained in a scaffold which is generally polymeric and obviously hydrophilic. As a result, hydrogels resemble each other even though obtained from different polymers. Nevertheless, the polymeric matrix gives particular characteristics to the hydrogel leading to applications in different fields.

Water is the main element of the human body, thus hydrogels are excellent structures to favourably shelter proteins, cells etc., without altering their characteristics and properties. This is why hydrogels are mainly designed and synthesized for their use in the biological field; hence the name *biohydrogels*. Their properties point to their use as scaffolds for stem cells which has turned out to be a very promising technique for tissue and organ regeneration. For this reason their investigation falls within the Biomaterials Science.

Paradoxically, the conceptual simplicity of hydrogels up to now has led to a superficial study of their chemistry, chemical physics and mechanics preventing their wider application in the human body due to a lack of knowledge of biological component interactions. For example, it is not clear, yet, how to store hydrogels without altering their characteristics. In fact, hydrogels re-hydrated after lyophylization or oven drying, generally show corrupted properties once swollen in water, in comparison with their native counterparts. This is why the properties of water and its capacity to bind to hydrophilic chemical groups must be taken into account, as well as how the water is organized around hydrophobic groups and also the organization of the layers of water molecules surrounding a polymer. Obviously, all of this determines the hydrogel swelling degree in water and consequently its biological response.

This book aims to give a contribution to hydrogel knowledge from the chemical, physico-chemical, mechanical, biological and biomedical point of view.

My warmest thanks to the authors who gave their contribution to this work.

November 2008 *Rolando Barbucci*

Contents

Hydrogels and Tissue Engineering
Barbara Zavan, Roberta Cortivo and Giovanni Abatangelo 1

Structure–Property Relationships in Hydrogels
Assunta Borzacchiello and Luigi Ambrosio 9

Water and Surfaces: a Linkage Unexpectedly Profound
Gerald H. Pollack 21

Polysaccharide Based Hydrogels for Biomedical Applications
Gemma Leone and Rolando Barbucci 25

Hydrogels for Healing
Buddy D. Ratner and Sarah Atzet 43

Stereocomplexed PEG-PLA Hydrogels
Christine Hiemstra, Zhiyuan Zhong, Pieter J. Dijkstra and Jan Feijen 53

Hybrid Hydrogels Based on Poly(vinylalcohol)-Chitosan Blends and Relevant CNT Composites
Sangram K. Samal, Federica Chiellini, Cristina Bartoli, Elizabeth G. Fernandes and Emo Chiellini 67

Poloxamine Hydrogels: from low Cell Adhesion Substrates to Matrices with Improved Cytocompatibility for Tissue Engineering Applications
Alejandro Sosnik, Omar F. Khan, Mark Butler and Michael V. Sefton 79

Biohydrogels for the *In Vitro* Re-construction and *In Situ* Regeneration of Human Skin
Liudmila Korkina, Vladimir Kostyuk and Liliana Guerra 97

Chitosan-Based Beads for Controlled Release of Proteins
Mamoni Dash, Anna Maria Piras and Federica Chiellini 111

Synthesis of Stimuli-Sensitive Hydrogels in the µm and sub-µm Range by Radiation Techniques and their Application
Karl-Friedrich Arndt, Andreas Richter and Ingolf Mönch 121

Stimuli-Sensitive Composite Microgels
Haruma Kawaguchi 141

Novel pH/Temperature-Sensitive Hydrogels Based on Poly(β-Amino Ester) for Controlled Protein Delivery
Dai Phu Huynh, Chaoliang He and Doo Sung Lee 157

On-Off Switching Properties of ultra thin Intelligent Temperature-Responsive Polymer Modified Surface
Yoshikatsu Akiyama and Teruo Okano 179

List of Contributors

Giovanni Abatangelo
Dipartimento di Istologia, Microbiologia e Biotecnologie Mediche
University of Padova, Italy
g.abatangelo@unipd.it

Yoshikatsu Akiyama
Institute of Advanced Biomedical Engineering and Science
Tokyo Women's Medical University, TWIns, Tokyo, Japan
yakiyama@abmes.twmu.ac.jp

Luigi Ambrosio
Institute of Composite & Biomedical Materials
National Research Council, Naples, Italy
ambrosio@unina.it

Karl-Friedrich Arndt
Physical Chemistry of Polymers
University of Dresden, Germany
karl-friedrich.arndt@chemie.tu-dresden.de

Sarah Atzet
Department of Chemical Engineering
University of Washington, USA

Rolando Barbucci
Department of Chemical and Biosystem Sciences and Technologies and Interuniversity Research Center for Advanced Medical Systems (C.R.I.S.M.A.)
University of Siena, Italy
barbucci@unisi.it

Cristina Bartoli
Department of Chemistry & Industrial Chemistry
University of Pisa, Italy
cribart@ns.dcci.unipi.it

Assunta Borzacchiello
Institute of Composite & Biomedical Materials
National Research Council, Naples, Italy
bassunta@unina.it

Mark Butler
Institute of Biomaterials and Biomedical Engineering
University of Toronto, Canada
mark.butler@utoronto.ca

Emo Chiellini
Department of Chemistry & Industrial Chemistry
University of Pisa, Italy
emochie@dcci.unipi.it

Federica Chiellini
Department of Chemistry & Industrial Chemistry
University of Pisa, Italy
federica@dcci.unipi.it

Roberta Cortivo
Dipartimento di Istologia, Microbiologia e Biotecnologie Mediche
University of Padova, Italy
roberta.cortivo@unipd.it

Mamoni Dash
Department of Chemistry & Industrial Chemistry
University of Pisa, Italy
mdash@ns.dcci.unipi.it

Pieter J. Dijkstra
Department or Institute: Department of Science and Technology
University of Twente, Netherlands
p.j.dijkstra@tnw.utwente.nl

Jan Feijen
Department or Institute: Department of Science and Technology
University of Twente, Netherlands
j.feijen@utwente.nl

Elizabeth G. Fernandes
Department of Chemistry & Industrial Chemistry
University of Pisa, Italy
beth@ns.dcci.unipi.it

Liliana Guerra
Lab. Tissue Engineering & Skin Pathophysiology
Istituto Dermopatico dell'Immacolata IRCCS,
Rome, Italy
l.guerra@idi.it

Chaoliang He
Department of Polymer Science and Engineering
SungKyunKwan University, Suwon, Kyungki, Korea
hechaoliang@hotmail.com

Christine Hiemstra
Department or Institute: Department of Science and Technology
University of Twente, Netherlands
christinehiemstra@gmail.com

Dai Phu Huynh
Department of Polymer Science and Engineering
SungKyunKwan University, Suwon, Kyungki, Korea
huynh_daiphu@yahoo.com

Haruma Kawaguchi
Department of Applied Chemistry
Keio University, Yokohama, Japan
haruma@applc.keio.ac.jp
haruma@mvg.biglobe.ne.jp

Omar F. Khan
Institute of Biomaterials and Biomedical Engineering
University of Toronto, Canada
omar.khan@utoronto.ca

Liudmila Korkina
Lab. Tissue Engineering & Skin Pathophysiology
Istituto Dermopatico dell'Immacolata IRCCS,
Rome, Italy
l.korkina@idi.it

Vladimir Kostyuk
Lab. Tissue Engineering & Skin Pathophysiology
Istituto Dermopatico dell'Immacolata IRCCS,
Rome, Italy
u.kastsiuk@idi.it

Doo Sung Lee
Department of Polymer Science and Engineering
SungKyunKwan University, Suwon, Kyungki, Korea
dslee@skku.edu

Gemma Leone
Department of Chemical and Biosystem Sciences and Technologies
University of Siena, Italy
leone10@unisi.it

Ingolf Mönch
Institute for Integrative Nanosciences, IFW Dresden, Germany
i.moench@ifw-dresden.de

Teruo Okano
Institute of Advanced Biomedical Engineering and Science,
Tokyo Women's Medical University, TWIns, Tokyo, Japan
tokano@abmes.twmu.ac.jp

Anna Maria Piras
Department of Chemistry & Industrial Chemistry
University of Pisa, Italy
apiras@ns.dcci.unipi.it

Gerald H. Pollack
Department of Bioengineering
University of Washington, USA
ghp@u.washington.edu

Buddy D. Ratner
University of Washington Engineered Biomaterials (UWEB)
Departments of Bioengineering and Chemical Engineering
University of Washington, USA
ratner@uweb.engr.washington.edu

Andreas Richter
Polymeric Microsystems
University of Dresden, Germany
andreas.richter7@tu-dresden.de

Sangram K. Samal
Department of Chemistry & Industrial Chemistry
University of Pisa, Italy
sksamal@ns.dcci.unipi.it

Michael V. Sefton
Institute of Biomaterials and Biomedical Engineering
University of Toronto, Canada
michael.sefton@utoronto.ca

Alejandro Sosnik
Institute of Biomaterials and Biomedical Engineering
University of Toronto, Canada
alesosnik@gmail.com

Barbara Zavan
Dipartimento di Istologia, Microbiologia e Biotecnologie Mediche
University of Padova, Italy
barbara.zavan@unipd.it

Zhiyuan Zhong
Department or Institute: College of Chemistry and Chemical Engineering
Soochow University, China
zyzhong@suda.edu.cn

Hydrogels and Tissue Engineering

Barbara Zavan, Roberta Cortivo and Giovanni Abatangelo

Abstract. Hydrogels are water-swollen polymeric materials that maintain a distinct three-dimensional structure. They were the first biomaterials designed for use in the human body. Traditional methods of biomaterial synthesis include crosslinking copolymerization, crosslinking of reactive polymer precursors, and crosslinking via polymer–polymer reaction. These methods of hydrogel synthesis were limited in the control of their detailed structure. Other inadequacies of traditional hydrogels have been poor mechanical properties and slow or delayed response times to external stimuli. The huge field of biomaterials research has received a strong revitalization by several novel approaches in hydrogel design. Enhanced biomechanical properties of hydrogel preparation, superporous and comb-type grafted hydrogels with fast response times, and self-assembly are just a few examples of hydrogel biomaterials with a smart future. Potential applications of all the types of hydrogels include: tissue engineering, synthetic extracellular matrix, implantable devices, biosensors, separation systems (valves to control permeability across porous membranes, or materials for affinity separation based on the specific recognition of monomeric strands), materials controlling the activity of enzymes, phospholipid bilayer destabilizing agents, materials controlling reversible cell attachment, nanoreactors with precisely placed reactive groups in three-dimensional space and smart microfluidics. With regard to the applications of hydrogels in recent years, particular attention has been devoted to drug delivery, clinical application as well as to the use of hydrogels as scaffolds for tissue engineering and regenerative medicine. Among the materials used for regenerative applications, hydrogels seem very promising and are receiving increasing attention due to their ability to entrap large amount of water, good biocompatibility and the ability to mimic tissue environment.

1 Introduction

Tissue Engineering (TE) and regenerative medicine aim to investigate the deposition, growth and remodeling of tissue by drawing together approaches from a range of disciplines.

Recent developments in the multidisciplinary field of TE have yielded many novel tissue replacements and implementation strategies. Scientific advances in biomaterials, stem cell isolation, growth and differentiation factors and biomimetic environments have created unique opportunities to fabricate tissues in the laboratory. One of the major challenges now facing TE is to optimize 3D functional recovery, a factor

Barbucci R. (Ed): Hydrogels. Biological Properties and Applications.

dependent on 3D structural complexity, as well as the biomechanical and functional stability of the laboratory-grown tissues destined for transplantation.

The field of tissue engineering has developed to meet the tremendous need for organs and tissues. In the most general sense, tissue engineering seeks to fabricate living replacement parts for the body. The necessity for tissue engineering is illustrated by the ever-widening supply and demand mismatch of organs and tissues for transplantation.

Approximately half of medical spending in Europe is attributable to tissue loss/damage and organ failure, with approximately 8 million surgical procedures and 40–90 million hospital days per year required to treat these disorders. In 2006, approximately 29,000 patients received organ transplants, while almost 100,000 patients remain on the waiting list and many will probably die without treatment. The demand for tissue and organ replacement or regenerative strategies following tissue damage (e.g. bone fractures, liver failure and severe burns) or disease (e.g. diabetes, cancer and cardiomyopathy) is expanding. Thus, the scientific and medical communities are working together to develop engineered tissues and regenerative approaches by utilizing various combinations of stem and progenitor cells, biomaterials, growth factors and gene therapy. However, after three decades, the provision of tissues and organs to millions of patients suffering from trauma, congenital defects and chronic disease has yet to be fully accomplished.

On the whole, TE appears to be the new frontier of medicine due to its clinical impact on regenerative and reconstructive procedures. In fact, its ultimate goal is to develop powerful new therapies, namely "biological substitutes", for structural and functional disorders that have proven to be difficult or impossible to tackle successfully with the current approaches of interventional medicine. In addition, by providing "cell-to-tissue replacement parts" for the human body, it can ultimately resolve the problem of the irremediable shortage of transplantable organs.

Among the materials used for regenerative applications, hydrogels (HGs) are receiving increasing attention due to their ability to retain a great quantity of water, good biocompatibility, low interfacial tension, and minimal mechanical and frictional irritation, all appealing features from the perspective of mimicking a bioenvironment.

But what is a hydrogel? The term hydrogel is composed of "hydro" (=water) and "gel", and refers to aqueous (water-containing) gels, or, to be more precise, to polymer networks that are insoluble in water. Hydrogels used in these applications are typically degradable, can be processed under relatively mild conditions, have mechanical and structural properties similar to many tissues and the ECM, and can be delivered in a minimally invasive manner.

2 Materials

A variety of synthetic and naturally derived materials may be used to form hydrogels for tissue engineering scaffolds. Synthetic materials include poly(ethylene oxide) (PEO), poly(vinyl alcohol) (PVA), poly(acrylic acid) (PAA), poly(propylene furmarate-co-ethylene glycol) (P(PF-co-EG)), and polypeptides. Representative nat-

urally derived polymers include agarose, alginate, chitosan, collagen, fibrin, gelatin, and hyaluronic acid (HA).

2.1 Synthetic materials

Synthetic hydrogels are appealing for tissue engineering because their chemistry and properties are controllable and reproducible. For example, synthetic polymers can be reproducibly produced with specific molecular weights, block structures, degradable linkages, and crosslinking modes. These properties in turn, determine gel formation dynamics, crosslinking density, and material mechanical and degradation properties. Examples of such synthetic materials are PEO, PVA, and P(PF-co-EG).

2.2 Naturally derived materials

Naturally derived hydrogel forming polymers have frequently been used in tissue engineering applications because they are either components of or have macromolecular properties similar to the natural ECM. For example, collagens are the main protein of mammalian tissue ECM and comprise 25% of the total protein mass of most mammals. Similarly, HA is found in varying amounts in all tissues of adult animals. Like HA, both alginate and chitosan are hydrophilic, linear polysaccharides. They have also been shown to interact in a favorable manner in vivo and thus have been utilized as hydrogel scaffold materials for tissue engineering.

Collagen is an attractive material for biomedical applications as it is the most abundant protein in mammalian tissues and is the main component of natural ECM. There are at least 19 different types of collagen, but the basic structure of all collagen is composed of three polypeptide chains, which wrap around one another to form a three-stranded rope structure. The strands are held together by both hydrogen and covalent bonds. Collagen strands can self-aggregate to form stable fibers. In addition, collagen fibers and scaffolds can be created and their mechanical properties enhanced by introducing various chemical crosslinkers (i.e. glutaraldehyde, formaldehyde, carbodiimide), by crosslinking with physical treatments (i.e. UV irradiation, freeze-drying, heating), and by blending with other polymers (i.e. HA, PLA, poly(glycolic acid) (PGA), poly(lactic-co-glycolic acid) (PLGA), chitosan, PEO). Collagen is naturally degraded by metalloproteases, specifically collagenase, and serine proteases, allowing for its degradation to be locally controlled by cells present in the engineered tissue.

HA is the simplest glycosaminolglycan (GAG) and is found in nearly every mammalian tissue and fluid. It is especially prevalent during wound healing and in the synovial fluid of joints. It is a linear polysaccharide composed of a repeating disaccharide (Fig. 1) of (1–3) and (1–4)-linked β-D-glucuronic acid and N-acetyl-β-D-glucosamine units. Hydrogels of HA are formed by covalent crosslinking with hydrazide derivatives, by esterification, and by annealing. HA is naturally degraded by hyaluronidase, again allowing cells in the body to regulate the clearance of the material in a localized manner.

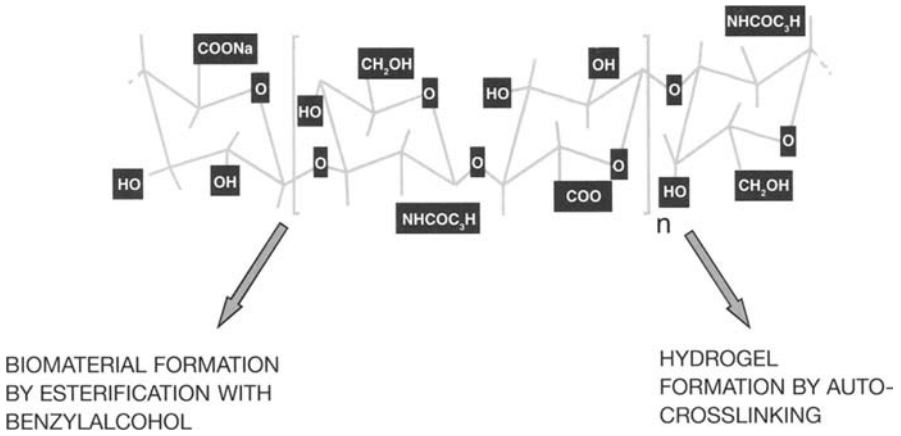

Fig. 1 HA is a linear polysaccharide composed of a repeating disaccharide of (1–3) and (1–4)-linked β-D-glucuronic acid and N-acetyl-β-D-glucosamine units. Hydrogels of HA are formed by covalent crosslinking with hydrazide derivatives, by esterification, and by annealing

Alginate has been used in a variety of medical applications including cell encapsulation and drug stabilization and delivery, because it gels under gentle conditions, has low toxicity, and is readily available. It is a linear polysaccharide copolymer of (1–4)-linked β-D-mannuronic acid (M) and *-L-guluronic acid (G) monomers and is derived primarily from brown seaweed and bacteria. Hydrolytically degradable forms of alginate have been synthesized by partial oxidation of alginate and an alginate derivative, polyguluronate, to form oxidized alginate and poly(aldehyde guluronate) (PAG), respectively.

Chitosan has been investigated for a variety of tissue engineering applications because it is structurally similar to naturally occurring GAGs and is degradable by enzymes in humans. It is a linear polysaccharide of (1–4)-linked D-glucosamine and *N*-acetyl-D-glucosamine residues derived from chitin, which is found in arthropod exoskeletons. Chitosan is degraded by lysozyme; the kinetics of degradation are inversely related to the degree of crystallinity. [1]

3 Scaffold design

Selection or synthesis of the appropriate hydrogel scaffold material is governed by the physical property, mass transport property, and biological interaction requirements of each specific application. These properties or design variables are specified by the intended scaffold application and environment into which the scaffold will be placed. In addition, the biological properties are designated by the requirement of non-toxicity.

Many scaffolds for tissue engineering initially fill a space otherwise occupied by natural tissue, and then provide a framework by which that tissue may be regenerated.

In this capacity, the physical properties of the material are inherent to the success of the scaffold. Specific physical properties include gel formation mechanisms and dynamics, mechanical characteristics, and degradation behavior. In hydrogels, these properties are prescribed by the intrinsic properties of the main chain polymer and the crosslinking characteristics (i.e. amount, type, and size of crosslinking molecules), as well as environmental conditions.

Gel formation mechanisms and dynamics dictate how molecules and cells are incorporated into a scaffold and how that scaffold is then delivered.

Once the scaffold is produced and placed, formation of tissue with desirable properties relies on scaffold material mechanical properties on both the macroscopic and microscopic level. Macroscopically, the scaffold must bear loads to provide stability to the tissue as it forms and to fulfill its volume maintenance function. On the microscopic level, evidence suggests that cell growth and differentiation and ultimate tissue formation are dependent on mechanical input to the cells. As a consequence, the scaffold must be able to both withstand specific loads and transmit them in an appropriate manner to the surrounding cells and tissues [2].

4 Degradation

Besides appropriate mechanical properties and mass transport characteristics, degradation of the hydrogel is essential for many tissue-engineering applications. Admittedly, most hydrogels formed by the crosslinking of macromers exhibit a strong interdependency of crosslink density, mechanical properties, and degradation rate. With regard to the desired characteristics of the hydrogel, however, independent control of degradation rate and mechanical properties will be crucial.

Degradability and degradation rate of the supportive matrix were identified as having a strong influence on cell migration, proliferation, differentiation, and morphology of the newly formed tissue. The observed biological responses may be due to the given mechanical properties of the matrix or to the ongoing loss of material during degradation.

The desired kinetics for scaffold degradation depends on the tissue engineering application. Degradation is essential in many small and large molecule release applications and in functional tissue regeneration applications.

Ideally, the rate of scaffold degradation should mirror the rate of new tissue formation or be adequate for the controlled release of bioactive molecules. Thus, it is important to understand and control both the mechanism and the rate by which each material is degraded. For hydrogels, there are three basic degradation mechanisms: hydrolysis, enzymatic cleavage, and dissolution. Most of the synthetic hydrogels are degraded through hydrolysis of ester linkages. As hydrolysis occurs at a constant rate in vivo and in vitro, the degradation rate of hydrolytically labile gels (e.g. PEG-PLA copolymer) can be manipulated by the composition of the material but not the environment. As discussed in the materials section above, collagen, HA and chitosan are all degraded by enzymatic action [3, 4].

5 Diffusion

The success of scaffolds for tissue engineering are typically coupled to the appropriate transport of gases, nutrients, proteins, cells and waste products into, out of, and/or within the scaffold. Here, the primary mass transport property of interest, at least initially, is diffusion. In a scaffold, the rate and distance a molecule diffuses depend on both the material and molecule characteristics and interactions. Gel properties such as polymer fraction, polymer size, and crosslinker concentration determine the gels nanoporous structure. As a consequence, diffusion rates will be affected by the molecular weight and size of the diffusion species (defined by Stokes radii) compared to these pores [5].

6 Biological properties

In tissues, cells are embedded within the extracellular microenvironment, a highly hydrated network that comprises three classes of stimuli or cues that stem from the following sources: insoluble hydrated macromolecules (e.g. fibrillar proteins, proteoglycans, or polymer chains), soluble molecules (e.g. growth factors or cytokines) and membrane-associated molecules of neighboring cells. By contrast, the pure biochemical information provided by ligands attached to an extracellular structure, such as the extracellular matrix (ECM), is supplemented by additional degrees of information including the spatial distribution of ligands and the mechanical properties of the structure to which the ligands are attached.

In the past, great efforts have been made to elucidate how physical forces, applied to either the ECM or the cell surface, induce biochemical alterations inside the cell. Today, there is much evidence that mechanical signals are transferred into the cell across transmembrane molecules, such as integrins, which couple extracellular anchors to the cytoskeleton. Integrins constitute a large family of transmembrane, heterodimeric receptors that bind to specific amino acid sequences, such as the arginine–glycine–aspartic acid (RGD) recognition motif, present in all major ECM proteins. After binding to ECM ligands, integrins cluster together to form dot-like adhesive structures termed focal complexes. Depending on the stiffness of the underlying substrate, focal complexes can disappear or evolve into focal adhesions.

In general, all hydrogels used in biomedical applications must be biocompatible. Because the apparent mesh size of polymeric gels is typically much smaller than a cell's diameter, it would be useful to introduce cells into the liquid precursors of the gel, rather than to the preformed hydrogel itself. Due to their hydrophilic nature, most synthetic hydrogels are known to prevent the adsorption of ECM proteins [6–8].

Once placed at the application site, the hydrogel scaffolds should be able to bear local mechanical loads until the cells have produced their own functional ECM. Moreover, the hydrogel should provide an appropriate mechanical environment to support cell migration, proliferation, and differentiation.

Materials used to form gels engineered to exist in the body must simultaneously promote desirable cellular functions for a specific application (i.e. adherence, pro-

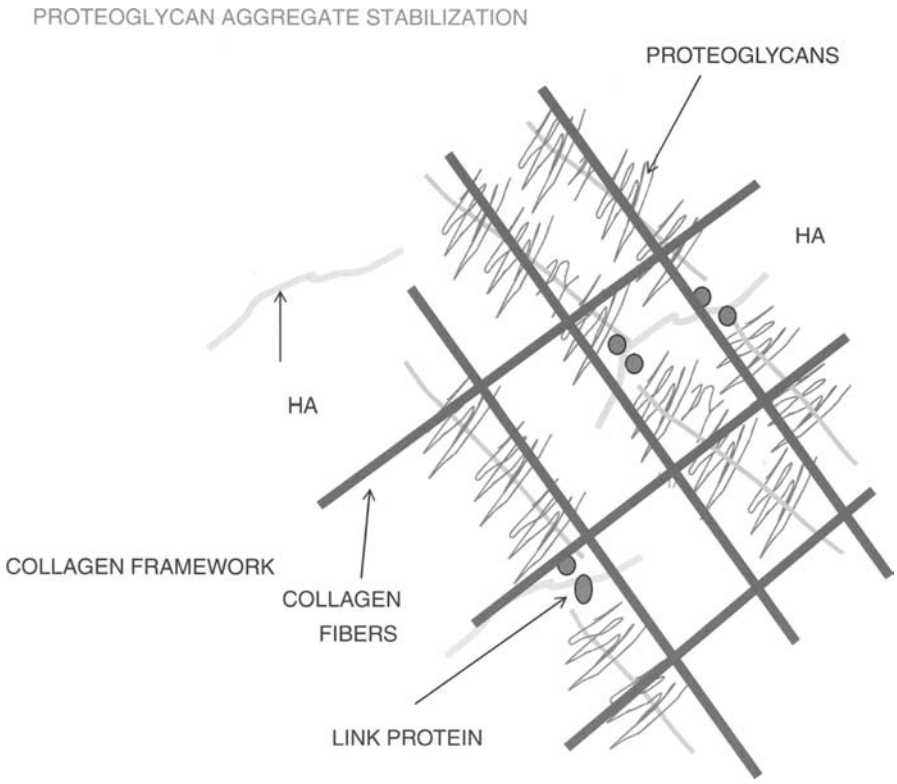

Fig. 2 Interaction of HA and the proteoglycans (PG). Along a linear molecule of hyaluronan numerous PG adhere and are closely associated by the presence of link-proteins

liferation, differentiation) and tissue development, while not eliciting a severe and chronic inflammatory response. Hydrogel forming polymers are generally designed to be non-toxic to the cells they are delivering and to the surrounding tissue. Both collagen and HA are major components of the native ECM and tissue.

While many hydrogels are non-toxic and do not activate a chronic immune response, they also do not readily promote cellular adhesion and function [9–12].

A natural model of a complex hydrogel is represented by the extracellular matrix of cartilage where collagen fibrils, glycosaminoglycans and water form a very well organized gel whose mechanical properties fulfill the correct function of the tissue, namely resistance to mechanical load and elasticity. An important role in the organization of these hydrogels is played by hyaluronan. In Fig. 2 the interaction between HA and proteoglycans (PG) is represented. Along a linear molecule of hyaluronan, numerous PG adhere and are closely associated by the presence of link-proteins. These huge PG aggregates, capable of binding a high quantity of water, are entrapped in a collagen framework and give rise to highly swollen hydrogel dominions. The mechanical forces applied on the articular cartilage induce a compression of the hy-

drogel with a leakage of water. As soon as the mechanical load ceases, water is again attracted to the inside of the hydrogel network to restore the initial configuration. Since cartilage is an avascular tissue, the flow of water triggered by the on-and-off articular loading favors the diffusion of nutrients and catabolites, thus ensuring correct metabolism of the cartilage tissue.

References

[1] Baroli B (2007) Hydrogels for tissue engineering and delivery of tissue-inducing substances. J Pharm Sci 96(9):2197–2223

[2] Brandl F, Sommer F, Goepferich A (2007) Rational design of hydrogels for tissue engineering: Impact of physical factors on cell behavior. Biomaterials 28(2):134–146

[3] Lutolf MP, Hubbell JA (2005) Synthetic biomaterials as instructive extracellular microenvironments for morphogenesis in tissue engineering. Nat Biotechnol 23(1):47–55

[4] Mann BK (2003) Biologic gels in tissue engineering. Clin Plast Surg 30(4):601–609

[5] Tessmar JK, Göpferich AM (2007) Matrices and scaffolds for protein delivery in tissue engineering. Adv Drug Deliv Rev 59(4–5):274–291

[6] Mano JF, Silva GA, Azevedo HS, Malafaya PB, Sousa RA, Silva SS, Boesel LF, Oliveira JM, Santos TC, Marques AP, Neves NM, Reis RL (2007) Natural origin biodegradable systems in tissue engineering and regenerative medicine: present status and some moving trends. J R Soc Interface 4(17):999–1030

[7] Tsang VL, Bhatia SN (2004) Three-dimensional tissue fabrication. Adv Drug Deliv Rev 56(11):1635–1647

[8] Kashyap N, Kumar N, Kumar MN (2005) Hydrogels for pharmaceutical and biomedical applications. Crit Rev Ther Drug Carrier Syst 22(2):107–149

[9] Drury JL, Mooney DJ (2003) Hydrogels for tissue engineering: scaffold design variables and applications. Biomaterials 24(24):4337–4351

[10] Hoffman AS (2001) Hydrogels for biomedical applications. Ann N Y Acad Sci 944: 62–73

[11] Hoffman AS (2002) Hydrogels for biomedical applications. Adv Drug Deliv Rev 54(1):3–12

[12] Lee KY, Mooney DJ (2001) Hydrogels for tissue engineering. Chem Rev 101(7):1869–1879

Structure–Property Relationships in Hydrogels

Assunta Borzacchiello and Luigi Ambrosio

Abstract. The structure and properties of a specific hydrogel are extremely important in selecting which materials are suitable for the specific application. Knowledge of the structure–property relationship is, then, fundamental to tailor hydrogel properties to their final goal.

In this chapter, the theory describing the mechanical, both static and dynamic, and the swelling behavior of hydrogels is examined and the relationship between these properties and structural parameters is discussed.

1 Hydrogel classification and basic structure

Hydrogels are highly swollen solids which are water soluble polymers crosslinked via chemical or physical bonds [1]. The structure and properties of a specific hydrogel are extremely important in selecting which material is suitable for the specific application. Hydrogels can be classified on the basis of different properties. On the basis of preparation method [2] they can be classified as homo-polymer hydrogels or network when they are composed of one type of hydrophilic monomer, as copolymer hydrogels if made of two types of monomers, at least one hydrophilic, as multi-polymer hydrogels when more than three types of monomers are present, or interpenetrating polymeric networks when they are prepared by swelling a network of polymer1 in monomer2, to make an intermeshing network of polymer1 and polymer2 [3]. They can be further classified, on the basis of the ionic charges [4], as neutral hydrogels, anionic hydrogels, cationic hydrogels, and ampholytic hydrogels when both charges are present on the same hydrogel. They can be classified on the basis of physical structure [5], as amorphous hydrogels when the chains are randomly arranged, semi-crystalline hydrogels when dense regions of ordered macromolecules, i.e. crystallites, are present or as hydrogen-bonded hydrogel structures, as supermolecular network structures and hydrocolloidal aggregates. They can be also classified on the basis of the nature of their crosslinks, as chemical hydrogels when the crosslinks are covalent bonds, or physical hydrogels when the links are secondary weak bonds such as Van der Waals and electrostatic interactions or hydrogen bonds or molecular entanglements [6–8].

Barbucci R. (Ed): Hydrogels. Biological Properties and Applications.

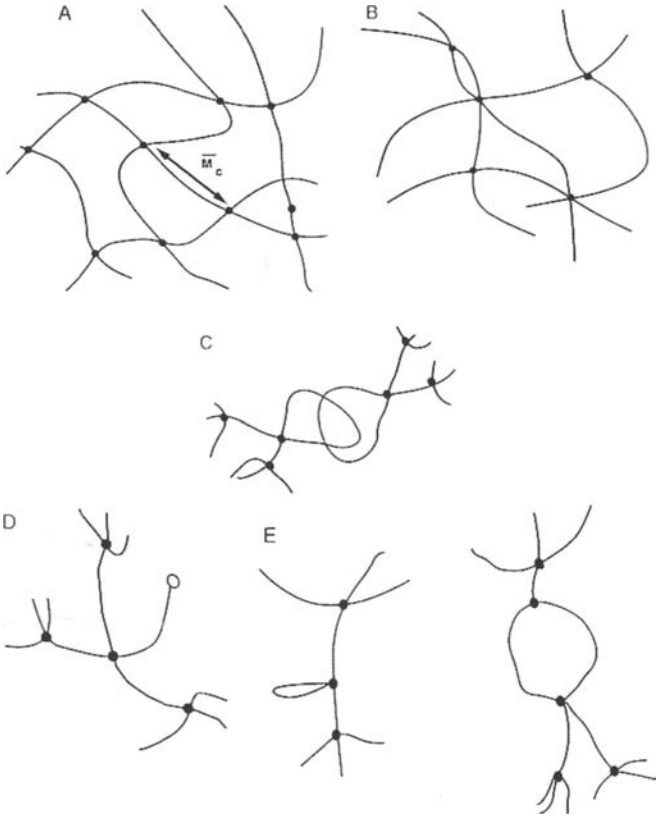

Fig. 1 Network structure. **a** ideal network with tetrafunctional crosslinks; **b** multifunctional junctions; **c** molecular entanglements; **d** unreacted functionality; **e** chain loops. Mc: Molecular weight between crosslinks. Note that neither of the two configurations d and e contribute to mechanical strength or physical properties of the network

Hydrogels can be prepared by swelling crosslinked structures in water or in biological fluids containing water. The crosslinks can be induced by radiation or chemical reaction. In particular, in the first case, the radiation reactions include electron beams, γ -rays, X-rays, or UV light. In the second case of chemical crosslinking, the crosslink reaction can occur between small molecular weight crosslinking agents and a polymer chain, and the crosslinking agent links two chains together through its di- or multifunctional groups or a copolymerization-crosslinking reaction can occur between the monomers and a multifunctional monomer that is present in small quantities. It is very common to have a combination of the above procedures [1].

The ideal network structure of hydrogels is constituted by tetra-functional crosslinks in which M_c is the average weight between crosslinks (ideal network, Fig. 1a), but also, multifunctional junctions (Fig. 1b) or molecular entanglements (permanent or semi-permanent, Fig. 1c) can be present. These kinds of mentioned links can, of

course, be observed simultaneously. Hydrogels with molecular defects are always possible. Unreacted functionality (Fig. 1d) and/or chain loops (Fig. 1e) are examples of such defects; in this case, neither of the two configurations contribute to mechanical strength or the physical properties of the network [9].

1.1 Structural parameters

Hydrogel structure can be defined by three parameters: the polymer volume fraction in the swollen state, $\nu_{2,s}$, the average molecular weight between crosslinks, M_c, and the correlation length ξ, also known as the network mesh (or pore) size [10].

The equilibrium polymer volume fraction in the gel, $\nu_{2,s}$, is the ratio of the polymer volume, V_p, to the volume of the swollen gel, V_{gel}, and the reciprocal of the volume swelling ratio, Q:

$$\nu_{2,s} = V_p / V_{gel} = Q^{-1} \tag{1}$$

It can be determined by equilibrium swelling experiments [11]. The average molecular weight between crosslinks, M_c, can be related theoretically to the degree of crosslinking, X:

$$M_c = M_0 / 2X \tag{2}$$

where M_0 is the molecular weight of the repeating unit of the polymer.

The correlation length or the network mesh size, ξ, is indicative of the distance between consecutive junctions, crosslinks, or tie points. All of these network parameters can be measured through a range of experimental techniques or calculated by the application of the network deformation theory [12]

2 Hydrogel mechanical properties

The understanding of the hydrogel mechanical properties is extremely important for gathering information on their structure. Indeed, their mechanical behavior can be described by using theories that allow to analyze the polymers structure and determine the effective molecular weight between crosslinks and provide information about the number of elastically active chains and cyclization versus crosslinking tendency [13].

2.1 Dynamical mechanical analysis

Dynamical mechanical analysis provides information on the viscoelastic properties of hydrogels by measuring the response of a sample when it is deformed under periodic oscillation (stress or strain) [14].

In a dynamic experiment the material is subjected to a sinusoidal shear strain (or stress):

$$\gamma = \gamma_0 \sin(\omega t) \tag{3}$$

where γ_0 is the shear strain amplitude, ω is the oscillation frequency (which can also be expressed as $2\pi gf$ where f is the frequency in Hz) and t the time. The mechanical

response, expressed as shear stress σ of viscoelastic materials, is intermediate between an ideal pure elastic solid (++in phase with the deformation) and an ideal pure viscous fluid (90 ° out of phase with the deformation) and therefore is out of phase with respect to the imposed deformation as expressed by:

$$\sigma = G^*(\omega)\gamma_0 \sin(\omega t + \delta p \tag{4}$$

and consequently

$$\sigma = G^*(\omega)\gamma_0 \sin(\omega g t)\cos(\delta) + G''(g\omega)\gamma_0 \cos(\omega t)\sin(\delta) \tag{5}$$

and if it is defined

$$\begin{aligned} G'(\omega) &= G^* \cos(\delta) \\ G''(\omega) &= G^* \sin(\delta) \end{aligned} \tag{6}$$

we obtain

$$\sigma = G'(\omega)\gamma_0 \sin(\omega t) + G''(g\omega)\gamma_0 \cos(\omega t) \tag{7}$$

where $G'(\omega)$ is the shear storage (or elastic) modulus and $G"(\omega)$ is the shear loss (viscous) modulus. G' gives information about the elasticity or the energy stored in the material during deformation, whereas $G"$ describes the viscous character or the energy dissipated as heat. The dependences of the elastic and viscous moduli upon frequency are called mechanical spectra.

The combined viscous and elastic behavior is given by the absolute value of complex shear modulus G^*:

$$B^*(\omega) = \sqrt{G'^2 G''^2} \tag{8}$$

or by the absolute value of complex viscosity η^* defined as:

$$\eta^*(\omega) = \frac{\sqrt{G'^2 + G''^2}}{\omega} \tag{9}$$

which is usually compared with the steady shear viscosity in order to evaluate the effect of large deformations and shear rates on the material structure.

The ratio between the viscous modulus and the elastic modulus is expressed by the loss tangent:

$$\tan\delta = \frac{G''}{G'} \tag{10}$$

where δ is the phase angle. The loss tangent is a measure of the ratio of energy lost to energy stored in the cyclic deformation [14].

In general the ratio between the stress and strain may depend both on time and stress. The ratio will depend only on time if the deformations are kept small in order to obtain liner material behavior. To determine the region of linearity, preliminary strain sweep tests at fixed oscillation frequency are performed. Specifically, the dynamic moduli are monitored while logarithmically varying the strain amplitude γ_0.

2.2 Hydrogel viscoelastic properties

The mechanical spectra analysis allows to distinguish clearly between concentrated (entangled) polymer solutions and gels [15, 16].

In the case of a concentrated solution at low frequency the solution presents viscous behavior ($G'' > G'$) while at high frequency an elastic behavior ($G' > G''$) is observed. The transition between viscous and elastic behavior, indicated by the cross point of G' and G'' curves, as a function of frequency, occurs at a given value of the frequency (f^*) (Fig. 2a). This behavior is typical of the concentrated solution or entangled networks, as in the terminal zone (low frequency), the polymer chains are able to regain equilibrium configuration through Brownian motion within the time scale of the experiment, and the solution behaves as a viscous liquid. On the other hand, at high frequency, above the intersection of G' and G'' curves, the chains cannot disentangle during the short period of oscillation and therefore they behave as a temporary crosslinked network in which the principal way to accommodate stress is by network deformation and elastic behavior ($G' > G''$) is observed. The cross-over frequency (f^*) corresponds to the intrinsic rate of disentanglement of polymer chains [17–19].

The mechanical spectra of a gel is substantially different [6].

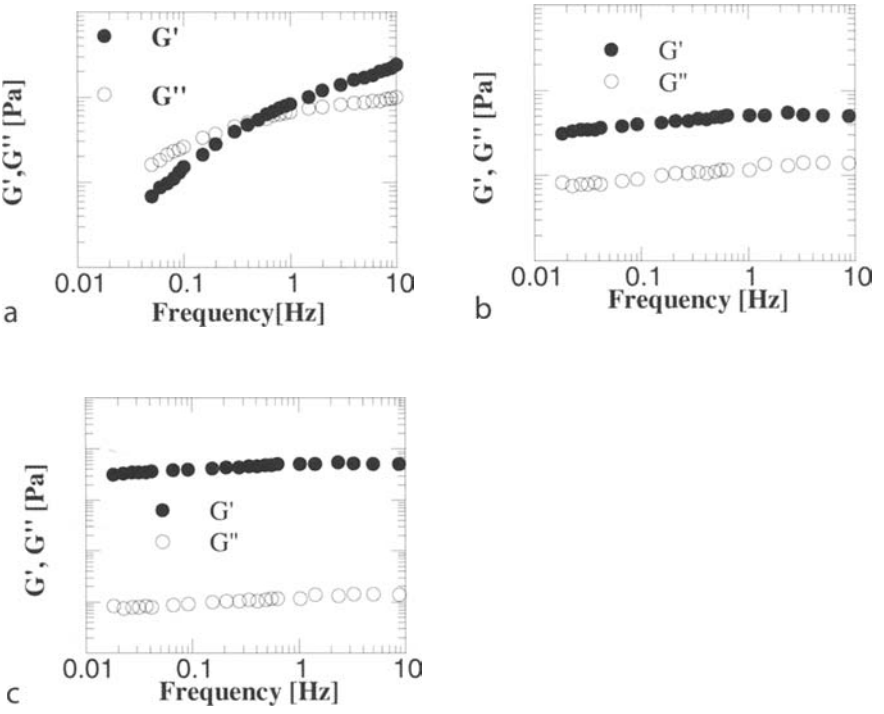

Fig. 2 Mechanical spectra of entangled solution **a**; weak **b** and strong **c** gels

The elastic modulus curve is higher than that of G'' over the frequency range analyzed (generally $10^{-2} - 10^{2}$ rad/s). In particular, from the mechanical spectra, it is possible to distinguish between chemical (strong) gel and physical (weak) gels [7, 8]. The typical strong gel spectrum (Fig. 2b) consists of an almost horizontal straight line, G' and G'' curves are, indeed, almost frequency independent and parallel to each other; moreover G' values are typically 1–2 orders of magnitude greater than G'' values (G''/G' lower than 0.1) [20–25].

In the case of a weak gel, the profile of G' and G" moduli (Fig. 2c) can show slight frequency dependence and the ratio G"/G' is higher than 0.1 [26]. Such rheological behavior is typical of biological gels such as protein and polysaccharide based networks (collagen, Hyaluronic acid) and soft tissues [27, 28]

It is worth underlining that the critical deformation γ_0^c characterizing the limit of the linear viscoelastic regime also allows to distinguish between the different systems. Physical gels, indeed, are essentially strain independent for deformations of lower than 0.2–0.3, whereas the linear viscoelastic region my extend to large strains of the order of the units [29].

2.3 Stress–strain behavior

Most hydrogels in their swollen state can be considered as rubber, that are lightly crosslinked networks with a rather large free volume that allows them to respond to external stresses with a rapid rearrangement of polymer segments. When a hydrogel is in the region of rubber-like behavior, its mechanical behavior is dependent mainly on the architecture of the polymer network [13]. To derive a relationship between the network characteristics and the mechanical stress–strain behavior, classical and statistical thermodynamics and phenomenological approaches have been used to develop an equation of state for rubber elasticity. The state equation for rubber elasticity, from classical thermodynamics can be expressed as [30–32]:

$$f = \left(\frac{\partial U}{\partial L}\right)_{T,V} + \left(\frac{\partial f}{\partial T}\right)_{L,V} \tag{11}$$

where f is the retractive force of the elastomer in response to a tensile force, U is the internal energy, L is the length, V is the volume and T the temperature.

For elastomeric materials it can be considered that the change in length does not cause internally driven retractive forces, indeed for those materials, bonds are not stretched with a change in L and an increase in length brings about a decrease in entropy because of the changes in the end-to-end distances of the network chains. The retractive force and entropy are related through the Maxwell equation:

$$-\left(\frac{\partial S}{\partial L}\right)_{T,V} = \left(\frac{\partial f}{\partial L}\right)_{L,V} \tag{12}$$

The entropic model for rubbery elasticity is a reasonable approximation for hydrogels. Indeed the entropy accounts for more than 90% of the stress.

By expressing the retractive force using the statistical thermodynamics, assuming no volume change upon deformation and that the free energy change on straining the polymer chains is due to the restraints placed on configurational rearrangements and is considered to be totally entropic in origin [8], it is possible to write the equation of state for rubber elasticity as follow [14, 30–32]:

$$\tau = \left(\frac{\partial A}{\partial \lambda}\right)_{T,V} = \frac{\rho RT}{\bar{M}_C}\frac{\bar{r}_0^2}{\bar{r}_f^2}\left(\lambda - \frac{1}{\lambda^2}\right) \tag{13}$$

where τ is the shear stress per unit area, ρ is the density of the polymer, M_c is the average molecular weight between crosslinks, and λ is the extension ratio. The quantity, $\bar{r}_0^2 / \bar{r}_f^2$, is the ratio of the end-to-end distance in a real network versus the end-to-end distance of the isolated chains; it is generally approximated as 1 when it is unknown. From equation 13 it can be deduced that the stress is directly proportional to the number of network chains per unit volume (i.e. ρM_c). The equation assumes that the network is ideal in that all chains are elastically active and contribute to the elastic stress and network imperfections such as cycles, chain entanglements and chain ends are not taken into account [33–35]. To correct for chain ends:

$$\tau = \frac{\rho RT}{\bar{M}_C}\frac{\bar{r}_0^2}{\bar{r}_f^2}\left(1 - \frac{2\bar{M}_C}{\bar{M}_n}\right)\left(\lambda - \frac{1}{\lambda^2}\right) \tag{14}$$

where M_n is the average molecular weight of the linear polymer chain before crosslinking. The correction can be neglected when $M_n \gg M_c$

From the constitutive equation the modulus can be expressed as:

$$G = \frac{\rho RT}{\bar{M}_C}\frac{\bar{r}_0^2}{\bar{r}_f^2}\left(1 - \frac{2\bar{M}_C}{\bar{M}_n}\right) \tag{15}$$

and the force per unit area as:

$$\tau = G\left(\lambda - \frac{1}{\lambda^2}\right) \tag{16}$$

The rubber elasticity theory predicts a non-linear stress strain behavior. The theory predictions describe the experimental results fairly well at low extension but are less accurate at higher elongations (Fig. 3).

3 Hydrogel swelling properties

The swelling behavior of biomedical hydrogels in biological fluids can be described by a variety of theoretical models aiming at the prediction of swelling behavior, mesh size for solute diffusion, and related parameters. Even if no theory can predict exact behavior, due to the highly non-ideal thermodynamic behavior of polymer networks in electrolyte solutions, the Flory-Rehner analysis can however be used with reasonable

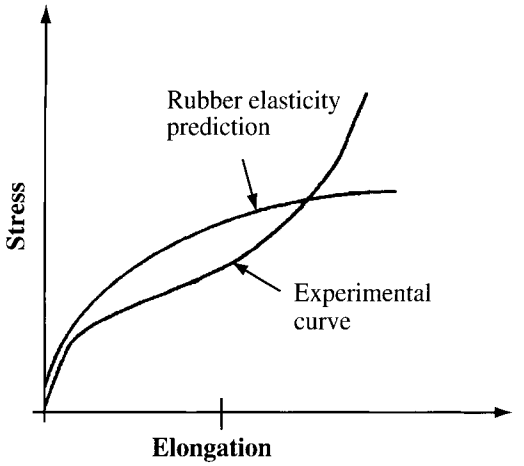

Fig. 3 Experimental and rubber elasticity predictions for the stress-strain behavior of crosslinked materials

success [36]. In this theoretical frame, gels are described as neutral, tetrafunctionally–cross-linked networks with polymer chains exhibiting a Gaussian distribution. When a polymer network is in contact with an aqueous solution or a biological fluid, it starts to swell due to the thermodynamic compatibility of the polymer chains and water. The swelling force is counterbalanced by the retractive force induced by the crosslinks of the network. Swelling equilibrium is reached when these two forces are equal.

The chemical potential change of water can be calculated at constant temperature and pressure as follows:

$$\mu_1 - \mu_{1,0} = \Delta\mu_{\text{mix}} + \Delta\mu_{\text{elastic}} \tag{17}$$

Here, $g\mu_1$ is the chemical potential of water in the system, $\mu_{1,0}$ is the chemical potential of pure swelling water, and $\Delta\mu_{\text{mix}}$ and $\Delta\mu_{\text{elastic}}$ are the mixing and elastic contributions to the total chemical potential change. The parameter $\Delta\mu_{\text{mix}}$ can be determined from the thermodynamics of the biomedical polymer-water mixing process and $\Delta\mu_{\text{elastic}}$ can be determined from the rubber elasticity theory [34] as shown below:

$$\Delta\mu_{\text{mix}} = RTln(1 - \nu_{2,s}) + \nu_{2,s} + \chi_x g\nu_{2,s}^{y} \tag{18}$$

and

$$\Delta\mu_{\text{elastic}} = (RTV_1/\overline{v}M_c)(1 - 2M_c/M_n)(\nu_{2,s}^{1/3} - \frac{\nu_{2,s}}{2}) \tag{19}$$

where, χ_{xg} is the biomedical polymer-water interaction parameter, V_1 is the molar volume of water, $\overline{v}$ is the specific volume of the biomedical polymer, $\nu_{2,s}$ is the volume fraction of the swollen gel, M_c is the average molecular weight between the crosslinks, and M_n is the molecular weight of linear polymer chains prepared under the same conditions without crosslinking. Equation 19 is written for hydrogels that were crosslinked in the absence of a solvent. Equations 17 to 19 lead to the expression

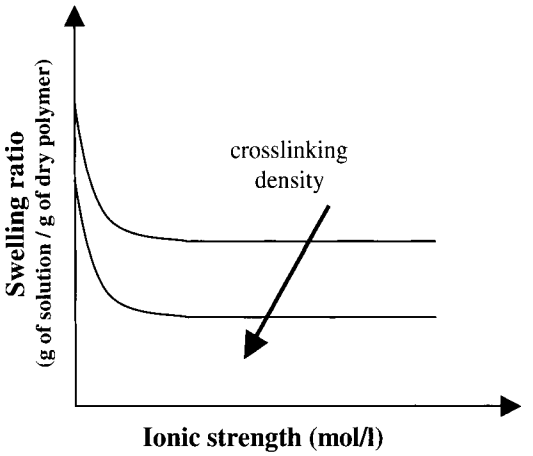

Fig. 4 Swelling ratio for polyelectrolyte gels as a function of the ionic strength and crosslinker concentration

for the true Mc of a non-ionized hydrogel:

$$\frac{1}{M_c} = \frac{2}{\bar{M}_n} - \frac{\frac{\bar{v}}{V_1}\ln(1-\nu_{2,s}) + \nu_{2,s} + \chi\nu_{2,s}^2}{\left[\nu_{2,s}^{1/3} - \nu_{2,s}\left(\frac{2}{\varphi}\right)\right]} \tag{20}$$

For the case of bio-hydrogels crosslinked in the presence of water, equation 20 is modified to account for the water-induced elastic contribution swelling:

$$\frac{1}{M_c} = \frac{2}{\bar{M}_n} - \frac{\frac{\bar{v}}{V_1}\left[\ln\left(1-\nu_{2,s}\right) + \nu_{2,s} + \chi\nu_{2,s}^2\right]}{\nu_{2,r}\left[\left(\frac{\nu_{2,s}}{\nu_{2,r}}\right)^{1/3} - \frac{\varphi}{2}\left(\frac{\nu_{2,s}}{\nu_{2,r}}\right)\right]} \tag{21}$$

where, $\nu_{2,r}$ is the volume fraction of the polymer in the relaxed state, i.e. immediately after crosslinking but prior to swelling/deswelling [37], and φ is the functionality of the crosslinking agent.

Most biomedical hydrogels contain ionizable pendant groups. In these gels, the force influencing swelling may be greatly increased due to localization of charges within the hydrogel. These ionizable groups may be partially or completely dissociated in solution. Due to the existence of ionic interactions, an ionic contribution term, $\Delta\mu_{\text{ion}}$, has to be added to the right-hand side of the chemical potential term of equation 17. The ionic interactions are strongly dependent on the degree of ionization, ionization equilibrium, and the nature of the counterions [38–40]. In the case of electrolyte gels, M_c will depend on the above mentioned gel parameters.

To calculate M_c, the $\nu_{2,r}$ values can be evaluated experimentally by equilibrium swelling experiments as they are inversely related to the swelling ratio Q (equation 1). The Q values will depend on the degree of crosslinking and for electrolyte gels on the ionic strength of the medium. (Fig. 4).

The knowledge of the average molecular weight between crosslinks Mc, permits the calculation of the characteristic correlation length, defined as the average distance between consecutive crosslinks, or mesh size [41]. From the value of Mc it is possible to estimate the end-to-end distance of the unpertubated (solvent free) state, $(r_0^{-2})^{1/2}$:

$$(r_0^{-2})^{1/2} = l\left(2\frac{M_c}{M_r}\right)^{1/2} C_n^{1/2} \tag{22}$$

where l is the bond length, C_n is the characteristic ratio of the polymer and M_r is the molecular weight of the repeating unit.

Finally, the mesh size, ξ, can be calculated from:

$$\xi = (r_0^{-2})^{1/2} V_{2,s}^{-1/3} \tag{23}$$

References

[1] Peppas NA, Huang Y et al (2000) Physicochemical foundations and structural design of hydrogels in medicine and biology. Annu Rev Biomed Eng 02:9–29

[2] Peppas NA (1986) Hydrogels in medicine and pharmacy. CRC Press, Boca Raton, Florida.

[3] Sperling LH (1981) Interpenetrating polymer Networks. Plenum Press, New York

[4] Ratner BD, Hoffman AS (1976) Synthetic hydrogels for biomedical applications. In: Andrade JD (ed) Hydrogels for medical and related applications. ACS symposium series, 31, ACS Washington

[5] Park H, Park K, Shalaby Waleed SW (1993) Biodegradable Hydrogels for Drug Delivery. CRC Press, Boca Raton, Florida

[6] Borzacchiello A, Ambrosio L, Netti PA, Nicolais L (2004) Rheology of biological fluids and their substitute. In: Yaszemski MJ, Trantolo DJ, Lewandroski KU, Hasirci V, Altobelli DE, Wise DL (ed), Tissue Engineering and Novel Drug Delivery Systems. Marcel Dekker Inc, New York

[7] Ross-Murphy SB (1991) Physical gelation of synthetic and biological macromolecules. In: De Rossi D, Kajiwara K, Osada Y and Yamauchi A (ed) Polymer Gels. Fundamentals and Biomedical Applications. Plenum Press, New York

[8] Clark AH, Ross-Murphy SB (1987) Structural and mechanical properties of biopolymers gels. Adv Pol Sc 83: 61

[9] Brannon-Peppas L (1994) Preparation and characterization of cross-linked hydrophilic networks. In: Superabsorbent Polymers: Science and Technology ACS Symp. Ser. 573, American Chemical Society, Washington, DC

[10] Peppas NA, Mikos AG (1986) Preparation methods and structure of hydrogels. In: Peppas NA (ed) Hydrogels in Medicine and Pharmacy, Vols 1, 2. CRC press Boca Raton, Florida

[11] Peppas NA, Barr-Howell BD (1986) Characterization of the cross-linked structure of hydrogels. In: Peppas NA (ed) Hydrogels in Medicine and Pharmacy, Vols 1, 2. CRC press Boca Raton, Florida

[12] Peppas NA, Huang Y, Torres-Lugo M, Ward JH, Zhang J (2000) Physicochemical foundations and structural design of hydrogels in medicine and biology. Annu Rev Biomed Eng 02:9–29

[13] Anseth KS et al. (1996) Mechanical properties of hydrogels and their experimental determination. Biomaterials 17:1647–1657

[14] Ferry JD (1970) Viscoelastic Properties of Polymers. Wiley, New York
[15] Ambrosio L, Borzacchiello A, Netti PA, Nicolais L (1998) Rheological properties of hyaluronic acid based solutions. Polymeric Materials Science and Engineering 79: 244–245
[16] Ambrosio L, Borzacchiello A., Netti PA, Nicolais L (1999) Rheological study on Hyaluronic acid and its derivatives solutions. J. of Macromolecular Science-Pure and Applied Chemistry A 36(7 and 8):991–1000
[17] Borzacchiello A, Netti PA, Ambrosio L, Nicolais L (2000) Hyaluronic acid derivatives mimic the rheological properties of vitreous body. In: Abatangelo G, Weigel PH (ed) New Frontiers in Medical Sciences: Redefining Hyaluronan. Elsevier, Amsterdam, pp 195–202
[18] Borzacchiello A, Ambrosio L (2001) Network formation of low molecular weight hyaluronic acid derivatives. Journal of Biomaterials Science Polymer Edition 12(3):307–316
[19] Maltese A, Bucolo C, Maugeri F, Borzacchiello A, Mayol L, Nicolais L, Ambrosio L (2006) Novel polysaccharides based viscoelastic formulations for ophthalmic surgery: rheological characterization. Biomaterials 27:5134–5142
[20] Barbucci R, Ruoppoli R, Borzacchiello A, Ambrosio L (2000) Synthesis, chemical and rheological characterisation of new hyaluronic based hydrogels. Journal of Biomaterials Science Polymer Edition 11(4):383–399
[21] Borzacchiello A, Ambrosio L, Netti PA, Nicolais L, Peniche C, Gallardo A, San Roman J (2001) Chitosan-based hydrogels: Synthesis and Characterization. J. of Materials Science: Materials in Medicine 12:861–864
[22] Barbucci R, Lamponi S, Borzacchiello A, Ambrosio L, Fini M, Torricelli P, Giardino R (2002) Hyaluronic acid hydrogel in the treatment of osteoarthritis, Biomaterials 23(13): 4503–4513
[23] Leone G, Barbucci R, Borzacchiello A, Ambrosio L, Netti PA, Migliaresi C (2004) Preparation and physico-chemical characterisation of microporous polysaccharidic hydrogels. J Mater Sci: Mater in Med 15(4):463–467
[24] Borzacchiello A, Mayol L, Ramires PA, Di Bartolo C, Pastorello A, Ambrosio L, Milella E (2007) Structural and rheological characterization of hyaluronic acid-based scaffolds for adipose tissue engineering. Biomaterials 28:4399–4408
[25] D'Errico G, De Lellis M, Mangiapia G, Ortona O, Fusco S, Borzacchiello A, Ambrosio L (2008) Structural and mechanical properties of UV photocrosslinked poly(N-vinyl-2-pyrrolidone) hydrogels. Biomacromolecules 9 (1): 231–240
[26] Xuejun Xin, Borzacchiello A, Netti PA, Ambrosio L, Nicolais L (2004) Hyaluronic Acid Based Semi Interpenetrating Materials. J Biomater Sci Polymer Edn 15:1223–1236
[27] Battista S, Guarnieri D, Borselli C, Zeppetelli S, Borzacchiello A, Mayol L, Gerbasio D, Keene DR, Ambrosio L, Netti PA (2005) The effect of matrix composition of 3D constructs on embryonic stem cell differentiation. Biomaterials 26(31):6194–6207
[28] Guarnirei D, Battista S, Borzacchiello A, Mayol L, De Rosa E, Kene DR, Muscariello L, Barbarisi A, Netti PA (2007) Effect of fibronectin and laminin on structural, mechanical and transoprt properties of 3D collageneous network. Journal of Materials Science: Materials in Medicine 18 (2): 245–253
[29] Lapasin R, Pricl S (1995) Rheology of industrial polysaccharides Theory and applications. Blackie Academic and Professional, London
[30] Aklonis JJ, MacKnight WJ (1983) Introduction to polymer viscoelasticity. Wiley, New York
[31] Ward IM, Hadley PW (1993) An introduction to the mechanical properties of solid polymers. Wiley, New York

[32] Sperling LH (1986) Introduction to physical polymer science. Wiley, New York
[33] De Smedt SC, Dekeyser P, Ribitsch V, Lauwers A, Demeester (1993) Viscoelastic and transient network properties of hyaluronic acid as a function of the concentration. Biorheology 30:631
[34] Flory PJ (1953) Principles of Polymer Chemistry. Cornell University Press, New York
[35] Schurz J (1991) Rheology of polymer solutions of the network type. Prog Polym Sci 16:1–53
[36] Flory PJ, Rehner BD. (1943). Statistical mechanics of cross-linked polymer networks. J Chem Phys 11:521–526
[37] Peppas NA, Merrill EW (1976). PVA hydrogels: reinforcement of radiation-crosslinked networks by crystallization. J Polym Sci Polym Chem 14:441–457
[38] Ricka J, Tanaka T (1984) Swelling of ionic gels: quantitative performance of the Donnan theory. Macromolecules 17:2916–2921
[39] Tanaka T (1979) Phase transition in gels and a single polymer. Polymer 20:1404–1412
[40] Brannon-Peppas L, Peppas NA (1990) The equilibrium swelling behavior of porous and non-porous hydrogels. In: Brannon-Peppas L, Harland RS (ed) Absorbent polymer technology. Elsevier, Amsterdam
[41] Canal T, Peppas NA (1989) Correlation between mesh size and equilibrium degree of swelling of polymeric networks. J Biomed. Mater Res 23:1183–1193

Water and Surfaces: a Linkage Unexpectedly Profound

Gerald H. Pollack

Abstract. The impact of surfaces on the contiguous water is thought to project no more than a few molecular layers from the surface. On the contrary, we have found that solutes are profoundly excluded from a several-hundred-micrometer-wide zone next to various hydrophilic surfaces, including gels. Such large "exclusion zones" appear to be quite general. Recent studies have shown that the underlying basis is a reorganization of interfacial water molecules into a liquid crystalline array, which then excludes solutes. The impact of this "fourth phase" of water appears to be broad, especially in biology.

For most, water is fairly boring. In biology especially, water is considered merely a background carrier for the interesting molecules in life – a largely neutral entity that bears responsibility mainly for suspending the molecules of central interest. Likewise, in the physical sciences, except for the water immediately adjacent to surfaces and except for situations (such as atmospheric science) where water is the central protagonist, water is considered to play only a secondary role in most physical or chemical processes.

Contrastingly, we have found evidence that water plays an unexpectedly profound role – one that may inevitably impact practically all phenomena that take place in aqueous solution.

Recent data from this laboratory show that in the vicinity of common hydrophilic materials, water molecules become ordered. Properties of this ordered zone – mechanical, chemical and optical – all differ from those of bulk water. These findings stem from an original core observation: colloids and solutes are profoundly excluded from the region next to hydrophilic materials. The exclusion zone (EZ) commonly extends up to hundreds of micrometers from the surface (see Fig. 1).

The core findings are detailed in two papers, Zheng and Pollack [1] and Zheng et al. [2]. More easily accessible is the link to a lecture [3] delivered as recipient of the 2007/2008 University of Washington Annual Lectureship Award. This lecture describes the evidence as well as the implications in a manner easily accessible for non-experts.

The first of the two cited papers deals with the question of whether the finding of long-range exclusion of solutes may have some trivial explanation. Plausible candi-

Barbucci R. (Ed): Hydrogels. Biological Properties and Applications.

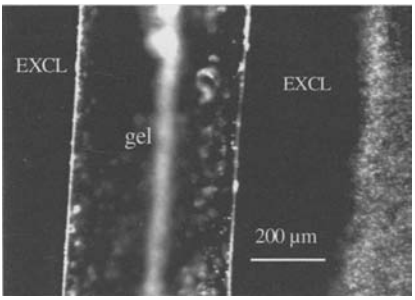

Fig. 1 Solute exclusion (EXCL) in the vicinity of polyacrylic acid gel. Gel runs vertically. The blurred vertical white element to the right of the "gel" is an optical artifact. The gel was placed on a coverslip, superfused with a suspension of 1-μm carboxylate-coated microspheres, and observed with an inverted microscope equipped with a 20x objective. The image was obtained 20 min after superfusion. Microspheres (seen on the right edge) undergo active thermal motion, but do not enter the exclusion zone

dates were ruled out by an extensive series of controls. Since then, at least ten groups worldwide have informally tested and confirmed the basic finding. In fact, a similar result had been published four decades ago: in addressing the origin of the so-called "unstirred layer" adjacent to biological tissues [4] , a region where mixing is known to be extremely slow, Green and Otori [5] showed in both corneal tissue and contact lenses that the unstirred layer excludes microspheres; exclusion zones several hundred micrometers wide were found – essentially the same as we have found in our studies. Hence, there is little question of the existence of unexpectedly large exclusion zones next to hydrophilic surfaces. The question is what such zones might mean.

The second Zheng paper [2] shows that the physical chemical properties of the EZ differ from those of bulk water. Four sets of results were presented:

- NMR rotational relaxation time in the EZ is shorter than in bulk water;
- Infrared radiation from the EZ is less than from bulk water;
- Potential gradients exist in the EZ, but not in bulk water;
- UV-Vis absorption spectra are markedly different in the EZ.

Two additional features have recently been added. They are:

- Polarizing microscopy shows that the EZ is birefringent, confirming molecular ordering in that zone;
- Falling-ball viscometry shows that EZ water is considerably more viscous than bulk water.

Hence, six independent approaches show that EZ water differs from the water beyond the EZ. Collectively, they imply that EZ water may be more ordered and more stable than bulk water. It is understood that this conclusion deviates substantially from accepted theoretical expectations; nevertheless, the results of these studies show this feature consistently.

Two additional features are relevant to a fuller understanding of the implications:

The EZ is charged: typically, the charge is negative [2]. The "reason" the EZ is negatively charged is that as it forms, constituent water molecules lose protons, which then accumulate in the bulk water beyond. This accumulation is confirmed using two independent methods: pH-sensitive dyes and pH electrodes. Both show that the pH of the bulk water beyond the EZ is sharply diminished, indicating excess protons. In other words, the EZ and the complementary region beyond the EZ effectively constitute a battery – negative in the EZ and positive in the region beyond. Substantial current can be drawn from this battery, confirming genuine charge separation.

The energy needed to build the EZ comes from radiant sources [3]. That is, photons from the environment, including wavelengths in the UV, visible, and particularly infrared region, expand the EZ. Even infrared-intensity levels weak enough to cause insignificant heating (on the order of 1 °C) expand the EZ by three to four times within five minutes. Hence, radiant energy is extremely effective in charging this battery.

The results outlined above are critically important for applications involving water. Any particle or solute suspended in water will be richly endowed with the kinds of features outlined above. Examples: (1) With ordered water surrounding each particle, the effective size of the particle exceeds the presumed size, possibly by an unexpectedly sizable amount. (2) With protons released by the ordered moiety, the pH of the rest of the solution is likely to be lower than expected. (3) Light, especially infrared, is likely to have an impact on all suspensions.

The same is true of water adjacent to extended surfaces. The region immediately adjacent to hydrophilic surfaces will be extensively ordered, and the zone beyond is likely to be amply endowed with protons. Hence, the latter will have a pH lower than anticipated. The presence of positive charge may have an unexpectedly profound effect on reactions occurring in reasonable proximity of the surface.

The EZ may constitute the long-anticipated "fourth phase" of water. This was suggested almost a century ago by the eminent physical chemist Sir Wm. Hardy, but largely forgotten over the years. The bottom line, available by visiting [3] (for review, visit [6]), is that the role of interfacial water in all aqueous suspensions is far more profound than generally expected. Indeed, this unexpectedly profound role may open doors to numerous practical applications.

References

[1] Zheng JM, Pollack GH (2003) Long range forces extending from polymer surfaces. Phys Rev E 68: 031408

[2] Zheng JM, Chin WC, Khijniak E, Khijniak E Jr, Pollack GH (2006) Surfaces and Interfacial Water: Evidence that hydrophilic surfaces have long-range impact. Adv Colloid Interface Sci 127: 19–27

[3] http://uwtv.org/programs/displayevent.aspx?rID=22222. Accessed 15 September 2008

[4] Pollack GH, Clegg, J (2008) Unsuspected Linkage Between Unstirred Layers, Exclusion Zones, and Water. In: Pollack GH, Chin, WC (ed) Phase Transitions in Cell Biology. Springer, pp 143–15

[5] Green K, Otori, T (1970) Direct measurement of membrane unstirred layers. J Physiol London 207: 93–102
[6] http://www.i-sis.org.uk/liquidCrystallineWater.php. Accesed 15 September 2008

Polysaccharide Based Hydrogels for Biomedical Applications

Gemma Leone and Rolando Barbucci

Abstract. Polysaccharide based hydrogels for their physico-chemical and biological properties can be used as scaffolds for soft tissue regneration and as vehicles for drug controlled release. For both these applications, Hyaluronan shows optimal characteristics even though its quick enzymatic degradability makes this natural polysaccharide unsuitable for applications which require prolonged presence in the human organism.

For this reason, new semisynthetic polysaccharides based on carboxymethylcellulose alginate and guar were developed and tested as cartilage substitutes, nucleus pulposus substitutes and as a vehicle for biologically active substances directed towards bone tissue regeneration.

Naturally derived hydrogel forming polymers have frequently been used in tissue engineering applications because they are either components of, or have macromolecular properties similar to, the natural ECM. Among the natural polymers forming hydrogels, an important role is played by polysaccharides. Recognition of the potential utility of this class of materials in the biomaterial field is growing and the field of polysaccharide biomaterials is poised to experience rapid growth. Three factors have specifically contributed to this growing recognition of polysaccharide-based biomaterials. First is the large and growing body of information pointing to the critical role of saccharide moieties in cell signaling schemes and in particular in the area of immune recognition. Secondly, has been the recent development of powerful new synthetic techniques with the potential for automated synthesis of biologically active oligosaccharides. The third factor is the explosion of tissue engineering research and the associated need for new materials with specific, controllable biological activity and biodegradability [1]. Among the polysaccharides, Hyaluronic acid, Alginate and Carboxymethylcellulose are widely used in the biomedical field.

On the basis of the physico-chemical and biological response of polysaccharide based hydrogels, two main applications in the biomedical field can be foreseen:

- hydrogels for soft tissue regeneration;
- hydrogels for delivery of biologically active substances (i.e. growth factors and drugs).

Barbucci R. (Ed): Hydrogels. Biological Properties and Applications.

1 Hydrogels for soft tissue regeneration

The degradation of Hyaluronan can be considered one of the crucial events in the loss of funcionality of several soft tissues, such as cartilage or the nucleus pulposus [2]. Several attempts were made to counteract these degenerative processes. In particular, injection of exogeneous hyaluronan obtained from different sources, with different molecular weights and different formulation was tested [3]. No lasting effects have ever been obtained because of the very quick degradation rate of hyaluronan which cannot be blocked without changing drastically its chemistry or activity.

So new polysaccharides with similar compatibility and bioactivity to hyaluronan, but more stable against enzymatic attack, seem to represent optimal substitutes. Regarding the chemical composition of Hyaluronan, the main difference between this polysaccharide and other polysaccharides is represented by the presence of an amidic group along its chain. Considering this, we modified polysaccharides, such as carboxymethylcellulose [4] and alginate [5], by converting their carboxylic groups, chemically correlated with those present along the hyaluronan chains, into amidic ones.

1.1 Hydrogel for cartilage regeneration

Most approaches to cartilage engineering involve delivery of cells via biodegradable scaffolds to regenerate tissue [6]. However, the time necessary for cell colonization and new tissue development is not comparable with the time necessary for hydrogel degradation. One of the most utilized materials for cartilage regeneration is alginate hydrogel because alginate supports chondrocytes and has shown to be biocompatible when delivering cells in human trials. However, its degradation rate is too fast in comparison to cartilage regeneration [7]. The same trend has been found also with chondritin sulphate or Hyal based hydrogels. A cellulose derivative seems to overcome these disadvantages. In particular, an amidic carboxymethylcellulose hydrogel was realized and analyzed.

1.2 Amidic Carboxymethylcellulose hydrogel

The amidation reaction was carried out by dissolving the tetrabutylammonium salt of carboxymethylcellulose in organic solvent (N-N'-Dymethylformamide) under nitrogen flow. Chloro-methyl-pyridin-iodide (CMPI) was used as an activating agent of carboxylic groups towards the nucleofilic attack of the amidating agent. As an amidating agent, the methylamine (CH_3NH_2) was chosen to obtain an amidic group which was similar, although not identical, to the one which is present along the hyaluronan chain.

The amidation reaction on the CMC polysaccharide was qualitatively confirmed by infrared analysis. The IR spectrum of the modified polysaccharide (CMCA) was compared with that of the native polysaccharide (CMC). The CMCA IR spectrum showed a new shoulder centered at 1645 cm^{-1} which is relative to the amidic C=O stretching [4].

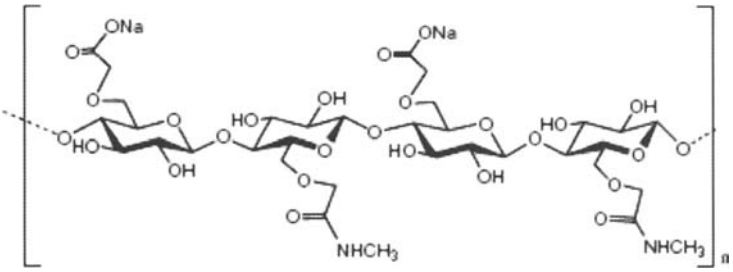

Fig. 1 Schematic representation of the regular structure of CMCA polymer characterized by alternating carboxylic and amidic groups (Reprinted from [8], with permission from Elsevier)

A complete structural NMR analysis of the polymer was carried out, from which the amidation degree was also obtained. The ^{1}H NMR spectra showed broad and unresolved peaks, due to the size of the macromolecules and to the presence of resonance arising from different substitution positions, so univocal assignments were possible only on the basis of 2D ^{1}H NMR homonuclear COSY and TOCSY, and 2D heterocorrelated inverse ^{13}C techniques like HMQC and HMBC. The peak relative to the carbonyl group was identified and assigned by comparing the NMR spectra of native CMC and CMCA. In the CMCA spectrum, a new complex signal was present at a higher field (178.3 ppm) which can be related to the amidic carbonyl group. ^{13}C experiments carried out without NOE allowed for the amidation degree to be calculated. It was about 39%, in agreement with potentiometric data.

Furthermore, 2D NOESY experiments performed on differently diluted samples showed that the amidic and carboxylic groups were strictly alternated along the polysaccharide chains, thus confirming the regularity of the structure guaranteed by the chemical procedure performed. All these data allowed the polysaccharide structure to be determined as reported in Fig. 1.

The amidic polysaccharide chains were crosslinked through an alkylic bridge deriving from the formation of amidic bonds between the free carboxylic groups of the polysaccharides and the aminic groups of the crosslinking agent (1.3 diaminopropane). A 100% hydrogel (i.e., all the carboxylic groups not involved in the amidation reaction were involved in the crosslinking reaction) was obtained by adding an excess of chloromethyl pyridine iodide to utilize all the free COOs. The crosslinking reaction and degree to which it had occurred were confirmed by FT-IR spectroscopy. The two different amidic groups in the hydrogel were also mapped using the FT-IR imaging technique. As shown in Fig. 2, the dark grey dots relative to the $-CONHCH_3$ amidic groups of the polymer were positioned closed to the light grey dots which were relative to the new amidic groups formed on the carboxylic groups during the crosslinking reaction. This distribution confirmed the hypothesis of a regular distribution of $-CONHCH_3$ along the polymer chain.

The ^{13}C NMR spectrum of CMCA in the crosslinked form showed no evidence of free carboxylic groups, whereas a new peak centered at about 175 ppm was found. This new peak was relative to the new amidic C=O groups deriving from the crosslinking reaction (Fig. 3) [8].

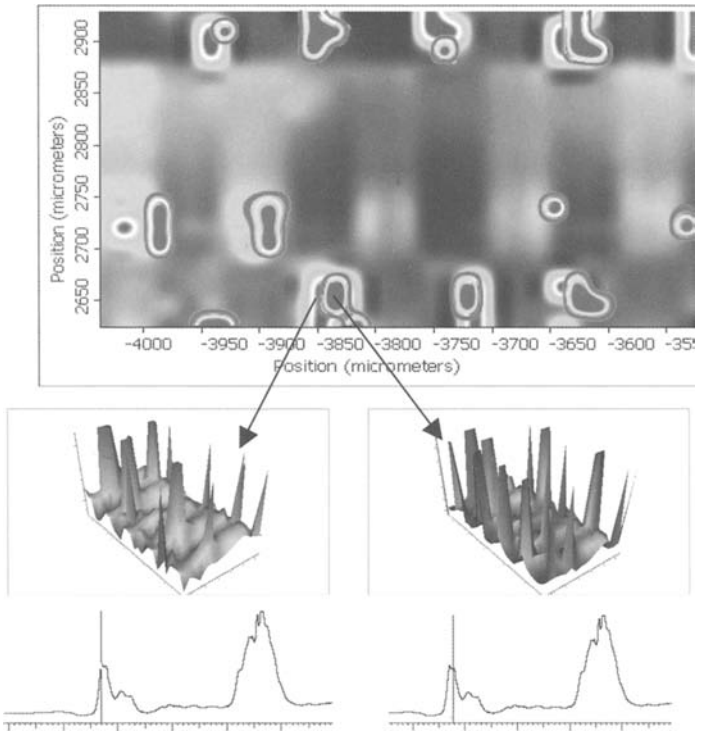

Fig. 2 FT-IR image in which the dark grey dots are relative to $CONHCH_3$ amidic groups (1647 cm^{-1}) and the light grey dots to crosslinking amidic groups (1659 cm^{-1}). The two different amidic groups are very close to each other indicating regular alternation (Reprinted from [8], with permission from Elsevier)

Measurements of diffusional domains by low-resolution NMR performed on hydrogels, showed that a regular hydrogel structure could be obtained with reproducible meshes whose dimensions depend on either the synthesis procedure or the amount of activating agent added, but not on the polysaccharide. Four different kinds of water were present.

The component with the longer T2 can be ascribed to water molecules remote from the polymer network, called free water. The component with a lower T2 can be ascribed to the water molecules whose motion is slightly affected by the polymer presence and therefore called bulk water. The reduced T2 of bulk water can be simply explained as being due to the anisotropic motion that water molecules can undergo in a restricted region, with possible further lowering due to proton exchange with polymer exchangeable protons. The fast relaxing component (mesh water) was attributed to the water molecules within the interstitial spaces of the polymer. Finally, the lowest T2 can be ascribed to the water molecules bound strictly to the polymer chains [8].The same analysis was previously performed on different hyaluronan based hydrogels with a 50% crosslinking degree [9]. By comparing the T2 values relative to the mesh water,

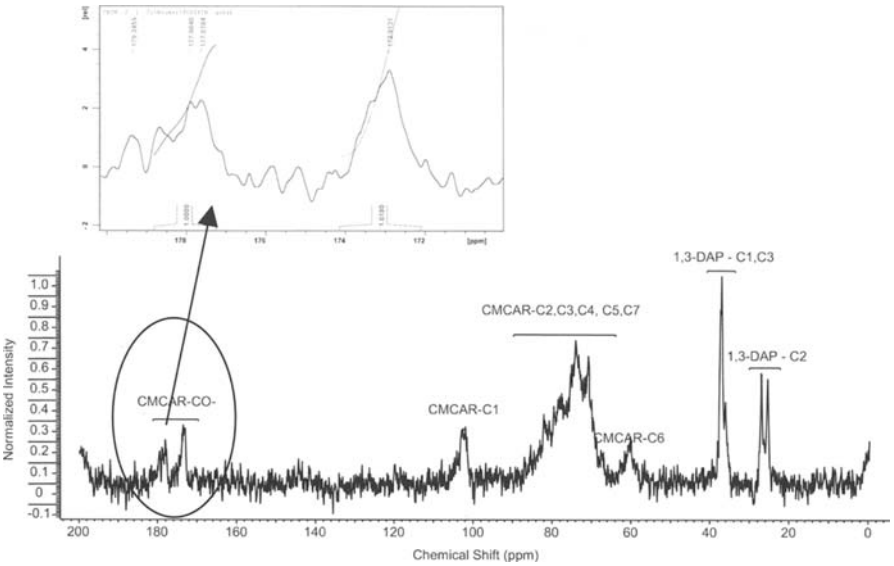

Fig. 3 ^{13}C NMR spectrum of CMCA hydrogel. The spectrum was recorded on hydrogel swollen in deuterium oxide at the controlled temperature of 310 ± 1 K (Reprinted from [8], with permission from Elsevier)

comparable values were found despite the higher degree of crosslinking for the CMCA hydrogels. This suggests a high level of hydrophilicity of the CMCA polysaccharide. This hypothesis was also confirmed by the fact that for CMCA hydrogels, a fourth slower water component was found which is related to the water bound strictly to the polymer (Table 1).

Table 1 Transverse relaxation times and signal percentages of the four components of water in crosslinked amidic carboxymethylcellulose hydrogel at 310 K

Components	T2(ms)	%
Free Water	2423±30	22.5±0.4
Bulk Water	680±14	39.1±0,7
Meshes Water	274.6±3.6	36.2±1.0
Bound Water	12.25±0.48	2.2±0.1

Rheological Analysis. The equilibrium modulus (μ), a measure of the intrinsic matrix shear stiffness at equilibrium, and the dynamic modulus (|G*|), a measure of combined elastic and viscous effects in dynamic shearing, are important material properties for cartilage substitutes. The loss angle (delta) is a measure of the dissipation associated with viscous-elastic effects and can range from 0° for a perfectly elastic solid to 90° for a perfectly viscous fluid. The frequency sweep test evidenced a "gel-like" behavior for CMCA hydrogel, with the storage modulus (G') greater than the loss

Table 2 Trend of CMCA hydrogel complex modulus (|G*|) and loss angle (δ) in the frequency range 0.01–20 Hz

	0.01Hz	20Hz
|G*| (Pa)	7400±250	10800±300
δ(deg)	10±1	13±2

modulus (G") within the frequency range analyzed. CMCA hydrogel exhibited the typical behavior of viscous-elastic solids under small deformation conditions. From both G' and G" values it was possible to obtain the trend of the complex shear modulus |G*| within the frequency range tested. It changed from 0.7 MPa (0.01 Hz) to 1.0 MPa (20 Hz) for CMCA. On the contrary, δ of the hydrogel did not change significantly over the range of frequencies tested (~13 ° for CMCA) (Table 2). Samples exhibited a predominantly elastic behavior in dynamic shearing, as evidenced by the value of $\delta < 45$ °, reflecting a more solid-like rather than a fluid-like behavior of the hydrogel under dynamic conditions. The stress-relaxation test at a strain of 0.1 rad, performed to evaluate either the time dependent sensitivity to load or deformation of CMCA hydrogel, showed a very rapid relaxation time within the first second after loading, then slow decay (Fig. 4).

The regularity of the polymer structure, characterized by alternating amidic and carboxylic groups, permitted a homogeneous network to be obtained which was, as a consequence, able to respond to stress and dissipate quickly undergoing no fracture. This aspect, together with the hydrogel's ability to absorb a very large amount of water (W.U = 6000 at pH 7.4), renders the hydrogel very similar to highly viscous solutions, allowing for the thixotropic behavior of the polysaccharide[10] also in the hydrogel form.

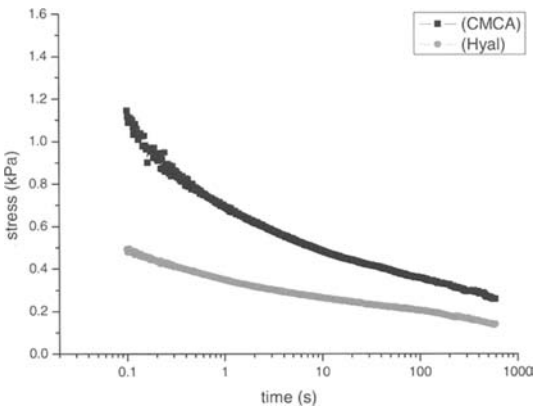

Fig. 4 Behaviour of CMCA (black) hydrogel subjected to a ramp stress-relaxation experiment with an imposed shear strain $\gamma_0 = 0.10$ rad (Reprinted from [8], with permission from Elsevier)

In fact, the hydrogel obtained using the described procedure, can be considered as formed by several macroparticles connected to each other by a diffused water network. When an appropriate stress is applied, the macroparticles slide onto the water layer which connects them, and so under stress the system behaves as a fluid. Once the stress is removed, the hydrogel network formed again and the structrure resumed its three-dimensional form. This property was observed in all the polysaccharide hydrogels obtained using our crosslinking procedure.

Cell proliferation and synthetic activity (NHAC): The ability of the 100% CMCA hydrogel to stimulate chondrocyte proliferation and metabolic activity was compared with a 100% Hyal-based hydrogel whose activity towards chondrocytes is well known [11, 12]. The results of the WST1 test showed that chondrocytes proliferated in both CMCA. Furthermore, chondrocytes seeded on CMCA and Hyal hydrogels maintained their phenotype as indicated by cathepsin B values. Actually, cathepsin B, which can be used as a soluble marker to evaluate the phenotype of cultured chondrocytes, is known to be produced by chondrocytes grown in a monolayer culture, while decreasing significantly when cells are cultured on substrates that promote a re-differentiation process. To verify chondrocyte anabolic activity, the production of collagen type II (CPII) and proteoglycans (PG) were evaluated. Chondrocytes cultured on hydrogels showed significantly higher values of CPII (CMCA, Hyal versus CTR, $p < 0.0001$) and aggrecan (CMCA versus CTR, $p < 0.005$; Hyal versus CTR, $p < 0.0001$) in comparison with CTR on plate polystyrene culture (Table 3).

In vitro results suggested that CMCA ameliorated chondrocyte differentiation as well as ECM synthetic activity with respect to CRT, exhibiting a behavior similar to better and optimal materials for OA therapy, or Hyaluronan [12]. Actually, the chondrocytes seeded on CMCA hydrogel showed significantly increased Aggrecan production. This increase was important for the role of the proteoglycan network in the cartilage, since it is responsible for the maintenance of the integrity of the structure, bringing unique biomechanical properties to the tissue. Also in terms of type II collagen production and degradation, CMCA showed good performance, significantly increasing the production of this extracellular matrix component. Therefore, CMCA hydrogel did not stimulate the release of MMP1 and MMP13, collagenases which are

Table 3 Proliferation and bioactivity of different polysaccharide based hydrogels towards NHAC (Normal Human Articular chondrocytes)

	control	Hyal	CMCA
WST1 (OD450650nm)	1.16±0. 03	0.70±0.04	0.73±0.03
Cathepsin B(ng/mL)	4.28±0.54	2.06±0.09	2.25±0.51
MMP13 (pg/mL)	68.0±12.7	121.5±16.7	93.0±15.0
MMP1 (ng/mL)	1.33±0.70	1.88±0.30	0.81±0.50
Collagen II (ng/mL)	133.9±11.2	312.8±17.2	203.2±12.2
IL-6 (pg/mL)	3.64±0.20	4.40±0.76	3.80±0.35
Aggrecan (ng/mL)	731.8±83.4	1294.5±82.6	1126.5±114.8

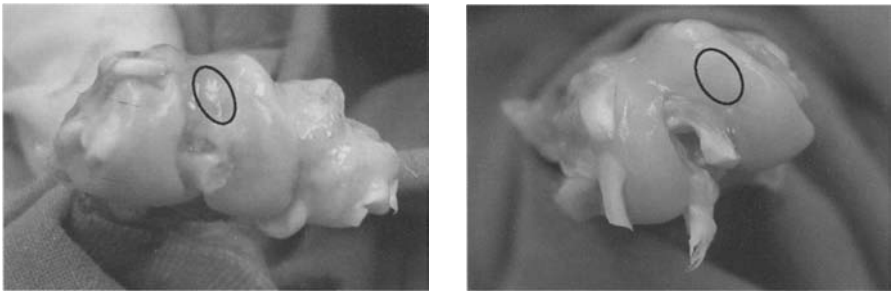

a b

Fig. 5 Macroscopic photographs of the chondral lesion after 50 days. **a** Control group; **b** CMCA hydrogel group [13]

the most effective enzymes for initiating the cleavage of native helical collagen. So, on the basis of good rheological performance and optimal action towards normal human chondrocytes, CMCA hydrogel can be considered a potentially good filler for cartilage defects. Since the aim of this study was to find a substitute for Hyal-based hydrogel for the treatment of OA, the effect of this new hydrogel has been evaluated in vivo.

In vivo study: In all the animals, wounds healed without complication, and no edema or inflammation of the treated articulations were observed. At explant, gross examination of untreated condyles showed that after 50 days, the surface lesion was well visible because of a rough and opaque area. In treated condyle groups, after 50 days, the area of the initial defect was less clearly definable from the adjacent intact cartilage (Fig. 5).

From histomorphometric analysis, as expected, tissue healing was not observed in untreated lesions. In the group treated with CMCA hydrogel, the histological analysis showed that after 50 days, a layer of mixed fibro cartilaginous and hyaline-like tissue was present. The defect was completely filled in 3 out of 4 samples, their surface being regular and smooth (Fig. 6). Local treatment with CMCA improved healing of cartilage lesions, showing a more regular filling of the defect when compared with untreated samples. The staining of the matrix was only slightly reduced, while cluster and columnar formations of chondrocytes were observed in the new hyaline-like cartilage.

In vivo results obtained using the amidic derivative of carboxymethylcellulose in the form of hydrogel showed that intra-articular injection of CMCA stimulated cartilage healing, even if long-term studies are needed to exclude further tissue degeneration [13].

To conclude, on the basis of these preliminary results, CMCA can be considered a potential product for cartilage regeneration and OA therapy. Using CMCA hydrogel, an identical result in terms of tissue regeneration with respect to Hyal was obtained, but with a lower cost. The reduced degradation rate of CMCA in comparison to Hyal will allow fewer administrations and, consequently, reduce discomfort and the risk of infection for the patient. Furthermore, the tixotropy of CMCA hydrogel permits it to

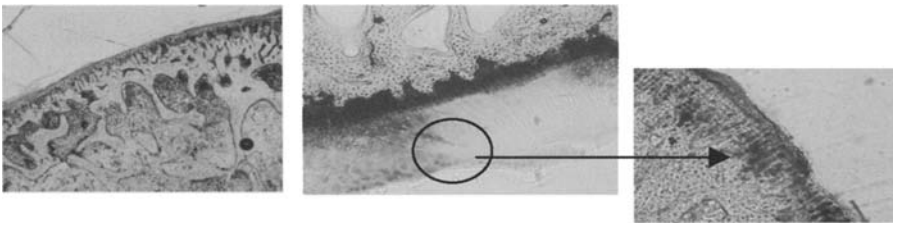

Fig. 6 Histological sections from the chondral defect after 50 days. **a** control group: no tissue regeneration; **b** CMCA hydrogel group: mixed hyaline and new fibrous tissue; **c** columnar formations of chondrocytes dipped into a hyaline-like matrix [13]

be included in the injectable hydrogel class which guarantee minimally invasive and localized therapy.

1.2.1 Hydrogels for nucleus pulposus replacement

Degeneration of intervertebral discs is the most common cause of back pain. The first phase of this degenerative process involves the nucleus pulposus. Rapid recovery of this structure can prevent further degradation of the annulus fibrosus. The composition of the human nucleus pulposus (NP) can be considered as water dispersed in a matrix of proteoglycan, collagen and other proteins. In particular, the water content of the nucleus pulposus changes from 90% at birth to less than 70% at over 60 years of age. The other most abundant macromolecules present in the nucleus pulposus, proteoglycans, account for as much as 65% of the dry weight, decreasing to as little as 30% with advancing age [14]. Among these, several molecular species of glycosaminoglycan have been identified in the nucleus pulposus, such as versican and hyaluronan [15]. On the basis of these characteristics, hyaluronan was tested for NP replacement but was rapidly degraded, even in the form of very highly viscous solutions [16]. A Hyal based hydrogel was therefore tested, as it is well known that crosslinking decreases the degradation rate [17]. This seemed to meet several of the requirements for NP regeneration, but its rate of enzymatic degradation was not sufficiently lowered and this hindered its use in this application. In fact, an optimal nucleus pulposus substitute should not degrade.

An amidic alginate based hydrogel with potential use as a nucleus prosthesis was tested.

1.3 Amidic alginate hydrogel

The amidation reaction was carried out as previously reported for carboxymethylcellulose polysaccharide [5].

Infrared analysis was performed to verify the amidation reaction. The IR spectrum of the amide modified alginate (AAA_lin) showed a new peak centered around $1650\,cm^{-1}$ relative to the amidic C=O stretching which was absent in the IR spectrum of the native AA.

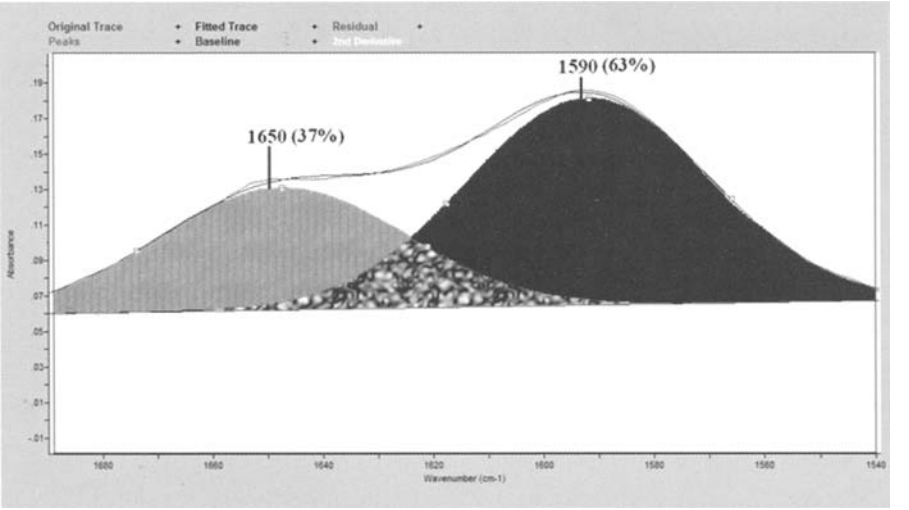

Fig. 7 Curve fitting of the 1700–1540 cm^{-1} ATR-FTIR spectrum region. The COO^- component represented about 63% whereas the C=O component reached about 37% (modified from [5])

The degree of amidation was estimated by Curve-fitting the 1700–1540 cm^{-1} ATR-FTIR spectrum region. The band at 1590 cm^{-1}, corresponding to COO^- stretching, and the band at 1650 cm^{-1}, ascribable to amidic CO vibrations, were found in the ratio (expressed in percentages) of 63 ± 3% (free COO^-) and 37 ± 3% (amidic C=O), respectively (Fig. 7) [5].

The hydration kinetics of AAA_cr were evaluated to determine the time necessary to reach swelling equilibrium. Overnight, the nucleus pulposus reabsorbs the fluids that it loses during daily activities [18]: a material that is able to recover the initial swelling after a short time is therefore advisable. The hydration kinetics of AAA_cr were monitored at 37 °C in a thermostated bath (humidity chamber). The hydrogel (AAA_cr) reached swelling equilibrium (8700) in 1 h.

The AAA hydrogel swelled up to 250% in volume, showing similar behavior to the nucleus pulposus, which is able to swell up to 200% [19].

Furthermore, the hydrogel (AAA_cr) showed thixotropic properties, i.e. it was able to become fluid under appropriate mechanical stimulus and, once the mechanical stimulus was removed, it resumed its original consistency as a hydrogel [20]. In fact, as shown in Fig. 8, once the stress value of 1270 Pa was reached, a gel-sol transition was observed. This stress made the AAA_cr hydrogel change its consistency, showing a G' (storage modulus) of lower than the G" (viscous modulus). Once mechanical stimulation was removed, the original hydrogel consistency was immediately regained, with G' becoming greater than G" once again. This property makes the hydrogel suitable for injection into the annulus fibrosus using a syringe. By pressing the piston with the adequate pressure, the gel-sol transformation was achieved. Once in situ, the fluid hydrogel resumed the consistency of a gel.

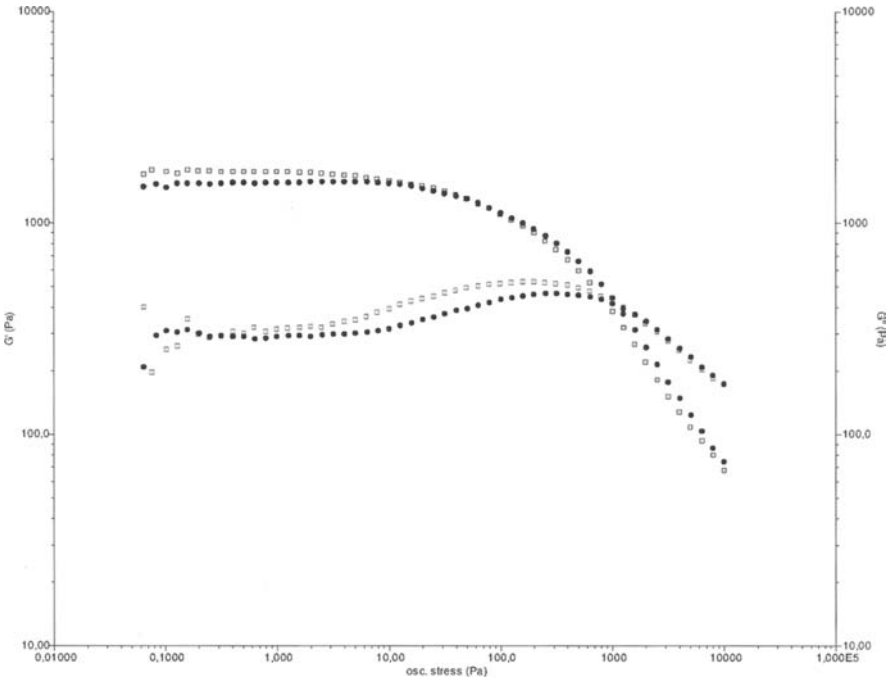

Fig. 8 Storage (G') and loss (G") moduli trend of the AAA hydrogel as functions of increasing (G' and G"), and decreasing stress (G'- and G"-) (n = 5) (modified from [5])

The rheological analysis of the AAA_cr was performed following the same protocol used to determine the characteristics of the human nucleus pulposus under shear, dynamic conditions [21]. The dynamic frequency sweep test showed that the magnitude of complex shear modulus increased with frequency over the range of 1 to 100 rad/sec, indicating that the material became stiffer with higher frequency. Consistently, both storage and loss moduli increased with angular frequency, with the value of G' always greater than G", showing the hydrogel to be predominantly elastic under dynamic conditions in the range of frequencies tested.The same behavior was found for non-degenerate nucleus pulposus. The influence of frequency on the phase shift angle δ values of the polysaccharide hydrogel was also evaluated. In Table 4, the $|G^*|$ and δ of the polysaccharide hydrogel as functions of the frequencies tested were reported. The dependence of δ on frequency was less pronounced with respect to $|G^*|$, not changing significantly over the range of frequencies tested. The sample exhibited predominantly elastic behavior during dynamic shearing, as demonstrated by the value of $\delta < 45\,^\circ$, reflecting a more solid-like, rather than fluid-like, behavior of crosslinked polysaccharides under dynamic conditions, as for the NP. The $|G^*|$ values of the AAA_cr hydrogel were very close to those found for the NP.

The values reported in Table 4 show that the nucleus pulposus became slightly more dissipative with frequency, whereas the AAA_cr hydrogel did not change its

Table 4 Dynamic material properties |G*| (kPa) of Human lumbar NP and AAA_cr hydrogel (mean ± S.D.). Angular frequency and dissipation energy (δ) (degree) of Human lumbar NP and AAA_cr hydrogel (mean ± S.D.) with angular frequency

	|G*| (ω=1rad/s)	|G*| (ω=10rad/s)	|G*| (ω=100rad/s)
NP[#]	7. 40±115.60kPa	11.30±17.90 kPa	19.80±31.40 kPa
AAA hydrogel	15.00±3.00 kPa	16.00 ±3.00 kPa	21.00±4.00 kPa
	δ(ω=1rad/s)	δ(ω=10rad/s)	δ(ω=100rad/s)
NP[#]	23±5 deg	24±5 deg	30±6 deg
AAA hydrogel	18.7±0.3 deg	19.7±0.6 deg	19.6±0.80 deg

[#]*Iatridis et al. J Biomechanics, 1997, 1005.*

dissipative behavior. It also showed a more pronounced elastic component with respect to the NP.

Stress-relaxation tests were performed to evaluate the time-dependent sensitivity to load or deformation of the hydrogel. The stress-relaxation test makes it possible to evaluate how a material changes under stress over time. The NP under imposed shear strain of $\gamma_0 = 0.10$ rad exhibited significant viscoelastic effects when subjected to shear stress relaxation experiments [14, 21]. In fact, the NP exhibited very rapid relaxation within the first second after loading, then it decayed more slowly for times greater than 1 sec [14]. The AAA hydrogel showed a trend similar to the NP when subjected to the same analysis. In fact, as shown in Fig. 9, both NP and the AAA_cr relaxed within the first second and showed similar peak stress (NP $\cong$ 0.46 kPa; AAA_cr: 0.63 kPa).

The bioactivity of the AAA_cr hydrogel was evaluated using human chondrocytes, since nucleus pulposus cells (i.e. notochordal cells) are chondrocyte-like [22]. The samples were incubated with NHAC and cell proliferation and metabolic activity were tested after 14 days. Chondrocytes proliferated on the AAA_cr hydrogel and maintained their phenotype, as demonstrated by cathepsin B values [23]. A significant increase in PG (i.e. aggrecan) production from chondrocytes seeded on AAA_cr with respect to cells seeded on CRT was also observed. This increase is very important for the role of the proteoglycan network in the nucleus pulposus. In fact, it is responsible for the considerable swelling of the nucleus (up to more than 200% of its initial volume) through its interaction with both collagen fibers and interstitial water. The PG network plays a major role in the static and dynamic mechanical properties of the intervertebral disc [24].

Furthermore, AAA_cr maintained chondrocyte production of type II collagen rather than type I collagen, which is an index of their dedifferentiation into fibroblast-like cells. Type II collagen, which gives structure and tensile strength to the nucleus pulposus, is principally degraded by Matrix Metalloprotease (MMP). A subgroup of MMPs, known as collagenases (MMP1, MMP8 and MMP13), are the most effective enzymes for initiating cleavage of native triple helical collagen that can be acted upon

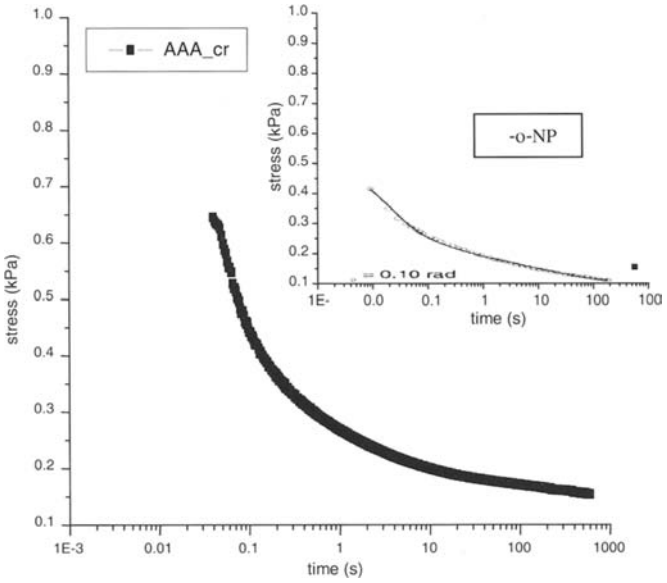

Fig. 9 Behavior of AAA_cr hydrogel (-■-) subjected to a ramp stress-relaxation experiment with an imposed shear strain of $\gamma_0 = 0.10$ rad ($n = 5$) compared to NP (-○-). For Nucleus pulposus trend data from [14] (modified from [5])

by other MMPs. Of these, MMP13 exhibits the highest activity towards degrading type II collagen [25]. Consequently, the production of MMP1 and MMP13 by chondrocytes seeded on AAA_cr was evaluated and compared with that of chondrocytes seeded on a PS dish (CRT). The values reported in Table 5 show that the chondrocytes seeded on AAA_cr hydrogel had a very low release of MMPs, as for CRT. Finally, the inflammatory action of the hydrogel was evaluated by monitoring the release of IL-6. After 14 days, no significant difference was found between IL-6 release found in the CTR and in the presence of AAA_cr (Table 5).

Table 5 Cytotoxicity and bioactivity of normal human chondrocytes (NHC) after 14 days

	control	Hyal	AAA
WST1 (OD450650nm)	1.16±0. 03	0.70±0.04	0.77±0.09
Cathepsin B(ng/mL)	4.28±0.54	2.06±0.09	2.72±0.34
MMP13 (pg/mL)	68.0±12.7	121.5±16.7	92.0±25.4
MMP1 (ng/mL)	1.33±0.70	1.88±0.30	0.85±0.09
Collagen II(ng/mL)	133.9±11.2	312.8±17.2	307.0±56.6
IL-6 (pg/mL)	3.64±0.20	4.40±0.76	4.40±0.59
Aggrecan (ng/mL)	731.8±83.4	1294.5±82.6	1255.2±117.4

From a rheological point of view, AAA_cr hydrogel displayed a behavior, in terms of complex modulus (|G*|) and phase shift angle (δ), strictly comparable with that of non-degenerated human nucleus pulposus. Finally, analysis of the behavior of the hydrogel towards chondrocytes showed that AAA_cr was able to perform a stimulating action. In fact, it ameliorated the synthetic activity of the ECM component, especially in terms of cathepsin B, aggrecan and type II collagen values. In conclusion, AAA_cr hydrogel appeared to be a good material as an NP substitute, due to its rheological characteristics and biological behavior.

1.4 Hydrogels for delivery of biologically active substances

Currently, there is great interest concerning controlled drug release systems. Several definitions for this have been given. One of the most exaustive is "a system that is capable of releasing a carried bioactive agent to a specific location at a specific rate". Thus, the main goal of controlled drug release systems is to facilitate the dosage and duration of the drug effect.

Polysaccharide hydrogels are able to respond to changes in the surrounding environment, such as temperature, pH or ionic strength modifications, by modifying their state (swollen/shrunken) and consequently, the amount of adsorbed water and the amount of drug dissolved and released.

1.4.1 Hydrogels as vehicles for bioactive substances for regeneration of bone tissue

The main requirements for a biomaterial to function properly in an osseous site include good biocompatibility and bioactivity (favoring of bone apposition), adequate mechanical properties, and the ability to assure skeletal function. These qualities are usually attributed to two key properties: ability to induce formation of an apatite layer on material surfaces in physiological conditions and ability to promote bone cell anchorage, attachment, spreading, growth and differentation [26]. Much effort has been made to find methods for improving the integration of polymeric biomaterials with natural hard tissues for orthopaedic applications such as bone replacement, repair and fixation [27]. The integration of biomimetic scaffolds into bone tissue takes place at the material-tissue interface and is often determined by initial cell and substrate interaction [28]. It is widely accepted that surface chemical structure exerts a significant influence over these two events [29]. Among the techniques available to turn polymeric biomaterials with limited or no tendency to mineralize into mineralizing ones, the most utilized is:

- formation of hydroxyapatite coating.

1.4.2 Guar gum based Hydrogel enriched with HA

Guar gum (GG), a hydrophylic, non-ionic polysaccharide extracted from the seed endosperm of the plant *Cyamopsis Tetragonalobus*, belonging to the wide family of

galactomannans and consisting of a (1 → 4) linked β-D-mannopyranosyl backbone partially substituted at O, linked at C6 with α-D-galactopyranosyl side groups, was crosslinked and the 3D matrix coated with nano-hydroxyapatite. The realized system was analyzed to evaluate how the nanocrystals affected its mechanical properties foreseeing its application in the bone field.

The GG was slowly dissolved in NaOH 0.1 M at a concentration of 1.6% w/v, using magnetic stirring. Prior to the addition of the crosslinking agent (poly-ethylene-glycol diglycidyl ether (CH_2OCH-$(CH_2CH_2O)_n$-$CHOCH_2$, $n = 10$, PEGDGE), the temperature of the mixture was brought up to 40 °C. The molar ratio of GG and PEGDGE used was 1:3 to obtain the best yield. The reaction was stirred for 15 h; at the end of the reaction, the product was dispersed in water and neutralized (pH=7) with acetic acid (96%). The hydrogel was washed with plenty of distilled water and freeze-dried. It was subsequently characterized in terms of swelling and rheological behavior [30].

The hydrogel was immersed in a nanocrystal hydroxyapatite suspension (1% in PBS) and a superficial coating of nanocrystals was observed (Fig. 10).

The effect of the nanocrystals on the rheological properties of the enriched hydrogel was analyzed. The presence of HA drastically increased the rheological properties of the hydrogel as shown in Table 6.

These very preliminary analyses were performed to evaluate the possibility of realizing a coating of nanoHA crystals on a polysaccharide hydrogel in order to enrich its biomineralizing properties and its mechanical behavior.

On the basis of these results, the developed system can be tested as a vehicle for growth factor (i.e BMP2) release in the osseous site.

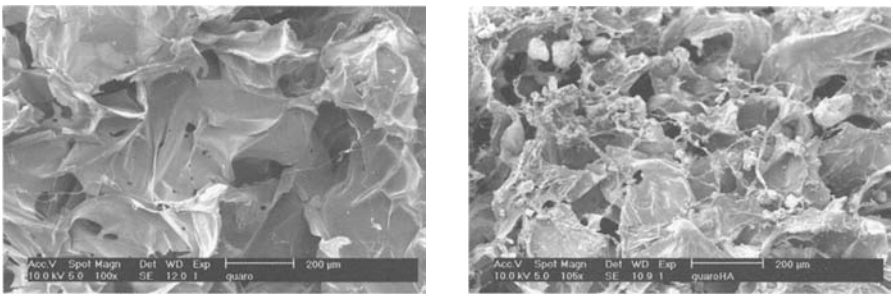

Fig. 10 SEM micrographs of native GG-hydrogel and GG-hydrogel coated with HA nanocrystals. A superficial coating was observed

Table 6 Dynamic material properties G' and G" with angular frequency of native GG-hydrogel and HA coated GG-hydrogel (Mean ± S.D.)

	G' (0.1-10Hz) Pa	G"(0.1-10Hz) Pa
$GUAR_{cr}$	5450–10100	~ 1600
$GUAR_{cr}$ + HA	1110–20500	3600–2800

2 Conclusions

This brief review on polysaccharide based hydrogels underlines the wide applicability of this class of polymers in the biomedical field. Polysaccharide chains have several functional groups, or potential reaction sites, which can be used to modify their chemical structure giving them not only new biological properties but also directing their physico-chemical properties widening their use in both tissue engineering and drug release.

Acknowledgements. Authors would like to thank Fondazione Monte dei Paschi di Siena and MIUR for financial support.

References

[1] Suh JKF, Matthew WTH (2000) Application of chitosan-based polysaccharide biomaterials in cartilage tissue engineering: a review. Biomaterials 21: 2589–2598

[2] Dahl LB, Dahl IM, Enstrom-Laurent A, Granath K. (1995) Concentration and molecular weight of sodium hyaluronate in synovial fluid from patients with rheumatoid arthritis and other arthropathies. Ann Rheum Dis 1985, 44:817–822

[3] Peyron JG, Balazs EA (1974) Preliminary clinical assessment of Nahyaluionate injection into human arthritic joint. Pathol Biol 22, 731–736

[4] Barbucci R, Leone G, Monici M, Pantalone D, Fini M, Giardino R (2005) The effect of amidic moieties on polysaccharides: evaluation of the physico-chemical and biological properties of amidic carboxymethylcellulose (CMCA) in the form of linear polymer and hydrogel. J Mater Chem 22:2234–2241

[5] Leone G, Torricelli P, Chiumiento A, Facchini A, Barbucci RJ (2008) Amidic alginate hydrogel for nucleus pulposus replacement. J Biomed Mater Res: part A 84:391–401

[6] Park H, Temenoff JS, Tabata Y, Caplan AI, Mikos AG (2007). Injectable biodegrdable hydrogel composites for rabbit marrow mesenchymal stem cell and growth factor delivery for cartilage tissue engineering. Biomaterials 28:3217–3227

[7] Lee CSD, Gleghorn NW, Choin NW, Cabodi M, Strook AD, Bonassar LJ (2007). Integration of layered chondrocytes-seeded alginate hydrogel scaffold. Biomaterials 28:2987–2993

[8] Leone G, Delfini M, Di Cocco ME, Borioni A, Barbucci R (2008) The applicability of an amidated polysaccharide hydrogel as a cartilage substitute: structural and rheological characterization. Carbohydr Res 343:317–327

[9] Barbucci R, Leone G, Chiumiento A, Di Cocco ME, D'Orazio G, Gianferri G, Delfini M (2006) Low and high resolution Nuclear Magnetic Resonance (NMR) characterisation of hyaluronan-based native and sulphated hydrogels. Carbohydr Res 341:1848–1858

[10] Zhang LM, Kong T (2006) Aqueous polysaccharide blends based on hydoxypropyl guar gum and carboxymethyl cellulose: synergistic viscosity and thixotropic properties. Colloid Polym Sci 285:145–151

[11] Barbucci R, Lamponi S, Borzacchiello A, Ambrosio L, Fini M, Torricelli P, Giardino R (2002) Hyaluronic acid hydrogel in the treatment of osteoarthritis. Biomaterials 23:4503–4513

[12] Barbucci R, Fini M, Giavaresi G, Torricelli P, Giardino R, Lamponi S, Leone G (2005) Hyaluronic acid hydrogel added with ibuprofen-lysine for the local treatment of chondral

lesions in the knee. In vitro and in vivo investigations. J Biomed Mater Res part B Appl Biomater 75B:42–48
[13] Leone G, Fini M, Torricelli P, Giardino R, Barbucci R. An amidated carboxymethylcellulose hydrogel for cartilage regeneration. J Mater Sci: Mater Med 19:2873–2880
[14] Iatridis JC, Weidenbaum M, Setton LA, Mow VC (1996) Is the nucleus pulposus a solid or a fluid? Mechanical behaviours of the nucleus pulposus of the human intervertebral disc. Spine 21:1174–1184
[15] Ayad S, Weiss JB (1987) Biochemistry of the intervertebral disc. In: Jayson MIV (ed), The Lumbar Spine and Back Pain. 3rd ed. New York: Churchill-Livingstone pp 100–137
[16] Zhong SP, Campoccia D, Doherty PJ, Williams RL, Benedetti L, Williams DF (1994) Biodegradation of hyaluronic acid derivatives by hyaluronidase. Biomaterials 15:359–365
[17] Barbucci R, Lamponi S, Borzacchiello A, Ambrosio L, Fini M, Torricelli P, Giardino R (2002) Hyaluronic acid hydrogel in the treatment of osteoarthritis. Biomaterials 23:4503–4513
[18] Hendry NGC (1958) The hydration of the nucleus pulposus and its realtion to intervertebral disc derangement. J Bone Joint Surg 40:132–144
[19] Wilke HJ, Neef P, Hinz B, Seidel H, Claes L (2001) Intradiscal pressure together with anthropometric data-a data set for he validation of models. Clinical Biomechancis 16:S111–S126
[20] Barbucci R, Leone G, Lamponi S (2006) Thixotropy property of hydrogels to evaluate the cell growing on the inside of the material bulk (Amber Effect). J Biomed Mater Res part B Appl Biomater 76B:33–40
[21] Iatridis JC, Setton LA, Weidenbaum M, Mow VC (1997) The viscoelastic behaviour of the non-degeneerate human lumbar nucleus pulposus in shear. J Biomechanics 30:1005–1013
[22] Mwale F, Roughley P, Antoniou J (2004) Distinction between the extracellular matrix of the nucleus pulposus and the hyaline cartilage: a requisite for tissue enigineering of intervertebral disc. European Cells and Materials 8:58–64
[23] Poiraudeau S, Monteiro I, Anract P, Blanchard O, Revel M, Corvol MT (1999) Phenotypic characteristics of rabbit intervertebral disc cells – Comparison with cartilage cells from the same animals. Spine 24:837–844
[24] Antoniou J, Steffen T, Nelson F, Winterbottom N, Hollander AP, Poole RA, Aebi M, Alini M. (1996) The human lumbar intervertebral disc: evidence for changes in the biosynthesis and denaturation of the extracellular matrix with growth, maturation, ageing and degeneration. J Clin Invest 98:996–1003
[25] Kanemoto M, Hukuda S, Komiya Y, Katsuura A, Nishioka J. (1996) Immunohistochemcial study of matrix metallo-proteinase-3 and tissue inhibitor of metalloproteinase-1 human intervertebral disc. Spine 21:1–8
[26] Ambrosio L, Netti PA, Revell PA (2002) Hard tissue pag 342. In: Barbucci (ed), Integrated Biomaterials Science. New York: Kluwer Academic
[27] Vacanti JP, Langer R (1999) Tissue engineering: the design and fabrication of living replacement devices for surgical reconstruction and transplantation. Lancet 354:32–34
[28] Puleo DA, Nanci A (1999) Understanding and controlling the bone-implant interface. Biomaterials 20:2311–2321
[29] Dalton BA, Mcfarland CD, Gengenbach TR, Griesser HJ, Steele JG (1998) Polymer surface chemistry and bone cell migration. J bioamter Sci Polym Ed 9:781–799
[30] Barbucci R, Pasqui D, Favaloro R, Panariello G (2008) A thixotropic hydrogel from chemically cross-linked guar gum: synthesis, characterisation and rheological behaviour. doi: 10.1016/j.carres.2008.08.029

Hydrogels for Healing

Buddy D. Ratner and Sarah Atzet

Abstract. Hydrogels are widely used in medicine and offer advantages in many implant situations. However, the body responds to them as with any other material – by walling them off in a foreign body capsule. We show here that by making hydrogels with uniform, interconnected spherical pores of about 35 microns, the healing reaction can be shifted to one of vascularization and little fibrosis. We have also developed a biodegradable form of poly(2-hydroxyethyl methacrylate) that can be used to fabricate these pro-healing, spherically pored materials.

1 Introduction

Hydrogels specifically designed for medical applications have roots which trace back to the 1960 paper by Lim and Wichterle describing crosslinked poly(2-hydroxyethyl methacrylate) (pHEMA) materials [1]. Since that seminal publication, pHEMA and other hydrogels have seen wide application in medicine as ophthalmologic devices, coatings and for other types of implants.

A general concern with hydrogels, and for that matter, with most all "biocompatible" implants, is that upon implantation they heal into a dense, avascular, collagenous bag. This healing process, generally referred to as the foreign body reaction (FBR), occurs over a period of about three weeks [2]. It is schematically illustrated in Fig. 1. Fig. 2 shows a Masson's trichrome stained histological specimen of a sheet of pHEMA that was implanted subcutaneously in a mouse for 28 days. The collagen capsule, as highlighted by the blue color from the trichrome stain (this region of the image is labeled as "collagen capsule" in the black and white image shown), totally isolates the implant from the body. This reaction is accepted by most medical device regulatory agencies as appropriate for a biocompatible implant if it is essentially complete by one month with a relatively thin capsule. However, this avascular, dense capsule electrically isolates electrodes, impedes drug delivery from controlled release devices, prevents diffusion of analytes to biosensors and generally adversely impacts many implants such as pacemakers, breast implants, heart valves, etc. There would be many advantages to achieving a less fibrotic, more vascularized healing of implanted devices.

Barbucci R. (Ed): Hydrogels. Biological Properties and Applications.

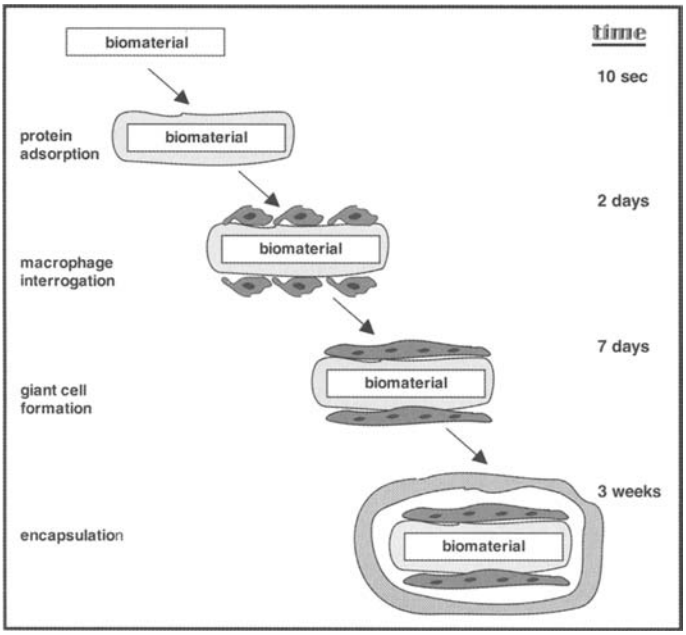

Fig. 1 A schematic diagram of the foreign body reaction (FBR) upon implantation

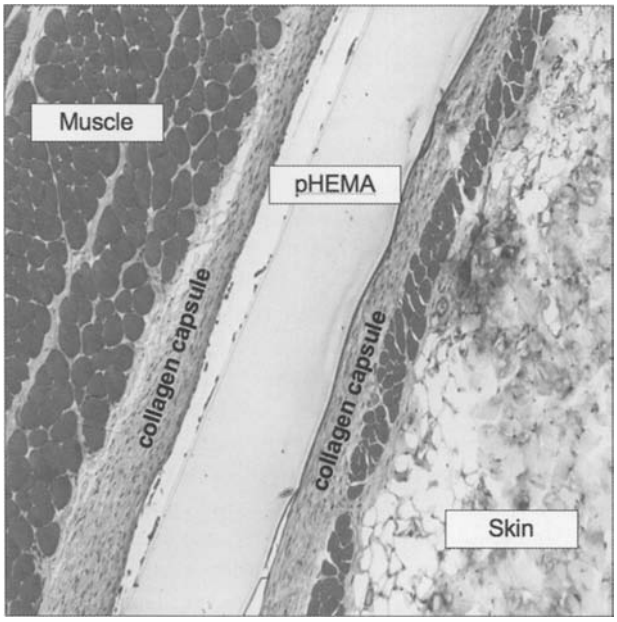

Fig. 2 A histological image of the FBR 1 month after implantation in a mouse

This paper focuses on a new hydrogel material that is an important component of a strategy for changing the course of healing and integration of material in medicine. The healing strategy involves sphere-templated polymers. Many types of polymers can be used to make these sphere templated materials. We describe here a methacrylate-based hydrogel polymer with good mechanical properties and biodegradability [3].

2 Sphere templated polymers

It has long been reported that rough or porous materials exhibit a different healing response in soft tissue from the same material in smooth or solid form. Typically, the *in vivo* response observed with rough or porous materials is less fibrotic and more vascularized [4–8]. However, all materials that have been used to explore this phenomenon have had a broad distribution of pore sizes. If we were to ask which pore size gives optimal healing, we could not discern this because of the impact on the outcome of "incorrect" pore sizes. For this reason we developed a sphere-templating method to create materials with only one pore size with all pores interconnected in three dimensions. We call his method 6S (sieve, shake, sinter, surround, solidify and solubilize) and it is illustrated schematically in Fig. 3. The 6S method, using commercially available poly(methyl methacrylate)(PMMA) microspheres, produces a porous structure with interconnected pores of a similar size (±5 %). The diameter of the interconnects can be adjusted by varying the sintering time. We have fabricated 6S materials from hydrogels, silicone elastomer and fibrin. A pHEMA 6S material is illustrated in Fig. 4.

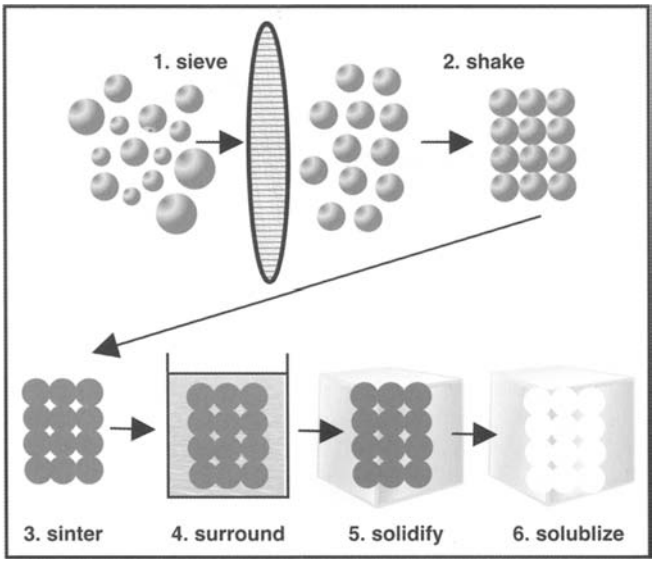

Fig. 3 The "6S" process to make sphere-templated polymers

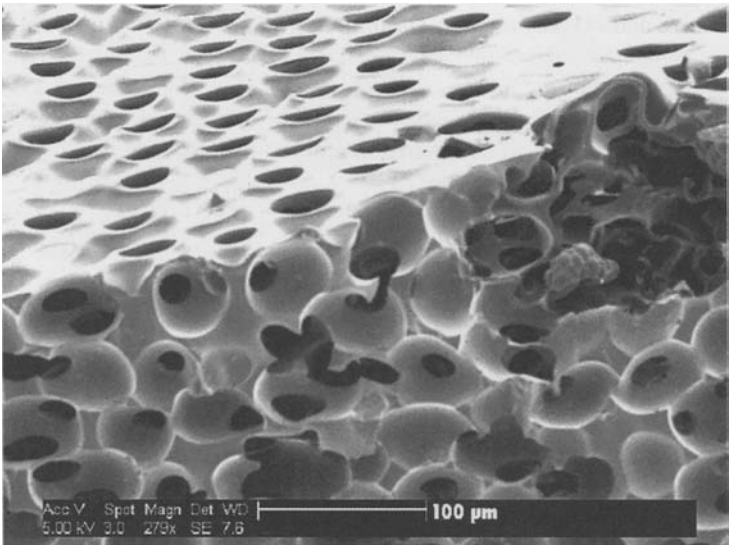

Fig. 4 A scanning electron micrograph image of a sphere-templated pHEMA hydrogel

6S scaffolds with pore sizes around 35 µm (±10 µm) have been found to heal in subcutaneous sites with extensive vascularization surrounding the implant and within the pore structure [9], and also with only a thin fibrous capsule of low collagen density. 6S materials will heal percutaneously with a reconstruction of both the epidermis and the dermis [10]. Other experiments have shown vascularized, non-fibrotic healing in heart muscle and in sclera. Good healing in skin has been seen with both pHEMA and silicone elastomers, essentially independently of the type of material.

3 A biodegradable pHEMA hydrogel

The unique, integrative healing of 6S materials has spurred the development of a biodegradable hydrogel polymer that is compatible with the 6S process. One of the primary criteria for compatibility is that the polymerization solvent must not dissolve the uncrosslinked PMMA microspheres prematurely (many solvents dissolve PMMA). The pHEMA gels originally explored for 6S scaffold manufacture, though showing good healing and integration, are highly biostable. In this section we show a macromolecular-engineering approach to create a biodegradable pHEMA gel.

There have been a number of published studies to create biodegradable pHEMA materials [11–15]. These studies have been predominantly *in vitro*, and have not addressed the ultimate clearance of biostable pHEMA degradation fragments. The specific design criteria for our biodegradable hydrogels are outlined in the next paragraph.

The rationale for this synthesis is discussed here. We address the following significant deficiencies with the majority of the scaffolds now being used for tissue engineering: (1) they break down to acidic products, (2) they are hydrophobic, (3) they

are hard to derivatize and (4) they are non-elastomeric. We start with the non-acidic HEMA monomer used to form the widely accepted hydrogel, pHEMA. Biodegradable crosslink units based on low molecular weight polycaprolactone (PCl) (a dimethacrylated PCl, DMAPCl) were synthesized, allowing the preparation of a crosslinked HEMA-PCl gel that can be formed in an ethylene glycol-dimethyl formamide solvent system (a solvent system that will not dissolve the PMMA microspheres). By hydrolyzing the PCl units, the gel breaks down to non-toxic pHEMA fragments. However, pHEMA is insoluble in water when its molecular weight is above 8–10 kDa. Also, renal clearance requires polymers of relatively low molecular weight. Since degraded fragments must be cleared through solubility mechanisms, we chose to keep all pHEMA segments at approximately 5 kDa. Atomic radical transfer polymerization (ATRP) permits us to synthesize low molecular weight pHEMA fragments that have very low molecular weight polydispersity [16]. Using, HEMA monomer, DMAPCl crosslinker and ATRP initiation, a biodegradable polymer was formed where the degradation products were pHEMA fragments of 5 kDa molecular weight and a small amount of caproic acid (the degradation product of PCl). However, the mechanical properties of this gel were poor. pHEMA chains of 5 kDa molecular weight incorporated into a crosslinked network simply did not exhibit classical macromolecular behavior. We postulated that longer backbone chains were needed. To obtain these, a difunctional ATRP initiator incorporating a PCl oligomeric segment was synthesized and used to initiate the polymerization of the HEMA monomer. Thus, a polymer was created with 10 kDa MW backbone segments (with PCl units in the center of these segments), and DMAPCl crosslinks. This polymer was hydrophilic, had good mechanical properties and offered possibilities to tune the degradation rate.

The synthesis of this pHEMA biodegradable gel is illustrated schematically in Fig. 5. The ATRP macroinitiator for the synthesis of 10 kDa units with a PCl oligo unit at the center of the molecule is shown in Fig. 6.

This biodegradable pHEMA was found to degrade slowly (next section). To tune the degradation rate, poly(ethylene glycol)(PEG) segments have been incorporated within the polymer structure to increase hydrophilicity. Also, poly(lactic acid)(PLA) segments have been introduced. The increased hydrophilicity from the PEG segments accelerates water penetration and therefore hydrolysis. The PLA segments hydrolytically degrade faster than the PCl segments.

4 Degradation studies

The degradation of the biodegradable pHEMA was studied five different ways: (1) by complete, rapid solubilization in basic solution, (2) by swelling studies, (3) by mass loss studies, (4) by mechanical property measurements, and (5) by animal implant studies with histological examination. Agents used to study in vitro degradation include lipase solutions and phosphate buffered saline.

When the biodegradable pHEMA is placed in a basic solution, rapid dissolution occurs yielding a clear solution. Gel permeation chromatography can be used to analyze breakdown products from this hydrolysis. Fig. 7 demonstrates that the un-

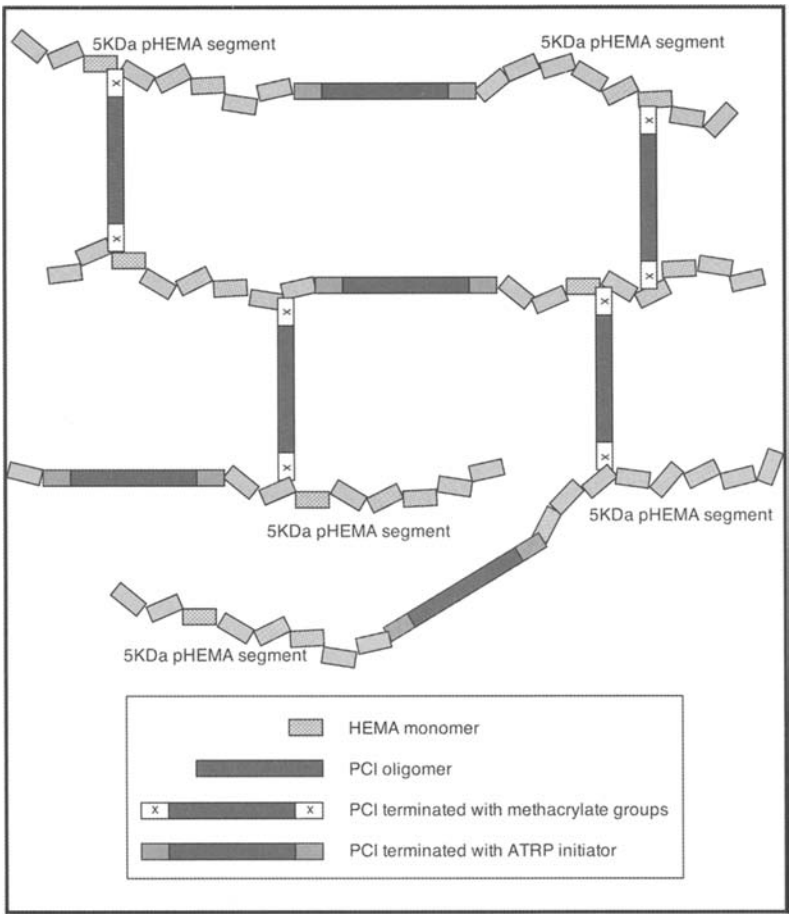

Fig. 5 A schematic representation of the biodegradable pHEMA gel. Note that 5KDa pHEMA oligomers will actually have about 34 monomer units

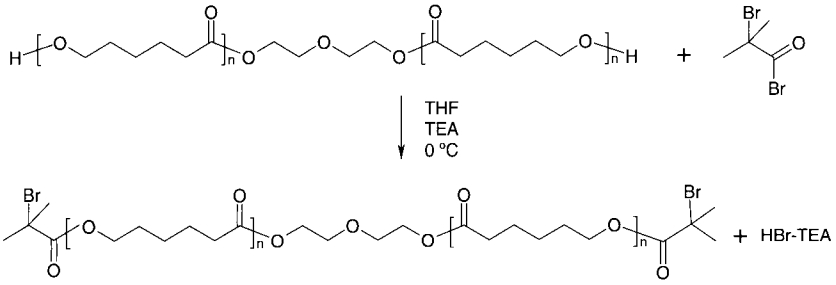

Fig. 6 PCL diol (Mw = 530) end-capped with bromoisobutyrl bromide to produce a difunctional macroinitiator

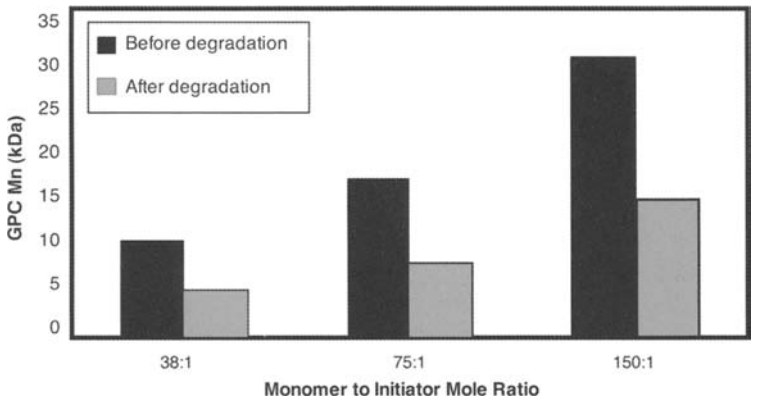

Fig. 7 pHEMA polymers made with the difunctional ATRP initiator break down to one half of their initial molecular weight upon exposure to 1N NaOH

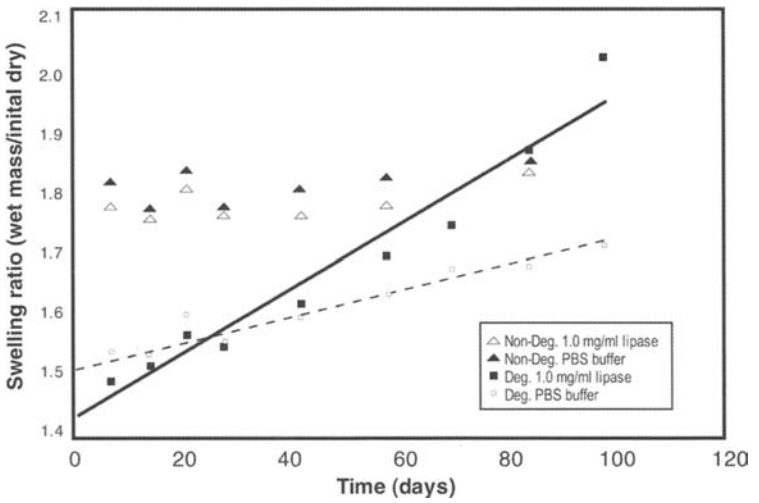

Fig. 8 Degradation of pHEMA gels as measured by increased swelling in PBS buffer and in lipase solution. Non-degradable hydrogels show no significant change in swelling with time in PBS or lipase while PCl-containing pHEMA hydrogels show increased swelling with time (indicative of degradation) in both PBS and lipase

crosslinked pHEMA units made with the ATRP initiator shown in Fig. 6 break down to segments that are one half the original molecular weight, consistent with the idea that small PCl blocks are integrated in a central location in each pHEMA chain.

Swelling studies showed expected increases in water content with time as crosslinks cleave. Amano Lipase PS, an esterase, at concentrations of 1.0 mg/ml and 0.5 mg/ml led to increases in swelling of the crosslinked network over time. Swelling data for buffer soaking and 1.0 mg/ml lipase are shown in Fig. 8.

Mass loss studies (not presented here) were consistent with the data in Fig. 8. Other degradation studies (not presented here) show that addition of poly(ethylene glycol) segments to the backbone chain, or addition of poly(lactic acid) segments can accelerate degradation over the rates suggested in Fig. 8. This polymer engineering permits "tuning" of degradation rates so that degradation profiles can match tissue reconstruction in tissue engineering scaffolds.

Toxicology studies have been completed. Using an MTT [(3-(4,5-dimethylthiazole-2-yl)-2,5-diphenyltetrazolium bromide)] test, the soluble, fully degraded pHEMA gel showed no appreciable toxicity when added to fibroblast cells at 5, 10 and 15 mg/ml. A latex positive control and tissue culture plastic negative control showed the expected low and high MTT colorimetric readings, respectively.

Finally, the first *in vivo* implants of 35 μm pore, sphere-templated (6S), biodegradable hydrogels in mice have been completed. Implant results from histological examination for the degradable gel are comparable to non-degradable pHEMA gels, i.e., much angiogenesis and little fibrosis. At six weeks, clear evidence of breakdown of the biodegradable gel (but not the biostable gel) is noted.

5 Conclusions

Tissue engineering that leads to accurate reconstruction of functional, living tissues and organs demands scaffolds that are engineered to meet precise requirements. These demands include the ability to stimulate angiogenesis, degradation at an appropriate rate to non-toxic products, easy fabrication to complex shapes and mechanics that match the target tissue. Other desirable qualities that are exhibited by scaffolds include the ability to immobilize bioactive molecules, the possibility to load diffusible molecules within the scaffold and component chemicals that are recognized as safe by regulatory agencies. The degradable pHEMA polymers described here meet these requirements. Coupled with sphere-templating (6S) technology, a new generation of tissue engineering scaffolds will evolve that actively stimulate reconstructive healing and then dissolve away.

Acknowledgment. This work was supported by the National Institutes of Health (Grant No. HL64387).

References

[1] Wichterle O, Lim D (1960) Hydrophilic gels for biological use. Nature 185:117–118

[2] Anderson JM, Rodriguez A, Chang DT (2008) Foreign body reaction to biomaterials. Seminars in Immunology 20:86–100

[3] Atzet S, Curtin S, Trinh P, Bryant S, Ratner B (2008) Degradable poly(2-hydroxyethyl methacrylate)-co-polycaprolactone hydrogels for tissue engineering scaffolds. Biomacromolecules, doi: 10.1021/bm800686h

[4] Brand KG, Buoen LC, Johnson KH, Brand I (1975) Etiological factors, stages and the role of the foreign body in foreign body tumorigenesis: a review. Cancer Res 35:279–286

[5] Picha GJ, Siedlak DJ (1984) Ion-beam microtexturing of biomaterials. MD & DI 6(4): 39–42
[6] Clowes AW, Kirkman TR, Reidy MA (1986) Mechanisms of arterial graft healing – rapid transmural capillary ingrowth provides a source of intimal endothelium and smooth muscle in porous PTFE prostheses. Am J Path 123(2):220–230
[7] Brauker JH, Carr-Brendel VE, Martinson LA, Crudele J, Johnston WD, Johnson RC (1995) Neovascularization of synthetic membranes directed by membrane microarchitecture. J Biomed Mater Res 29:1517–1524
[8] Sharkawy AA, Klitzman B, Truskey GA, Reichert WM (1997) Engineering the tissue which encapsulates subcutaneous implants. I. diffusion properties. J Biomed Mater Res 37:401–412
[9] Marshall AJ, Irvin CA, Barker T, Sage EH, Hauch KD, Ratner BD (2004) Biomaterials with tightly controlled pore size that promote vascular in-growth. ACS Polymer Preprints 45(2):100–101
[10] Isenhath SN, Fukano Y, Usui ML, Underwood RA, Irvin CA, Marshall AJ, Hauch KD, Ratner BD, Fleckman P, Olerud JE (2007) A mouse model to evaluate the interface between skin and a percutaneous device. J Biomed Mater Research A 83:915–922
[11] Khelfallah NS, Decher G, Mesini PJ (2007) Design, synthesis, and degradation studies of new enzymatically erodible poly(hydroxyethyl methacrylate)/poly(ethylene oxide) hydrogels. Biointerphases 2(4):131–135
[12] Bölgen N, Yang Y, Korkusuz P, Güzel E, El Haj AJ, Piskin E (2008) Three-dimensional ingrowth of bone cells within biodegradable cryogel scaffolds in bioreactors at different regimes. Tissue Engineering A 14:1743–1750
[13] Van Thienen TG, Lucas B, Flesch FM, van Nostrum CF, Demeester J, De Smedt SC (2005) On the synthesis and characterization of biodegradable dextran nanogels with tunable degradation properties. Macromolecules 38(20):8503–8511
[14] Lim DW, Choi SH, Park TG (2000) A new class of biodegradable hydrogels stereocomplexed by enantiomeric oligo (lactide) side chains of poly(HEMA-g-OLA)s. Macromol Rapid Commun 21:464–471
[15] He B, Wan E, Chan-Park MB (2006) Synthesis and Degradation of Biodegradable Photo-Cross-Linked Poly (a,ß-malic acid)-Based Hydrogel. Chem. Mater 18:3946–3955
[16] Matyjaszewski K, Xia J (2001) Atom transfer radical polymerization. Chem Rev 101(9):2921–2990

Stereocomplexed PEG-PLA Hydrogels

Christine Hiemstra, Zhiyuan Zhong, Pieter J. Dijkstra and Jan Feijen

Abstract. In this paper we give an overview of our studies on stereocomplexed hydrogels upon mixing aqueous solutions of enantiomeric linear poly(ethylene glycol)-poly(L-lactide) triblock (PEG-PLA) copolymers and eight-arm (PEG-PLA) star block copolymers and methacrylate functionalized PEG-PLA star block copolymers [1–3]. Stereocomplexation and photopolymerization were combined and enhanced the stability of the hydrogels. For all polymers, the critical gel concentrations of the mixed enantiomer solutions were considerably lower compared to polymer solutions containing only the single enantiomer. The gel-sol transition temperatures were increased and gel regions were expanded due to stereocomplexation.

1 Introduction

Hydrogels are water-swollen, insoluble networks of crosslinked hydrophilic polymers. Due to their similarity with the extracellular matrix, hydrogels have been investigated for use in biology and medicine since Wichterle and Lim discovered them in the early 1960s [4]. They are important materials for biomedical applications [5], such as drug delivery [6–8] and tissue engineering [9–11]. Many hydrogels were found to be biocompatible with strongly reduced protein interaction, and their soft and rubbery nature minimizes damage to surrounding tissue [12]. The mechanical properties of hydrogels parallel those of soft tissue, such as cartilage, making them especially suitable for engineering of these tissues.

Recently, in situ forming hydrogels have been prepared for biomedical applications. In situ forming hydrogels are preferred over preformed hydrogels, since in situ formation allows homogeneous mixing of e.g. cells and proteins with the polymer solutions prior to gelation. Moreover, in situ formation allows for preparation of complex shapes and applications using minimally invasive surgery.

Hydrogels can be classified in several ways. According to their composition, they can be classified into synthetic, natural or hybrid hydrogels. According to the crosslinking mechanism, hydrogels can be classified into chemically and physically crosslinked hydrogels. In chemical crosslinking covalent bonds are formed, while in physical crosslinking non-covalent interactions, such as hydrophobic and ionic interactions, are established. Furthermore, hydrogels can be classified into in situ forming

Barbucci R. (Ed): Hydrogels. Biological Properties and Applications.

or preformed hydrogels. In situ forming hydrogels form in the body after injection of the precursors, in contrast to preformed hydrogels that have to be implanted by surgery.

2 Hydrogels

2.1 General requirements

Materials used for biomedical applications should be biocompatible. The materials should not elicit an unresolved inflammatory reaction and should not demonstrate immunogenicity or cytotoxicity. In addition, this must be true for any unreacted compounds or additives and in the case of biodegradable materials, also for their degradation products.

It is important that hydrogels can degrade in the body, in order to avoid subsequent surgery to remove the implant after it has performed its function. The degradation products should be either metabolized or excreted by the kidneys. Excretion of such products is limited to a certain size. For instance, the cut-off molecular weight of globular proteins is approximately 60,000. In particular, for tissue engineering applications the progressive loss of mechanical strength of the material simulates the healing process of the tissues.

The best known synthetic, degradable polymers are the poly(hydroxy acid)s, including poly(glycolide) (PGA), poly(lactide) (PLA), poly(glycolide-*co*-lactide) (PLGA) and poly(ε-caprolactone) (PCL). These polymers degrade via hydrolytic cleavage of their ester bonds, finally resulting in the corresponding hydroxy acids as non-toxic degradation products.

2.2 Synthetic polymers used for hydrogel preparation

Synthetic hydrogels can be tailored to have a wide range of mechanical and chemical properties. However, cell-material interactions and biocompatibility may be an issue and have to be taken into account in the development of these hydrogels. The most commonly used synthetic hydrogels are based on poly(ethylene glycol) (PEG) [13, 14]. Due to its high hydrophilicity, PEG shows hardly any interaction with proteins and can be excreted through the kidneys up to molecular weights of approximately 30,000. Amphiphilic block copolymers, consisting of hydrophilic PEG blocks and hydrophobic blocks have been widely applied for the preparation of hydrogels (Fig. 1). PLA and PLGA have been mostly used as the hydrophobic blocks. Other hydrophobic blocks include PCL and poly(D,L-3-methylglycolide) (PMG). These amphiphilic block copolymers self-assemble in water due to hydrophobic interactions and may form physically crosslinked hydrogels. PEG has also been derivatized with polymerizable (meth)acrylate groups for the formation of hydrogels by photoirradiation or redox initiation.

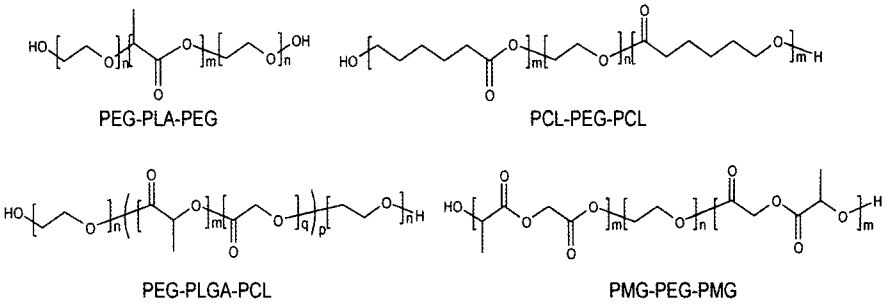

Fig. 1 Examples of PEG- poly(hydroxy acid) block copolymers used for hydrogel preparation

2.3 In situ forming hydrogels

In situ forming hydrogels are those that can form in the body, i.e. under (near) physiological conditions, wherein the gel precursors should be non-toxic and the gelation reaction should not cause any toxicity or substantial temperature rise. In the past few years an increasing number of in situ forming hydrogels have been reported in literature. These hydrogels offer several advantages over preformed hydrogels, which are shaped into their final form before implantation. The precursors of in situ forming hydrogels are injectable fluids that can be introduced into the body in a minimally invasive manner prior to gelation within the desired tissue, organ or body cavity. Their flowing nature ensures a good fit and contact with surrounding tissue. Since hydrogels are fluid prior to gelation, bioactive components, such as cells, proteins and drugs, can be easily mixed with the polymer solutions, ensuring high loading and homogeneous distribution. The gelation should occur within a few minutes to prevent leakage of the gelling solution to the surrounding tissue and to minimize the length of the procedure, while on the other hand allowing surgeons ample time for placement before hardening.

In situ hydrogels have been formed by physical or chemical crosslinking methods. Since the conditions for physical crosslinking are generally mild, most physically crosslinked hydrogels can be formed in situ. For the in situ formation of chemically crosslinked hydrogels often a compromise needs to be found between fast gelation (i.e. crosslinking reaction rate) and reaction conditions (such as temperature and pH). For instance, photopolymerization, which is a common method for in situ preparation of chemically crosslinked hydrogels, can give rise to substantial heat effects due to the polymerization exotherm. Furthermore, toxicity may be an issue in chemical crosslinking, since the gel precursors have reactive groups and often auxiliary compounds such as initiators, co-crosslinkers and organic solvents are needed.

2.4 Physical crosslinking

Physical crosslinking offers the advantage that the crosslinking conditions are generally mild compared to chemical crosslinking, since no reactive groups, crosslinking

agents, (photo)initiators or photoirradiation are needed. These mild crosslinking conditions allow for in situ hydrogel formation and entrapment of labile compounds, such as proteins. Moreover, many physical interactions are reversible, allowing for repeated gelation and sol formation. In general however, physical hydrogels are mechanically weak compared to chemically crosslinked hydrogels and changes in the external environment (e.g. ionic strength, pH, temperature) may give rise to disruption of the hydrogel network.

2.5 Thermosensitive hydrogels

Physically crosslinked hydrogels have been prepared by a variety of non-covalent interactions. Most commonly, hydrogels have been formed by self-assembly of thermosensitive polymers. The hydrophobicity of these polymers increases upon increasing the temperature to around body temperature, causing decreased hydrogen bonding with the surrounding water and increased hydrophobic interactions. Subsequently, the polymers self-assemble and form physical crosslinks. Water-soluble, amphiphilic block copolymers with both hydrophobic and hydrophilic blocks represent an important class of thermosensitive polymers [15, 16]. In these hydrogels the crosslinks are formed by the hydrophobic blocks. The proposed self-assembly mechanisms of amphiphilic block copolymers with outer hydrophilic blocks like PEG-PLGA-PEG or outer hydrophobic blocks like PCL-PEG-PCL [17] however are different. The gelation for PEG-PLGA-PEG copolymers is thought to be due to self-assembly into closely packed micelles, while the gelation of PCL-PEG-PCL copolymers is thought to be due to self-assembly of micelle aggregates that are bridged by polymers having both hydrophobic ends in different micelles. Other well-known thermosensitive hydrogels are those based on PNIPAAm and its copolymers, which have an LCST around body temperature [17–19]. More recently, thermosensitive hydrogels based on elastin-like peptides [20], hydroxybutyl chitosan [21], PEG-grafted chitosan [22], mixtures of chitosan with anionic polyol salts [23] and poly(organophosphazenes) bearing thermosensitive side groups [24, 25] have been reported. Thermosensitive hydrogels are generally rapidly formed upon temperature increase and have been applied as in situ forming hydrogels.

2.6 Stereocomplexation

Stereocomplexation refers to co-crystallization of poly(L-lactide) (PLLA) and poly(D-lactide) (PDLA). Recently, this type of physical interaction has been used for in situ hydrogel formation. It is well-known that blending of PLLA and PDLA results in the formation of stereocomplex crystals, having a melting temperature of approximately 230 °C, which is 50 °C above the melting temperature of homocrystallites of non-blended PLLA or PDLA [26]. The PLLA and PDLA chains in a stereocomplex crystal are packed side-by-side [27]. The higher melting point of the stereocomplex crystals is ascribed to a denser packing of the PLLA and PDLA helices as compared to the packing of the single enantiomer helices. PLLA forms a left-handed helix and PDLA forms a right-handed helix. The van der Waals forces between opposite oxygen

atoms and hydrogen atoms of the two helices are suggested to be the driving force for the dense packing of the helices in the stereocomplex [28].

Stereocomplexation offers an attractive crosslinking method for in situ hydrogel formation using water-soluble PLLA and PDLA block copolymers. Since stereocomplex formation takes place at shorter block lengths than for homocrystallization, an operation window exists in which mixing of aqueous solutions of these block copolymers results in hydrogel formation through stereocomplexation. De Jong et al. formed hydrogels by stereocomplexation of dextran grafted with monodisperse L-lactic acid and D-lactic acid oligomers. At least 11 lactyl units were required to form stereocomplex crystals [29].

Li et al. [30] prepared stereocomplexed PLA-PEG-PLA triblock copolymer hydrogels and showed that bovine serum albumin (BSA) can be released from these hydrogels over a prolonged period of time without denaturation (up to 15 days).

2.7 Chemical crosslinking by photopolymerization

Chemically crosslinked hydrogels have been mostly prepared via photopolymerization [31], in particular by UV-irradiation of (meth)acrylate functionalized PEG [32]. Photopolymerization offers the advantage of spatial and temporal control, polymerization takes place where and when the polymer is exposed to the light. The main disadvantage is that its *in vivo* application, i.e. transdermal photopolymerization, is hampered by the absorption of UV-light by the skin (> 99%) [33]. Visible light is less attenuated by the skin, but more efficient and cytocompatible initiators are needed. Another drawback of photopolymerization is that the energy of the polymerizing light, the heat and the radical species produced during the polymerization and the toxicity of the photoinitiators and monomers may damage the surrounding tissue and/or the entrapped molecules [34].

Hubbell et al. were the first to report on photopolymerized, hydrolytically degradable PEG-PLA diacrylate hydrogels [35]. Anseth et al. reported on biodegradable PEG-PLA dimethacrylate hydrogels. It was shown that by using combinations of PEG and PEG-PLA dimethacrylates and/or by changing the PLA block length, the hydrogel degradation rate, compressive modulus and crosslinking density could be tuned to provide suitable scaffolds for cartilage tissue engineering [36]. Though photopolymerization has been proposed for in situ hydrogel formation by transdermal photoirradiation, photopolymerized hydrogels have mostly been preformed and subsequently implanted. Currently, there are still problems with efficient in situ formation of hydrogels by photopolymerization *in vivo* due to UV absorption by the skin. Elisseeff et al. have formed hydrogels by transdermal irradiation of an aqueous PEG methacrylate solution with UV-light, which were successfully applied for the generation of cartilage in nude mice [37].

2.8 Synthesis

Along with earlier work, this work has shown that a convenient way to prepare PEG-PLA block copolymers is the $Sn(Oct)_2$ catalyzed ring opening polymerization of

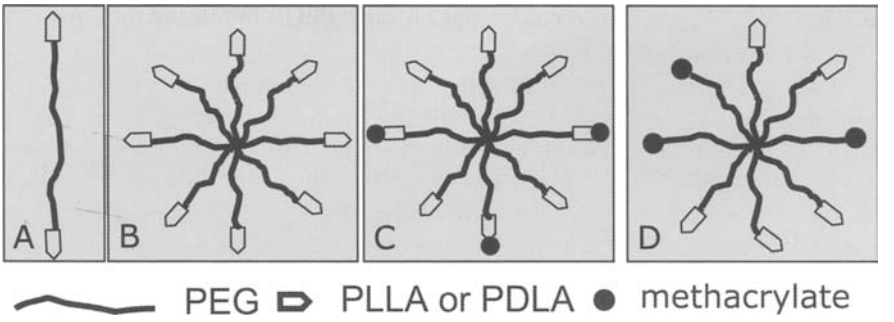

Fig. 2 Molecular structures of **a** linear triblock; **b** 8-arm PEG-PLA$_n$ star block copolymers and **c** PEG-PLA$_n$/MA and **d** PEG-MA/ PLA$_n$ star block copolymers. As an example, three methacrylate groups per molecule are drawn

Table 1 Composition and molecular weight of PLA-PEG12500-PLA and (methacrylated) PEG21800-(PLA)$_8$ block copolymers (also see Fig. 2)

Polymer	Conversion (%)	N_{LA}[a]		M_n	PEG content (wt%)
		Theory[b]	Found[c]		
PDLA-PEG12500-PDLA	83	10	10	14000	90
	89	16	15	14700	85
	88	20	19	15200	82
PLLA-PEG12500-PLLA	88	9	10	13900	90
	86	16	15	14700	85
	90	20	19	15300	82
PEG21800-(PLLA)$_8$	97	10	9	27200	81
	98	12	12	28400	76
	98	14	14	29500	74
PEG21800-(PDLA)$_8$	97	10	10	27400	79
	99	12	12	28700	76
	98	14	14	29800	73
				MA%	PEG wt%
PEG21800-PLLA$_{12}$/MA	94	12	12	28800 40	76
PEG21800-PDLA$_{12}$/MA	96	12	12	28900 42	76
PEG21800-MA/PLLA$_{12}$	95	12	12	25600 46	85
PEG21800-MA/PDLA$_{12}$	94	12	12	25600 46	85

[a] Number of lactyl units per PLA block. [b] Based on feed composition and conversion. [c] Calculated from ^{1}H NMR integral ratios.

lactides initiated by hydroxyl end groups of linear PEG's in toluene [38]. All PEG hydroxyl groups initiate the ring opening polymerization and polymers with a well-defined block copolymer structure were obtained (Fig. 2, Table 1). Poly(ethylene glycol)-poly(lactide) star block copolymers (PEG-$(PLA)_8$) were preferably synthesized by the single site Zn-complex (Zn(Et)[$SC_6H_4(CH(Me)NC_5H_{10})$-2]) catalyzed ring-opening polymerization of lactides, initiated by the 8-arm star PEG. The advantage of the use of a single site catalyst is the prevention of gelation of the reaction mixture in the solution polymerization reaction.

To obtain amphiphilic polymers that are well soluble in water, poly(ethylene glycol)-poly(L-lactide) triblock and star-block copolymers were prepared with a defined degree of polymerization of the poly(lactide) blocks. As shown in Table 1, the obtained PLA block lengths are close to the theoretical values based on the feed composition and conversion.

Two types of methacrylate functionalized poly(ethylene glycol)-poly(lactide) star block copolymers were prepared by a two-step synthesis procedure. In the first case, 8-arm PEG-PLA star block copolymers with 12 lactyl units per PLA block were synthesized. Subsequently, the PLA hydroxyl end groups were reacted with methacrylic anhydride using triethylamine as a catalyst in dichloromethane to give PEG-PLA/MA. A degree of methacrylation of approximately 40% was obtained. In a second procedure approximately 40% of the hydroxyl end groups of the 8-arm star PEG were methacrylated. Subsequently, the ring opening polymerization of L-lactide or D-lactide was initiated by the remaining hydroxyl groups, using the single-site Zn-complex. In this way PEG-MA/PLA copolymers with 12 lactyl units per PLA block were prepared.

Differential Scanning Calorimetry thermograms of triblock and PEG-PLA star block copolymers in the solid state showed a single melting endotherm of between 40 and 60 °C due to melting of the PEG crystals. The absence of a melting endotherm at higher temperatures revealed that the PLA blocks are in the amorphous state.

2.9 Solubility

The solubility of linear and star block copolymers in distilled water at room temperature decreases rapidly upon increasing the PLA block length. When the number of lactyl units per PLA block was higher than 22 for the triblock copolymers or higher than 14 for the star-block copolymers, the copolymers were hardly water-soluble.

2.10 Gelation behavior

The triblock copolymers studied showed gelation upon mixing of both enantiomer solutions, while the single enantiomer solutions did not form a gel at similar concentrations and temperatures. The critical gel concentration (CGC) (Table 2) at room temperature was found to decrease sharply upon increasing the PLA block length from 10 to 15 lactyl units, while a further increase to 19 lactyl units only caused a minor decrease in CGC. The decrease in CGC can be explained by an increase in micelle number and size and increased intermolecular and intermicellar association

Table 2 Critical gel concentrations of PLA-PEG-PLA triblock copolymers and PEG-PLA_8, PEG-$PLLA_8$/MA and PEG-MA/$PLLA_4$ star block copolymers in distilled water at room temperature

Polymer	Critical gel concentration (w/v%)	
	Single enantiomer	1:1 mixture of D- and L-enantiomers
PLA_{10}-PEG12500-PLA_{10}	80	30
PLA_{15}-PEG12500-PLA_{15}	15	10
PLA_{19}-PEG12500-PLA_{19}	10	7.5
PEG21800-$(PLA_{10})_8$	40	25
PEG21800-$(PLA_{12})_8$	20	10
PEG21800-$(PLA_{14})_8$	15	5
PEG21800-$(PLA_{12})_8$/MA	17.5	7.5
PEG21800-MA/$(PLA_{12})_4$	30	22.5

upon increasing the hydrophobic block length. Furthermore stereocomplexation enhances interactions between the hydrophobic blocks and thereby lowers the CGC. The decrease in CGC may also be due to an increase in crystallinity or the chain packing tendency of the hydrophobic block, as has been proposed by Jeong et al. in their study on PEG-PLLA and PEG-PDLLA diblock copolymers [39].

The star block copolymers also showed stereocomplex mediated gelation even at short PLA blocks of 10 lactyl units. These stereocomplexed hydrogels were formed at a low CGC, which is attributed to the lower PEG content of 76 wt% and increased number of stereocomplex interaction sites compared to the linear triblock copolymers. When half of the number of star PEG arms was acrylated and the other half contained a PLA block as in PEG21800-MA/$(PLA_{12})_4$, the CGC increased as was expected.

Increasing the temperature of single enantiomer and stereocomplexed hydrogels of PLA_{15}-PEG12500-PLA_{15} and PEG21800-$(PLA_{14})_8$ polymers may turn the gel into a mobile (sol) phase (Fig. 3). The PLA_{15}-PEG12500-PLA_{15} hydrogels formed a clear fluid phase. On the contrary, the PEG21800-$(PLA_{14})_8$ hydrogels exhibited phase separation, resulting in a clear fluid and a viscous opaque phase, caused by dehydration of the PEG chains at elevated temperatures. Remarkably, the gel-sol transition temperatures of these two polymers in the concentration range studied are similar, which indicates that the hydrogel gel to sol transition temperature depends predominantly on the PLA block length. The stereocomplexed hydrogels showed the same trend, but the gel-sol transitions are shifted to much higher temperatures (Fig. 3).

The influence of the methacrylate groups on the formation of stereocomplex hydrogels was only studied up to now at room temperature. The critical gel concentrations (CGCs) for stereocomplexation of PEG-PLA_{12}/MA and PEG-PLA_{12} are similar indicating that the methacrylate end groups do not influence the stereocomplexation. The higher CGC for stereocomplexation of PEG-MA/PLA_{12} compared to PEG-PLA_{12}/MA is likely due to the lower number of PLA blocks per molecule.

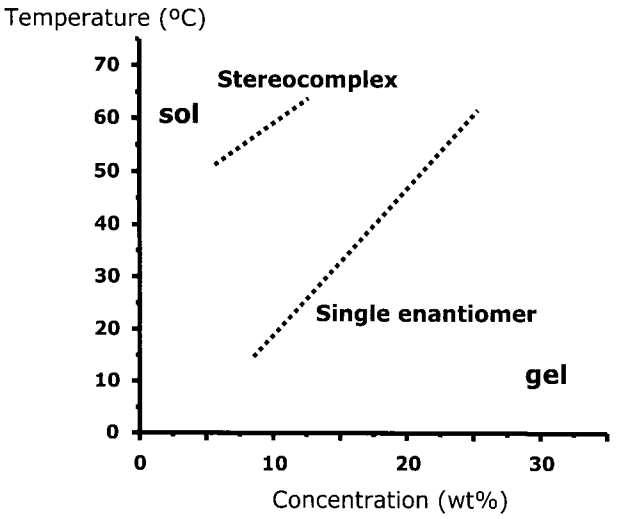

Fig. 3 General gel-sol phase diagram of hydrogels comprising linear triblock or star block copolymers containing either a single enantiomer or D- and L-enantiomers in equimolar amounts

2.11 Rheology

After mixing enantiomeric triblock or star block copolymer solutions (PBS, 37 °C), gels were formed almost instantaneously. The gels stabilized further in time as determined by oscillatory rheology experiments monitoring the storage modulus (G') and loss modulus (G"). The PEG21800-$(PLA_{14})_8$ hydrogels have higher storage moduli ($\sim$ 1.9 kPa) compared to the PLA_{15}-PEG12500-PLA_{15} hydrogels (0.8 kPa), which can be ascribed to the increased stereocomplex interaction sites of the PEG21800-$(PLA_{14})_8$ polymer, causing an increase in crosslinking density. However, the lower water solubility of PEG21800-$(PLA_{14})_8$ compared to the linear triblock copolymer cause a considerable decrease in the storage modulus upon an increase in temperature. This is reflected by an increased turbidity of PEG21800-$(PLA_{14})_8$hydrogels with increasing temperature, while PLA_{15}-PEG12500-PLA_{15} hydrogels remained clear. This lower solubility may hamper mixing of D- and L-enantiomers and stereocomplexation.

Increasing the concentration increases the storage and loss moduli of PEG21800-$(PLA_{14})_8$ stereocomplexed hydrogels due to the formation of a denser crosslinked network. Storage moduli of 14.0 kPa were obtained at 37 °C in PBS. These results showed that stereocomplexation is a promising method for in situ formation of hydrogels and may be used in biomedical applications. To increase the stability of the hydrogels, the concept of combining stereocomplexation and photopolymerization was introduced. As described in the sections above, two new types of star block copolymers were prepapred, PEG-PLA/MA and PEG-MA/PLA polymers (Fig. 2).

Stereocomplexed hydrogels were prepared by mixing aqueous solutions of equimolar amounts of PEG-$PLLA_{12}$/MA and PEG-$PDLA_{12}$/MA, or PEG-MA/$PLLA_{12}$

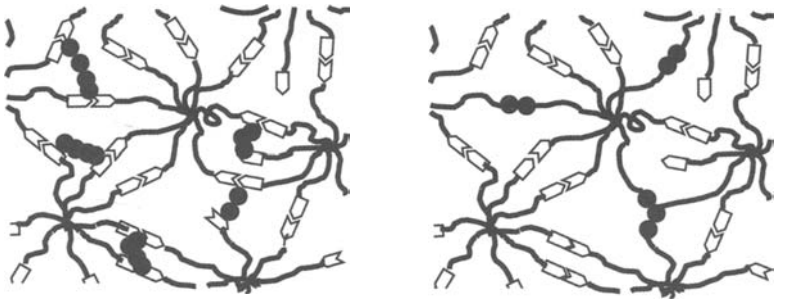

Fig. 4 A schematic representation of the stereocomplexed-photo hydrogels PEG-PLA/MA (left) and PEG-MA/PLA copolymers (right)

and PEG-MA/PDLA$_{12}$ star block copolymers in HEPES buffered saline (pH 7) in a polymer concentration range of 12.5 to 17.5 w/v%. The storage modulus evolutions and plateau values of PEG-PLA$_{12}$/MA and PEG-PLA$_{12}$ copolymers were similar, showing that the methacrylate groups hardly influence the stereocomplexation. The storage modulus of the stereo hydrogels of PEG-MA/PLA$_{12}$ (15 wt%) were in general a factor 3 lower compared to PEG-PLA$_{12}$/MA hydrogels and most importantly are becoming higher with increasing stereocomplexation equilibration time.

2.12 In situ monitoring of mechanical properties during photopolymerization

Similarly, as described above, the streocomplexed hydrogels were prepared on the rheometer. The rheometer was equipped with a UV-cell allowing the samples to be irradiated at 350-400 nm. Polymer solutions were prepared in HEPES buffered saline (pH 7) at 37 °C. UV-irradiation after 6 h of equilibration of the PEG-PLA$_{12}$/MA stereocomplexed hydrogel resulted in a storage modulus of 31.6 kPa. Since the hydrophobic methacrylate groups are at the PLA chain ends, the chemical crosslinks are most probably formed in the PLA domains. A schematic representation of the stereocomplexed-photo hydrogels PEG-PLA/MA and PEG-MA/PLA copolymers is shown in Fig. 4. Combining stereocomplexation and photocrosslinking thus may provide fast gelation *in vitro* and *in vivo*, yielding hydrogels with good mechanical properties.

3 Conclusions

Hydrogels are important materials for biomedical applications, such as drug or protein delivery and tissue engineering. Besides serving as a depot or support, hydrogels are nowadays designed with additional functionalities, such as cell-adhesion and cell-dependent degradation and release, thus mimicking the natural ECM. Hydrogels can be formed by physical or chemical crosslinking. Stereocomplexation is an attractive method to form physically crosslinked hydrogels, since hydrogels can be rapidly

formed in situ in the presence of proteins, without damaging proteins. Furthermore, stereocomplexed hydrogels are degradable due to the presence of PLA blocks. Stereocomplexed hydrogels that are based on PLA-PEG-PLA triblock copolymers show weak mechanical properties and can be improved using star block copolymers. Stereocomplexation followed by photopolymerization appears to be a convenient method for preparation of robust chemically crosslinked hydrogels.

References

[1] Hiemstra C, Zhong ZY, Dijkstra PJ, Feijen J (2005) Stereocomplex mediated gelation of PEG-(PLA)2 and PEG-(PLA)8 block copolymers. Macromol Symp 224:119–131

[2] Hiemstra C, Zhong ZY, Li L, Dijkstra PJ, Feijen J (2006) In-situ formation of biodegradable hydrogels by stereocomplexation of PEG-$(PLLA)_8$ and PEG-$(PDLA)_8$ star block copolymers. Biomacromolecules 7:2790–2795

[3] Hiemstra C, Wouters MEL, Zhong ZY, Feijen J (2007) Rapidly in situ forming PEG-PLA hydrogels prepared by combined stereocomplexation and photocrosslinking. J Am Chem Soc 129 32:9918–9926

[4] Wichterle O, Lim D, Dreifus M (1961) On the problem of contact lenses. Cesk Oftalmol 17:70–75

[5] Peppas NA, Hilt JZ, Khademhosseini A, Langer R (2006) Hydrogels in biology and medicine: From molecular principles to bionanotechnology. Adv Mater 18:1345–1360

[6] Kashyap N, Kumar N, Kumar M (2005) Hydrogels for pharmaceutical and biomedical applications. Crit Rev Ther Drug Carrier Syst 22:107–149

[7] Peppas N, Bures P, Ichikawa H (2000) Hydrogels in pharmaceutical formulations. Eur J Pharm Biopharm 50:27–46

[8] Malmsten M (2006) Soft drug delivery systems, Soft Matter 2:760–769

[9] Hubbell JA (2003) Materials as morphogenetic guides in tissue engineering. Curr Opin Biotech 14:551–558

[10] Nerem RM (2006) Tissue engineering: The hope, the hype, and the future. Tissue Eng 12:1143–1150

[11] Lavik E, Langer R (2004) Tissue engineering: current state and perspectives. Appl Microbiol Biotechnol 65:1–8

[12] Hennink WE, van Nostrum CF (2002) Novel crosslinking methods to design hydrogels. Adv Drug Deliv Rev 54:13–36

[13] Benoit DSW, Durney AR, Anseth KS (2006) Manipulations in hydrogel degradation behavior enhance osteoblast function and mineralized tissue formation. Tissue Eng 12:1663–1673

[14] Patel PN, Gobin AS, West JL, Patrick CW (2005) Poly(ethylene glycol) hydrogel system supports preadipocyte viability, adhesion, and proliferation. Tissue Eng 11:1498–1505

[15] Bae SJ, Joo MK, Jeong Y, Kim SW, Lee WK, Sohn YS, Jeong B (2006) Gelation behavior of poly(ethylene glycol) and polycaprolactone triblock and multiblock copolymer aqueous solutions. Macromolecules 39:4873–4879

[16] Shim WS, Kim JH, Park H, Kim K, Kwon IC, Lee DS (2006) Biodegradability and biocompatibility of a pH- and thermo-sensitive hydrogel formed from a sulfonamide-modified poly(epsilon-caprolactone-co-lactide)-poly(ethylene glycol)-poly(epsilon-caprolactone-co-lactide) block copolymer. Biomaterials 27:5178–5185

[17] Lee BH, West B, McLemore R, Pauken C, Vernon BL (2006) In-situ injectable physically and chemically gelling NIPAAm-based copolymer system for embolization. Biomacromolecules 7:2059–2064

[18] Liu YY, Shao YH, Lu J (2006) Preparation, properties and controlled release behaviors of pH-induced thermosensitive amphiphilic gels. Biomaterials 27:4016–4024

[19] Xu FJ, Kang ET, Neoh KG (2006) pH- and temperature-responsive hydrogels from crosslinked triblock copolymers prepared via consecutive atom transfer radical polymerizations. Biomaterials 27:2787–2797

[20] Betre H, Setton LA, Meyer DE, Chilkoti A (2002) Characterization of a genetically engineered elastin-like polypeptide for cartilaginous tissue repair. Biomacromolecules. 3: 910–916

[21] Dang JM, Sun DDN, Shin-Ya Y, Sieber AN, Kostuik JP, Leong KW (2006) Temperature-responsive hydroxybutyl chitosan for the culture of mesenchymal stem cells and intervertebral disk cells. Biomaterials 27:406–418

[22] Bhattarai N, Ramay HR, Gunn J, Matsen FA, Zhang MQ (2005) PEG-grafted chitosan as an injectable thermosensitive hydrogel for sustained protein release. J Controlled Release 103:609–624

[23] Chenite A, Chaput C, Wang D, Combes C, Buschmann MD, Hoemann CD, Leroux JC, Atkinson BL, Binette F, Selmani A (2000) Novel injectable neutral solutions of chitosan form biodegradable gels in situ. Biomaterials 21:2155–2161

[24] Lee BH, Lee YM, Sohn YS, Song SC (2002) A thermosensitive poly(organophosphazene) gel. Macromolecules 35:3876–3879

[25] Seong JY, Jun YJ, Jeong B, Sohn YS (2005) New thermogelling poly (organophosphazenes) with methoxypoly(ethylene glycol) and oligopeptide as side groups. Polymer 46:5075–5081

[26] Garlotta D (2001) A literature review of poly(lactic acid). J Polym Environ 9:63–84

[27] Ikada Y, Tsuji H (2000) Biodegradable polyesters for medical and ecological applications. Macromol Rapid Commun 21:117–132

[28] De Jong SJ, van Nostrum CF, Kroon-Batenburg LMJ, Kettenes-van den Bosch JJ, Hennink WE (2002) Oligolactate-grafted dextran hydrogels: Detection of stereocomplex crosslinks by X-ray diffraction. J Appl Polym Sci 86:289–293

[29] De Jong SJ, De Smedt SC, Wahls MWC, Demeester J, Kettenes-van den Bosch JJ, Hennink WE (2000) Novel self-assembled hydrogels by stereocomplex formation in aqueous solution of enantiomeric lactic acid oligomers grafted to dextran. Macromolecules 33:3680–3686

[30] Li S, Vert M (2003) Synthesis, characterization, and stereocomplexation-induced gelation of block copolymers prepared by ring-opening polymerization of L(D)-lactide in the presence of poly(ethylene glycol). Macromolecules 36:8008–8014

[31] Nguyen KT, West JL (2002) Photopolymerizable hydrogels for tissue engineering applications. Biomaterials 23:4307–4314

[32] Zhu J, Beamish J, Tang C, Kottke-Marchant K, Marcant R (2006) Extracellular Matrix-like Cell-Adhesive Hydrogels from RGD-Containing Poly(ethylene glycol) Diacrylate. Macromolecules 39:1305–1307

[33] Elisseeff J, Anseth K, Sims D, McIntosh W, Randolph M, Langer R (1999) Transdermal photopolymerization for minimally invasive implantation. PNAS 96:3104–3107

[34] Baroli B (2006) Photopolymerization of biomaterials: issues and potentialities in drug delivery, tissue engineering, and cell encapsulation applications. J Chem Technol Biotechnol 81:491–499

[35] Sawhney AS, Pathak CP, Hubbell JA (1993) Bioerodible hydrogels based on photopolymerized poly(ethylene glycol)-co-poly(alpha-hydroxy acid) diacrylate macromers. Macromolecules 26:581–587

[36] Bryant SJ, Bender RJ, Durand KL, Anseth KS (2004) Encapsulating Chondrocytes in degrading PEG hydrogels with high modulus: Engineering gel structural changes to facilitate cartilaginous tissue production. Biotechnol Bioeng 86:747–755

[37] Elisseeff J, Anseth KS, Sims D, McIntosh W, Randolph M, Yaremchuk M, Langer R (1999) Transdermal photopolymerization of poly(ethylene oxide)-based injectable hydrogels for tissue-engineered cartilage. Plast Reconstr Surg 104:1014–1022

[38] Stevels WM, Ankone MJA, Dijkstra PJ, Feijen J (1995) Stereocomplex formation in ABA triblock copolymers of poly(lactide)(A) and poly(ethylene-glycol)(B). Macromol Chem Phys 196:3687–3694

[39] Jeong B, Lee D, Wu CH, Bae YH, Kim SW (1999) Thermoreversible gelation of poly(ethylene oxide) biodegradable polyester block copolymers. J Polym Sci Polym Chem 37:751–760

Hybrid Hydrogels Based on Poly(vinylalcohol)-Chitosan Blends and Relevant CNT Composites

Sangram K. Samal, Federica Chiellini, Cristina Bartoli, Elizabeth G. Fernandes and Emo Chiellini

Abstract. The present paper reports on the preparation of hybrid polymeric hydrogels consisting of poly(vinylalcohol) (PVA) and Chitosan (CHI) blends and relevant composites loaded with multiwalled carbon nanotubes (MWCNT). The hydrogels, prepared by the physical freeze-drying method were specifically characterized in the merit of their morphological, thermal and swelling/deswelling behavior. The obtained results indicate that PVA/CHI/MWCNTs hydrogel nanocomposites appear good candidates for biomedical and pharmaceutical applications. The presence of up to 0,5 % MWCNTs in the investigated polymeric hydrogel composites does not negatively affect the biocompatibility of the PVA/CHI hybrid polymeric blends used as continuous matrix.

1 Introduction

Hydrogels are crosslinked macromolecular networks of hydrophilic polymer chains that swell in water or biological fluids. They turned out to be appealing biomaterials for biomedical and pharmaceutical applications including, among other practices, drug delivery, tissue engineering, bioseparation and protein folding. Polymeric hydrogels are carbon based functional materials and even though studied and used for centuries, they are far from constituting a mature field. Nowadays, the tissue engineering field is requiring materials with tailor-made and modulated structural features. Among these, biocompatible hydrogel composites become structural items of ever growing interest. Carbon nanotubes (CNTs) are also attracting interest for their inherent structural features that appear to open new interesting avenues for novel applications in science and technology. The electronic structure and morphology (surface energy and roughness) of CNTs, which certainly should affect their biocompatibility, are typical of graphite-like structures [1]. They can be distinguished by a tubular construction in the nanometer range and by high strength and Young modulus [2]. Due to their high electrical conductivity, the latter process can be additionally assisted by electrostimulation during cell culture and eventually tissue formation [3]. CNTs have the potential to carry drugs into living organisms thanks to their hollow structure and size, which is even smaller than blood cells. The accessible canals of open-ended nanotubes may

Barbucci R. (Ed): Hydrogels. Biological Properties and Applications.

facilitate the flow and migration of metabolites or bioactive agents, and hence may also be used as convenient drug carriers at nanoscale level.

Incorporation and manipulation of CNTs into different polymeric matrices is always problematic due to poor solubility and low dispersibility of CNTs in water or organic solvents [4, 5]. There have been several recent reports on research activities regarding the use of CNTs. They have been used for supramolecular self-assembly of lipid derivatives [6] and in the spontaneous uptake of DNA oligonucleotides [7]. Since CNTs have successfully been made soluble in both organic solvents by chemical functionalization [8] and in aqueous media by non-covalently association with linear polymer [9], CNTs /gelatin hybrid hydrogels have been prepared and shown to allow efficient separation of proteins [10]. The CNTs/PVA hybrid hydrogels, prepared by a freeze/thaw method were characterized by effectively improved mechanical properties and good swelling capability at high temperature [11]. The MWCNT were used for crystallization of protein in helical arrays [12] and growth of embryonic rat-brain neurons [13], whereas hybrid alginate/SWCNT have been successfully used as scaffolds for tissue engineering with beneficial efforts on structural, mechanical and biological responses specifically in the case of vascular grafts [14]. In very recent studies, composites based on a major fraction of MWCNTs (up to 89 %-wt.) and a minor content of Chitosan (CHI) have been found well suited components for the fabrication of biocompatible biodegradable scaffolds for cell culture growth [15]. All these results indicate that CNTs can be ideal candidates to modify the performance of polymeric hydrogels and promising possibilities can be expected by introducing CNTs into synthetic polymers to reinforce and provide some specific requested functionalities to tissue engineered multifunctional scaffolds.

In this context, we have chosen a water soluble polyhydroxy polymer [poly(vinyl-alcohol) (PVA)] that is known as one of the most utilized synthetic polymers which received increasing attention in biomedical and pharmaceutical applications thanks to its permeability, biocompatibility and biodegradability in water media under physiological conditions. The specific structure and properties of PVA increases the possibilities of tailoring its properties by blending it with other compatible polymers of synthetic and natural origin. PVA is also known to provide good stress transfer to CNTs when used as continuous matrix in CNTs loaded constructs [16]. MWCNTs displays better reinforcement characteristics with respect to SWCNTs, most likely due to tight bundle formation. This feature strongly suggests that low-diameter MWCNT can be taken as optimal fillers for polymeric material reinforcement [4].

Chitosan, [poly-β-(1-4)-2-amino-2-deoxy-β-D-glucose] (CHI), is a hydrophobic/amphiphilic biopolymer obtained by hydrolyzing the amino acetyl groups of chitin, which is the main component of the exoskeleton of insects, crabs, shrimps and krills. The main driving force in the development of new applications for Chitosan is due to its polysaccharidic nature, and natural abundance. More important is its bifunctional chemical character allowing for convenient conversion to hydrogels specifically thanks to the presence of two hydroxyl groups and one primary amino group per glycosidic unit upon complete acetyl group removal. Chitosan is structurally related to other bioactive polysaccharides such as glycosaminoglycans (GAG) including heparin, heparin sulfate, hyaluronic acid, and keratin sulfate. These GAGs

are remarkable derivatives of 2-amino-2-deoxy-D-glucose and are present in nearly all mammalian body compartments. The non-toxic, biocompatible, biodegradable, and antigenic pH-sensitive cationic biopolymer Chitosan represents on its own, a promising candidate for employment in the design of hydrogels used in a variety of areas such as medicine, pharmaceutics [17], tissue engineering [18], antimicrobial prophylaxis [19], and other industrial applications within the biomedical and environmental fields.

To the best of our knowledge, there is no research report aimed at addressing the incorporation of water dispersed MWCNT into PVA/Chitosan for the preparation of bioerodible polymeric scaffold systems. Thus, we tried to examine whether incorporation of MWCNTs into PVA/CHI polymer blends was feasible, and how the structure, morphology, and properties of the resultant novel hybrid scaffolds would have been influenced by the incorporation of the nanofiller. Understanding of the interaction of CNTs with biological systems is essential for the realization of bio-hybrid systems. The present investigation was aimed at finding a simple and effective method to obtain intimate and uniform loading of the water-dispersed MWCNTs into PVA and PVA/CHI blends. Polymeric scaffolds incorporating CNT, other than showing improvement in mechanical strength, structural coherence and electrical conductivity, should be effective in influencing cell growth as well as bone, cartilage and other soft and hard tissue regeneration.

2 Experimental procedures

2.1 Materials

Poly(vinylalcohol) PVA with a molecular weight (MW) of 146–186 KDa and 99% hydrolysis, and Chitosan (CHI) with more than 85% eacetylation (with respect to the parent chitin) were purchased from Sigma-Aldrich. Water dispersion of MWCNTs was kindly provided by Nanocyl Company, Belgium.

For cell culture, Dulbecco's modified eagles medium (DMEM), glutamine, penicillin/streptomycin and calf serum were purchased from Gibco brl. The cell proliferation reagent WST-1 was obtained from Roche and used as indicated by the manufacturer.

2.2 Processing

Chitosan/MWCNT solution was prepared by first dissolving 1% CHI into 1% acetic acid solution and then adding a 0.5% solution of water dispersed MWCNT. PVA at 99% hydrolysis is practically insoluble in water at room temperature but dissolution does occur at 80–90 °C. To speed up the dissolution, the PVA solutions were prepared at water's boiling temperature by refluxing in an atmosphere of nitrogen for 3 h until a transparent homogeneous system was obtained. The CHI/MWCNTs mixture was added to the PVA solutions and the refluxing treatment was repeated for a further 3 hr until a homogeneous solution was obtained. The solution was then sonicated

for 20 min at 70 °C until a complete dispersion was obtained, free of air bubbles. The viscous black color dispersion was allowed to cool down to room temperature for 30 min and poured into a syringe. Approximately 2 mL of PVA/CHI/MWCNTs dispersion was injected into a mold of cylindrical shape. The filled mould was kept for 15 min at room temperature and then placed in a freezer at approximately −20 °C. After 24 h at −20 °C, the sample was thawed for 5 h at room temperature to obtain the desired gel. The freeze/thaw cycle was repeated twice and lyophilized at a temperature of −55 °C for 24 h. The PVA and PVA/CHI hydrogels were also prepared according to the same procedure for comparison.

The resulting hydrogels were stored in parafilm closed falcon tubes at −4 °C to prevent possible degradation before submitting them to test evaluations.

2.3 Characterization

Morphology. Morphological characterization of the hydrogel specimen was carried out using a field emission scanning electron microscopy (FE-SEM) (Tescan- Mod Mira LMU – Czech Republic) at an acceleration voltage of 5 kV and working distance of about 7.6 mm with the secondary electron image as a detector.

Cytotoxicity of hydrogel extracts. Extracts were prepared by incubating the hydrogel samples in cell growth medium (DMEM) supplemented with 10% calf serum, 4 mM glutamine and penicillin/streptomycin (100 units/mL–100µg/mL) for 24 h at a concentration of 0.2 g/mL. Each extract was then used to incubate a subconfluent monolayer of 3T3/BALB-C clone A31 mouse embryo fibroblasts for 24 h and cell viability was then measured using WST-1 (Roche) tetrazolium salts. Cells grown in the presence of DMEM were used as a negative control.

Swelling. The swelling behavior of the hydrogels was evaluated by immersing the pre-weighed dried specimens into different aqueous media that were deionized water (Wm), phosphate buffer medium (Bm, ionic strength = 0.1 mol/L) and growth media (Gm) at pH 7.4 and pH 2.2 at 37 °C. Hydrogel swelling was followed over a period of 165 min. At intervals of 15 min, specimens were withdrawn from aqueous medium and the excess of surface water was removed gently with filter paper. Immediately after, their weights were recorded using an analytical balance and the specimen then returned to the aqueous medium.

The hydrogel swelling ratio (*Hsr* in %-wt) was calculated using the following equation

$$\mathrm{Hsr}(\%) = \left[\frac{(\mathrm{Ws} - \mathrm{Wd})}{\mathrm{Ws}}\right] \times 100 \tag{1}$$

where W_d and W_s are the weights of dried and swollen hydrogel, respectively.

The equilibrium of water content (E_{wc} in %-wt) was determined by weighing the samples after 96 h of permanence in the medium of choice, and was calculated by means of the following equation

$$\mathrm{Ewc}\ (\%) = \left[\frac{(\mathrm{We} - \mathrm{Wd})}{\mathrm{We}}\right] \times 100 \tag{2}$$

where W_e and W_d represent the weights of hydrogel in the swollen state at equilibrium and the dried state respectively.

Deswelling. A dried gel disk specimen was immersed in distilled water at 37 °C for 5 days to obtain a fully swollen state at equilibrium. The sample was removed from the distilled water and the deswelling kinetic was assessed by isothermal TGA treatment at 37 °C. Weight loss of specimens weighing 10–15 mg in a nitrogen atmosphere at a flow rate of 60 mL/min was followed for 4 h.

State of the water in hydrogels. The state of water as *bound water* (W_b), and *free water* (W_f) in hydrogels obtained by repeated freeze-thaw cycles was investigated by differential scanning calorimetry (DSC) analysis [20]. The DSC measurements were performed by means of a Mettler Toledo DSC-820 instrument fitted with a cooling accessory in a nitrogen atmosphere at 80 mL/min of flow rate. Samples of 1 to 3 mg of hydrogel were weighed in 40 μL aluminum hermetic pans and an empty pan was used as a reference. DSC temperature calibration was performed using indium, lead and zinc standards. Measurements were performed according to the following protocol:

1. Cooling scan from 25 °C to −70 °C at 10 °C/min and isotherm of 5 min at the end temperature; and,
2. Heating scan from −70 °C to 50 °C at 10 °C/min.

Water content sorbed by hydrogel samples were determined using the following equations.

$$\mathrm{Wf}\ (mg) = \left[\frac{\mathrm{Qendo}}{\Delta \mathrm{Hw}}\right] \tag{3}$$

$$\mathrm{Wb}\ (mg) = \left[\frac{\mathrm{Ewc} \times \mathrm{Wh}}{100}\right] - \mathrm{Wf} \tag{4}$$

where W_h is the swelled hydrogel weight (mg), Q_{endo} (mJ) is the heat of fusion for *freezable water* in the hydrogels and ΔH_w is the melting enthalpy of water determined in the present work with the same water used to prepare aqueous media. The mean value obtained was 346 J/g.

Thermogravimetric Analysis (TGA). TGA traces were obtained by means of a TA Instrument - Series Q500. Measurements were performed on specimens of 10–15 mg at 10 °C/min from 25 °C to 900 °C, in a nitrogen flow rate of 60 mL/min.

3 Results and discussion

Physical crosslinking has become a straightforward method of choice for the attainment of polymeric hydrogels with desirable properties for practical applications in the biomedical field. In particular, in the present work, a series of polymeric blends based on poly(vinylalcohol) (PVA) and Chitosan (CHI) have been prepared, either loaded or not with multiwalled carbon nanotubes (MWCNTs). The designation and composition of the prepared blend and composite hydrogels are summarized in Table 1.

Table 1 Designations and compositions of hydrogels based on Poly(vinyl alcohol) (PVA) and Chitosan (CHI)

Sample	PVA (%-w/v)	CHI (%-w/v)	MWCNTs (%-w/v·10^2)
PVA5	5	0	0
PVCH5	5	1	0
PVCHNT5	5	1	0.25
PVCHNT5	5	1	2.5
PVCHNT5	5	1	50
PVA7	7	0	0
PVCH7	7	1	0
PVCHNT7	7	1	0.25
PVCHNT7	7	1	2.50
PVCHNT7	7	1	50
PVA10	10	0	0
PVCH10	10	1	0
PVCHNT10	10	1	0.25
PVCHNT10	10	1	2.5
PVCHNT10	10	1	50

FE-SEM photomicrographs of the PVCHNT10 sample taken as a typical example of the hybrid hydrogel composites containing 0.5%-w/v MWCNT is reported in Fig. 1. The hydrogel, prepared by freeze-thaw cycles, presented a rugous surface at 6.5 kX magnification (Fig. 1a). This magnification was not sufficient to show the arrangement of the MWCNT in the polymeric matrix. In Fig. 1b, the photomicrograph, at 40 kX magnification, of the cryogenic fracture in the transversal direction of the hydrogel specimen suggests the presence of a small phase that can be supposed to be either microporous or agglomerate of MWCNT.

In Fig. 2a–c the results of cytotoxicity tests carried out on extracts of the hydrogel samples (PV10, PVCH10 and PVCHNT10) at different dilutions are collected. Any major difference in cell proliferation was observed, thus indicating that the presence of MWCNT in the hydrogel composites, at least up to a concentration of 0.5% w/v, is not a significant variable. Hydrogel samples did not release toxic compounds, thus suggesting their possible safe employment as materials for contact with living tissues.

The swelling behavior of hydrogels in aqueous media constitutes an important parameter to be taken into consideration in view of their utilization in formulation of carriers of bioactive macromolecules. The applications of hydrogels include many biological processes such as control of micro flows and drug and protein delivery.

In Fig. 3a–c, the swelling kinetics at different pH and aqueous media of the typical PV10, PVCH10 and PVCHNT10 samples is reported. The swelling ratio of the PVCHNT10 composite sample is remarkably higher in acidic medium with respect to the parent blend PVCH10 principally in water and growth media. This

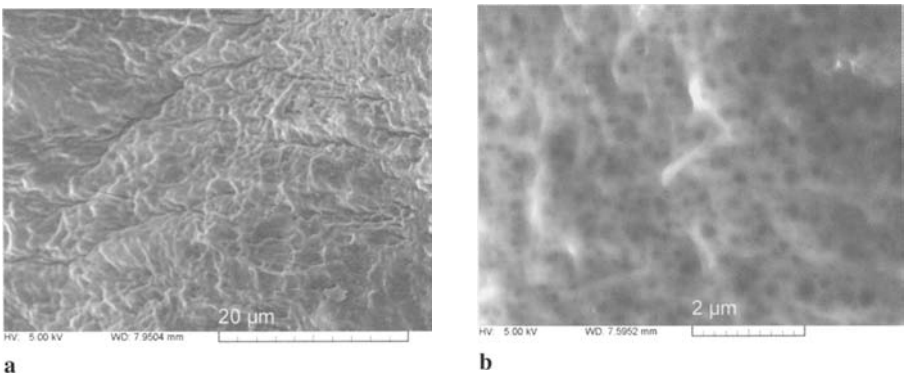

Fig. 1 FE-SEM photomicrographs of the composite PVCHNT10 (0.5%-w/v MWCNT). **a** Surface and **b** Transversal fracture at 6.5 kX and 40 kX magnification respectively

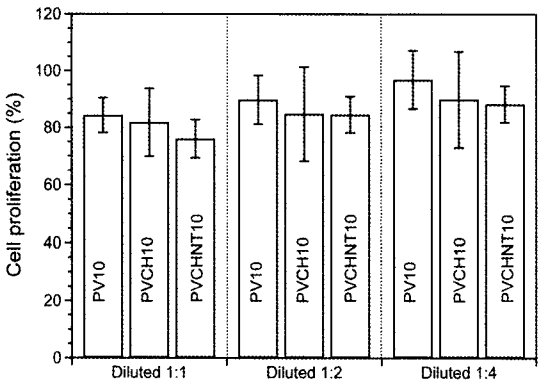

Fig. 2 Cytotoxic test **a** PV10, **b** PVCH10 and **c** PVCHNT10 (0.5%-w/v MWCNTs)

can be attributed to the capillary action exploited by MWCNT in the matrix, which facilitates solvent diffusion into the gel matrix that is maximized in acid medium (pH 2.2) when compared to the neutral medium (pH 7.4).

In Fig. 4, the deswelling profiles of the typical hydrogel samples PV10, PVCH10 and PVCHNT10 recorded at 250 min time intervals at 37 °C are reported.

The PVCH10 sample exhibited much faster deswelling with a %-weight loss of about 70 in the first 60 min. PV10 and PVCHNT10 showed a weight loss of 46% and 61% respectively. A higher content of interconnected pores in the Chitosan containing blend (PVCH10) and composite (PVCHNT10) could be taken as the principal reason for why *free water* is able to diffuse out easily from the hydrogel network thus leading to a quicker and more extensive shrinking of the porous structure.

MWCNT in the PVA/CHI blend apparently act like crosslinking sites which make the uptake and release of water more difficult.

Water frozen in a hydrogel is known as supercooled water, in which the melting enthalpy is different from normal water which freezes at 0 °C. The water in a hydrogel

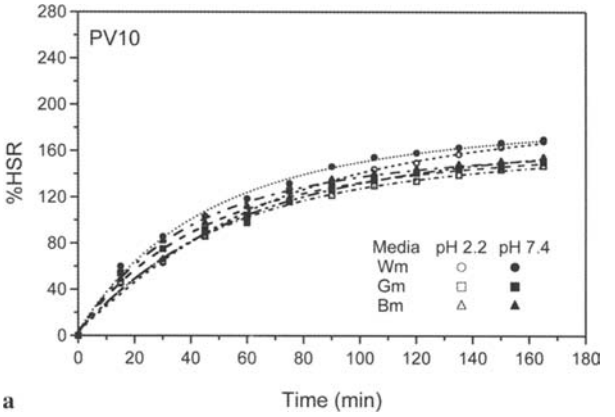

a

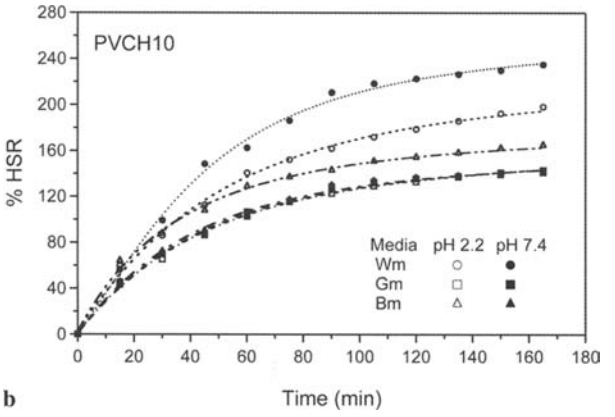

b

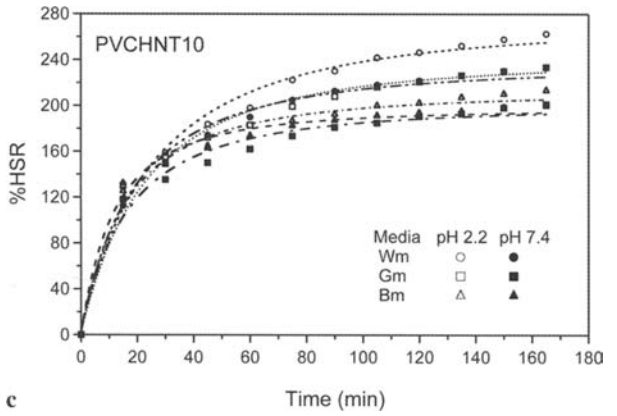

c

Fig. 3 Swelling behavior of PV10 **a**; PVCH10 **b** and PVCHNT10 (0.5%-w/v MWCNTs); **c** at 37 °C and with different aqueous media (water:Wm; Buffer: Bm and Growth: Gm) and pH

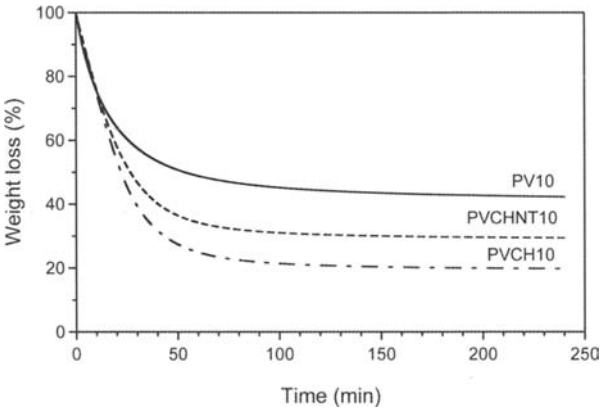

Fig. 4 Deswelling kinetics of PV10, PVCH10 and PVCHNT10 (0.5%-w/v MWCNTs) hydrogels after water equilibrium at 37 °C for 6 h

can be classified into *bound water* (W_b), and *free water* (W_f). Compared to W_b, the W_f in a hydrogel has high mobility and can be easily released. The percentage of W_b and W_i content in swollen hydrogels is related to the number of hydrophilic groups per unit volume of the super absorbent.

The total water content, as determined by DSC measurements, is higher in PVCH10 than that observed for PV10 and PVCHNT10 as reported in Table 2. The DSC endothermic peak shown by hydrogels is reported in Fig. 5. In the PV10 sample, W_b is almost double that found in PVCHNT10. This could be due to the association of a large quantity of water molecules with the amino groups of Chitosan in the swelling process. A further explanation could be bound related to the presence of the hydrophilic chains in PV10 that induce an osmotic effect in the network during the swelling. This graph also indicates that incorporation of MWCNT gives two endothermic peaks. The MWCNT based hydrogel has at least two types of W_b and there is an increase of the overall bound water content with respect to the PVCH10 sample, most likely due to the trapping of water in MWCNTs.

Table 2 State of water estimated using DSC analysis carried out on typical hydrogel samples based on Poly(vinyl alcohol) (PVA) and Chitosan (CHI)

Sample	Water in hydrogel		
	E_{wc} (%-wt)	W_f (%-wt)	W_b (%-wt)
PVA10	75.5	53.3	22.2
PVCH10	79.3	68.6	10.7
PVCHNT10[a)]	76.7	58.8	17.9

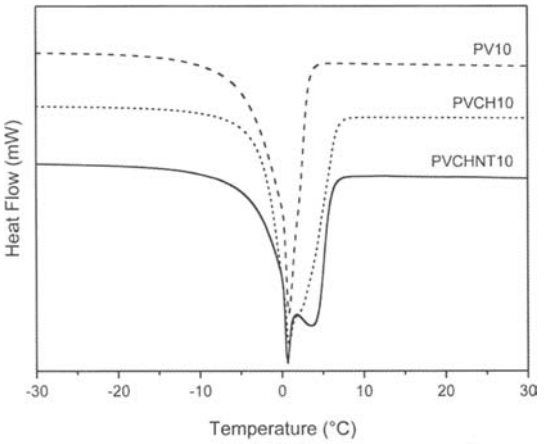

Fig. 5 DSC profiles of free water melting peak sorbed by PV10, PVCH10 and PVCHNT10 (0.5%-w/v MWCNTs) hydrogels after water equilibrium at 37 °C for 6 h

TGA traces of hydrogels in Fig. 6 are reminiscent of the profiles reported for the homopolymers (PVA & CHI), that constitute hybrid hydrogels. The PVA-based hydrogel shows thermal stability higher than that detected for pristine dry PVA with decomposition at 237 °C compared to 230 °C respectively. PVCHNT10 shows higher thermal stability than that of pristine dry PVA and lower thermal stability than that of pristine dry CHI with decomposition at 250 °C compared to 230 °C and 264 °C respectively for PVA and CHI. The MWCNTs hybrid hydrogels show lower thermal stability 246 °C when compared to the PVA/CHI blend as a continuous matrix. In Fig. 6b, we can clearly observe the exact shifting of the first derivative peak for the pristine dry polymer component of the hydrogel matrices. The transition peaks located around 80–150 °C of all samples are due to the elimination of volatile substances. The pristine dry CHI displays only a single step degradation whereas the pristine dry PVA and corresponding PVA based hydrogels show 2 or 3 degradation steps. It was observed that when a less thermally stable species (PVA) is combined with a species of high thermal stability (CHI), the blend will increase its thermal stability.

4 Conclusions

Hybrid scaffolds based on Poly(vinylalcohol) (PVA) and Chitosan (CHI) blends loaded or not with MWCNTs retained the basic characteristics of PVA, Chitosan and pristine MWCNTs. The loading of water dispersed MWCNTs into PVA/CHI blends did not cause any appreciable cell cytotoxicity as determined by the water extracts of the composite specimen. The presence of even small percentages of MWCNTs does not alter appreciably the overall structure of the PVA/CHI blends, but does have beneficial effects on overall continuous polymeric matrix reinforcement. Carbon nanotube

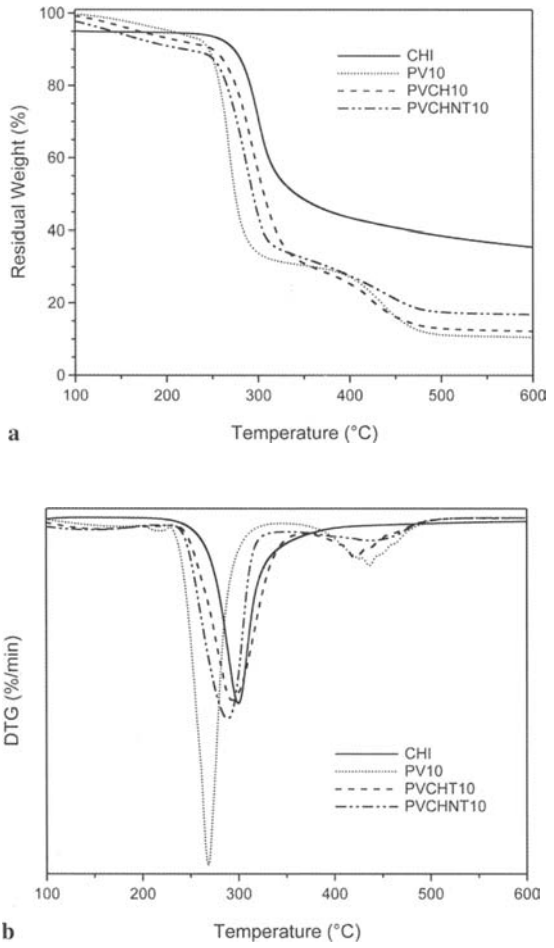

Fig. 6 Thermogravimetric analysis of PV10, PVCH10 and PVCHNT10 (0.5%-w/v MWCNT) hydrogel samples. **a** Weight loss profiles and **b** derivative of weight loss profiles

based scaffolds appear to be good candidates with good potential for biomedical and pharmaceutical applications.

Acknowledgement. The authors would like to express sincere thanks to "NOE-Expertissues" CT-2004-500328 and PRIN-2006 for supporting the present ongoing research activity at BIOlab of the University of Pisa. Nanocyl SA, Belgium, is acknowledged for the kind supply of CNT samples within the framework of the IP-Ambio (NMP4CT2005011827). The rock was also implemented with the partial support of FIRB 2005RBIN043BCP.

References

[1] Tanaka K, Yamabe T, Fukui K (1999) The science and technology of carbon nanotubes. Elsevier, Amsterdam

[2] Salvetat JP, Kulik A, Bonard JM et al (1999) Elastic modulus of ordered and disordered multiwalled carbon nanotubes. Adv Mater 2:161–165

[3] Supronowicz PR, Ullman KR, Ajayan PM et al (2001) Cellular/molecular responses of electrically stimulated osteoblasts cultured on novel polymer/carbon nanophase substrates. In: Carbon OI, An International Conference on Carbon, Lexington, KY, United States, July 14–19. University of Kentucky, Center for Applied Energy Research Library, Lexington, pp 1–2

[4] Cadek M, Coleman JN, Ryan KP et al (2004) Reinforcement of Polymers with Carbon Nanotubes: The Role of Nanotube Surface Area. Nano Lett 4:353–356

[5] Calvert P (1999) Nanotube composites: A recipe for strength. Nature 399:210–211

[6] Richard C, Balavoine F, Schultz P et al (2003) Supramolecular self-assembly of lipid derivatives on carbon nanotubes. Science 300:775–778

[7] Gao HJ, Kong Y, Cui DX et al (2003) Spontaneous insertion of DNA oligonucleotides into carbon nanotubes. Nano Lett 3:471–473

[8] Chen J, Hamon MA, Hu H et al (1998) Solution properties of single-walled carbon nanotubes. Sciente 282:95–98

[9] O'Connell MJ, Boul P, Ericson LM et al (2001) Reversible water-solubilization of single-walled carbon nanotubes by polymer wrapping. Chem Phys Lett 342:265–271

[10] Li H, Wang DQ, Chen HL et al (2003) A novel gelatin-carbon nanotubes hybrid hydrogel. Macromol Biosci 3:720–724

[11] Tong X, Zheng J, Lu Y et al (2007) Swelling and mechanical behaviors of carbon nanotube/poly (vinyl alcohol) hybrid hydrogels. Mater Lett 61:1704–1706

[12] Balavoine F, Schultz P, Richard C et al (1999) Helical crystallization of proteins on carbon nanotubes: A first step towards the development of new biosensors. Angew Chem. Int Edit 38:1912–1915

[13] Mattson MP, Haddon RC, Rao AM (2000) Molecular functionalization of carbon nanotubes and use as substrates for neuronal growth. J Mol Neurosci 14:175–182

[14] Yildirim ED, Yin X, Ko FK et al (2006) Evaluation of 3D Hybrid Alginate/Single Wall Carbon Nanotube Tissue Scaffolds in Terms of Process and Cytocompatibility. Bioengineering Conference, Proceedings of the IEEE 32nd Annual Northeast, 01-02 April, pp 5–6

[15] Abarrategi A, Gutierrez MC, Moreno-Vicente C et al (2008) Multiwall carbon nanotube scaffolds for tissue engineering purposes. Biomaterials 29:94–102

[16] Cadek M, Coleman JN, Barron V et al (2002) Morphological and mechanical properties of carbon-nanotube-reinforced semicrystalline and amorphous polymer composites. Appl Phys Lett 81:5123–5125

[17] Gong HP, Zhong YH, Li JC et al (2000) Studies on nerve cell affinity of chitosan-derived materials. J Biomed Mater Res 52:285–295

[18] Drury JL, Mooney DJ (2003) Hydrogels for tissue engineering: scaffold design variables and applications. Biomaterials 24:4337–4351

[19] Zhao L, Mitomo H, Zhai ML et al (2003) Synthesis of antibacterial PVA/CM-chitosan blend hydrogels with electron beam irradiation. Carbohyd Polym 53:439–446

[20] Fernandes EG, Krauser S, Samour CM, Chiellini E (2000) Symmetric block oligomers. Gelation characteristics by DSC. J Therm Anal Cal 61:551–564

Poloxamine Hydrogels: from low Cell Adhesion Substrates to Matrices with Improved Cytocompatibility for Tissue Engineering Applications

Alejandro Sosnik, Omar F. Khan, Mark Butler and Michael V. Sefton

Abstract. Polyethylene glycol based hydrogels are being considered as tissue substitutes. Here we describe the preparation of synthetic collagen-mimetic material that are stiffer than collagen but that like collagen allow for both cell encapsulation and cell growth on the surface. These materials are poloxamine based hydrogels with and without collagen; poloxamine is a four-arm PEO-PPO block copolymer derivative, Tetronic™1107.

1 Introduction

The materials and constructs used in tissue engineering need to satisfy a number of fundamental constraints: (a) have sufficient mechanical properties; (b) satisfy mass transfer requirements; and (c) have biological tolerance. Hydrogel matrices comprise high water-content systems based on very hydrophilic materials that crosslink by physical or chemical bonds and superficially mimic the extracellular matrix. In addition to their structural versatility, gels display a unique combination of relatively high mechanical properties, high water contents, good biocompatibility and allow for fine tuning of porosity and pore size that will govern transport mechanisms (e.g., nutrient supply, waste clearance). Hence, they have become important materials in the design of tissue-engineered devices [1, 2].

Poly(ethylene oxide)-poly(propylene oxide) (PEO-PPO) block copolymers are a noteworthy family of gel-forming polymers [3, 4]. Due to their amphiphilic character (PEO and PPO blocks display high and low hydrophilicity, respectively), aqueous solutions undergo a distinctive and reversible sol-gel transition upon heating. Several mechanisms have been described in the literature as the driving force for gelation [5–8]. *In vivo* studies demonstrated that at most, only minor irritation was produced when PEO-PPO derivatives were administered in subcutaneous, intramuscular and intraperitoneal sites. [9]. Even though these polymers do not degrade under physiological conditions, the kidneys can clear unmodified molecules with molecular weights of up to 15 kDa [10–12]. According to their molecular structure, commercially available PEO-PPO block copolymers can be classified as: (a) linear PEO-PPO-PEO triblocks known as poloxamers (Pluronic®) and (b) their 4-arm counterparts, namely polox-

Barbucci R. (Ed): Hydrogels. Biological Properties and Applications.

amines (Tetronic®) [13]. The wide range of existing molecular weights and EO/PO ratios constitute one of the main advantages of these materials [13]. In addition, because a number of these block copolymers were approved by the FDA and EPA for use as food additives, pharmaceutical ingredients and in agricultural products, they are poised for use in biotechnology [14, 15, 16]. In the context of tissue engineering, drug delivery and pharmaceutical technology, poloxamers have been the major focus of investigational work. Poloxamines display two remarkable advantages worthy of comment:

a) The presence of an ethylenediamine central block gives the molecule two tertiary amine groups. These moieties contribute to thermal stability and confer both temperature and pH-dependency in aqueous media [17]. Moreover, they enable further chemical modification.
b) The branched structure and concomitant higher functionality provides a better platform for the design of highly crosslinked networks using polymer concentrations as low as 3–4 wt% [18].

Since pioneering investigations on PEO-PPO derivatives for biomedical applications focused on poloxamers, the first part of this work is dedicated to briefly highlighting their application in tissue engineering. In the second section, we summarize the developments involving their branched counterparts, including our own contributions to the field.

2 Poloxamers (Pluronic®)

Poloxamers have a variety of compositions [13]. However, only highly hydrophilic representatives like Pluronic F127 (MW 12 kDa, 70% PEO) have been studied as matrices for cell culture. This Pluronic has been used in FDA approved devices. In order to obtain relatively stable gels, polymer concentrations need be around 15 wt% [19, 20]. The first reports appeared in the late 1990s and described the use of a scaffold (polymeric [21] or metallic [22]) impregnated or superficially "painted" with cell-containing poloxamer solutions that maintained cells in place upon heating. The main applications included cartilage regeneration [23–26] but uses in nipple-areolar complex [27], bone [28, 29] and neuronal tissue [30] were also reported. The poor cell-adhesion properties of these derivatives were stressed by Liu *et al.* by using Pluronic F108 in order to create anti-adhesive domains in micropatterned surfaces for cell culture [31]. For the main work describing the use of the FDA-approved Pluronic F127 in cell culture and tissue engineering read References [21–30] and [32–47].

Poloxamer-based gels display relatively high permeability but their short residence times in the physiological environment limited clinical application [48]. Aiming at overcoming these drawbacks, Cohn and co-workers introduced a number of molecular modifications that led to systems combining sol-gel transitions at lower polymer concentrations and substantially improved stability and integrity in aqueous environments [49–51].The chain extension of commercially available poly(ethylene glycol) and poly(propylene gycol) precursors also enabled the design of polymers with

finely tuned hydrophilic/hydrophobic balance [52, 53]. Finally, chemical modification of terminal functional groups in PEO-PPO-PEO derivatives with methacryloyl [54, 55] or silane moieties [54, 56], and later covalent crosslinking of the polymeric chains, generated stiffer and more mechanically stable matrices. These modifications extended the applicability of the thermo-responsive systems tissue engineering to soft and hard tissues [57].

3 Poloxamines (Tetronic®)

As noted above, poloxamines have been less well studied as substrates for cell culture and growth. Some have investigated the basic aggregation pattern of some hydrophobic poloxamines [58–60]. Poloxamines have found application in the surface modification of particles [61, 62] and as preservatives in multi-purpose solutions for contact lenses [63]. One drawback stems from the fact that for similar molecular weights, 4-arm molecules are shorter than linear derivatives and hence, higher concentrations (20–30%) are often required to form gels. In recent years, interest in these derivatives displaying pH and temperature responsiveness has increased, especially in pharmaceutical sciences, for the solubilization of water-insoluble drugs by means of inclusion into polymeric micelles [13, 64, 65]. In tissue engineering, Cellesi et al. reported an initial application for poloxamine in 2004 [66]. The authors described a process denoted as "tandem gelation." First, the aqueous solution of the polymer underwent a fast thermal gelation and then, chemical crosslinking through a Michael-type addition rendered a mechanically stable matrix. High compatibility was observed when gelling systems were evaluated with fibroblasts. The proposed strategy was used for the preparation of cell-containing beads and was introduced as an alternative to alginate for immunoisolation [67]. However, due to the high content of the very hydrophilic PEO, these materials have limited cell attachment [31, 68, 69]. Thus, in order to attain matrices that would efficiently perform as substrates for cell embedding and cell growth on the surface, further modifications are needed. In the context of the design of a novel tissue engineered-modular construct that aims to maximize nutrient diffusion [70], our research group has investigated a number of approaches in order to enhance the compatibility of poloxamine networks for cell culture.

3.1 Poloxamine/collagen hybrids

3.1.1 Design of semi-interpenetrating networks and their characterization

Collagen, a main constituent of the extracellular matrix, displays a number of properties (e.g., biodegradability, low antigenicity and cell-binding properties) that make it an almost ideal material for cell culture in tissue engineering applications [71]. However, the poor mechanical properties are a main limitation in the design of matrices able to perform under physiological conditions such as during flow or in load bearing applications. This is the case of the modular construct designed in our laboratory [70].

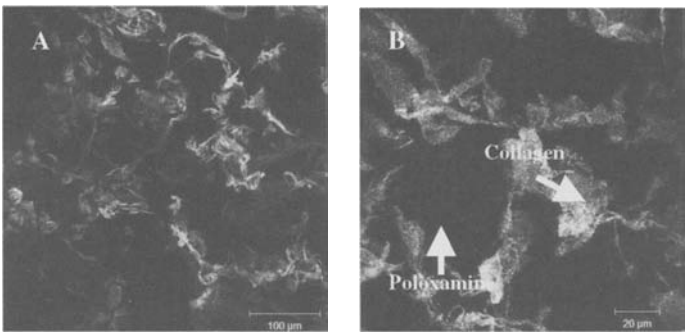

Fig. 1 A poloxamine/collagen matrix immunostained with a primary collagen antibody followed by secondary staining with AlexaFluor 568. Collagen (see arrow) stains while poloxamine (see arrow) is unstained and appears black. Collagen appeared in patches with regions of no staining dispersed among the collagen. **a** Scale bar = 100 µm and **b** Scale bar = 20 µm

Our concept was that a semi-synthetic material (hybrid) combining the higher stiffness of poloxamine crosslinked networks with the biological properties of collagen would result in matrices showing improved performance [18]. Poloxamine terminal –OH groups were reacted with isocyanate ethylmethacrylate. The introduction of unsaturated moieties enabled covalent crosslinking through a photoinitiated free radical polymerization reaction to generate mechanically stable hydrogels. Irgacure 2959 was chosen as the photoinitiator because of its relatively high cytocompatibility and its higher water solubility that enabled its solubilization in buffer. In order to produce collagen-containing systems, poloxamine precursor and collagen were thoroughly mixed and then photopolymerization was carried out under mild conditions [18]. Immonustaining of the gel with a primary collagen antibody followed by secondary staining with AlexaFluor 568 showed the heterogenicity of the hybrid (Fig. 1).

This was thought to reflect phase separation of the two macromolecules and is influenced to some extent by the pH of the mixture. This phenomenon is likely the result of collagen aggregation and precipitation following neutralization of the solution. Prior to neutralization, poloxamine/collagen mixtures were macroscopically homogeneous and transparent mixtures. Neutralization of poloxamine/collagen mixtures did not lead to gelation; systems became solid only after the photo-initiated chemical crosslinking of the modified poloxamine.

Measurements of the viscoelastic properties indicated that poloxamine-based matrices were substantially stiffer than pure collagen. Also, the addition of collagen did not affect the storage modulus of pure poloxamine networks [18]. The poloxamine/collagen mixtures were used in the production of cylindrical rods (modules) by crosslinking the system within a polyethylene tubing [70]. Surface analysis by a "deep freezing" ToF-SIMS methodology confirmed the presence of collagen molecules at the interface [72].

3.1.2 Cell embedding

The cytocompatibility of the network for cells embedded before crosslinking was evaluated. Preliminary studies were conducted with a human hepatoma cell line (HepG2) [18]. Cell viability studies indicated that photoinitiator concentrations in the range of 0.04 to 0.06% led to very good viability levels (around 80–90%). In the absence of collagen, cell viability was about 50% at day 1 [73]. An important criterion to assess the success of cell encapsulation was to measure the secretion of a marker for cell specific function. Hence, the release of α-antitrypsin by cells embedded in poloxamine/collagen matrices was monitored over 3 weeks and compared to pure collagen systems [73]. Findings showed a relatively constant release and even though poloxamine/collagen matrices displayed lower secretion levels than collagen, the maintenance of a functional phenotype was apparent [73]. In addition, cells stained with Vybrant CFDA SE, a fluorescent cytoplasmatic tracer, appeared to remain alive for about 2 months supporting the cytocompatibility of the matrix [73]. The behavior of other cell types has also been investigated. CRL-2481, an umbilical vein smooth muscle cell line (UVSMC), also showed good survival levels after crosslinking as seen by the small number of dead cells. Similar results were obtained with primary UVSMC.

The laboratory is investigating the applicability of the collagen/poloxamine matrices for adipose tissue engineering. Human adipose-derived stem cells (ASC) embedded in collagen/poloxamine and cultured in adipogenic medium accumulated intracellular lipid by Oil Red O staining indicative of ASC differentiation into mature adipocytes. ASC embedded in poloxamine hydrogels without collagen became nonviable over 7 days in culture, highlighting the importance of the collagen component in the hydrogel to provide sites for cell attachment.

3.1.3 Cell attachment on poloxamine/collagen hydrogels

These hydrogels are intended to support cell attachment and growth on the surface (especially of endothelial cells). As noted above, due to the PEO-rich nature of poloxamine-based matrices, negligible attachment was expected without the introduction of pro-adhesive modifications. Not surprisingly, there was a sharp increase in viability of HepG2 cells seeded on the surface (from 50 to 90%) when collagen was included in the composition [18]. Attached cells showed their characteristic morphology. The effect of cell density on attachment to poloxamine/collagen was measured with bovine aortic (BAEC) and human umbilical vein (HUVEC) endothelial cells (EC), and compared to collagen-free systems. In general, higher seeding cell density led to higher initial attachment. However, on pure poloxamine gels cells did not spread at all [18,73]. On the contrary, addition of collagen improved the initial attachment and a spread morphology was observed. When the number of attached cells was monitored with time, a decrease in cell density on the surface was apparent by day 5. Thus, even though surface analysis confirmed the presence of collagen [72], the concentration did not appear to be high enough to enable cell adhesion over time. Finally, the ability of the attached HUVEC to produce VE-Cadherin (a specific gap junction protein) was used to evaluate the phenotype of attached EC [73].

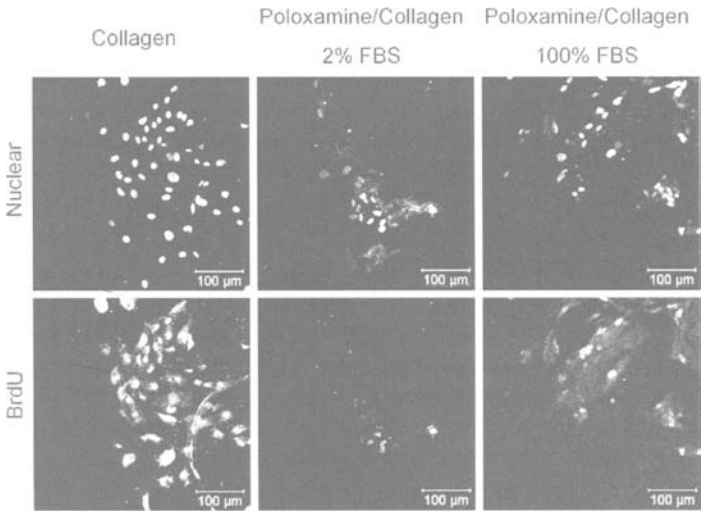

Fig. 2 HUVEC proliferation on poloxamine/collagen gels 6 days after initial seeding. BrdU stains newly synthesized DNA while SYTOX Green was used as a nuclear-counter stain. Each stain is shown separately. Poloxamine/collagen gels were pre-incubated in medium containing 2% FBS or 100% FBS overnight prior to cell seeding. Cells continued to proliferate 6 days after initial seeding but showed poor attachment for gels pre-incubated in 2% FBS. Cell attachment was much better after a 100% FBS pre-treatment. Scale bar = 100 µm

To further investigate the proliferative capacity of cells grown on poloxamine/collagen hydrogels and the effect of serum pre-incubation, HUVEC at passage 7 were seeded on the gels at a concentration of 10^5 cells/mL. The thymidine analog 5-bromo-2-deoxyuridine (BrdU) was used to label DNA synthesis in proliferating HUVEC. Sytox Green was used to assess nuclear staining (and hence cell attachment) (Fig. 2).

When grown on poloxamine/collagen gels pre-incubated in either 2% or 100% fetal bovine serum (FBS), HUVEC proliferated the day after seeding for both conditions. After 6 days of culture on hydrogels pre-incubated in 2% FBS, cells remained proliferative, however, there were fewer cells present. In contrast, cells were both proliferative and showed good adhesion to gels pre-incubated in 100% FBS. No cells were found on pure poloxamine gels, regardless of FBS pre-treatment. Thus, pre-incubation in 100% FBS improved cell adhesion to semi-synthetic gels and facilitated their growth over and coverage of the surface. In addition to EC morphology, cell phenotype was also explored.

Attached HUVEC are expected to display a non-activated phenotype. Because ICAM-1 and VCAM-1 are ligands for circulating leukocytes and aid their attachment and transendothelial migration *in vivo*, their level of expression on HUVECs grown on poloxamine/collagen is of interest as markers of EC activation. HUVEC (passage 7) grown on collagen/poloxamine gels for 8 days showed ICAM-1 expression, but no VCAM-1 expression (Fig. 3). In contrast, HUVEC grown on collagen-only

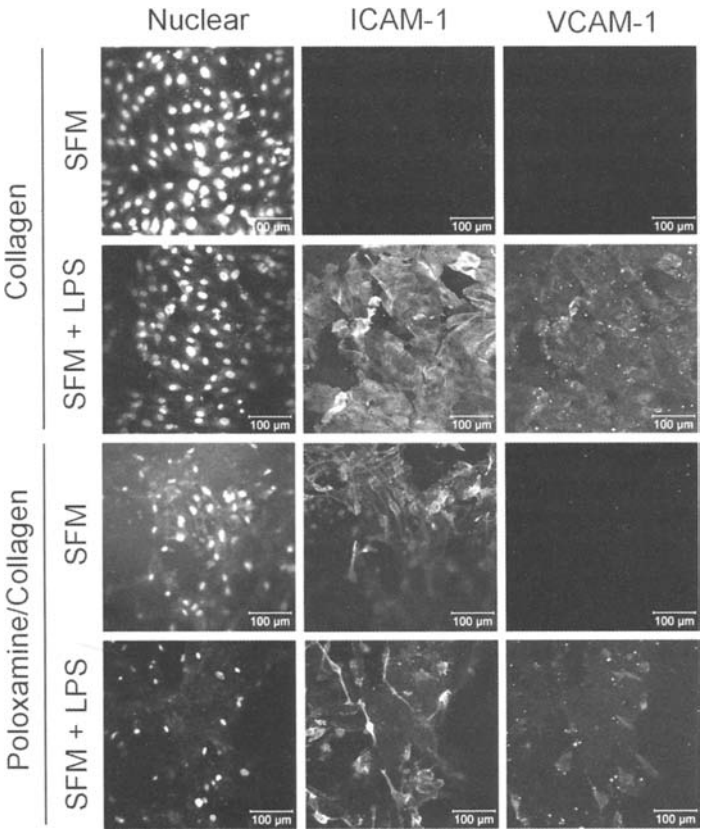

Fig. 3 ICAM-1 and VCAM-1 expression of HUVEC on collagen-only or poloxamine/collagen gels. Nuclei are stained with Hoechst. Each stain is shown separately. Cells incubated in serum-free medium (SFM) for 44.5 hours were compared to positive controls (incubation in SFM containing LPS). Higher ICAM-1 expression was seen on poloxamine/collagen gels as compared to collagen-only gels, thus indicating a slightly higher level of activation. No VCAM-1 expression was detected. Scale bar = 100 µm

gels showed neither ICAM-1 nor VCAM-1 expression. As before, there were almost no cells attached to poloxamine-only gels; however, for the exceptional cases where several cells remained, they showed high ICAM-1 expression. This behavior was similar to HUVEC behavior on other polymers such as tissue culture polystyrene, polypropylene and polyethylene terephthalate which show high ICAM-1 expression but poor VCAM-1 expression [74–76]. Thus, interactions with the semi-synthetic polymer may have induced some degree of HUVEC activation. The expected constitutive expression of ICAM-1 and poor expression of VCAM-1 in EC was not seen on collagen-only gel controls, perhaps because expression fell below the detection limit of confocal microscopy.

3.2 Positively-charged matrices

Aiming to further enhance EC attachment, other modifications and strategies were explored. With a view to exploring a fully synthetic means of enhancing cell attachment, especially on modules, we introduced positively-charged groups in the matrix to improve cell-matrix interaction. The rationale was that we would exploit two mechanisms: (a) primary electrostatic cell-surface interactions due to the electronegative nature of the cell membrane and (b) adsorption of pro-adhesive molecules (e.g., fibronectin) containing specific adhesion segments that are present in the culture medium. Materials were modified by two different synthetic pathways. The first comprised the introduction of positive charges by means of a photo-initiated free radical copolymerization reaction between the poloxamine-methacrylate derivative previously described and ([2-(methacryloyloxy)ethyl]-trimethylammonium chloride (MAETAC), a bifunctional molecule displaying a pH-independent cationic head (quaternary ammonium) and a reactive methacryloyl moiety [77]. The second relied on chemical modification of the poloxamine molecule by methylating the tertiary amine groups of the central ethylenediamine block [78].

3.2.1 Copolymerization of reactive poloxamine with quaternary ammonium methacrylates

This strategy involved the mixture of the two components for the production of a co-network. Different levels of modification were obtained by changing the poloxamine/modifier ratio. Thus, hydrogels with poloxamine contents of 6 to 12 wt% and MAETAC amounts from 0 to 0.48 M were synthesized and fully characterized [77]. Incorporation of quaternary ammonium groups was evaluated by elemental analysis; a gradual increase in nitrogen content was seen in agreement with calculated theoretical values, indicating an almost complete copolymerization. The modification was also supported by swelling assay. While MAETAC-free crosslinked poloxamine hydrogels showed slight shrinkage, specimens containing increasing concentrations of positively-charged groups gradually swelled. In addition, higher water uptake values in distilled water as opposed to PBS, was consistent with an increase in the osmotic gradient. As expected, the analysis of the viscoelastic behavior showed increasing values of storage (G') and loss (G") moduli for increasing concentrations of MAETAC (for similar poloxamine-methacrylate contents).

The main goal of the modification was to enhance cell-surface interaction. HepG2 cells attached well to MAETAC containing films and showed some spreading. HUVEC attached although they maintained a rounded morphology, characteristic of a non-adhesive phenotype. On the contrary, when prior to cell seeding, films were incubated in serum-containing medium, both cell types were well-spread and confluent monolayers were obtained (Fig. 4a). In addition, the production of VE-Cadherin indicated the formation of gap junctions, characteristic of EC maturation (Fig. 4b). These findings suggested that even if a better cell-surface interaction was attainable by cationic modification and cells attached, only after the pre-adsorption of serum proteins, would cells have the expected morphology. Since MAETAC and poloxam-

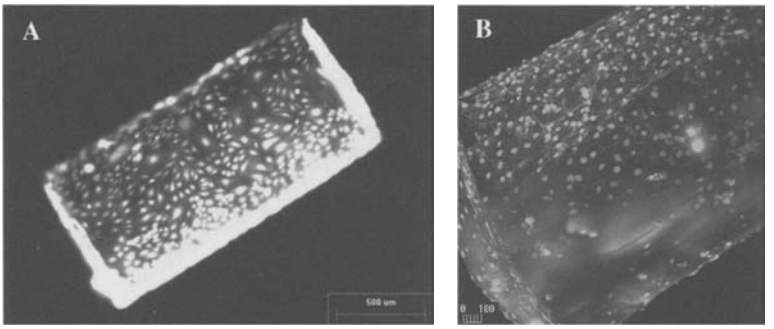

Fig. 4 HUVEC seeded on positively-charged poloxamine/MAETAC modules. **a** High viability levels (live cells stained green) and a relatively high surface coverage was observed at Day 5. Scale bar = 500 μm; **b** VE-Cadherin staining supported the formation of gap junctions (Day 5). Scale bar = 100 μm

ine have opposite effects on cell adhesion, the poloxamine-methacrylate/MAETAC ratio (i.e. the positive charge density) requires fine tuning for each poloxamine concentration and cell type [77].

A problem with the use of MAETAC was that HepG2 cells embedded in the gelling mixture rapidly lost viability in this system [77], precluding the use of the material for cell encapsulation. It constituted a proof of concept however, that by introducing positively-charged moieties, better cell attachment could be achieved in poloxamine hydrogels.

3.2.2 Methylation of poloxamine central block (quaternized poloxamine)

In order to improve the attachment properties of poloxamine hydrogels while minimizing the cytotoxicity of the system for encapsulated cells, tertiary amine groups of the central diamine block were methylated with iodomethane, resulting in quaternary ammonium groups in the polymer backbone. The subsequent incorporation of double bonds resulted in crosslinkable materials. The extent of methylation was ~ 60% as determined by means of the argentometric titration of chloride ions after replacing I^- counterions with Cl^- [78]. This was done due to some level of quenching of the free radical polymerization by I^- ions. As seen with poloxamine/MAETAC systems [77], the introduction of positive charges increased the osmotic gradient between the hydrogel and the aqueous environment. Tests in water led to high swelling [78], while in PBS, the values decreased substantially, reflecting the ionic nature of the hydrogel. Rheometric measurements indicated that these matrices displayed lower stiffness than un-methylated counterparts of similar concentration suggesting a less complete polymerization and a lower degree of crosslinking.

Here, the presence of tertiary amine groups capable of being exhaustively methylated was exploited in order to introduce positive charges to the network without increasing the concentration of reactive double bonds in the precursor mixture that would adversely affect cell viability. HepG2 cells stained with the Vybrant CFDA

tracer and encapsulated, showed better survival levels than with MAETAC or in poloxamine gels without collagen. However, a gradual decrease in viability was apparent during the first week of the study. Also, due to the low viscosity of the polymer solution, cells settled within the mixture resulting in a non-homogeneous distribution. With respect to surface properties, HepG2 displayed better attachment on methylated films pre-incubated in serum-containing medium [78]. Good attachment and the characteristic elongated shape were also apparent for HUVEC.

It is noteworthy that the PEO/positive charge ratio of the methylated derivative was lower than the optimal one as determined from MAETAC-containing systems [77]. Unfortunately, this ratio could not be fine tuned; increasing the concentration of quaternary ammonium groups in the precursor system meant an increase in the PEO-containing polymer. In contrast to their behavior on films, HUVEC seeded on modules attached poorly. This difference between films and modules was also seen on poloxamine/collagen rods [18]. These findings suggested that the static seeding procedure used for films enabled cells in suspension to settle on the surface and even if forming a loose interaction with the surface, they apparently attached and spread. In contrast, on modules, weak cell-surface forces probably resulted in limited initial attachment and later detachment.

3.3 The combined approach

While introduction of either collagen or positive charges had a favorable effect on the cell attachment properties of the poloxamine hydrogels, individually these were not enough to obtain the desired well-attached confluent monolayer. Thus, we investigated the potential synergistic effect of combining both modifications in the same system; modules made of collagen-containing methylated poloxamine networks were produced and evaluated. HepG2 cells were suspended in the precursor mixture and exposed to crosslinking conditions. A Live-Dead™assay revealed that cells remained mainly viable, suggesting good cytocompatibility of the process [78]. Furthermore, when ECs were cultured on methylated poloxamine/collagen modules, improved attachment and proliferation was noted (Fig. 5).

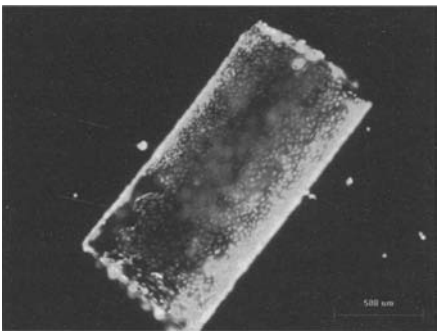

Fig. 5 Live HUVEC seeded on the surface of methylated-poloxamine/collagen modules, at day 1

While cells did not attach to poloxamine/collagen or methylated-poloxamine modules, the combination of the modifications led to a synergistic phenomenon and a high surface coverage was obtained. Scale bar = 500 μm.

This combination appears to result in the desired and controllable matrix characteristics. However long-term compatibility studies are needed to confirm the applicability of these systems in tissue engineering.

3.4 The degradable strategy

Due to the stability of methacrylate ester bonds against hydrolysis, all the poloxamine derivatives described in previous sections were considered non-degradable. There was some motivation, however, to modify the materials in order to obtain degradability under physiological conditions: (a) good integration of the construct with tissue in the implantation site is desired and (b) by enabling matrix remodelling including partial modification of the composition of the hydrogel (replacement of the original matrix by extracellular matrix), surfaces displaying higher pro-adhesive properties and, in consequence, better EC attachment could be generated.

The chemical modification involved the introduction of short poly(ester) blocks, a broadly used approach to confer hydrolytic sensitivity to water-containing systems [50]. In this framework, the first stage consisted of the reaction between terminal –OH groups of poloxamine with a lactone, epsilon-caprolactone or L-lactide, by a ring opening polymerization reaction in the presence of an organic tin (IV) catalyst, resulting in the generation of oligo(ester) blocks of about two repeating units [79]. The number of repeating units in the degradable block was an important consideration. In general, the longer the segment, the higher the probability of chain linkage and the faster the degradation rate. Observations indicated that longer poly(ester) blocks resulted in relatively low crosslinking density (higher molecular weight between crosslinks) and substantially affected the mechanical properties of the hydrogel; with longer degradable segments the resulting hydrogels were soft and disintegrated under normal manipulation conditions. Aiming at attaining stiffness levels similar to those displayed by non-degradable poloxamine/collagen systems, while rendering the materials sensitive to hydrolytic or enzymatic degradation, a minimal number of degradable units was incorporated. Subsequently the poloxamine-oligo(ester) derivative was acylated with methacryloyl chloride under mild conditions (room temperature) [54]. Preliminary studies were carried out with methacryloyl isocyanate [18]. However, crosslinking reactions failed, suggesting that a partial or total breakage of oligo(ester) blocks took place.

First, a derivative containing 2 caprolactone units *per* arm (8 total units *per* poloxamine molecule) was synthesized. In order to explore the cytocompatibility of the produced material, HepG2 cells were suspended in the mixture and exposed to UV light to produce modules. A relatively high survival was apparent after the crosslinking of the caprolactoyl-poloxamine/collagen matrix, as expressed by the large number of cells traced with Vybrant CFDA (Fig. 6a,b). Samples were incubated in serum-containing cell medium and followed over time to show the changes in the modules due to eventual cell proliferation. There was some proliferation, mainly on the surface

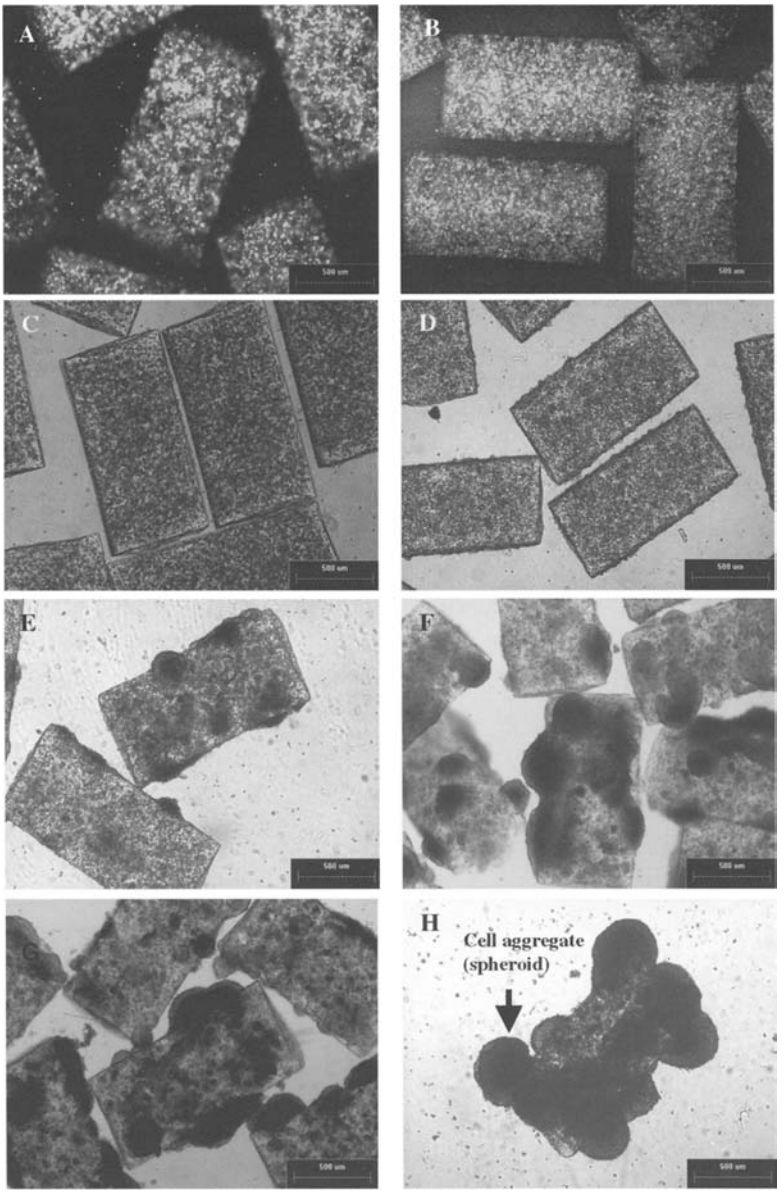

Fig. 6 HepG2 cells embedded in degradable PCL-poloxamine modules. A,B) Fluorescent micrographs of Vybrant CFDA traced HepG2 cells embedded in CL-containing poloxamine/collagen modules. **a** Day 0 and **b** Day 3; **c–h** Micrographs of HepG2 cells embedded in CL-containing poloxamine/collagen modules over time; **c** Day 0; **d** Day 3; **e** Day 18; **f** Day 21; **g** Day 27 and **h** Day 32. A very low remodelling extent was found, as apparent from the regular and uniform shape of the modules. Proliferation was apparent only at the surface and the presence of large HepG2 aggregates (spheroids) at the module surface was found. Scale bar = 500 μm

of the modules (see the formation of large cell groups at Day 18, Fig. 6e) and a very low extent of remodelling, as expressed by the regular and uniform shape that was apparent (see the sharp unchanged edges of the rods throughout the study, Fig. 6c–h).

Proliferation was apparent only at the surface and the presence of large HepG2 aggregates (spheroids) at the module surface was found. In this case, module size and shape remained practically unchanged, consistent with the relatively high stability of polycaprolactone-containing hydrogels [50]. In vitro degradation studies on films also showed no relevant weight losses over several months.

Since we were looking for more rapid degradation (2 to 4 weeks), further studies focused on lactoyl-based materials. Degradation was estimated with cell-free discs. While non-degradable poloxamine hydrogels lost about 8% of the initial weight after 14 days, lactoyl-based specimens had weight loss values between 20 and 39% after 5 days at 37 °C, depending on the concentration of the polymer and the crosslinking density [79]. Studies with HepG2 cells showed high cytocompatibility of the matrix for cell encapsulation [79]. In addition, in compositions with lower poloxamine content, some contraction of the matrix was seen, suggesting some remodelling of the network [79]. A gradual contraction of the matrix, changes in shape and surface roughening were found over time for both a UVSMC cell line and primary cells [79]. Fig. 7 shows the gradual remodelling process of the hydrogel for a UVSMC cell line-embedded matrix.

In order to study cell morphology and proliferation, both cell types were stained with Alexa Fluor 568 phalloidin (for filament actin) and Sytox Green (for nuclei), at different time points. The UVSMC cell line initially presented a rounded shape

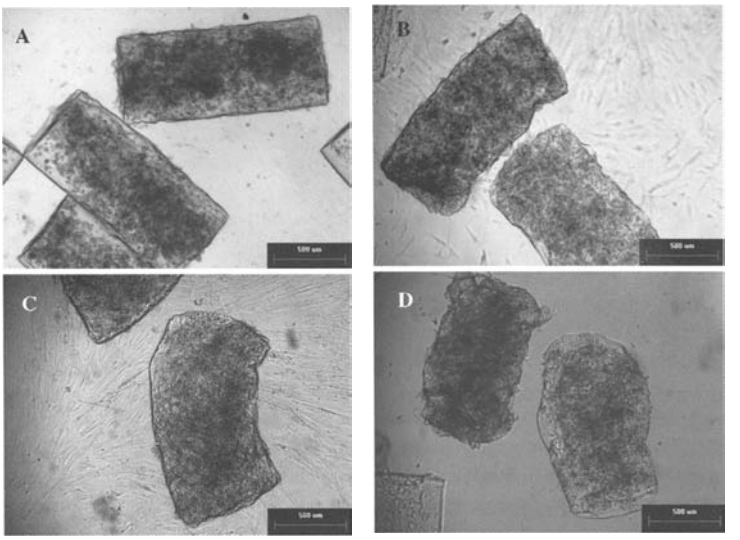

Fig. 7 Micrographs of a UVSMC cell line (CRL-2481) embedded in lactoyl poloxamine-methacrylate/collagen modules over time. **a** Day 1; **b** Day 21; **c** Day 27 and **d** Day 34. Scale bar = 500 μm

and a homogeneous distribution across the matrix [79]. Later on, cells spread to adopt the characteristic elongated pattern. Finally, the decrease in the observed cell density indicated that cells were dying. Primary UVSMC also displayed a uniform distribution upon crosslinking [79]. Unlike the cell line however, primary cells formed rounded clusters, and based on the apparent decrease in cell density, also a faster loss of viability [79]. It is remarkable however, that as empty areas appeared in the module, cell agglomerates grew in size, suggesting some extent of cell migration and proliferation. These results highlight the variability of the cell-matrix interaction not only in terms of different cell types but also among cells from different sources [79].

A central goal in making the matrix remodellable was to attain favourable conditions for embedded cells to secrete components of the extracellular matrix and hence improve the attachment of EC onto the surface. For example, in contrast to hydrogels without encapsulated cells where EC detached after a few days, in the presence of embedded CRL-2481 UVSMC, EC remained attached for about 9 days [79]. With primary UVSMC embedded in the degradable gel, HUVEC attachment was more limited, but VE-cadherin staining showed the formation of gap junctions [79]. In the present study, medium containing a low serum concentration as is appropriate for HUVEC was used. However, this medium may not have been adequate for the UVSMC and there were detrimental changes in UVSMC phenotype [80, 81]. Optimizing the co-culture medium in the context of this particular gel matrix was beyond the scope of this study, but is a necessary next step. Nonetheless, the premise that in a remodelable matrix, the underlying cells can enhance HUVEC attachment appears to be supported by our experience here and a full study to this effect is warranted.

4 Summary and perspectives

Until the mid 2000s, most of the work on PEO-PPO based materials focused on the linear counterparts. Branched derivatives however, present a number of characteristics that make them attractive for the design of mechanically robust substrates for cell encapsulation and attachment. Since these polymers display very low cell adhesion properties, we have been investigating the preparation of modified poloxamine networks that combine the higher mechanical properties of the crosslinked poloxamine with more cell-friendly features like cell adhesiveness. Two approaches were pursued: 1) the production of poloxamine/collagen hybrids and 2) the introduction of positively-charged moieties into the matrix. For example, we have shown that adipose-derived stem cells differentiated to a mature cell type as one indication of the cytocompatibility of the collagen-poloxamine matrix. In the context of endothelial cell-surface interaction, we have focused on analyzing the cell phenotype when attached to the poloxamine/collagen matrix and on optimizing the hydrogel composition in order to attain confluent EC covered modules that would enhance the blood-compatibility of the construct. While the goal of a fully synthetic collagen-mimetic material with high stiffness, high compatibility with embedded cells and strong attachment of endothelial cells has not yet been reached, several novel materials have been created which may find application in the creation of novel tissue engineering constructs.

References

[1] Drury JL, Mooney DJ (2003) Hydrogels for tissue engineering: scaffold design variables and applications. Biomaterials 24:4337–4351

[2] Hoffman AS (2002) Hydrogels for biomedical applications. Adv Drug Del Rev 54:3–12

[3] Moghimi SM, Hunter AC (2000) Poloxamers and poloxamines in nanoparticle engineering and experimental medicine. TIBTECH 18:412–420

[4] Aliabadi HM, Lavasanifar A (2006) Polymeric micelles for drug delivery. Exp Op Drug Del 3:139–162

[5] Rassing J, Atwood D (1983) Ultrasonic velocity and light-scattering studies of polyoxyethylene–polyoxypropylene–polyoxyethylene copolymer Pluronic F127 in aqueous solution. Int J Pharm 13:47–55

[6] Vadnere M, Amidon GL, Lindenbaum S et al (1984) Thermodynamic studies on gel–sol transition of some Pluronic polyols. Int J Pharm 22:207–218

[7] Wang P, Johnston TP. Kinetics of sol–gel transition for poloxamer polyols. J Appl Polym Sci 43:283–292

[8] Mortensen K (1992) Phase behavior of poly(ethylene oxide)-poly(propylene oxide)-poly(ethylene oxide) triblock-copolymer dissolved in water. Europhys Lett 19:599–604

[9] Reeve L (1997) The poloxamers: their chemistry and medical applications. In: Domb A, Kost Y, Wiseman D (ed) Handbook of Biodegradble Polymers (Drug Targeting and Delivery, vol. 7), Harwood Academic Publishers, London, Great Britain

[10] Pec EA, Wout ZG, Johnston TP (1992) Biologicalactivity of urease formulated in poloxamer 407 after intraperitoneal injection in the rat. J Pharm Sci 81:626–630

[11] Grindel JM, Jaworski T, Piraner O, Emanuele RM, Balasubramanian M (2002) Distribution, metabolism, and excretion of a novel surface-active agent, purified poloxamer 188, in rats, dogs, and humans. J Pharm Sci 91:1936–1947

[12] Batrakova EV, Li S, Li Y, Alakhov VYu, Elmquist WF, Kabanov AV (2004) Distribution kinetics of a micelle-forming block copolymer Pluronic P85. J Control Rel 100:389–397

[13] Chiappetta DA, Sosnik A (2007) Poly(ethylene oxide)-Poly(propylene oxide) block copolymer micelles as drug delivery agents: Improved hydrosolubility, stability and bioavailability of drugs. Eur J Pharm Biopharm 66:303–317

[14] Bromberg LE, Ron ES (1998) Temperature-responsive gels and thermogelling polymer matrices for protein and peptide delivery. Adv Drug Del Rev 31:197–221

[15] Kabanov AV, Alkhov VYu (2002) Pluronic®block copolymers in drug delivery: From micellar nanocontainers to biological response modifiers. Critical Rev Therap Drug Carrier Syst 19:1–72

[16] Kibbe AH (2000) Handbook of Pharmaceutical Excipients. American Pharmaceutical Association, Washington DC

[17] Dong J, Chowdhry BZ, Leharne SA (2003) Surface activity of poloxamines at the interfaces between air–water and hexane–water. Colloids and Surfaces A: Physicochem Eng Aspects 212:9–17

[18] Sosnik A, Sefton MV (2005) Semi-synthetic collagen/poloxamine matrices for Tissue Engineering. Biomaterials 26:7425–7435

[19] Barichello JM, Morishita M, Takayama K et al (1999) Absorption of insulin from Pluronic F-127 gels following subcutaneous administration in rats. Int J Pharm 184:189–198

[20] Scherlund M, Brodin A, Malmsten M (2000) Micellization and gelation in block copolymer systems containing local anesthetics. Int J Pharm 211:37–49

[21] Are'valo-Silva CA, Eavey, RD, Cao Y et al (2000) Internal support of tissue-engineered cartilage. Arch Otolaryng - Head Neck Surg 126:1448–1452

[22] Kamil SH, Vacanti MP, Aminuddin BS et al (2004) Tissue Engineering of a human sized and shaped auricle using a mold. Laryngoscope 114:867–870
[23] Cao Y, Rodriguez A, Vacanti M et al (1998) Comparative study of the use of poly(glycolic acid), calcium alginate and pluronics in the engineering of autologous porcine cartilage. J Biomater Sci Polym Ed 9:475–487
[24] Saim, AB, Cao Y, Weng Y et al (2000) Engineering autogenous cartilage in the shape of a helix using an injectable hydrogel scaffold. Laryngoscope 110:1694–1697
[25] Are'valo-Silva CA, Cao Y, Vacanti M et al (2000) Influence of growth factors on tissue-engineered pediatric elastic cartilage. Arch Otolaryng-Head Neck Surg 126:1234–1238
[26] Are'valo-Silva CA, Cao Y, Weng Y et al (2001) The effect of fibroblast growth factor and transforming growth factor-β on porcine chondrocytes and tissue-engineered autologous elastic cartilage. Tissue Engineering 7:81–88
[27] Cao YL, Lach E, Kim TH et al (1998) Tissue-engineered nipple reconstruction. Plastic Reconst Surg 102:2293–2298
[28] Weng Y, Cao Y, Silva CA et al (2001) Tissue-engineered composites of bone and cartilage for mandible condylar reconstruction. J Oral Maxillofacial Surg 59:185–190
[29] Weinand C, Pomerantseva I, Neville CM et al (2006) Hydrogel-β-TCP scaffolds and stem cells for tissue engineering bone. Bone 38:555–563
[30] Komiyama T, Nakao Y, Toyama Y et al (2004) Novel technique for peripheral nerve reconstruction in the absence of an artificial conduit. J Neurosci Methods 134:133–140
[31] Liu VA, Jastromb WE, Bhatia SN (2002) Engineering protein and cell adhesivity using PEO-terminated triblock polymers. J Biomed Mater Res 60:126–134
[32] Kamil SH, Eavey RD, Vacanti MP et al (2004) Tissue-engineered cartilage as a graft source for laryngotracheal reconstruction: A pig model. Arch Otolaryng-Head Neck Surg 130:1048–1051
[33] Terada S, Yoshimoto H, Fuchs JR et al (2005) Hydrogel optimization for cultured elastic chondrocytes seeded onto a polyglycolic acid scaffold. J Biomed Mater Res 75A: 906–917
[34] Zhou G, Liu W, Cui L et al (2005) In vivo chondrogenesis of BMSCs at non-chondrogenesis site by co-transplantation of BMSCs and chondrocytes with pluronic as biomaterial. Key Eng Mater 288–289:1–6
[35] Chua KH, Aminuddin BS, Fuzina NH et al (2005) Insulin-Transferrin-Selenium prevent human chondrocyte dedifferentiation and promote the formation of high quality tissue engineered human hyaline cartilage. Eur Cells Mater 9:58–67
[36] Ruszymah BHI, Chua K, Latif MA et al (2005) Formation of in vivo tissue engineered human hyaline cartilage in the shape of a trachea with internal support. Int J Ped Otorhinolaryng 69:1489–1495
[37] Roberts A, Wyslouzil, BE, Bonassar L (2005) Aerosol delivery of mammalian cells for tissue engineering. Biotech Bioeng 91:801–807
[38] Xu X, Lou J, Tang T et al (2005) Evaluation of different scaffolds for BMP-2 genetic orthopedic tissue engineering. J Biomed Mater Res-Part B 75:289–303
[39] Weinand I, Pomerantseva C, Neville R et al (2006) Hydrogel-β-TCP scaffolds and stem cells for tissue engineering bone. Bone 38:555–563 C
[40] Cortiella J, Nichols JE, Kojima K et al (2006) Tissue-engineered lung: An in vivo and in vitro comparison of polyglycolic acid and pluronic F-127 hydrogel/somatic lung progenitor cell constructs to support tissue growth. Tissue Eng 12:1213–1225
[41] Lee YJ, Kim IA, Park SA et al (2007) A tissue engineering based approach to regeneration of intervertebral disc. Key Eng Mat 342–343:397–400
[42] Monroy A, Kojima K, Ghanem M et al (2007) Tissue engineered cartilage "bioshell" protective layer for subcutaneous implants. Int J Ped Otorhinolaryng 71:547–552

[43] Hu H-L, Cao Y-L, Chen T-T et al (2007) Tissue engineered allogeneic cartiage induces local immune privilege in rabbits. J Clin Rehab Tissue Eng Res 11:2757–2760
[44] Idrus RBH, Hui CK, Ibrahim FW et al (2007) The expansion potential of human nasal septum chondrocytes for the formation of engineered cartilage. Science Asia 33:145–152
[45] Jeong JH, Moon YM, Kim SO et al (2007) Human cartilage tissue engineering with pluronic and cultured chondrocyte sheet. Key Eng Mat 342–343:89–92
[46] Vashia AV, Keramidarisa E, Abbertona KM et al (2008) Adipose differentiation of bone marrow-derived mesenchymal stem cells using Pluronic F-127 hydrogel *in vitro*. Biomaterials 29:573–579
[47] Thonhoff JR, Lou DI, Jordan PM et al (2008) Compatibility of human fetal neural stem cells with hydrogel biomaterials in vitro. Brain Res 1187:42–51
[48] Dumortier G, Grosslord JL, Agnely F et al (2006) A review of poloxamer 407 pharmaceutical and pharmacological characteristics. Pharm Res 23:2709–2728
[49] Cohn D, Sosnik A, Levy A (2003) Improved reverse thermo-responsive polymeric systems. Biomaterials 24:3707–3714
[50] Cohn D, Lando G, Sosnik A et al (2006) PEO-PPO-PEO based poly(ether ester urethane)s as degradable thermo-responsive multiblock copolymers. Biomaterials 27:1718–1727
[51] Cohn D, Sosnik A, Malal R et al (2007) Chain extension as a strategy for the development of improved reverse thermo-responsive polymers. Poym Adv Tech 18:731–736
[52] Cohn D, Sosnik A (2003) Novel reverse thermo-responsive injectable poly(ether carbonate)s J Mat Sci Mater Med 14:175–180
[53] Sosnik A, Cohn D (2005) Reverse thermo-responsive poly(ethylene oxide) and poly(propylene oxide) multiblock copolymers. Biomaterials 26:349–357
[54] Sosnik A, Cohn D, San Román J et al (2003) Crosslinkable PEO-PPO-PEO-based reverse thermo-responsive gels as potentially injectable materials. J Biomater Sci Pol Ed 14:227–239
[55] Cohn D, Sosnik A, Garty S (2005) Smart hydrogels for in situ-generated implants. Biomacromolecules 6:1168–1175
[56] Sosnik A, Cohn D (2004) Ethoxysilane-capped PEO-PPO-PEO triblocks: a new family of reverse thermo-responsive polymers. Biomaterials 25:2851–2858
[57] Slavin S, Gurevitch O, Kullkarni BG et al (2006) Compositions comprising bone marrow cells, demineralized bone matrix and various site-reactive polymers for use in the induction of bone and cartilage formation, US Pt Appl #20060177387
[58] Armstrong JK, Chowdry BZ, Snowden MJ et al (2001) The effect of pH and concentration upon aggregation transitions in aqueous solutions of poloxamine T701. Int J Pharm 229:57–66
[59] Dong J, Chowdry BZ, Leharne SA (2003) Solubilisation of polyaromatic hydrocarbons in aqueous solutions of poloxamine T803. Colloids and Surfaces A: Physicochem Eng Aspects 246:91–98
[60] Dong J, Armstrong J, Chowdry BZ et al (2004) Thermodynamic modelling of the effect of pH upon aggregation transitions in aqueous solutions of the poloxamine, T701. Therm Acta 417:201–206
[61] Storm G, Belliot SO, Daemen T et al (1995) Surface modification of nanoparticles to oppose uptake by the mononuclear phagocyte system. Adv Drug Del Rev 17:31–48
[62] Redhead HM, Davis SS, Illum L (2001) Drug delivery in poly(lactide-co-glycolide) nanoparticles surface modified with poloxamer 407 and poloxamine 908: In vitro characterisation and in vivo evaluation. J Control Rel 70:353–363
[63] Sumide T, Tsuchiya T (2003) Effects of multipurpose solutions (MPS) for hydrogel contact lenses on gap-junctional intercellular communication (GJIC) in rabbit corneal keratocytes. J Biomed Mater Res- Part B 64:57–64

[64] Alvarez-Lorenzo C, Gonzalez-López CJ, Fernández-Tarrio M et al (2007) Tetronic micellization, gelation and drug solubilization: Influence of pH and ionic strength. Eur J Pharm Biopharm 66:244–252

[65] Chiappetta DA, Degrossi J, Teves S et al (2008) Triclosan-loaded poloxamine micelles for enhanced antibacterial activity against biofilm (in press)

[66] Cellesi F, Tirelli N, Hubbell JA (2004) Towards a fully-synthetic substitute of alginate: development of a new process using thermal gelation and chemical cross-linking. Biomaterials 25:5115–5124

[67] Cellesi F, Weber W, Fussenegger M et al (2004) Towards a fully synthetic substitute of alginate: Optimization of a thermal gelation/chemical cross-linking scheme ("tandem" gelation) for the production of beads and liquid-core capsules. Biotechn Bioeng 88:740–749

[68] Winblade ND, Schmokel H, Baumann M et al (2002) Sterically blocking adhesion of cells to biological surfaces with a surface-active copolymer containing poly(ethylene glycol) and phenylboronic acid. J Biomed Mater Res 59:618–631

[69] Llanos GR, Sefton MV (1993) Immobilization of poly(ethylene glycol) onto a poly(vinyl alcohol) hydrogel. 2. Evaluation of thrombogenicity. J Biomed Mater Res 27:1383–1391

[70] McGuigan AP, Sefton MV (2006) Vascularised organoid engineered by modular assembly enables blood perfusion. Proc Natl Acad Sci USA 103:11461–11466

[71] Lee CH, Singla A, Lee Y (2001) Biomedical applications of collagen. Int J Pharm 221:1–22

[72] Sosnik A, Brodersen P, Sodhi RNS et al (2006) Surface study of collagen/poloxamine hydrogels by a 'deep freezing' ToF-SIMS approach. Biomaterials 27:2340–2348

[73] Sosnik A, Leung B, McGuigan AP et al Collagen/poloxamine hydrogels: Cytocompatibility of embedded HepG2 cells and surface attached endothelial cells. Tissue Eng 11:1807–1816

[74] Margiotta MS, Robertson FS, Greco RS (1992) The adherence of endothelial cells to Dacron induces the expression of the intercellular adhesion molecule (ICAM-1). Ann Surg 216: 600–604

[75] Cenni E, Granchi D, Ciapetti G et al (1997) Expression of adhesion molecules on endothelial cells after contact with knitted Dacron. Biomaterials 18:489–494

[76] Granchi D, Cenni E, Verri E et al (1998) Adhesive protein expression on human endothelial cells after in vitro contact with woven Dacron. Biomaterials 19:93–98

[77] Sosnik A, Sefton MV (2005) Poloxamine hydrogels with a quaternary ammonium modification to improve cell attachment. J Biomed Mater Res-Part A 75:295–307

[78] Sosnik A, Sefton MV (2006) Methylation of poloxamine for enhanced cell adhesion. Biomacromolecules 7:331–338

[79] Sosnik A, Leung BM, Sefton MV (2008) Lactoyl-poloxamine/collagen matrix for cell-containing modules. J Biomed Mater Res-Part A (in press)

[80] Leung BM (2005) A modular vascularized Tissue Engineering construct containing smooth muscle cells and endothelial cells. M.Sc. Thesis. University of Toronto, Toronto, Canada

[81] Leung BM, Sefton MV (2007) A modular Tissue Engineering construct containing smooth muscle cells and endothelial cells. Ann Biomed Eng 35:2039–2049

Biohydrogels for the *In Vitro* Re-construction and *In Situ* Regeneration of Human Skin

Liudmila Korkina, Vladimir Kostyuk and Liliana Guerra

Abstract. Natural and synthetic biohydrogels are of great interest for the development of innovative medicinal and cosmetic products feasible for the treatment of numerous skin diseases and age-related changes in skin structure and function. Here, the characteristics of bio-resorbable hydrogels as scaffolds for the *in vitro* re-construction of temporary skin substitutes or full skin equivalents for further transplantation are reviewed. Another fast developing area of regenerative medicine is the *in situ* regeneration of human skin. The approach is mainly applicable to activate and facilitate the skin regeneration process and angiogenesis in chronic wounds with impaired healing. In this case, extracellular matrix resembling polymers are used to stimulate cell growth, adhesion, and movement. Better results could be achieved by activation of biocompatible hydrogels either with proteins (growth factors, adhesion molecules or/and cytokines) or with allogenic skin cells producing and releasing these molecules. Hydrogels are widely applied as carriers of low molecular weight substances with antioxidant, anti-inflammatory, anti-ageing, and wound healing action. Incorporation of these substances into hydrogels enhances their penetration through the skin barrier and prevents their destruction by oxidation. Potential roles of hydrogel-based products for modern dermatology and cosmetology are also discussed.

1 Biohydrogels as scaffolds for *in vitro* produced skin equivalents

In humans, skin is the largest organ with essential physical, chemical, and biological barrier properties. Skin damage such as trauma, disease, burns or surgery brings dramatic consequences for the whole organism. Bioengineered skin substitutes represent a modern tool in treating acute and chronic skin wounds by advanced cell-based therapies. Although there are no examples of bioengineered skin that completely replicate anatomy (Fig. 1a), physiology, biological stability, and aesthetic aspect of intact skin, *in vitro* expanded skin equivalents could be auto-transplanted in cases of severe burns, chronic ulcers of different origin, and pigment defects with long-lasting satisfactory clinical and aesthetic outcomes [1–3]. To our knowledge, the first company commercializing world-wide cultured autografts was the Biosurface Technology Inc. (now Genzyme Biosurgery, Cambridge, MA). Its product (Epicel®) is manufactured fol-

Barbucci R. (Ed): Hydrogels. Biological Properties and Applications.

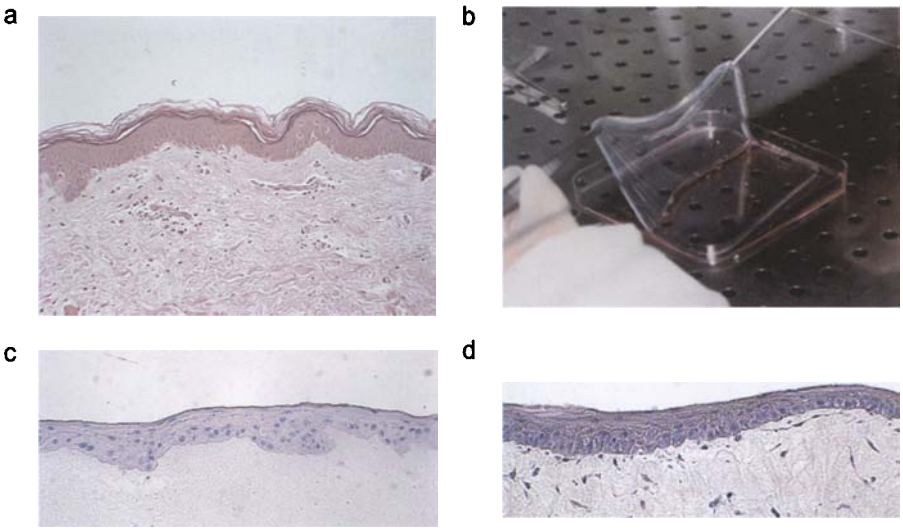

Fig. 1 Histology of human skin and reconstructed *in vitro* skin equivalents. **a** Histology of normal human skin, with well differentiated epidermal cell layers, evenly distributed ridges and complex dermal compartment (Hematoxylin-eosin staining; ×20 magnification); **b** Appearance of the fibrin gel prepared with a commercially available fibrin glue; **c** Histology of an epidermal equivalent reconstituted on fibrin gel (Hematoxylin-eosin staining; ×20 magnification). Only two/three cell layers are present in the *in vitro* reconstructed epidermis. However, when cultured keratinocytes are applied to the wound bed, they take, proliferate and differentiate, resulting in fully regenerated epidermis; **d** Histology of a skin equivalent reconstituted on a fibroblast-containing collagen gel (Hematoxylin-eosin staining; ×20 magnification)

lowing the original technique described previously [4], and epidermal sheets, which are transplanted using a petrolatum gauze support, are currently successfully applied in several Burn Units in the USA and Europe on massive full-thickness burns (reviewed in [3]). Patients successfully treated with this technology now have a follow up of almost 25 years. Mechanical fragility was considered among the major disadvantages of Epicel [5]. In order to i) optimize production, ii) make handling of cultured autografts easier and iii) render long-distance transportation less complicated, companies and public institutions developed new culture technologies using cultivation of epidermal cells on different carriers.

Skin re-construction on the appropriate scaffold could take place either in *in vitro* laboratory conditions or *in situ* directly at the site of skin damage. For *in vitro* tissue engineering, matrices are developed to support cultured cells and promote their differentiation and proliferation towards the formation of new tissue. Substrates-scaffolds enabling proper wound coverage should have some essential characteristics which include: 1- being easy to handle and apply to the wound site; 2- provide appropriate barrier function; 3- be readily adherent; 4- have appropriate physical and mechanical properties; 5- undergo controlled degradation; 6- be sterile, non-toxic, and non-antigenic; 6- evoke minimal inflammatory reactivity; 7- incorporate into the

host with minimal pain and low risk of further scarring; 8- facilitate angiogenesis; 9- be cost effective [6].

Different materials have been proposed to be used as scaffolds for skin cells. For example, three-dimensional (3D) biodegradable natural or synthetic hydrogels, which undergo polymerization in the presence of cells mixed with the monomer solution. Natural polymers similar to macromolecules of the extracellular matrix (ECM) are recognized by skin and immune cells as the body's own substances that allows avoidance of a primary inflammatory response, chronic immunological reactions and toxicity, often induced by synthetic polymers [7].The principal structural elements of ECM are formed by collagens, a family of closely related but distinct extracellular matrix proteins. More than 20 genetically different forms have been identified, type I being the most abundant and most investigated for biomedical applications [8]. Only collagen types I, II, III, V, and XI self-assemble into fibrils, whereas some collagens form networks (types IV, VIII and X), a typical example of which is the basement membrane, mostly made of collagen IV [9]. The important role of collagens in maintaining the extracellular structure resulted in numerous tissue engineering applications, employing collagen as an ideal scaffold or matrix for cell growth and proliferation [10]. Particular characteristics such as high mechanical strength, excellent biocompatibility and water-uptake properties, biodegradation and low antigenic potential make collagen a golden standard for polymers to be used for tissue engineering purposes [7].

Statistically, fibrin and hyaluronic acid are the most frequently used scaffolds for *in vitro* skin engineering. Commercially available hyaluronic acid-based *in vitro*-engineered skin substitutes for clinical application are Hyalograft 3D® and Laserskin® (Fidia Advanced Biopolymers, Padova, Italy). Hyalograft 3D® is a 100% benzyl-esterified derivative of hyaluronic acid (Hyaff-11) processed into fibres and prepared as a flat, non-woven dressing which is seeded with autologous fibroblasts before clinical application. Laserskin is a 100% benzyl-esterified hyaluronic acid-membrane for the culture and delivery of autologous keratinocytes. Laser drilled microperforations allow keratinocytes to migrate through the membrane onto the wound bed [11].

Fibrin substrates may be prepared *ad hoc* from commercially available surgical fibrin glues [12], which contain clot-forming fibrinogen, fibronectin, and factor XIII. Human thrombin is also present in the fibrin glue kit. In order to prepare a biological substrate for cultured cells, fibrinogen and thrombin are diluted with a sterile physiological solution and mixed together [3,13]. When the two substances are mixed, thrombin, in the presence of calcium, converts fibrinogen into fibrin. The mixture is gently poured onto the bottom of culture dishes and is quickly and evenly distributed before the fibrin is completely polymerized, which usually occurs in less than 4 min [13]. Under these conditions, the fibrin matrix is a homogeneous and transparent gel (Fig. 1b) where cell growth may be easily monitored. When keratinocyte-containing fibrin gels (Fig. 1c) are applied to the wounds, fibrin is quickly degraded, allowing cells to take on the wound bed. Accurate quality controls have demonstrated that keratinocyte clonogenic ability, growth rate and long-term proliferative potential are not affected by fibrin and that human epidermal stem cells are preserved when

keratinocytes are cultivated on a fibrin substrate [3,13]. BioSeed®-S (BioTissue Technologie, Freiburg, Germany) is a fibrin gel-based autologous epidermal replacement product [14]. The product consists of autologous keratinocytes grown for 2–3 weeks in the laboratory and finally suspended in a gel-like fibrin adhesive. The gel-like skin graft is applied to the patient's wound with a syringe, so that it is easy to handle. The fibrin adhesive fixes the cells to the wound and allows better in-growth.

Synthetic gels have been introduced for a greater control over physical and chemical properties of the 3D culture environment. The homogeneous nature of synthetic hydrogels provides matrix uniformity and simplifies biochemical assays [15]. Usually, synthetic hydrogels are not explicitly bioactive, and harsh polymerization conditions (i.e., free radical initiation and limited biocompatibility of monomeric components) may prevent their use as cell-entrapping materials [15].

PEG hydrogels are commonly used synthetic gels because of their high biocompatibility and precise control of reaction kinetics during rapid photopolymerization, providing a spatially well-controlled 3D gel-scaffold for skin cells [15].

Natural and synthetic polymers are frequently hybridized to compensate for the shortcomings each may possess alone. For example, copolymerization of PEG with natural polymers such as hyaluronan and collagen, enables a better control over the physical and biochemical properties of natural and synthetic cell entrapping materials [15].

Chitosan (Cs), gelatin (Gel) and polylactic-co-glycolic acid (PLGA) in combination with hyaluronic acid or collagen have also been used to form a bilayered skin equivalent as well as collagen–poly caprolactone (PCL), cellulose derivatives, carrageenan, polyacrylates, polyvinyl alcohol, polyvinyl pyrrolidone and silicones [16].

2 Biohydrogels for *in situ* human skin regeneration

Another fast developing approach for the treatment of skin lesions is the use of combined tissue engineering products consisting of hydrogels bioactivated with growth factors, and low molecular weight molecules [17] that facilitates wound closure by directing keratinocyte/fibroblast migration and vascular network formation. The major aim of this emerging approach is to develop and apply bioactivated 3D degradable hydrogels, which can stimulate wound closure by activating skin cells and promoting angiogenesis *in situ* at the site of the skin lesion. The biological activation of a hydrogel could be achieved by chemical binding of growth factors approved for medicinal use such as VEGF (vascular endothelial growth factor), RGDS tetra-peptide [18], and its synthetic analogue RAM with the polymer (see below).

A hydrogel could be activated in the presence of cultivated skin cells, where cells act as "biological factories" producing cytokines and growth factors to stimulate the patient's own wound repair mechanism [19]. Indeed, the graft take of autologous cells inserted into a hydrogel is rather poor in chronic non-healing wounds. The lack of dermis is a critical factor for cell engraftment in chronic and acute wounds. However, many other factors can impair healing in chronic wounds such as local factors (presence of foreign bodies, tissue maceration, ischaemia, and infection) as well as

systemic factors (advanced age, venous insufficiency, ischemia, diabetes) [20]. In addition, reduction in tissue growth factors, an imbalance between proteolytic enzymes and their inhibitors, and the presence of senescent cells seem to be particularly important in chronic wounds [20, 21]. Thus, hydrogel-containing skin substitutes may stimulate wound healing in chronic ulcers by production of growth factors and extracellular matrix (ECM) components, with re-epithelialization proceeding from the edge of the wound and from islands of epithelium in the wound bed. Numerous autologous and allogenic skin substitutes have been utilized to treat chronic leg ulcers in patients with impaired wound healing [5, 22–25]. Collagen is one of the most popular materials for the majority of dermal substitutes (Fig. 1d). Apligraf® (formerly Graftskin®, Organogenesis Inc, Canton, MA) is an allogenic bilayered skin substitute consisting of a dermal equivalent composed of type I bovine collagen which contains human fibroblasts and an overlying epidermal layer of human keratinocytes derived from neonatal foreskin. The mechanism of action of Apligraf has not been clearly elucidated but it may work inducing wound closure by re-epithelialization from the wound margins and stimulation of wound healing through growth factors and ECM components [24].

Integra® (Integra LifeSciences, Plainsborough, NJ) is a bioengineered, cell-free dermal matrix composed of a porous matrix of crosslinked bovine type I collagen and glycosaminoglycans (chondroitin-6-sulphate) overlayered with a temporary substitute made of semi-permeable polysiloxane (silicone). It is used as a dermal template in the surgical management of diabetic foot ulcers and stimulates production of endogenous collagen and growth of resident fibroblasts and keratinocytes [22, 26].

The extracellular matrix (ECM) is the optimized milieu that has evolved to maintain homeostasis and to direct tissue development. Its biochemical and biophysical properties are responsible for integrity of individual cells, their migration, adhesion, nutrition and differentiation as well as for angiogenesis and formation of intracellular contacts [27].

A great effort has been made to mimic the ECM to guide morphogenesis in tissue repair and tissue engineering [28]. As the ECM plays an instructive role in cell activities, the hypothesis here is that biopolymers could maintain the biological information and other physical and chemical features, which would preserve a potential space for new tissue development after cell seeding. In some cases, the surface of synthetic hydrogels for *in situ* tissue engineering is modified by the ECM proteins [29]. The ECM is composed of proteins (collagenous and non-collagenous) and polysaccharides. Fibronectin is an example of a non-collagenous multifunctional component of the ECM. It is known to induce cell attachment and spreading. Intracellular signaling induced by cell adhesion on fibronectin plays a critical role in cytoskeletal organization, cell cycle progression and cell survival [5]. Glycosoaminoglycans (GAGs) are linear chains consisting of repeating units of a disaccharide, generically a hexosamine (glucosamine or galactosamine) and a uronic acid component [8]. Owing to their ionic character, GAGs are able to absorb large quantities of water, and this osmotic swelling provides compressive strength. The most spectacular example of a GAG is hyaluronic acid, a linear polysaccharide composed of linked disaccharide units, which consists

of D-glucuronic acid and N-acetyl-D-glucosamine (GlcNAc). The disaccharide units of hyaluronic acid are extended, forming a rigid molecule whose numerous repelling anionic groups bind cations and water molecules. Being applied externally to a skin wound, hyaluronic acid promotes epithelial migration and differentiation, improves angiogenesis, and enhances collagen production. Industrial production of hyaluronic acid as a medical device accelerating wound healing is based on microbial fermentation, enabling the scale-up of derived products and avoiding the risk of animal-derived pathogens. Chemical modifications of natural hyaluronic acid have brought an array of hyaluronan-based materials widely used as biodegradable hydrogel scaffolds for *in situ* regeneration of the skin. A family of Hylan products is characterized by two specific functional groups of the hyaluronic acid chain, i.e. the carboxylic and N-acetylic groups. The majority of cross-linked materials are water-insoluble gels with a higher viscosity and chemical stability than the parent molecule of hyaluronic acid [30]. New hyaluronic acid-derivative polymers called Hyaff® have been obtained by a coupling reaction. The benzyl esters Hyaff-11 and Hyaff-11p75 induce (under test conditions) the hydrolytic degradation of ester bonds in the absence of enzymatic activity. The degradation periods for Hyaff vary from 1–2 weeks to 2–3 months, and degradation rates depend on the degree of esterification [30]. The previously described hyaluronic acid-based products Hyalograft 3D® and Laserskin® have been reported to improve healing in diabetic dorsal foot ulcers in a controlled, randomized clinical trail [31].

Dermagraft® (Advanced BioHealing Inc, La Jolla, CA) is a cryopreserved living dermal structure manufactured by cultivating allogenic fibroblasts on a synthetic polymer scaffold (polyglycolic acid or polyglactin-910). The fibroblasts become confluent within the polymer mesh, secrete growth factors and dermal matrix proteins such as collagens, tenascin, vitronectin and glycosaminoglycans, thus creating a living dermal substitute. Dermagraft was designed to restore the dermal bed, thereby improving healing in chronic diabetic foot ulcers and venous ulcers [32, 33].

TransCyte® (originally developed by Advanced Tissue Sciences Inc as Dermagraft-TC, and now a product of Smith & Nephew, London, UK) consists of an inner nylon mesh in which newborn human fibroblast cells are embedded, and an outer silicone layer. As fibroblasts proliferate, they secrete human dermal collagen, matrix proteins and growth factors. At the final stage, the composite product is exposed to low temperature to destroy fibroblasts while the tissue matrix and bound growth factors remain intact. This dermal substitute provides a temporary protective barrier and facilitates wound healing [34].

3 Biohydrogels as carriers of topical drugs facilitating wound healing and attenuating cutaneous inflammation

Hydrogels are feasible not only as scaffolds for both *in vitro* and *in situ* tissue regeneration but also as slow releasers and stabilizers of easily metabolized drugs and proteins. Numerous recent studies have demonstrated that the tetra-peptide RGDS is a potent modulator of cellular adhesion [35]. This *motif* is expressed on the surface

of a number of ECM substances, thus providing strong and controlled anchorage for cells and molecules. Notwithstanding its extremely potent biological activity, the tetra-peptide is easily degraded by proteolytic enzymes, heavily expressed in the skin, particularly under inflammatory circumstances. Therefore, several non-peptide analogues of RDGS with similar biological action and higher *in vivo* stability have been developed [36]. For example, RGDS itself and RGDS-mimicking RAM molecule immobilized on a hydrogel could increase (i) adhesion of the hydrogel-containing layer to the wound surfaces thus playing a role as a biological glue, (ii) selective adhesion of circulating progenitor endothelial cells, which initiate and maintain the process of angiogenesis, and (iii) directed movement of keratinocytes to close the skin defect. Covalent binding of hydrogels with proteins and peptides results in the bio-activation of the polymer.

The adhesion properties of polymers towards cells and proteins greatly depends on the nature of the polymer and could be changed by chemical modification of polymer molecule. Polysaccharide hydrogels, both natural and synthetic, subjected to strictly controlled phosphorylation, carboxylation or modification by starch, change their adhesive properties and ability to stimulate an immune response depending on the degree of chemical modification and the modifying moiety.

In a similar way, low molecular weight substances with anti-inflammatory and wound healing action could be covalently bound to polysaccharide-containing hydrogel using the functional hydroxyl and carboxyl groups of the polymer and appropriate groups in the bio-active molecule. For example, phenylpropanoid glycosides (see below) with the chemical structure β-(3,4-dihydroxyphenyl)ethyl- O-a-L-rhamnopyranosyl (1"-3')- O-β D-galactopyranosyl (1"'-2")-β-D-(4'-O-caffeoyl) glucopyranoside, are excellent candidates for binding covalently to hydrogels using either their carbohydrate moieties or polyphenyl nuclei. Also, the same phenylpropanoid glycosides could be safely entrapped in the reticulated hydrogel structure by mixing them before the sol-gel transition. The molecules would be slowly released from the hydrogel without any loss of their basic biological properties.

The multi-functional hydrogel-based product to accelerate *in situ* closure of chronic ulcers with impaired wound healing (diabetes, venous insufficiency or age-related degeneration) would be activated by chemically bound proteins or by growth factors and cytokines released by entrapped cells, angiogenic molecules, pain killers, and anti-inflammatory substances (Fig. 2).

4 Anti-oxidant properties of biohydrogels loaded with plant polyphenols

Polyphenols of plant origin such as bioflavonoids, phenylpropanoids, tannins, anthocyanins and resveratrol, have been reported to exert multiple biological effects and to exhibit positive health effects (anti-UV, anti- inflammatory, wound healing, antiviral, cancer chemopreventive, anti-ageing, etc.) [37–39]. These properties have been mainly attributed to the remarkable free radical scavenging, antioxidant, and chelating activities of polyphenols) [40]. The development of topical medicinal and

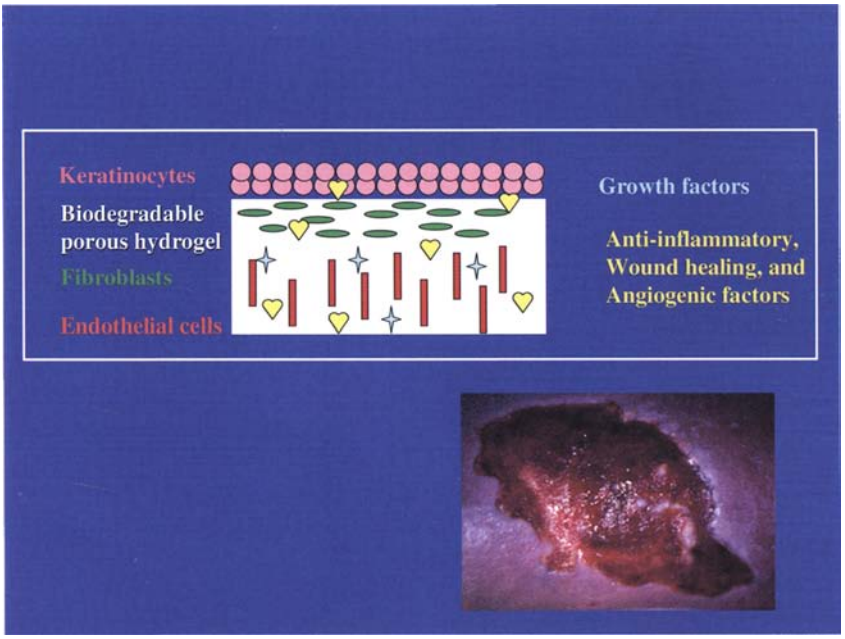

Fig. 2 Schematic presentation of bioactivated hydrogel for *in vivo* skin engineering

cosmetic preparations based on polyphenols is greatly limited by their low stability and susceptibility to oxidation by molecular oxygen, other oxidizing molecules, and specific drug-metabolizing enzymes in human skin [41, 42].

Three polymers (carboxymethyl cellulose, carboxymethyl cellulose modified with starch, and reticulated hyaluronic acid) were gelated in the presence of various concentrations of polyphenols (0.1–5% w/w, verbascoside, teupolioside, curcumin, rutin, and quercetin). The chemical stability, concentration of polyphenols introduced to hydrogen, their antioxidant and anti-inflammatory properties were monitored for 30 consecutive days. It has been shown that the polyphenols dissolved in physiological solution were extremely susceptible to oxidation: (1) their initial concentration dropped dramatically within one week of incubation; (2) the levels of their oxidized forms increased concomitantly; (3) in good agreement with rapid oxidation of polyphenols, their anti-oxidant, free radical scavenging, and anti-inflammatory properties diminished. At the same time, polyphenols "trapped" within the hydrogel remained chemically stable for up to 30 days (97–100% preservation). Moreover, the free radical scavenging activity of polyphenols was preserved completely for at least 30 days. Interestingly, hydrogels themselves exhibited remarkable anti-inflammatory action and maintained initial high levels of polyphenol-associated inhibition of inflammatory mediators released from activated and rested granulocytes. The conclusions have been drawn that both biodegradable and stable hydrogels could be feasible for topical preparations as a protective "cage" for easily oxidizable substances with anti-inflammatory, wound healing, and anti-age action [43].

5 Biohydrogels for drug delivery through the cutaneous barrier

Skin is the largest organ of the human body. It is extremely complex having a "sandwich-like" structure. The uppermost layer bordering the environment is stratum corneum, a unique, highly lipophilic two-compartment system of enucleated cells embedded in a lipid-enriched intercellular matrix, forming stacks of bilayers that are rich in fibrous proteins, mainly, keratins, ceramides, cholesterol and free fatty acids [44]. The underlying layer (epidermis) contains keratinocytes at different stages of differentiation. Moving upward from the deepest basal level of epidermis, young keratinocytes become mature and more differentiated, ending up in the stratum corneum as corneocytes. The bricks of epidermal keratinocytes are cemented by lipids and free fatty acids. Next is a dermal layer rich in various types of cells such as fibroblasts, melanocytes, endothelial cells, smooth muscle cells, immune cells (lymphocytes, granulocytes, monocytes, dendritic cells, Langerhans cells, and neurons). The extracellular space of skin derma is filled with specific proteins (collagens and fibrins) and polysaccharides (hyaluronic acid, glucosoaminoglycans, *etc.*). The highly effective barrier properties of the skin make the task of drug delivery to the skin itself and internal tissues an extremely complicated one. The intrinsic physical properties do not allow the penetration of certain matter and high molecular weight substances through the stratum corneum and epidermal layer of undamaged skin. Actually, all exogenous molecules with either a molecular weight higher than 500 Dalton [45] or low lipophilicity [46] have limited skin permeation. The majority of natural and synthetic drugs with antioxidant, anti-inflammatory and wound healing activity show limited skin permeability [47, 48]. Skin permeation and transdermal delivery of topically applied polyphenols could be enhanced substantially by combining them with hydrogels or liposomes [49–51], by electrically assisted methods such as electroporation and iontophoresis [47], or by the use of skin permeation enhancers [52]. For a comprehensive review on the subject see [53]. Once delivered to the depth of the skin, drugs, including polyphenols, could be either distributed in a homogeneous way through all layers, or concentrated in just one of them. It depends on the nature of the drug and delivery system. For example, phenylpropanoids caffeic and chlorogenic acid penetrated all skin layers with a rate of 0.32 and 0.48 mg/cm^2/h, respectively. At the same time, phenylpropanoid glycoside oraposide slowly penetrated the outermost stratum corneum [54]. Another phenylpropanoid, verbascoside, when inserted into liposomal or hydrogel vesicles has been mainly found in the epidermal layer [51]. Yang et al. [55] have recently reported that the green tea epigallocatechin gallate (EGCG) applied as a transdermal gel to SKH-1 mice showed very fast penetration through all skin layers with major concentration in the epidermis and three times lower levels in the dermal layer. Obviously, the penetration of wound healers and anti-inflammatory substances into impaired skin is much faster than into intact skin as was shown for the topical anti-psoriasis drug anthralin (1,8-dihydroxy-10H-anthracen-9-one) [56].

6 Perspectives of biohydrogels for dermatological and cosmetological applications

There are many possible directions for the use of non-toxic and biologically compatible hydrogels as topical preparations feasible for dermatology and cosmetology. Tissue- and cellular-based approaches to treat severe chronic skin diseases such as ulcers and vitiligo are extremely promising and appealing. Similarly, it will definitely improve the clinical and esthetic outcome of extended burns, scars and undesired adverse effects of plastic surgery. The next generation of hydrogel-based tissue substitutes for *in situ* skin regeneration will be undoubtedly highly sophisticated. They will contain carefully engineered smart biomaterial scaffolds to release, in a time-dependent fashion, various signalling molecules, differentiation factors and protein domains engineered to facilitate cell migration and adhesion. Stem-cell containing composite biomaterials will allow the re-construction not only of functional skin layers (epidermis and dermis) but of all the skin appendages such as hair follicles, sweat glands and sensory organs. Development of new modified and bio-activated hydrogels could tremendously accelerate wound healing providing that there is rapid establishment of tissue engineered product with simultaneous establishment of a functional vascular and nervous network and scar-free integration with the surrounding host tissue. A combination of hydrogels with substances possessing skin protecting and anti-inflammatory properties will bring a new generation of highly bio-available, stable and effective topical preparations.

References

[1] Guerra L, Primavera G, Raskovic D et al (2003) Erbium:Yag laser and cultured epidermis in the surgical therapy of stable vitiligo. Arch Dermatol 139:1303–1310

[2] Guerra L, Bondanza S, Raskovic D (2007) Transplantation of in vitro cultured epithelial grafts for vitiligo and piebaldism. In: Gupta S, Olsson MJ, Kanwar AJ, Ortonne JP (ed) Surgical Management of Vitiligo, 1st edn. Blackwell Publishing Ltd, Oxford, pp 180–190

[3] Pellegrini G, Ranno R, Stracuzzi G et al (1999) The control of epidermal stem cells (holoclones) in the treatment of massive full-thickness burns with autologous keratinocytes cultured on fibrin. Transplantation 68:868–879

[4] Rheinwald JG, Green H (1975) Serial cultivation of strains of human epidermal keratinocytes: the formation of keratinizing colonies from single cells. Cell 6:331–343

[5] Supp DM, Boyce ST. (2005) Engineered skin substitutes: practices and potentials. Clin Dermatol 23:403–412

[6] Metcalfe AD, Ferguson MWJ (2007) Tissue engineering of replacement skin: the crossroads of biomaterials, wound healing, embryonic development, stem cells and regeneration. J R Soc Interface 4:413–437

[7] Mano JF, Silva GA, Azevedo HS et al (2007) Natural origin biodegradable systems in tissue engineering and regenerative medicine: present status and some moving trends. J R Soc Interface 4:999–1030

[8] Hayashi T (1994) Biodegradable polymers for biomedical uses. Prog Polym Sci.19:663–702

[9] Rosso F, Marino G, Giordano A et al (2005) Smart materials as scaffolds for tissue engineering. J Cell Physiol 203:465–470
[10] Yang C, Hillas PJ, Baez JA et al (2004) The application of recombinant human collagen in tissue engineering. Bio Drugs 18:103–119
[11] Harris PA, Di Francesco F, Barisoni D et al (1999) Use of hyaluronic acid and cultured autologous keratinocytes and fibroblasts in extensive burns. Lancet 353:35–36
[12] Currie LJ, Sharpe JR, Martin R (2001) The use of fibrin glue in skin grafts and tissue-engineered skin replacements: a review. Plast Reconstr Surg 108:1713–1726
[13] Ronfard V, Rives JM, Neveux Y et al (2000) Long-term regeneration of human epidermis on third degree burns transplanted with autologous cultured epithelium grown on a fibrin matrix. Transplantation 70:1588–1598
[14] Vanscheidt W, Ukat A, Horak V et al (2007) Treatment of recalcitrant venous leg ulcers with autologous keratinocytes in fibrin sealant: a multinational randomized controlled clinical trial. Wound Repair Regen 15:308–315
[15] Lee J, Cuddihy MJ, Kotov NA (2008) Three-dimensional cell culture matrices: state of the art. Tissue Eng Part B Rev 14:61–86
[16] Priya SG, Jungvid H, Kumar A (2008) Skin tissue engineering for tissue repair and regeneration. Tissue Eng 14:105–118
[17] Chung Y-I, Tae G, Yuk SH (2006) A facile method to prepare heparin-functionalized nanoparticles for controlled release of growth factors. Biomaterials 27:2621–2626
[18] Hubbell JA (1999) Hydrogels in biological control during graft healing. In: Zilla P, Greisler HP (ed) Tissue engineering of vascular prosthetic grafts. RG Landes Company, Austin, Texas, pp 561–570
[19] MacNeil S (2007) Progress and opportunities for tissue-engineered skin. Nature 445:874–880
[20] Eming SA, Smola H, Krieg T (2002) Treatment of chronic wounds: state of the art and future concepts. Cells Tissues Organs 172:105–117
[21] Harding KG, Morris HL, Patel GK (2002) Science, medicine, and the future. Healing chronic wounds. BMJ 324:160–163
[22] Bello YM, Falabella AF, Eaglstein WH (2001) Tissue-engineered skin. Current status in wound healing. Am J Clin Dermatol 2:305–313
[23] Jimenez PA, Jimenez SE (2004) Tissue and cellular approaches to wound repair. Am J Surg 187:56S–64S
[24] Ehrenreich M, Ruszczak Z (2006) Update on tissue-engineered biological dressings. Tissue Eng 12:2407–2424
[25] Clark RAF, Ghosh K, Tonnesen MG (2007) Tissue engineering for cutaneous wounds. J Invest Dermatol 127:1018–1029
[26] Campitiello E, Della Corte A, Fattopace A et al (2005) The use of artificial dermis in the treatment of chronic and acute wounds: regeneration of dermis and wound healing. Acta Biomed 76 Suppl 1:69–71
[27] Kolácná L, Bakesová J, Varga F et al (2007) Biochemical and biophysical aspects of collagen nanostructure in the extracellular matrix. Physiol Res 56 Suppl 1:S51–S60
[28] Hubbell JA (2003) Materials as morphogenetic guides in tissue engineering. Curr Opin Biotechnol 14:551–558
[29] Brinda E, Pradny M, Lesny P et al (2007) Surface modification of hydrogels based on poly(2-hydroxyethyl methacrylate) with extracellular matrix proteins. Proc International Congress on Biohydrogels, pp 8
[30] Mori M, Yamaguchi M, Sumitomo S et al (2004) Hyaluronan-based biomaterials for tissue engineering. Acta Histochem Cytochem 37:1–5

[31] Caravaggi C, De Giglio R, Pritelli C et al (2003) HYAFF 11-based autologous dermal and epidermal grafts in the treatment of noninfected diabetic plantar and dorsal foot ulcers: a prospective, multicenter, controlled, randomized clinical trial. Diabetes Care 26:2853–2859
[32] Krishnamoorthy L, Harding K, Griffiths D et al (2003) The clinical and histological effects of Dermagraft in the healing of chronic venous leg ulcers. Phlebology 18:12–22
[33] Marston WA, Hanft J, Norwood P et al (2003) Dermagraft Diabetic Foot Ulcer Study Group. The efficacy and safety of Dermagraft in improving the healing of chronic diabetic foot ulcers: results of a prospective randomized trial. Diabetes Care 26:1701–1705
[34] Purdue GF (1997) Dermagraft-TC pivotal efficacy and safety study. J Burn Care Rehabil 18 (Pt 2):S13–S14
[35] Aguzzi MS, Giampietri C, De Marcis F et al (2004) RGDS peptide induces caspase 8 and caspase 9 activation in human endothelial cells. Blood 103:4180–418
[36] Aguzzi MS, Facchiano F, Ribatti D et al (2004) A novel RGDS-analog inhibits angiogenesis in vitro and in vivo. Biochem Biophys Res Commun 321:809–814
[37] Korkina L (2007) Phenylpropanoids as naturally occurring antioxidants: from plant defense to human health. Cell Mol Biol 53:13–23
[38] Korkina L, Mikhal'chik E, Suprun M et al (2007) Molecular mechanisms underlying wound healing and anti-inflammatory properties of naturally occurring biotechnologically produced phenylpropanoid glycosides. Cell Mol Biol 53:78–83
[39] Kostyuk V, Potapovich A, Suhan T et al (2008) Plant polyphenols against UV-C-induced cellular death. Planta Med 74:509–514
[40] Korkina L, Afanas'ev I (1997) Antioxidant and chelating properties of flavonoids. Advances in Pharmacology 38:151–163
[41] Denisov E, Afanas'ev I (2005) Oxidation and Antioxidants in Organic Chemistry and Biology, CBC Taylor & Francis Group, Boca Raton-London-New York-Singapore
[42] Korkina L, Pastore S, De Luca C et al (2008) Metabolism of plant polyphenols in human skin: beneficial versus deleterious effects. Curr Drug Met 9:710–729
[43] Kostyuk V, Potapovich A, Deeva I et al (2007) Biohydrogels as stabilizers against oxidation of polyphenols with antioxidant, anti-inflammatory, anti-ageing, and wound healing action. Proc. International Congress on Biohydrogels, pp 66
[44] Elias, PM (2005) Stratum corneum defensive functions: an integrated view. J Invest Dermatol 125:183–200
[45] Bos JD, Mainardi MM (2000) The 500 Dalton rule for the skin penetration of chemical compounds and drugs. Exp Dermatol 9:65–66
[46] Abdelouahab N, Heard CM (2008) Dermal and Transcutaneous Delivery of the Major Glycoside Constituents of Harpagophytum procumbens (Devil's Claw) in vitro. Planta Med 74:7–531
[47] Fang JY, Hung CF, Hwang TL et al (2006) Transdermal delivery of tea catechins by electrically assisted methods. Skin Phamacol Physiol 19:28–37
[48] Diniz A, Escuder-Gilabert L, Lopes NP et al (2007) Permeability profile estimation of flavonoids and other phenolic compounds by biopartitioning micellar capillary chromatography. J Agric Food Chem 55:8372–8379
[49] Casagrande R, Georgetti SR, Verri WA Jr et al (2007) In vitro evaluation of quercetin cutaneous absorption from topical formulations and its functional stability by antioxidant activity. Int J Pharm 328:183–190
[50] Cevc G (2004) Lipid vesicles and other colloids as drug carriers on the skin. Adv Drug Deliv Rev 56:675–711
[51] Sinico C, Caddeo C, Valenti D et al (2008) Liposomes as carriers for verbascoside: stability and skin permeation studies. J Liposome Res 18:83–90

[52] Touitou E. (2002) Drug delivery across the skin. Expert Opin Biol Ther 2:723–733
[53] Godin B, Touitou E (2007) Transdermal skin delivery: predictions for humans from in vivo, ex vivo and animal models. Adv Drug Deliv Rev 59:1152–1161
[54] Marti-Mestres G, Mestres JP, Bres J et al (2007) The "in vitro" percutaneous penetration of three antioxidant compounds. Int J Pharm 331:139–144
[55] Yang CS, Lambert JD, Ju J et al (2007) Toxicol Appl Pharmacol 224:265–273
[56] Peus D, Beyerle A, Vasa M et al (2004) Antipsoriatic drug anthralin induces EGF receptor phosphorylation in keratinocytes : requirement for H(2)O(2) generation. Exp Dermatol 13:78–85

Chitosan-Based Beads for Controlled Release of Proteins

Mamoni Dash, Anna Maria Piras and Federica Chiellini

Abstract. Chitosan is biocompatible polymer of natural origin widely investigated for applications in drug delivery and regenerative medicine. In this paper, Chitosan's capability of forming water gelling beads in the presence of non-toxic polyanion was exploited for the loading of two model proteins. Human Serum Albumin (HSA) and porcine trypsin were successfully loaded into Chitosan-tripolyphosphate (TPP) beads. Both proteins were highly incorporated when the crosslinking process was allowed to occur for 24 h at RT. The release profiles of the two proteins were compared and the faster diffusion of trypsin was associated to its smaller molecular weight. Moreover, *in vitro* degradation experiments, aimed at mimicking the physiological degradation pattern of the beads displayed a complete degradation of the material in almost 30 days. Certainly, the preliminary experimental data acquired in the present work represent a starting study for the promising application of Chitosan-TPP beads for the controlled release of proteins of therapeutic interest.

1 Introduction

Chitosan is primarily composed of β-1,4 linked 2-amino-2-deoxy-D-glucopyranose (D-glucosamine). In nature it is found in fungi, but it is conventionally produced by deproteinization, demineralization and deacetylation of chitinous material which is widely distributed in living organisms (arthropods, fungi, algae, mollusca, etc.) [1].

Chitosan is biocompatible, it does not cause allergic reactions and rejection. Under the action of ferments, it degrades slowly *in vivo* to harmless products (amino sugars), which are completely absorbed by the human body. It is known to possess antimicrobial property and absorbs toxic metals such as mercury, cadmium, lead, etc. In addition, it has good adhesion properties [2], ability to coagulate, and immunostimulating activity [3].

Chitosan is widely investigated nowadays thanks to its gelling capability and to the possibility of applying this natural polymer to regenerative medicine and drug delivery. The most applied processing methods include internal or external ionotropic gelation, which allow a wide range of products to be obtained, from micro beads to nano-sized particles. The advantage of ionotropic gelation is in the safeness of use for the operator, since it avoids the use of hazardous organic solvents and it is based

Barbucci R. (Ed): Hydrogels. Biological Properties and Applications.

on the cationic nature of Chitosan, which is able to crosslink with multivalent anions such as sulfate, citrate, and tripolyphosphate [4, 5]. Tripolyphosphate (TPP) is a non-toxic polyanion which easily interacts with Chitosan and has previously been used for the preparation of Chitosan beads, microspheres and nanoparticles [6]. In particular, Chitosan vehicles appear promising for the administration of therapeutic peptides and proteins, such as vaccines, cytokines, enzymes, hormones and growth factors, which are becoming a very important class of both therapeutics and agents for regenerative medicine. Despite the potential of many proteins and peptides, their application in medical treatments is hampered by difficulties in *in vivo* administration, related to their chemical and conformational instability, the presence of denaturing agents, pH and ionic strength changes.

In this paper, two model proteins are applied for the preparation of protein loaded Chitosan-TPP beads. Human serum albumin has been chosen as a middle-size protein model and applied for preliminary evaluation on loading and release kinetics. Porcine trypsin has been applied as a model of the active agent, due to its enzymatic activity it is generally applied for the assessment of activity maintenance after loading into a polymeric system [7, 8].

2 Materials and methods

2.1 Materials

Chitosan and sodium tripolyphosphate(TPP) were purchased from Sigma-Aldrich. The molecular weight was in the range of 190,000–375,000 as indicated by the supplier, viscosity was about 200 cps. The degree of deacetylation was > 85%. All other reagents and solvents were of reagent grade purity. Human Serum Albumin, used as a model protein and lysozyme (hen egg-white), was purchased from Sigma-Aldrich.

2.2 Preparation of crosslinked Chitosan beads

Chitosan powder (0.6 g) was dispersed in 20 mL of water containing 1 (v/v)% acetic acid. The mixture was stirred and left overnight. The TPP powder was dissolved in distilled water to prepare 1% (w/v) TPP aqueous solutions. The pH values of the TPP aqueous solutions was not changed (pH 9.0). The Chitosan solution was dropped through a syringe needle into gently agitated TPP solution and gelled spheres formed instantaneously.

2.3 Preparation of protein loaded Chitosan beads

Chitosan and TPP solutions of the same concentrations as described above were prepared. The model protein Human Serum Albumin was dissolved directly in the TPP solution. The concentration of the protein in the TPP solution was 0.1%. The solution of TPP and Albumin was stirred for 10 min to attain homogeneity. The Chitosan solution was dropped through a syringe needle into gently agitated TPP solution

and gelled spheres formed instantaneously. The Chitosan droplets were stood in the solution for 2 h and 24 h to crosslink the gel beads and examine the effect of time on crosslinking. To analyze the effect of temperature on crosslinking and encapsulation of the protein, the beads were allowed to crosslink at room temperature as well as at −4 °C. After crosslinking, the solidified gel beads were separated and the supernatant collected for further analysis.

Porcine trypsin was loaded under the same conditions of Albumin loading, by allowing crosslinking at room temperature for 24 h.

2.4 Morphological characterization

The surface and cross-sectional morphologies of the dried beads were examined using scanning electron microscopy (SEM) and Field Emission Microscopy (FEM).

2.5 Swelling of Chitosan-TPP beads

The water sorption capacity of the beads was determined by swelling them in three media: distilled water, phosphate buffer saline solution (PBS) pH 7.4 and cell growth media DMEM. A known weight (16 mg) of the Chitosan beads was placed in the different media. The wet weight of the swollen beads was determined by first blotting the beads with filter paper to remove the adsorbed water and then weighed immediately on an electronic balance. The percentage swelling of Chitosan beads in the media was calculated by the formula:

$$\text{BSR } \% = (W_e - W_o)/W_o * 100 \quad (1)$$

Where BSR is the beads swelling ratio percent at equilibrium. We denote the weight of the beads at equilibrium swelling and Wo is the initial weight of the beads.

2.6 Degradation of Chitosan-TPP beads

The in vitro degradation of Chitosan TPP beads was followed in 1ml PBS (pH 7.4) at 37 °C containing 1.5 µg/ml lysozyme. The concentration of lysozyme was chosen to correspond to the concentration in human serum [9]. Briefly, beads of known dry weights were incubated in the lysozyme solution with gentle mechanical agitation for the period of study. The lysozyme solution was refreshed daily to ensure continuous enzyme activity [10]. After 7, 14, 21 and 28 days, samples were removed from the medium, rinsed with distilled water, dried under vacuum and weighed. The extent of in vitro degradation was expressed as a percentage of weight loss of the beads after lysozyme treatment.

2.7 Evaluation of protein encapsulation efficiency

The supernatants of the drug loaded beads were analyzed both by UV spectrophotometric method for preliminary protein evaluation and by BCA Micro Assay Kit. The

BCA Micro Assay Kit was used as per the guidelines mentioned on the kit and the reading was taken at 540 nm. All the samples were analyzed in triplicate.

The Encapsulation Efficiency (EE %) was calculated from the following expression:

$$EE\ \% = [\text{Loaded Protein (mg)} / \text{Protein Formulation (mg)}] * 100 \quad (2)$$

The experiment was performed in two sets: one for 2 h crosslinking and 24 h crosslinking, and the other for temperature difference during the crosslinking process i.e. crosslinked at room temperature and at −4 °C.

The Loading (%) was also calculated by using the formula:

$$\text{Loading}\ (\%) = [\text{Loaded Protein(mg)/lyophilised beads (mg)}] * 100 \quad (3)$$

2.8 Protein release studies

Either albumin or trypsin loaded beads were suspended in 50 mL PBS (pH 7.4) and incubated on a shaking water-bath at 37 °C. A total of 2 ml supernatant was withdrawn at appropriate intervals, and protein content was determined by BCA Micro Assay Kit. An equal volume of the same dissolution medium was added immediately to maintain a constant volume.

The activity of the released trypsin was also evaluated by a colorimetric assay using N-α-benzoyl-DL-arginine-4-nitroanilide (BApNA) as synthetic substrate for the enzyme.

3 Results and discussion

3.1 Preparation of crosslinked Chitosan beads

The Chitosan gel beads were obtained by using the iontropic gelation method. This method employs the reinforcement of sodium tripolyphosphste (TPP) as a crosslinking agent. This results in the formation of insoluble Chitosan beads, without involving addition of dialdehydes. The electrostatic interaction between TPP and Chitosan has been reported and exploited in the pharmaceutical industry to prepare TPP crosslinked beads [11]. TPP treatment of Chitosan beads is expected to improve their stability and their applicability in controlled drug delivery [12].

3.2 Morphological observation

The prepared beads were mostly spherical in their hydrated state (Fig. 1). SEM micrographs of the dry Chitosan-TPP beads (Fig. 2a) display the formation of beads with a drop-like shape of about 800 μm diameter for the spherical portion, and a wrinkled surface with little cracks (Fig. 2b). The loading of the two model proteins, HSA and trypsin, did not affect the iontropic gelation process. Similarly to plain

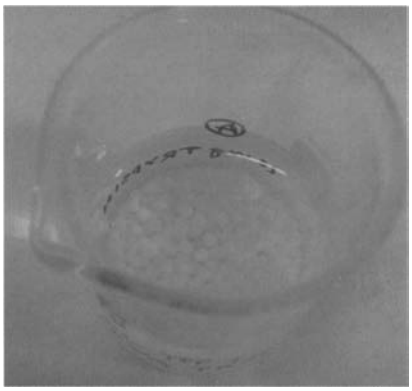

Fig. 1 Macroscopic features of TPP crosslinked Chitosan beads

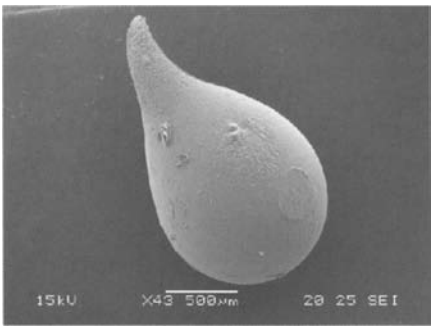

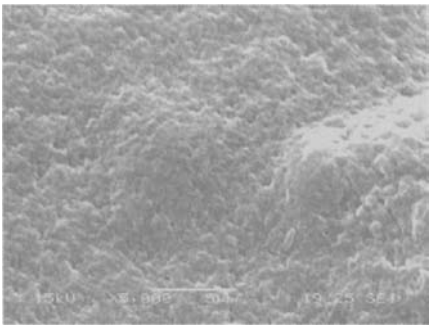

a **b**

Fig. 2 SEM micrographs of plain TPP crosslinked Chitosan beads. shape **a** and surface **b**

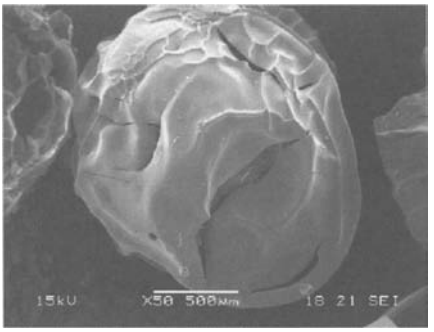

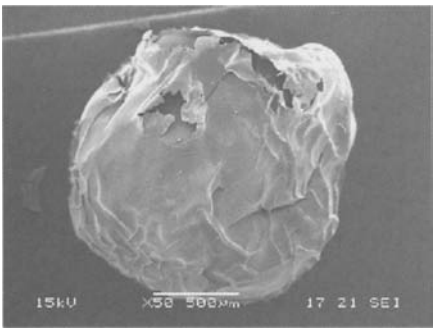

a **b**

Fig. 3 SEM micrographs of HSA. **a**, and trypsin loaded **b** TPP linked Chitosan beads

Chitosan-TPP beads, the prepared protein loaded beads were macroscopically spherical in the hydrated form. The SEM micrographs of the dry state display a preserved spherical shape, with about 1–1.5 mm diameter and a more irregular surface with higher rugosity. (Fig. 3a and 3b).

3.3 Swelling ratio

The swelling behavior of plain Chitosan-TPP beads was investigated in deionized water, PBS at pH 7.4 and DMEM cell growth medium (Table 1). The swelling equilibrium was reached in about 20 h in all the media, leading to swelling ratio values of 120–130%.

Table 1 Swelling ratios of TPP crosslinked Chitosan beads in water, PBS and DMEM

Medium	Water	PBS	DMEM
Swelling%±SD	119.4±3.5	121.2±1.1	131.0±1.9

3.4 Degradation of Chitosan-TPP beads

It is well known that in human serum, N-acetylated Chitosan is mainly depolymerized enzymatically by lysozyme and not by any other enzymes or other depolymerization mechanism [13]. The enzyme biodegrades the polysaccharide by hydrolyzing the glycosidic bonds present in the macromolecular backbone. Lysozyme contains hexameric binding sites [14] and hexasaccharide sequences, containing 3–4 or more acetylated units, which contribute mainly to the initial degradation rate of N-acetylated Chitosan [15]. The pattern of degradation of Chitosan found in our studies can, in part, be explained by this mechanism of enzymatic degradation. As can be seen in Fig. 4, almost linear enzymatic degradation occurred within 15–17 days and complete degradation of the beads is expected in about 30 days.

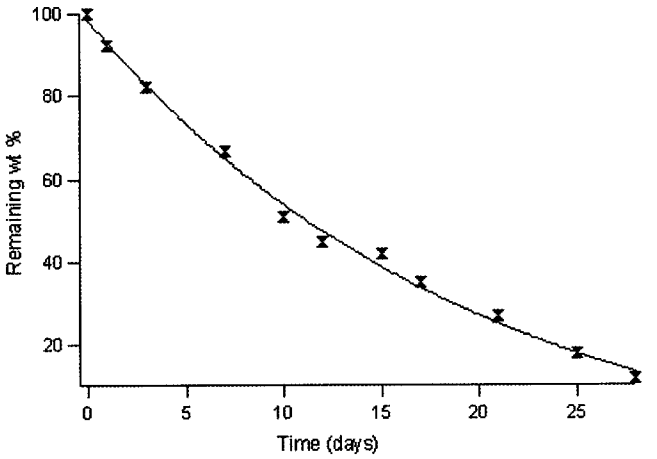

Fig. 4 Enzymatic degradation profile of TPP crosslinked Chitosan beads

3.5 Protein encapsulation and release studies

The model protein HSA was successfully encapsulated into Chitosan-TPP beads. The influence of the crosslinking time and temperature on encapsulation efficiency was evaluated. In particular, as reported in Table 2, 2 h of crosslinking were not sufficient to achieve a high EE %, and in fact 24 h were required. Moreover, when the process was performed at 4 °C, a lower value of EE % was recorded, probably due to kinetic limitations of the specific low temperature.

When trypsin was applied for loading, no significant variation of bead formation was observed macroscopically. The loading was performed in this case at room temperature for 24 h and the EE % was 55%.

The applied formulation parameters involve quite a small amount of protein which is highly incorporated into the beads, with EE % up to 64%, and corresponds to about 4.1% of the beads dry weight.

In vitro drug release was monitored for 5 h. Both proteins easily diffuse out of the Chitosan-TPP beads under physiological conditions. Results of drug release versus time for albumin and trypsin are shown in Fig. 5. As expected, in the case of albumin, the release of the protein was slower than for trypsin, reaching around 17% of cumulative release in 5 h, whereas under the same release conditions, trypsin was released up to a level of 50%. The difference in molecular weight of the two protein is reflected in their inherent volume and certainly in their diffusion constant.

The measurements of the activity of trypsin released from the beads (Fig. 6) highlight a loss of 15–20% of activity after 30 minutes. Actually, the enzyme released from the beads is accumulated in the releasing medium, because only a small amount of volume (2 ml out of 50 ml) is replaced when sampling. It is known that trypsin is extremely sensitive to auto-digestion under physiological conditions [16]. The correct evaluation of the activity of the released trypsin would be better performed with the complete withdrawl of medium at each time point, or after addition of calcium ions to the solution, to limit protein autolysis [17].

Table 2 Encapsulation Efficiency (EE %) and Loading % of Albumin into TPP crosslinked Chitosan beads, related to crosslinking temperature and duration

Run	Crosslinking		EE %	Loading %
	Temp °C	Time h		
B-HSA1	RT	2	49	4.1
B-HSA2	RT	24	64	4.1
B-HSA2	4	2	27	3.6

4 Conclusions

In this preliminary work, the conditions for the preparation of protein loaded TPP crosslinked Chitosan beads were optimized for the achievement of high protein loading. The activity of the model enzyme was not significantly affected by the process

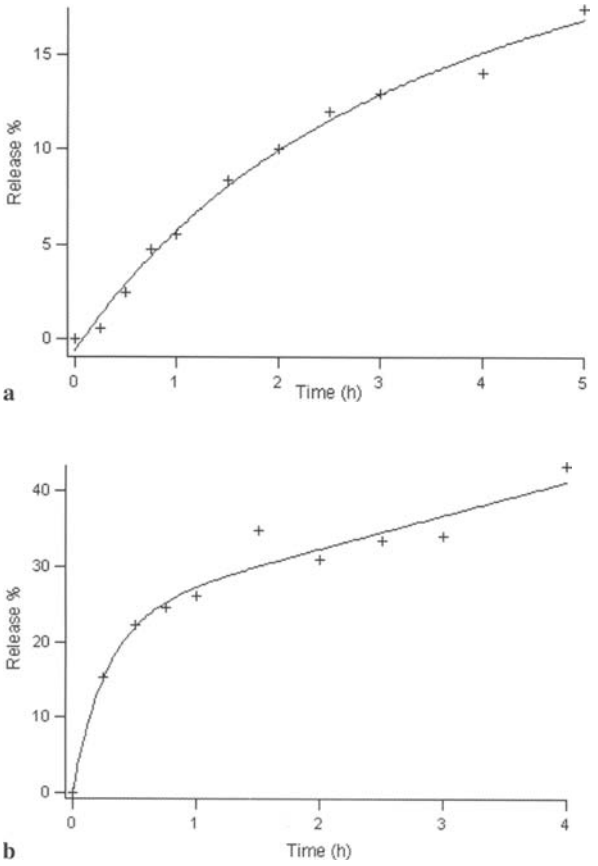

Fig. 5 Drug release profiles of HSA loaded (a), and trypsin loaded (b) TPP crosslinked Chitosan beads

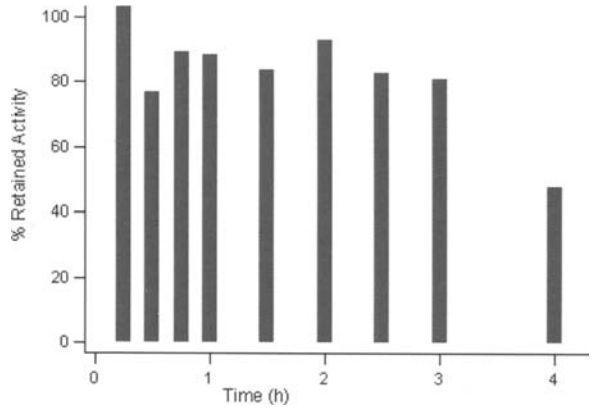

Fig. 6 Retained activity of trypsin loaded into TPP crosslinked Chitosan beads, in the releasing medium

and the observed reduction of activity of the released protein is mostly associated with trypsin autolysis under physiological conditions. The release profiles of the loaded proteins seem related to their molecular weight, and the complete degradation of the TPP crosslinked Chitosan beads under lysozyme digestion occurs in 30 days. The present work represent a starting study for the promising application of Chitosan-TPP beads for the controlled release of proteins of therapeutic interest. Forthcoming studies will be focused on the reduction of bead size to micro- nanostructures with the same properties of the prepared beads, but with the ability to reach all body areas after conventional administration.

Acknowledgments. The results reported in the present paper have been generated within the framework of the PRIN funded project PROT 200603854. The authors wish to acknowledge the financial support of MIUR and the contribution given by Mr. Piero Narducci in recording SEM images.

References

[1] Steinbüchel A (2002) Biopolymers. Vandamme EJ (ed) Volume 5. Polysaccharides~I: polysaccharides from eukaryotes and Volume 6. Polysaccharides II: polysaccharides from prokaryotes. Wiley-VCH Verlag GmbH, Weinheim, Germany

[2] Bravo-Osuna I, Vauthier C, Farabollini A, Palmieri GF, Ponchel G (2007) Mucoadhesion mechanism of Chitosan and thiolated Chitosan-poly(isobutyl cyanoacrylate) core-shell nanoparticles. Biomaterials 28(13):2233–2243

[3] Muzzarelli RAA, Muzzarelli C (2005) Chitosan chemistry: relevance to the biomedical sciences. Adv Adv Polym Sci 186:151–209

[4] Agnihotri SA, Mallikarjuna NN, Aminabhavi TM (2004) Recent advances on Chitosan-based micro- and nanoparticles in drug delivery. J Control Release 100:5–28

[5] Denkbas EB, Ottenbrite RM (2006) Perspectives on: Chitosan drug delivery systems based on their geometries. J Bioact Compat Polym 21(4):351–368

[6] Mi FL, Shyu SS, Lee ST, Wong TB (1999) Kinetic study of chitosan-tripolyphosphate complex reaction and acid-resistive properties of the chitosan-tripolyphosphate gel beads prepared by ni-liqiud curing method. J Polym Sci, Part B: Polym Phys 37:1551

[7] Chiellini F, Bartoli C, Dinucci D, Piras AM, Anderson R, Croucher T (2007) "Bioeliminable Polymeric Nanoparticles for Proteic Drug Delivery". International Journal of Pharmaceutics 343(1–2):90–99

[8] Piras AM, Chiellini F, Fiumi C, Bartoli C, Chiellini E, Fiorentino B, Farina C (2008) "A New Biocompatible Nanoparticle Delivery System for the Release of Fibrinolytic Drugs". International Journal of Pharmaceutics 357(1–2):260–271f

[9] Porstmann B, Jung K, Schmechta H, Evers U, Pergande M, Porstmann T, Kramm HJ, Krause H (1989) Measurement of lysozyme in human body fluids: comparison of various enzyme immunoassay techniques and their diagnostic application. Clin Biochem 22:349–355

[10] Masuda T, Ueno Y, Kitabatake N (2001) Sweetness and enzymatic activity of lysozyme. J Agric Food Chem 49:4937–4941

[11] Shu XZ, Zhu KJ (2002) Controlled drug release properties of ionically crosslinked Chitosan beads: the influence of anion structure. Int J Pharm 233:217–225

[12] Anal AK, Stevens WF, Remunan-Lopez C (2006) Ionotropic crosslinked Chitosan microspheres for controlled release of ampicillin. Int J Pharm 312:166–173

Synthesis of Stimuli-Sensitive Hydrogels in the µm and sub-µm Range by Radiation Techniques and their Application

Karl-Friedrich Arndt, Andreas Richter and Ingolf Mönch

Abstract. The macroscopic material properties (elasticity, volume in swollen state) of smart stimuli-sensitive hydrogels show a strong dependence on the properties of an aqueous environment (swelling agent). This behavior can be used for sensors or force-generating elements (actuators). Radiochemistry offers the possibility to synthesize smart gels in a wide range of dimensions. As an example of temperature-sensitive polymers we demonstrate the advantages of a radiochemical-based approach for hydrogel synthesis. Structures in the µm and sub-µm range on a support were synthesized using different techniques. The applications of particles and patterned layers in the µm range were demonstrated using the example of devices for handling liquids

1 Stimuli-sensitive hydrogels

Polymeric gels are most generally understood to be polymeric networks which absorb enough solvent to cause macroscopic changes in the sample dimension. Hydrogels are crosslinked hydrophilic polymers swollen in water. Most of their properties are directly influenced by the degree of swelling. The volume phase transition of certain hydrogels is one of the most fascinating and important phenomena in the physical chemistry of polymeric networks. Stimuli-sensitive hydrogels (they are also termed smart gels and responsive gels) are materials whose properties change in response to specific environmental stimuli (see Table 1). They change their volume (equilibrium degree of swelling), mechanical properties (elasticity, stiffness) and molecular transport properties, in response to a small change in the properties of the swelling agent, like temperature, solvent composition, pH value, mechanical strain, ion concentration, etc. The change in the degree of swelling may occur discontinuously at a specific value of stimulus or gradually over a (mostly small) range of stimulus values.

Polymer gels have found wide application in various fields: medicine, agriculture, biotechnology, nutritive industry, petrochemical industry, etc. For these applications only the ability of a gel to absorb solvent and to swell is important, not the relationship between changes in the environment and swelling.

The ability to directly convert chemical energy into mechanical work makes smart gels candidates for actuator and sensor systems, which can operate without additional

Barbucci R. (Ed): Hydrogels. Biological Properties and Applications.

Table 1 Sensitive Polymers. The VPT is measured in water. Addition of salt or organic components shifts the VPT. Under isothermal conditions a volume phase transition can be initiated by changing the concentration of ions or organic components

Polymer/sensitivity	Chemical structure	Reference
Poly(N-isopropyl-acrylamide) PNIPAAm/T VPT = 32–34 °C	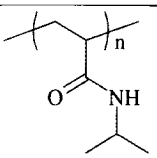	[33]
Poly(vinyl methyl ether) PVME/T VPT = 34–38 °C	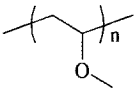	[34]
Hydroxypropyl-cellulose HPC/T VPT = 41–44 °C	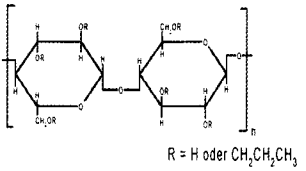 R = H oder $CH_2CH_2CH_3$	[35,36]
Poly(4-vinyl pyridine) P4VP/pH pH = 4.5	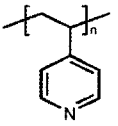	[37]
Poly(N-vinyl pyrrolidone) PVP/non sensitive	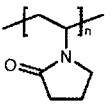	

measuring devices or external power supplies. Artificial muscles based on chemo-mechanical energy conversions in polyelectrolyte gels (response to pH-changes) were studied in the forties and fifties by Kuhn [1], Breitenbach [2], Katchalsky [3], and others. Later on, the unique properties of stimuli-sensitive hydrogels, the strong correlation between macroscopic phenomena, such as the degree of swelling, and properties of the swelling agent, resulted in substantial application research. These polymers have a great chance of finding applications in different fields, because they combine sensor and actuator properties. Nevertheless, only a few hydrogel-based devices are on the market.

Despite their remarkable behavior, there are some drawbacks. Gels' inherently weak mechanical properties strongly restrict their application properties. Gels are soft and can easily be destroyed by mechanical stress, e.g. large deformation forces. In the last few years, the synthesis of thermo-sensitive hybrid gels (e.g. poly(N-isopropylacryl-amide/clay) with improved mechanical properties has been described.

(Haraguchi et al. prepared hydrogels using hectorite as a cross-linker which shows excellent fracture strength and tensile elongation [4].) The most important fact for the application of smart gels is to take advantage of their swelling behavior. In our opinion, the prerequisites for their application are:

- The understanding of transport processes during swelling/shrinking. The swelling/shrinking response of hydrogels in response to physical or chemical stimuli has caught the attention of researchers for drug delivery, because volume change can be converted to a change in the rate of delivery or in the permeation rate of drugs.
- Controlling the degree of swelling, e.g. by determining the relationship between degree of swelling and temperature. In the case of temperature-sensitive gels, its volume is determined by the temperature in a given solvent and can be switched to another value by changing temperature. The temperature of the volume phase transition can be changed by copolymerization of a temperature sensitive monomer with other monomer units, e.g. hydrophobic monomers, or can be switched by changing the pH (acid or basic monomers). In this case, the swelling degree at a constant temperature is pH-dependent.
- Controlling the swell kinetics. The change of degree of swelling determines the time behavior of an actuator, or the time dependence of a sensor signal. The delivery of a drug is also determined by swell kinetics.
- Fast response to changes in environmental conditions. A fast response is usually desired for the application of smart gels. In this case, the degree of swelling directly follows the change in environmental conditions.

2 Materials and the swelling process

As a model to understand and to describe the processes during the response of a smart gel to changes of environmental properties, a two-step mechanism can be assumed. In the first step, the stimulus which triggers swelling/shrinking must permeate the gel itself. Heat transfer or mass transfer determines the rate of the first step. Typical diffusion coefficients for this are:

- The stimulus is a change in temperature, the rate of heat transfer is given by the thermal diffusivities (about 10^{-3} cm^2/s), see ref. [5]. The stimulus is a change in composition, e.g. diffusion of alcohol into a water swollen gel. A typical diffusion coefficient is about 10^{-5} cm^2/s, see ref. [6]. The swelling/shrinking starts if, thermodynamically, conditions for a volume phase transition are fulfilled, e.g. volume phase transition temperature (VPT), pH, mixing ratio of water with a hydrophobic agent, such as an organic solvent. Tanaka showed in 1979 that a cooperative diffusion coefficient, D_{coop}, determines the kinetics of swelling/ shrinking. Values of D_{coop} measured by dynamic light scattering (shift in frequency of scattered light due to the motion of net-chains could be used to predict the kinetics of gel swelling and shrinking. This fact is of fundamental significance: the dynamics of net-chains probed at the micro-scale have been linked with the macroscopic dynamic behavior of gels. Typically, the cooperative diffusion coefficient is in the

order of 10^{-7} cm^2/s, about 100 times lower than the mass transfer. According to Tanaka et al. [7], the swelling/shrinking rate, and thereby the response time for any application, during volume phase transitions of smart hydrogels depends on D_{coop} and on the square of their characteristic dimensions (response time $\sim$ length$^2/D_{coop}$). A faster response is achieved by a reduction in size. Gels with a fast response must have a small characteristic length, making them attractive materials for micro-scale actuation.

Different techniques have been described to acquire these gels:

- Synthesis of porous or sponge-like gels [8], in which the dimension of walls between the pores is crucial for the response time. These gels swell or shrink very fast compared with nonporous gels of the same size. Yan and Hoffman [9] have shown that polymerizing NIPAAm at temperatures above the volume phase transition results in gels having large pore sizes and faster swelling rates. The cross-linking of a polymer in a phase separated state, e.g. by irradiation of a high concentrated solution at high temperatures with γ - or electron rays, also results in porous gels [9–12].
- Formation of a hydrophobic cluster [13] n, a comb-grafted polymer gel, results in additional junction points and in an abrupt increase in cross-linking density.
- Synthesis of micro-gels [14], e.g. thermo-sensitive micro-gels based on NIPAAm by inverse suspension polymerization [15]; inverse emulsion polymerization [16]; irradiation of a phase-separated dilute solution [17].
- Thin (patterned) layers on a support. Patterning of hydrogels is important for their application in cell and tissue scaffolds, controlled drug release and microfluidics.

3 Patterning

Response times of hydrogels can be reduced to seconds or less by reducing their dimension and integrating them into MEMS (micro-electromechanical systems). Different applications need micro- or nano-sized smart hydrogels. This could be hydrogel particles or hydrogel layers, e.g. the need for stimuli-sensitive components in microfluidic systems has led to the synthesis of hydrogel-based patterned microstructures. Different patterning techniques for polymers have been described in the literature (see Table 2).

The current method of choice for patterning sensitive polymers is based on photochemistry. The in-situ photo-polymerization technique starts from monomers and ends with functionalized oligomers. In some cases it is possible to initiate a cross-linking reaction by mixing the polymer with a photo-initiator and UV irradiation. A direct photochemical approach to the synthesis of structured hydrogels is based on irradiation of polymers containing photo-crosslinkable groups. A film of the polymer is deposited onto silicon surfaces by spin coating. The thickness of the film depends on the concentration of the polymer solution and the rotation speed (typically from 10^2 nm to the µm-range). The film is irradiated with UV light through masks for different exposure times [18]. An indirect means of photo-patterning was demonstrated

Table 2 Overview of patterning techniques and application of patterned hydrogels

Patterning techniques
• micro-contact printing [38]
• photolithography [39–41]
• surface-initiated polymerization of brushes [42, 43]
• "dip-pen" nano-lithography [44]
• Plasma immobilization [45]
• ink-jet printing [46]
Application of patterned hydrogels
• cell adhesion/detachment devices [47, 48]
• protein adsorption [49]
• micro-reactors [50]
• automated fluidic valves [29, 30, 51]
• sensors [52, 53]

by Siegel et al. [19]. A dry hydrogel layer on a substrate was coated with a photoresist. A combination of resist lithography and dry etching in oxygen plasma yielded a hydrogel pattern with 2.5 μm resolution.

A direct means of patterning is photolithography [20].

In summary, one can say that photo-cross-linking is a very successful and often applied technique. It is suitable for patterning hydrogel features in the (1–100) μm range. Typical drawbacks are:

- UV irradiation of polymer with photo-crosslinkable groups needs modification of the sensitive polymer. The modification reaction gives way to a change in the conditions of the volume phase transition (increasing the hydrophobic part in the chain lowers the transition temperature).
- It often starts with a monomer or prepolymer in solution.
- Limited process control, complexity of sample handling.
- The penetration depth of light is limited.
- In the case of a filled polymer, weakening of intensity due to scattering of light limited resolution, state-of-the-art line width for hydrogels is (1–2) μm, see Fig. 1.
- Need for adhesion promoter if a gel layer on a support is the goal.

Considering the pros and cons of the photochemical method, we look for another method to synthesize structured smart polymers that can meet the requirements of MEMS and biotechnology. One goal is to overcome the limited resolution and the need for photo-initiators and/or modified polymers. For example, dots of hydrogels in the nanometer range can be used as scaffolds for growing cells and tissues: miniaturization needs nanofluidic channels to control or actuate fluid flow at that size scale.

Ionizing radiation has been recognized as a very suitable tool for the formation of hydrogels. The outstanding features of radiochemical cross-linking processes are:

- Easy process control, switching on and off of the cross-linking;
- the degree of cross-linking is correlated to the applied dose;

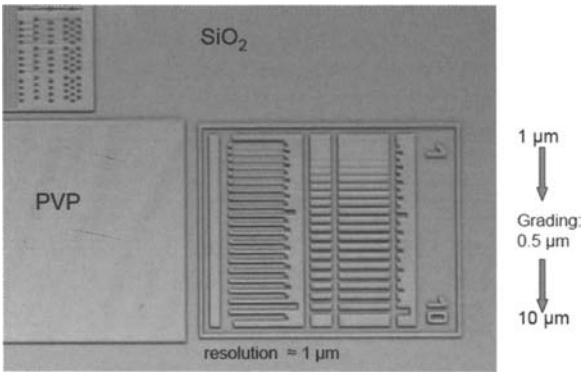

Fig. 1 Photopatterning of PVP. PVP (non-sensitive polymer) is often used in pharmaceutics (e.g. wound dressing, drug release)

- no need to add any initiators, cross-linkers etc., the mostly low molecular weight components are possibly harmful and difficult to remove;
- possibility of joining hydrogel formation and sterilization in one technological step, which could be important for medical application;
- relatively low running costs.

However, there are some limitations: High energy radiation can result in two processes: chain scission and cross-linking. In some cases, chain scission is the dominant process and it is not possible to form polymer gels with a good yield. The penetration depth of the radiation depends on its energy. This is important in using an electron beam for cross-linking. Irradiation with gamma rays needs long exposure times.

A polymer often applied, also as a hydrogel, in medicine and pharmacy is poly(N-vinyl pyrrolidone) [21]. Charlesby and Alexander first reported on the cross-linking of PVP and other polymers by irradiation [22]. After this pioneering work, various other water-soluble polymers were cross-linked to form hydrogels. From the literature and our own work, different smart polymers are known which can be cross-linked by high energy irradiation (γ -ray, mostly from the isotope Co^{60}, or electrons of different energies). A typical cross-linking procedure starts with the irradiation of an aqueous solution of the polymer with electrons or γ -rays. The structure of the gel formed depends on the polymer concentration and, in the case of a temperature-sensitive polymer, on the temperature.

In electron beam irradiation, it is difficult to prevent a change in temperature, due to the high amount of absorbed energy and the short irradiation time. The resulting gel is mostly heterogeneous, in contrast to γ -cross-linked gels. At low temperatures the polymer is in a good solution state. Irradiation at a low polymer concentration does not result in the formation of a gel. Highly branched polymers can be formed. Irradiation of a more highly concentrated polymer solution (concentration above the overlap concentration) results in a homogeneous macroscopic (bulky) gel. At a temperature higher than the critical temperature of the polymer, phase transition occurs. Aggregates are formed at a low concentration. The dimension of the gel particles formed is

determined by the aggregate-forming process, e.g. heating condition, and by the irradiation techniques applied and irradiation conditions. The dimension of the gel particles formed is between 10 nm and several 10^2 nm. Irradiation of a highly concentrated solution (again above the overlap concentration) yields a porous macroscopic gel.

Patterning is not, or not easily, possible by irradiation of an aqueous polymer solution, which is why irradiation conditions of different sensitive polymers in the dry state were investigated. Cross-linking a polymer in a dry state, e.g. in a thin layer, means different technological steps can be separated. In the first step, the layer of a defined thickness in a good quality is produced. After that, the layer is irradiated and the polymer cross-links. The film is immersed in water and the un-cross-linked polymer (sol content) is washed out. We were able to show that different stimuli-sensitive polymers were cross-linkable even in a dry state (Fig. 2). Generally, a higher radiation dose is necessary. Again, as in the photochemical approach, different techniques for patterning can be used.

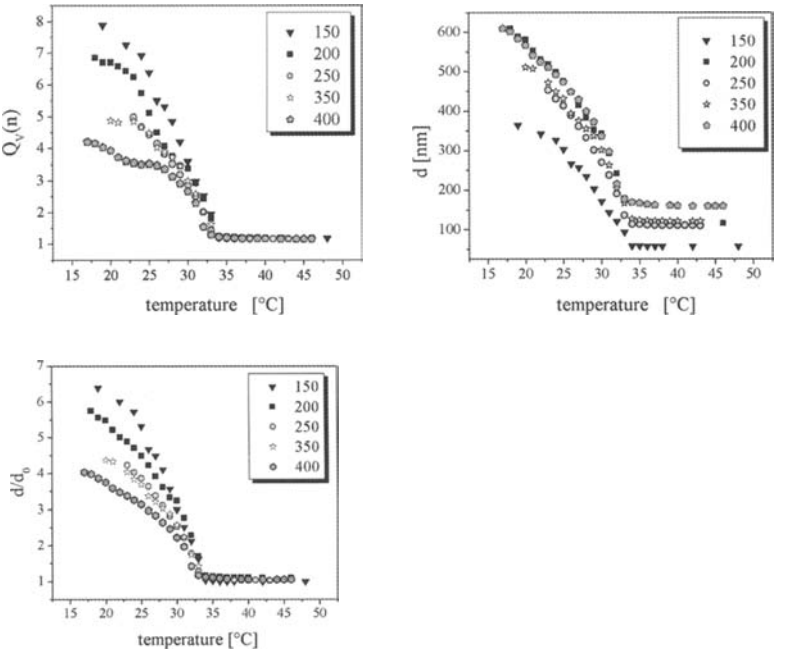

Fig. 2 Irradiation of a dry PVME film on a silicone wafer with different radiation doses (in kGy). The volume degree of swelling Q_V dependent on temperature was determined by ellipsometry [24]. The figures show the change of thickness in layer d as well as the ratio d/d_0 (d_0 = thickness of the dry layer) dependent on temperature

Irradiation through a mask

In the first step, a layer of the sensitive polymer on a substrate is generated by spin-coating. Due to the relation between the polymer concentration and the revolutions per minute, the thickness of the layer is adjustable. The dried layer is cross-linked by electron beam irradiation through a mask under an inert atmosphere.

A spin-coated layer is irradiated with 200 kGy. In a second step, the layer is irradiated through a mask with 300 kGy. Regions with different cross-linking density and therefore different degrees of swelling are formed [25].

By a subsequent irradiation it is possible to generate a layer with areas of different cross-linking densities. The layer has a flat surface in the dry state. At room temperature (high degree of swelling) the regions with a lower cross-linking density have a higher degree of swelling, and the regions with a higher cross-linking density have a lower degree of swelling (Fig. 3). By this technique it is possible to form bi-layers, e.g. of a sensitive and non-sensitive polymer [23–25].

One approach to further geometric reduction of the hydrogel structures presented on substrates is to use focused electron beams. This principle has been put into technological practice for a long time in electron beam lithography (EBL). In this process, an electron beam with a typical beam diameter of <10 nm is moved in a linear pattern across the sample and deflected to a defined extent in x and y directions using a coil system. As well as special devices developed for this purpose, scanning electron microscopes (SEMs) are often modified for this lithography method.

Fig. 4 shows the modification we used in schematic form. The SEM used was a Hitachi S4500 (cathode: cold field emission). Beam steering is no longer connected to the microscope and is carried out with an adapted electronic device, "ELPHY plus" (Raith GmbH, Dortmund, Germany). This device processes the structural design and converts it pixel for pixel into yes (electron beam hits the sample) or no (electron beam does not hit the sample) decisions. It also controls the beam blanker (on–off) and the coil system to deflect the electron beam in x and y directions. To increase precision when joining extended structures, the unit is fitted with a sample holder controlled by laser interferometry. This means registration accuracy can be achieved in the 10 nm range.

To perform the lithography, the electron beam, whose properties can be modified, is moved across the sample line by line. The main influencing factors in EBL are:

- acceleration voltage;
- dwell time (time the electron beam dwells on one pixel);
- step size;
- sample current;
- beam diameter.

Some of these parameters influence the dose, which can be seen as a central parameter of EBL. With this technology, the dose is indicated in $\mu C/cm^2$.

As with any technology, EBL presents a range of advantages, but also disadvantages.

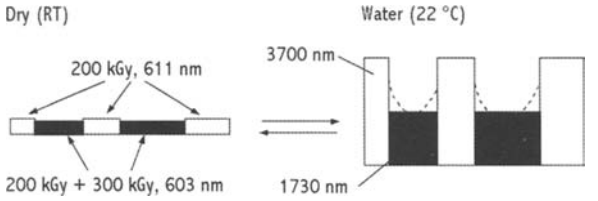

Fig. 3 Layer with regions of different crosslinking density

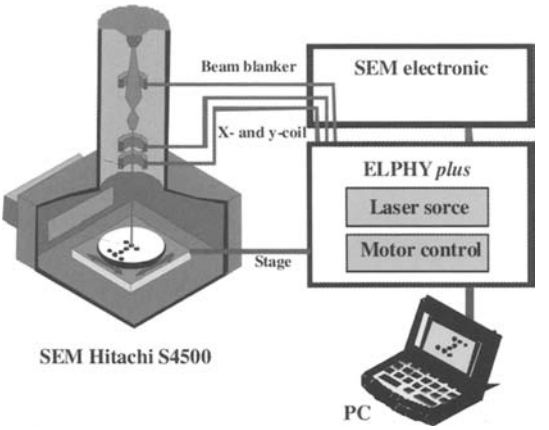

Fig. 4 Schematic diagram of the test set-up used

The main advantages worth mention are:

- Depending on the properties of the resist / polymer, geometric structures can be generated down to the range of a few nm.
- Structures made of different polymers can be created one after the other.
- By varying the dose above the minimum cross-linking dose, degrees of cross-linking can be produced which can cause different swelling patterns.
- The location of the structures can be defined very precisely.
- Structures can be created in indentations, e.g. in microfluidic channels.

The main disadvantages are:

- It is a slow process.
- The field to deflect the electron beam is limited in size – depending on the magnification selected during exposure on many commercial microscopes, $< 1 \times 1\ mm^2$. For this reason, to create extended structures, substructures may have to be lined up against one another, which requires very precise control of the sample holder.

During exposure, the electrons penetrate the polymer layer and lead to a modification of the polymer structure; in the case of hydrogels, crosslinking. Depending on the acceleration voltage in particular, the electrons also penetrate the substrate material

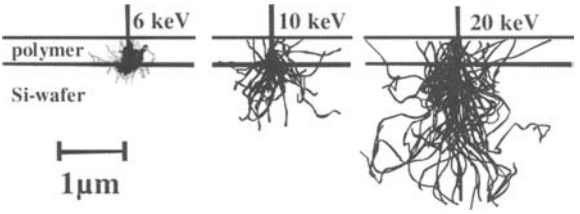

Fig. 5 Monte Carlo Simulation of the excitation volume for 6 keV, 10 keV and 20 keV of electron energy

and are scattered. Thus, they can influence the polymer again. With the help of theoretical simulations, it is possible to describe energy deposition and electron scattering in a polymer layer and in the substrate material. One means of numerical simulation often used for this purpose is the Monte Carlo method. Fig. 5 shows the result of a simulation calculation of this type for various energy values. One important result this demonstrates is that spatial energy distribution depends strongly on the acceleration voltage, and for low acceleration voltages the hydrogels which can be used are clearly less thick than for high acceleration voltages.

To create ideal structures, one thing which needs to be determined in particular is the ideal dose depending on the acceleration voltage, the structural geometry and the structural surroundings. This means that each substructure forming part of a whole may have to be allocated a different dose. Often, special test structures are used to determine the values important for the exposure. During the work process, first, an initial, overall dose is determined from rough structures; using these values, an adjustment is made for fine structures and different distances from neighbouring structures. Fig. 6 shows the result of a series of exposure tests to determine the overall dose, taking into account various acceleration voltages. The test structures used are comb structures where the individual structures are 5 µm in width, with the dose varied. Compared with the specified dose, the individual values for the exposure of the vertical lines are multiplied by factors of 0.125, 0.25, 0.5, 1.0, 2, 4, 8 and 10; i.e. for a specified dose of 100µC/cm^2 the actual dose varies from 12.5 μC/cm^2 to 1000 µC/cm^2.

After exposure and development (removal of the unexposed areas) the structures created are investigated in the AFM with regards to their geometrical shape. From the elevation profile in Fig. 6, it can be seen that the maximum value of the hydrogel structures is reached between the 2nd and 3rd value of the blue contour line. This is at a dose of between 25 µC/cm^2 and 50 µC/cm^2 (0.25 and 0.5 × 100 µC/cm^2, respectively). To establish the ideal dose more precisely, further experiments are required with a narrower variation between doses. However, upon looking at Fig. 6, the significant influence of the acceleration voltage is immediately recognizable. During the production of the structures depicted in Fig. 7, all experimental parameters – except the acceleration voltage – were kept constant. It can be seen that the dose required to achieve the maximum height of the hydrogel structures clearly rises along with the acceleration voltage, from approx. 50 µC/cm^2 at 3 kV to 200–400 µC/cm^2 at 20 kV.

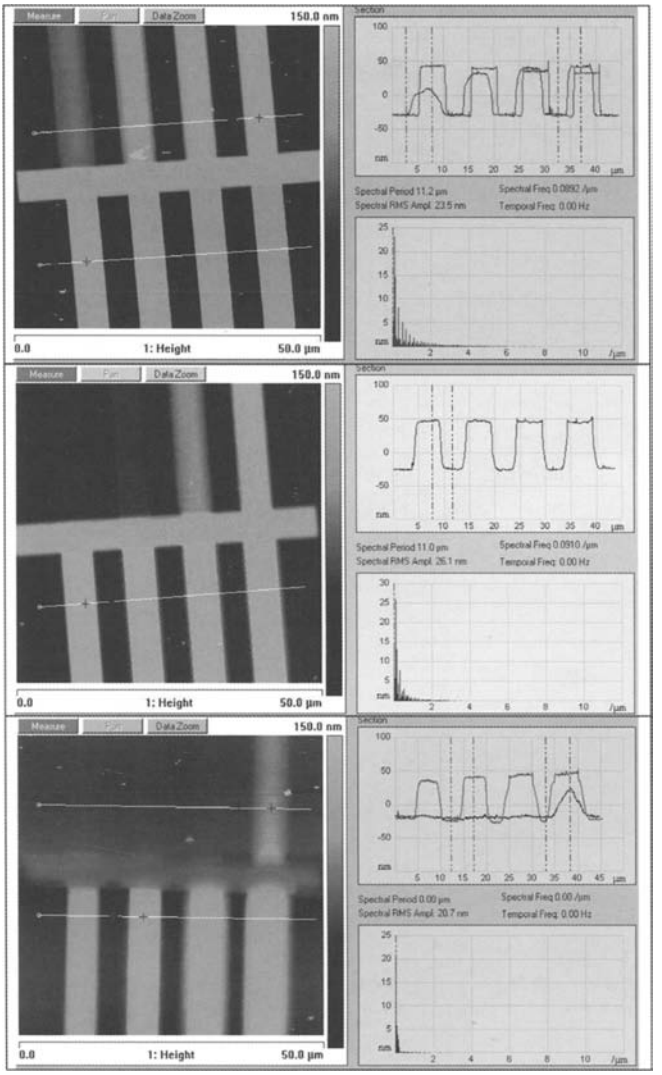

Fig. 6 AFM images of test structures, created with differing acceleration voltages

Furthermore, in Fig. 6, the extension of the structure at high doses is clearly visible.

In the next optimization section, a fine adjustment is made on test structures with very fine structures. One section of a test structure of this kind is depicted in Fig. 7. Squares were exposed which were 1.1 µm × 1.1 µm to 100nm × 100 nm in size, each with a dose variation of 50 to 290 µC/cm^2. It can be seen that small squares require a higher dose than large ones. Using test structures of this type, the ideal exposure conditions can be determined for any geometric layouts.

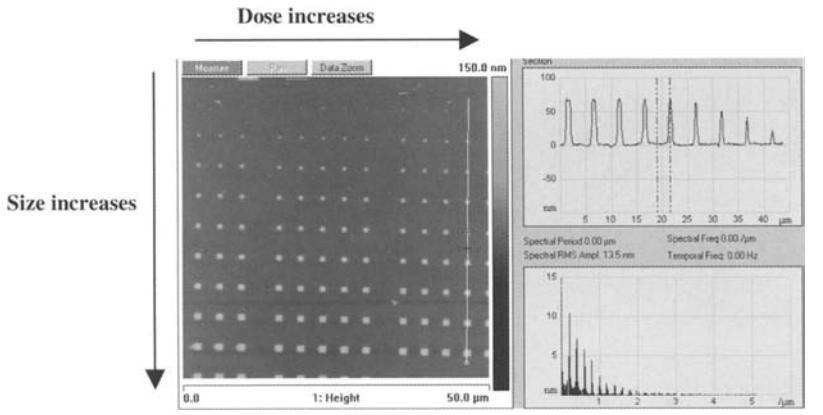

Fig. 7 AFM images of hydrogel structures in the µm and sub-µm range

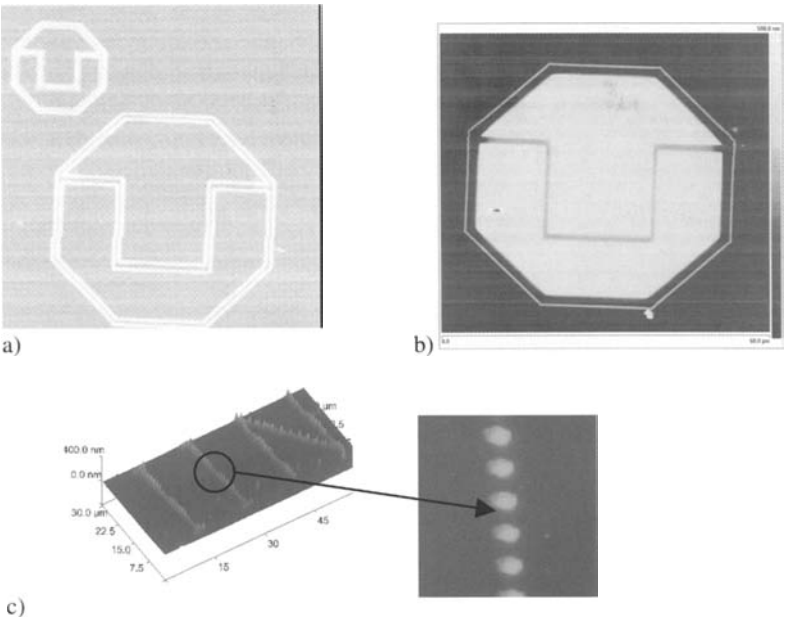

Fig. 8 AFM images of complex hydrogel structures. (**a** and **b** reproduced from [26], p. 759. Copyright Wiley-VCH Verlag GmbH & Co. KGaA. Reproduced with permission)

Using the procedures described above, the ideal dose for each hydrogel was determined and exposures were carried out. Using this technology, so far it has been possible to create structures from the following hydrogels on Si substrates:

PVP, P4VP, poly(vinyl caprolactam) (T-sensitive, ca. 31 °C), HPC, PNIPAAM, and Pluronic®F127, the width of the structure varying by several µm up to < 100 nm depending on the application.

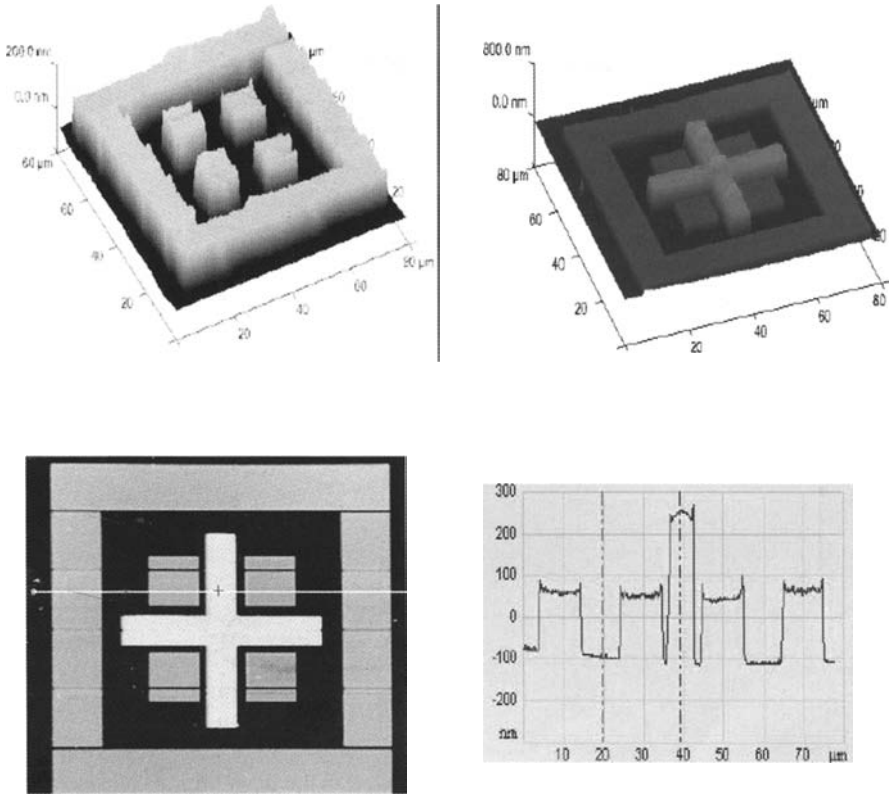

Fig. 9 Patterns from different hydrogels [27]

With the technology described here, in principle it is also possible to create more complex structures. As an example of this, Fig. 8 shows the logo of Dresden University of Technology in the form of individual lines (a), and individual lines and areas (b), and the letters IIN (for **I**nstitute for **I**ntegrative **N**anosciences) as dots. Although the same hydrogel is used for all materials, the ideal doses are different for all structures. From the example of the structure shown in Fig. 8, it was also shown, using fluid AFM, that the hydrogels keep their temperature-sensitive characteristics [26].

As well as preparing structures from a polymer, this technology can also be used to generate complex structures from several different hydrogels located next to one another. This can be shown from the example of the hydrogels HPC (temperature-sensitive) and P4VP (pH-sensitive). Using spin-coating, the polymer HPC was applied to a Si/SiO_2 substrate which had gold alignment marks applied to it using conventional thin-film technology methods. Depending on the overall structure required, first, a frame (10 µm in width), with four squares (10 µm × 10 µm) in it, was created in the first lithography step (Fig. 9).

After the necessary cleaning steps, the substrate was then coated with P4VP. Using the alignment marks, in the second lithography step, the cross (5 µm line width) was

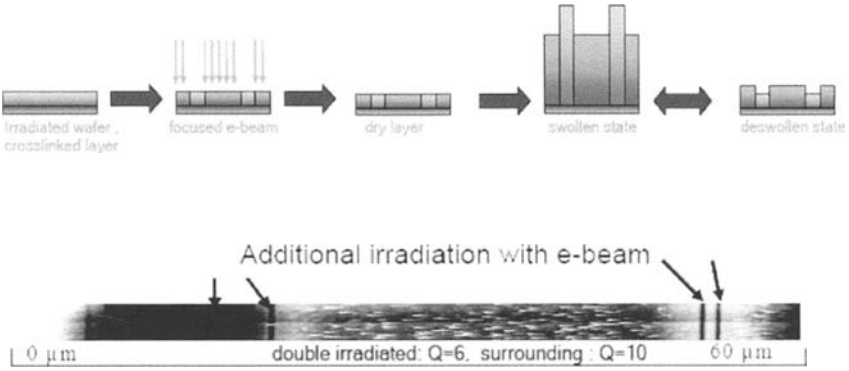

Fig. 10 Creation of crosslinking gradients. (Reproduced from [28], p. 535. Copyright Wiley International. Reproduced with permission)

added in the correct position in the first structure. From the contour lines on the AFM image, the thickness of the layers in a dry state can be estimated at 170 nm und 360 nm.

As well as the creation of separated structures, EBL can continue to be used to generate crosslinking gradients in a geometrically larger hydrogel structure. For this purpose, the technology shown in Fig. 10 can be used. The central element of this technology is taking hydrogel layers which have already been irradiated, and thus cross-linked, and applying another dose using EBL according to the pattern required.

In this way, crosslinking gradients are produced in the layer which can also result in different swelling behavior. The first and second irradiation can be carried out using only EBL or as a combination of EBL and other irradiation methods.

4 Application of gels in MEMS

The unique properties of stimuli-sensitive hydrogel are very interesting to develop microelectromechanical systems (MEMS). In particular, liquid handling fluidics and microfluidics could benefit from a hydrogel-based technology. However, only thermo-sensitive gels show the significant and reversible volume phase transition which is necessary for them to function as actuators. Therefore, the electronic control of active hydrogel elements is typically realized by an electrothermic interface [29, 30]. In the following two basic microfluidic basic devices, controllable microvalves and adjustable microchemostat valves basing based on the thermo-sensitive PNIPAAm (see Table 1) are described.

4.1 Microvalves

The basic function of such devices is to switch a liquid flow. By swelling, the gel actuator either closes a channel directly or performs mechanical work by displacing a distortable diaphragm to close the channel indirectly.

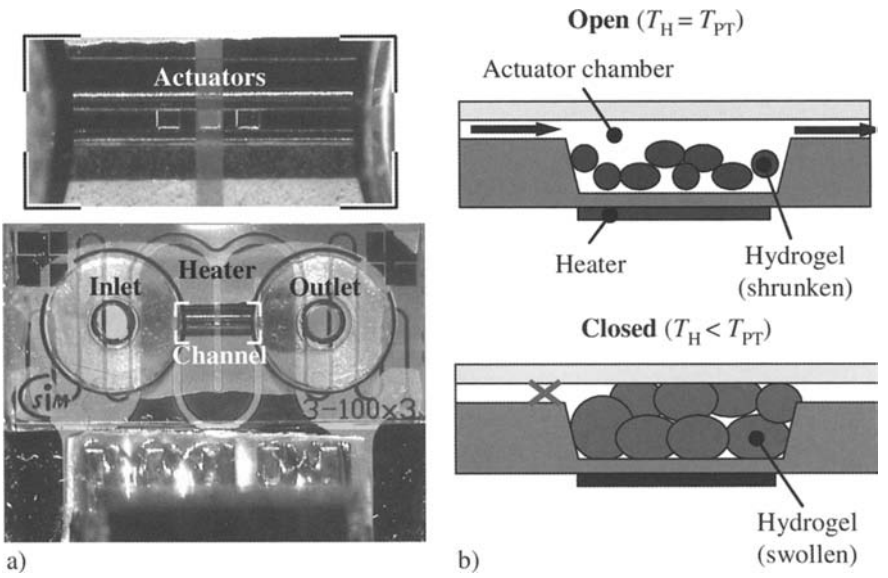

Fig. 11 Microvalves with electrothermic interface. a Photo-patterned actuators, each of the three actuators is (100 × 100 × 50) μm^3 in size; **b** Set-up and operating principle of a microgel-based microvalve [30, 31]

The actuators of the microvalves shown in Fig. 11 are directly placed within the channels, enabling the device to be set up simply. The electrothermic interface to control the actuator temperature is realized by heating elements.

The actuators can be fabricated *in-situ* by photo-patterning (Fig. 11a). The fixation of the hydrogel onto the substrate occurs by an adhesion promoter. When using microgels as actuator materials, the particles have to be enclosed in an actuator chamber (Fig. 11b). By heating the PNIPAAm actuator above the phase transition temperature {T_{PT} (PNIPAAm) ≈ 34 °C} the valve opens. To switch off the liquid flow the heating has to be disabled, the gel cools below the T_{PT} and closes the valve seat by swelling.

The opening time of the microvalve depends strongly on the applied heating power (Fig. 12a). For a valve with a chamber size of (500 × 500 × 200) μm^3 an optimal opening time of 300 ms was obtained at 350 mW. Increasing the power further leads only to a small time decrease. The closing time of the valve depends on the cooling rate of the microvalve due to heat transfer to the environment. The spontaneous shut-off time at room conditions is typically about 2 s. By active cooling, a closing time shorter than 1 s can be obtained. Fig. 12a also illustrates the effect of the heat capacity of the valve body. An increase in the heat capacity increases the heating power that is necessary to obtain short opening times.

Furthermore, the response times of the valves are influenced by the degree to which the actuator chamber is filled (Fig. 12b). If it is filled to a low degree this provides

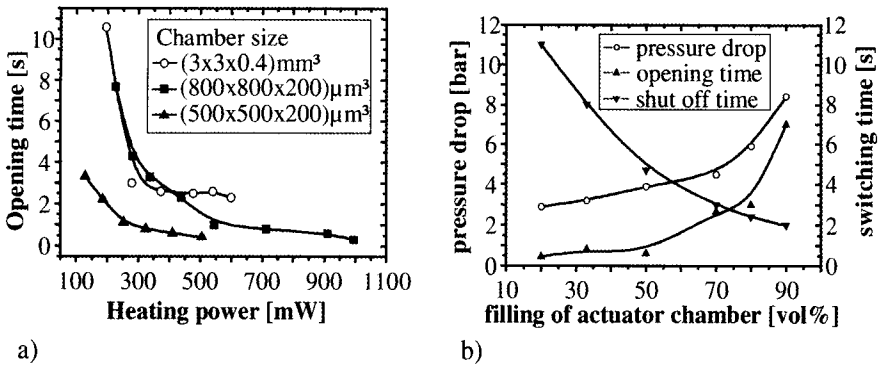

Fig. 12 Operating behavior of the microvalves. a The opening time depending on the applied heating power; **b** Influence of the degree to which the actuator chamber is filled on the pressure resistance and switching time of the microvalve [30, 31]

short opening times but long closing times, while a high degree decreases the closing time and increases the opening time. The degree to which the actuator chamber is filled with actuator material also influences the pressure resistance of the valve. The maximum pressure drop up to which no leakage flow can be observed is 8.4 bar when filled to 90%. Due to the softness of the actuator, hydrogel-based microvalves are very particle permissive. This feature makes hydrogel valves interesting for biological investigation. Since 2004, the company GeSiM mbH Großerkmannsdorf, Germany, has been producing hydrogel-based microvalves.

4.2 Microchemostat valves

The property of stimuli-sensitive hydrogels to combine both sensor and actuator properties allows a simple active device to be created for the automatic concentration regulation of chemical substances. The automatic flow control depending on concentration is interesting for regulating chemical and biochemical substances. In particular, case-sensitive drug release systems or devices acting as a substitute for body functions such as the pancreas could be developed. However, the lack of flow regulation adjustability of the operating conditions e.g. a critical concentration defined by the hydrogel used, inhibits the broad practical use of chemostats.

To electronically adjust the chemostats' operating conditions we use a controlled double-sensitivity hydrogel. At isothermal conditions the volume phase transition of the hydrogel occurs at a defined critical concentration of chemical substance. By changing the isotherm, the critical concentration is also changed. Therefore, control of the PNIPAAm actuator's temperature should enable the operating condition and/or switching concentration to be adjusted. The set-up of a microchemostat valve is shown in Fig. 13.

Both the temperature sensor and heater (Fig. 13b) realize a closed loop control to keep constant the device's temperature and isotherm.

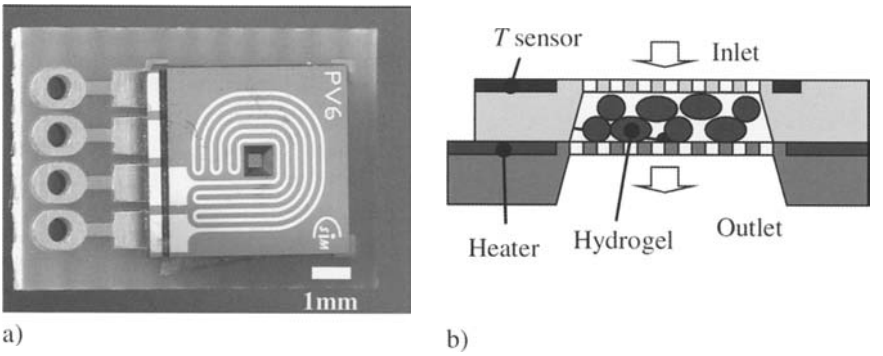

Fig. 13 Microchemostat valves. a Photograph of the device, **b** Schematic set-up of the chemostat valve [32]

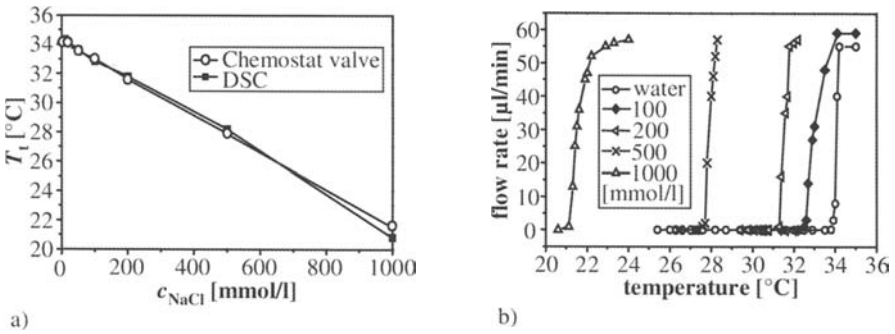

Fig. 14 The operating point characteristics of the chemostat valve regulating an aqueous NaCl solution. a The volume phase transition temperature determined by DSC measurements agrees with the operating point of the chemostat; **b** The position of the phase transition decreases as the salt concentration increases [32]

Fig. 14a compares the phase transition temperature for various sodium chloride solutions measured by DSC with the operating point characteristics of the chemostat valve. Both values are in good agreement. The average deviation of salt concentration investigated by repeated variations is 25 mmol/l. Furthermore, the regulation function of the chemostat valve is not affected at high salt concentrations (Fig. 14b).

5 Conclusions

Radiation chemistry gives possibilities to synthesize smart hydrogels in a broad range of dimension. The method is applicable to different sensitive polymers. The patterning of a layer on a substrate by electron lithography is possible. Writing with a focused e-beam onto a cross-linked layer results in changes in cross-linking density and

swelling behavior. Different combinations of polymers, e.g. multilayer, or a pattern of polymers with different sensitivities, were synthesized.

The examples of application show that smart gels can be integrated into microsystems and common technologies can be used. It has been shown that a hydrogel-based technology provides actuator devices. A chemostat functionality is unknown from other material-based technology. The principle opens broad possibilities for the application of hydrogel-based systems in chemical and biotechnological processes as well as medical treatment.

Acknowledgments. The authors wish to thank the DFG for financial support (AR 193/11-1, MO 887/2-1, RI 1294/2-1, RI 1294/4-1).

References

[1] Kuhn W (1949) Reversible Dehnung und Kontraktion bei Änderung der Ionisation eines Netzwerks polyvalenter Fadenmolekülionen. Experientia 5:318

[2] Breitenbach JW, Karlinger H (1949) Swelling of cross-linked polymethacrylic acid. Monatshefte Chem 80:312–313

[3] Katchalsky A, Oplatka A (1965) Mechanochemistry. In: Proc of the 4th Intern Congr Rheol, Providence Volume Date 1963 (Pt. 1):73–97

[4] Haraguchi K, Takeshi T, Fan S (2002) Effects of clay content on the properties of nanocomposite hydrogels composed of poly(N-Isopropylacryl-amide) and clay. Macromolecules 35:10162–10171

[5] Gehrke SH (1993) Synthesis, equilibrium swelling, kinetics, permeability and applications of environmentally responsive gels. Adv Polym Sci 110:81–144

[6] Arndt KF, Knoergen M, Richter S, Schmidt T (2006) NMR Imaging: Monitoring of swelling of environmental sensitive hydrogels. In: Webb GA (ed) Modern Magnetic Resonance Part 1, Springer-Verlag, Dordrecht, pp 183–189

[7] Tanaka T, Fillmore DJ (1979) Kinetics of swelling of gels. J Chem Phys 70:1214–1218

[8] Dong LC, A. S. Hoffman AS (1990) Synthesis and application of thermally-reversible heterogels for drug delivery. J Control Release 13:21–31

[9] Yan Q, Hoffman AS (1995) Synthesis of macroporous hydrogels with rapid swelling and deswelling properties for delivery of macromolecules. Polymer 36:887–889

[10] Arndt KF, Schmidt T, Menge H (2001) Poly(vinyl methyl ether) hydrogel formed by high energy irradiation. Macromol Symp 164:313–322

[11] Gotoh T, Nakatani Y, Sakohara S (1998) Novel synthesis of thermosensitive porous hydrogels. J Polym Sci 69:895–906

[12] Suzuki M, Hirasa O (1993) An approach to artificial muscle using polymer gels formed by micro-phase separation. Adv Polym Sci 110:241–261

[13] Yoshida R, Uccida K, Kaneko Y, Sakai K, Kikuchi A, Sakurai Y, Okano T (1995) Comb-grafted hydrogels with rapid de-swelling response to temperature changes. Nature 374(6519):240–242

[14] Pelton R (2000) Temperature-sensitive aqueous microgels. Adv Colloid Interface Sci 85:1–33

[15] English AE, Edelman ER, Tanaka T (2000) Polymer hydrogel phase transition. In: Tanaka T (ed) Experimental Methods in Polymer Science. Academic Press, pp 547–589

[16] Hirotsu S, Hirokawa Y, Tanaka T (1987) Volume-phase-transitions of ionoized N-isopropyl-acrylamide gels. J Chem Phys 87, 1392
[17] Arndt KF, Schmidt T, Reichelt R (2001) Thermo-sensitive poly(methyl vinyl ether) micro-gel formed by high energy radiation. Polymer 42:6785–6791
[18] Kuckling D, Hoffmann J, Plötner M, Ferse D, Kretschmer K, Adler HJ, Arndt KF, Reichelt R (2003) Photo cross-linkable poly(N-isopropylacrylamide) copolymers III: Micro-fabricated temperature responsive hydrogels. Polymer 44: 4455–4462
[19] Lei M, Gu Y, Baldi A, Siegel RA, Ziaie B (2004) High-resolution technique for fabricating environmentally sensitive hydrogel microstructures. Langmuir 20:8947–8951
[20] Chan-Park, Mary B, Yan Y, Neo WK, Zhou W, Zhang J, Yue CY (2003) Fabrication of high aspect ratio poly(ethylene glycol)-containing microstructures by UV embossing. Langmuir 19:4371–4380
[21] Peppas NA, Klier J (1991) Controlled release by using poly(methacrylic acid-g-ethylene glycol) hydrogels. J Control Release 16:203–214
[22] Charlesby A, Alexander P (1955) Reticulation of polymers in aqueous solution by γ-rays. J de Chim Phys et de Phys-Chim Biol 52:699–709
[23] Hegewald J, Schmidt T, Gohs U, Günther M, Stiller B, Reichelt R, Arndt KF (2005) Electron Beam Irradiation of Poly(vinyl methyl ether) Films: 1. Synthesis and Film Topography. Langmuir 21:6073–6080
[24] Hegewald J, Schmidt T, Eichhorn KJ, Kretschmer K, Kuckling D, Arndt KF (2006) Electron Beam Irradiation of Poly(vinyl methyl ether) Films. 2. Temperature-Dependent Swelling Behavior. Langmuir 22:5152–5159
[25] Hegewald J (2004) Strahlenmechanische Synthese und Charakterisierung dünner, temperatursensitiver PVME-Schichten, diploma thesis, TU Dresden
[26] Schmidt T, Mönch JI, Arndt KF (2006) Temperature-sensitive hydrogel pattern by electron-beam lithography. Macromol Mater Eng 291:755–761
[27] Kaiser C (2007) Strahlenmechanische Synthese und Charakterisierung dünner Hydrogel-Multi-Schichten, diploma thesis, TU Dresden
[28] Burkert S, Schmidt T, Gohs U, Mönch JI, Arndt KF (2007) Patterning of thin Poly(N-vinyl pyrrolidone) films on Si substrates by electron beam lithography. J Appl Polym Sci 106:534–539
[29] Arndt KF, Kuckling D, Richter A (2000) Application of sensitive hydrogels in flow control. Polym Adv Technol 11:496–505
[30] Richter A, Kuckling D, Howitz S, Gehring T, Arndt KF (2003) Electronically controllable microvalves based on smart hydrogels: magnitudes and potential applications. J Microelectromech Syst 12:748–753
[31] Richter A, Howitz S, Kuckling D, Arndt KF (2004) Influence of phenomena of volume phase transition at the behavior of hydrogel based valves. Sens Actuator B 99:451–458
[32] Richter A, Türke A, Pich A (2007) Controlled double-sensitivity of microgels applied to electronically adjustable chemostats. Adv Mater 19:1109–1112
[33] Schild HG (1992) Poly(N-isopropylacrylamide): experiment, theory and application. Progr Polym Sci 17:163–249
[34] Ichijo H, Hirasa O, Kishi R, Oowada M, Sahara K, Kokufuta E, Kohno S (1995) Thermo-responsive gels. Radiat Phys Chem 46:185–190
[35] Klug ED (1971) Properties of water-soluble hydroxyalkyl celluloses and their derivatives. J Polym Sci C 9:491–508
[36] Winnik FM (1987) Effect of temperature on aqueous solutions of pyrene-labeled (hydroxypropyl)cellulose. Macromolecules 20:2745–2750
[37] Giebeler E, Stadler R (1997) ABC triblock polyampholytes containing a neutral hydrophobic block, a polyacid, and a polybase. Macromol Chem Phys 198:3815–3825

[38] Xia Y, Whiteside GM (1998) Soft lithography. Angew Chem Inter Ed 37:550–557
[39] Chen C, Imanishi Y, Ito Y (1998) Photolithographic synthesis of hydrogels. Macromolecules 31:4379–4381
[40] Ward JH, Bashir R, Peppas NA (2001) Micropatterning of biomedical polymer surfaces by novel UV polymerization techniques. J Biomed Mater Res 56:351–360
[41] Kuckling D, Adler HJ, Arndt KF (2002) Poly(N-isopropylacrylamide) copolymers: Hydrogel formation via photocrosslinking. In: Bohindar HB, Dubin P, Osada Y (eds) Polymer Gels: Fundamentals and Applications, ACS Symp Series 833, ACS: Washington, pp 312–325
[42] Milner ST (1991) Polymer Brushes. Science 251:905–914
[43] Zhao B, Brittain WJ (2000) Polymer brushes: surface-immobilized macromolecules. Progr Polym Sci Jpn 25:677–710
[44] Wounters D, Schubert US (2003) Nanolithography and nanochemistry: Probe-related patterning techniques and chemical modification for nanmeter-sized devices. Angew Chem Int Ed 43:2480–2495
[45] Schmaljohann D, Nitschke M, Schulze R, Eing A, Werner C, Eichhorn KJ (2005) In: situ study of thermoresponsive behavior of micropatterned hydrogel films by imaging ellipsometry. Langmuir 21:2317–2322
[46] de Gans, BJ, Duineveld, PC, Schubert, US (2004) Inkjet printing of polymers: State of the art and future developments. Adv Mater 16:203–213
[47] Lutolf MP, Raeber GP, Zisch AH, Tirelli N, Hubbell JA (2003) Cell-responsive synthetic hydrogels. Adv Mater 15:888–892
[48] Koh WG, Revzin A, Siminian A, Reeves T, Pishko M (2003) Control of mammalian cell and bacteria adhesion on substrates micropatterned with poly(ethylene glycol) hydrogels. Biomed Microdev 5:11–19
[49] Hong Y, Krsko P, Libera M (2004) Protein surface patterning using nanoscale PEG hydrogels. Langmuir 20:11123–11126
[50] Harmon ME, Tang M, Frank (2003) A microfluidic actuator based on thermosensitive hydrogels. Polymer 44:4547–4556
[51] Beebe DJ, Moore JS, Bauer JM, Yu Q, Lui RH, Devadoss C, Jo BH (2000) Functional hydrogels for autonomous flow control inside microfluidic channels, Nature 404:588–590
[52] Marshall AJ, Blyth J, Davidson CAB, Lowe CR (2003) pH-sensitive holographic sensors. Anal Chem 75:4423–4431
[53] Richter A, Bund A, Keller M, Arndt KF (2004) Characterization of a microgravimetric sensor based on pH sensitive hydrogels. Sens Actuat B 99:579–585

Stimuli-Sensitive Composite Microgels

Haruma Kawaguchi

Abstract. Poly(N-isopropylacrylamide) (PNIPAM) microgels were prepared by precipitation polymerization and PNIPAM shell / hard core particles were obtained by soap-free emulsion copolymerization or seeded polymerization. Hairy particles were prepared by "grafting-to" modification or "grafting-from" living radical polymerization. They exhibited not only volume phase transition but also changes in some physical properties in a certain temperature range. Composite thermosensitive microgels including magnetite, Au, or titania were obtained by in situ formation of metal or metal oxide in polymeric particles. The functions of metal or metal oxide were tuned by reversible volume phase transition of the microgel as a function of temperature. Enzyme-carrying thermosensitive microgels exhibited unique temperature-dependence of enzyme activity.

1 Introduction

Soft matter is deformed by external forces or stimuli. A variety of stimuli, e.g., temperature, pH, ionic strength, light, electric field, magnetic field, biomolecules, etc. were applied for the deformation. Deformation generally occurs gradually or continuously. But some soft matter exhibits discontinuous deformation in a limited range of strength of stimuli. For example, poly(acrylic acid) gel swells and shrinks in the pH range of 4 to 6 although the volume of the gel does not change significantly below pH 4 and above pH 7. The deformation is generally reversible with repeated application of stimuli and such soft matter is called "smart matter". Stimuli may cause not only deformation, but also changes in physical properties such as density, surface potential, adsorbability, etc. In the case of particles, stimuli cause changes in specific surface area and response rate of such particles. The mobility and stability of particles in dispersion are also affected by stimuli. For example, stable dispersion and destabilized aggregation are reversibly possible by changing temperature, pH, etc. Such changes can be used for purposes such as sensing, control of particle recovery, drug delivery control, etc. In these cases, the particles are called as "smart particles". Here we focus on smart particles with temperature responsiveness, and their design, synthesis, function and application are described.

Barbucci R. (Ed): Hydrogels. Biological Properties and Applications.

2 The representative thermosensitive polymer, poly(N-isopropylacrylamide)

N-isopropylacrylamide (NIPAM) is a kind of amphiphilic monomer as expected from its molecular structure shown in Fig. 1. NIPAM has hydrophobic vinyl and isopropyl groups and a hydrophilic amide group. Due to their balance, NIPAM is soluble in water regardless of temperature. Poly(N-isopropylacrylamide) (PNIPAM) is also amphiphilic but the amphiphilicity is different from that of the monomer because of the difference in entropy between the monomer and polymer [1]. PNIPAM exhibits reversible transition between hydrophilic and hydrophobic states with temperature change, which is explained in several ways. Here, the most probable explanation for the reversible temperature dependence of PNIPAM is presented.

At low temperature, isopropyl groups in the polymer are swallowed by water molecules bound to each other through hydrogen bonds. This is referred to as hydrophobic hydration, in which the loss of entropy of water molecules is compensated by the gain of enthalpy of hydrogen bonding among water molecules. A rise in temperature causes a cut-off of hydrogen bonding, that is, a collapse of the water molecules cage. This is followed by cohesion of neighboring isopropyl groups. As a result, the PNIPAM molecule changes its conformation from a coil to globule when in water. This event occurs at so-called lower critical solution temperature (LCST). The phase diagram and LCST of PNIPAM in aqueous solution are shown in Fig. 1 [2]. A homogeneous solution is phase separated into two phases, that is, a polymer-rich phase and aqueous phase when the temperature of the solution exceeds the LCST. There are a large number of polymers which have their own LCST.

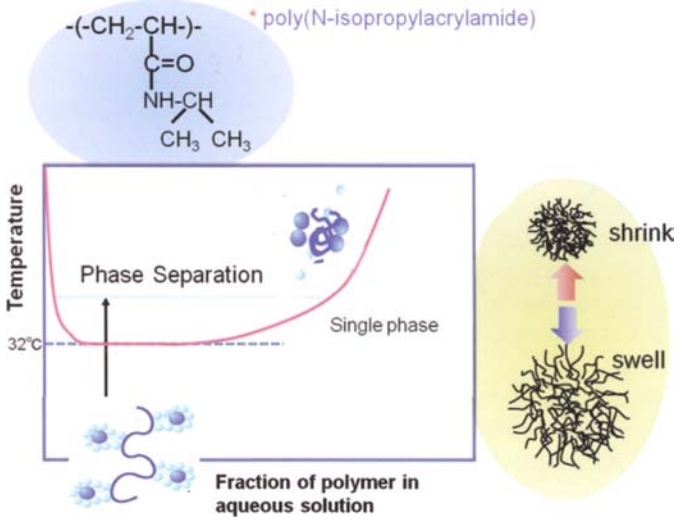

Fig. 1 Molecular structure of poly(N-isopropylacrylamide) (PNIPAM) and phase diagram of PNIPAM/water system

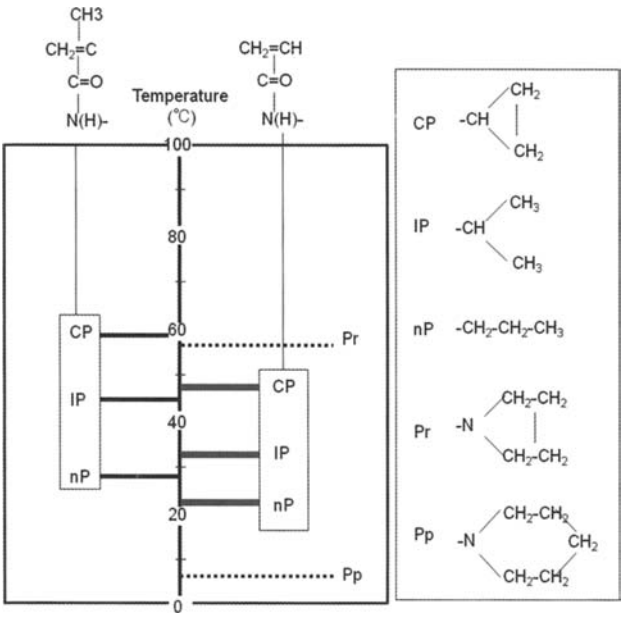

Fig. 2 Lower critical solution temperature of poly((meth)acrylamide) derivatives

Presented in Fig. 2 is a revision of some polymers exhibiting LCSTs [3]. Interestingly, three poly(propylacrylamide)s, poly(cyclopropylacrylamide) (PCPAM), PNIPAM, and poly(n-propylacrylamide) (PnPAM) have decreasing LCSTs. The LCSTs of PCPAM, PNIPAM and PnPAM are 43°, 32°, and 25°, respectively. The difference in LCST is attributed to the compactness of the propyl group. Namely, the water molecule cage surrounding the propyl group is the most stable for PCPAM out of the three poly(propylacrylamide)s because the cyclopropyl group is the most compact among propyl groups. In contrast, PnPAM's propyl group has the most extended and dangling structure and water molecules have difficulty forming a cage at relatively low temperature.

In general, the more hydrophobic the polymers are, the lower the LCSTs are. But this is not the case for poly(propylacrylamide)s and poly(propylmethacrylate)s. The latter have higher LCSTs than the former. This is attributed to the steadiness of the main chains of the polymers. The α-Carbon atom of methacrylamide possesses a methyl group and $CONR_2$ group, and so the main chain of methacrylamide has more symmetry and steadiness compared with acrylamide, whose α-carbon has hydrogen and $CONR_2$ unsymmetrically. As a result, poly(acrylamide) is too insecure for the main chain to hold the water molecule cage stably. This means that poly(methacrylamide) has a higher LCST than the corresponding poly(acrylamide), though the former is more hydrophobic than the latter.

When LCST-possessing polymers are crosslinked, they cannot be dissolved in water anymore, but they swell and their volumes drastically change at the LCST.

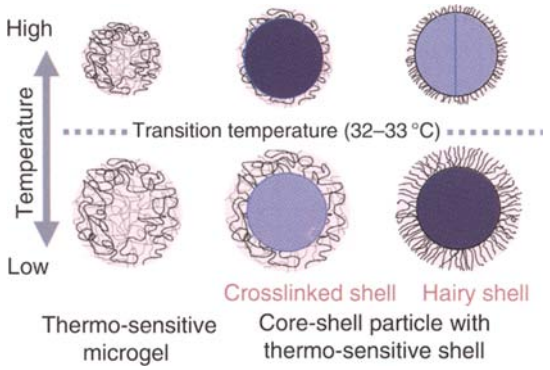

Fig. 3 Thermosensitive particles with different morphology

Swollen PNIPAM gel at low temperature in water shrinks above the LCST and, when it cools, the gel recovers its swollen state. This behavior is referred to as volume phase transition of gel.

3 Design and synthesis of smart particles

Different types of thermosensitive particles shown in Fig. 3 were designed and prepared.

3.1 PNIPAM microgel

There are two ways to prepare polymer particles. One is polymer molecule assembly from a dilute solution, followed by crosslinking. As mentioned in the previous section, a rise in temperature of the dilute aqueous solution of PNIPAM brought about the formation of nano-aggregates as a result of phase separation. Such aggregates dissolve reversibly when the solution is cooled down. To prevent this, aggregates should be crosslinked before the solution cools.

The other way to prepare polymer particles is particle-forming polymerization, which includes emulsion polymerization, suspension polymerization, dispersion polymerization, etc. Precipitation polymerization is also a particle-forming polymerization. It is defined as the polymerization by which polymer molecules come out of a monomer solution.

Chibante and Pelton prepared monodisperse PNIPAM microgels by precipitation polymerization in aqueous solution [4]. According to Fig. 1, formation of the polymer from a homogeneous aqueous solution of NIPAM at 70° results in immediate phase separation into a polymer-rich phase and an aqueous phase. The fraction of polymer-rich phase increases with increasing conversion. Polymer-rich phase is prone to form polymer aggregates, and aggregates accumulate during the course of polymerization. But, when the precipitation polymerization was initiated with persulfate, e.g., potas-

sium persulfate (KPS), the polymer molecule possessed an anionic group at the chain end which suppresses aggregation of polymer molecules at a certain level due to electrostatic repulsive forces between aggregates and, as a result, gives stable microgels. According to the observation of particles by transmission electron micrograph during the precipitation polymerization, the evolution of particle volume was proportional to the conversion. This means that polymerization contributed only to growth of particles but not to nucleation for new particles. In other words, the number of particles was fixed at a very early stage of polymerization and after that, existing particles grew evenly till the end of polymerization. As a result, PNIPAM particles were very monodispersed.

Addition of surfactant or stabilizer to the precipitation polymerization made the microgels smaller than in their absence. Smaller particles were targeted because of their merit stimuli can be transferred faster from their surface to their center. Quantitative analysis of the rate of stimuli transfer was studied by Tanaka et al. and equation 1 was presented [5],

$$\text{Log (rate of stimuli transfer)} \propto -2 \log \text{(particle diameter)} \quad (1)$$

Polymer molecules in microgels were usually entangled enough to prevent them coming apart below the LCST, but crosslinking is effective for their reinforcement.

Characteristic PNIPAM microgels were formed by modified preparative methods. Lyon, et al. created core-shell microgels whose core and shell are both composed of PNIPAM, but the polymers of the shell and core were not so mixable between themselves. The thermosensitive behavior of the core was modulated with the shell polymer [6, 7].

3.2 Hard core / PNIPAM gel shell particles

Microspheres composed of a hard core and gel shell are regarded as a kind of microgel. They are generally prepared by

1) soap-free emulsion copolymerization of hydrophobic and hydrophilic monomers, and;
2) seeded polymerization, in which hydrophilic polymers are formed or adsorbed onto seed particles covering them.

Concerning 1), one monomer combination for soap-free emulsion copolymerization to prepare hard core / PNIPAM shell particles is glycidyl methacrylate (GMA) and NIPAM [8]. Because GMA is more hydrophobic and more reactive than NIPAM, core-shell particles composed of polyGMA (PGMA)-rich core and PNIPAM-rich shell can be formed automatically. Epoxy groups in the core could be used as sites for chemical modification.

Concerning 2), seeded polymerization of NIPAM enabled the formation of well-structured core-shell particles whose shell is composed of PNIPAM. A small amount of NIPAM was added to styrene in seed particle forming polymerization as this helped effective pick-up of PNIPAM from aqueous medium in seeded polymerization to form the PNIPAM shell.

Compared with microgel formation by precipitation polymerization, gel shell-carrying particle formation by seeded polymerization has an advantage in terms of mass production of microgel-like particles.

3.3 Hairy particles

A hairy particle is defined as the particle whose core binds a number of polymer chains having free ends. A hairy particle is regarded as a special gel shell-carrying particle which has no crosslinks in the shell. Hairy particles can be obtained by several methods. They include

1) assembling amphiphilic diblock copolymers, hydrophobic blocks which contribute to assembly and hydrophilic blocks which form a hairy layer to stabilize the assembled material;
2) attaching hydrophilic polymer chains to existing particles at the chain ends (so-called grafting-to method);
3) polymerizing hydrophilic monomers from the surface of existing particles (so-called grafting-from method).

3.3.1 Molecular assemby method

Block copolymer assembly method was employed for the formation of hairy particles using poly(glycerol methacrylate) (PGLM)-block-PNIPAM which was prepared by quasi-living radical polymerization in water [9]. The living / dormant species was a water soluble photo-iniferter. PNIPAM core / PGLM shell particles can be prepared by elevating the temperature of the aqueous solution of polymer above the LCST of PNIPAM. Another hairy particle with inverse morphology, PGLM core / PNIPAM shell particle, was prepared by a method different from temperature change. The method was solvent composition change, that is, gradual addition of tetrahydrofuran (THF) into a methanol solution of block copolymer resulted in the formation of PGLM core / PNIPAM shell particles because THF is a poor solvent for PGLM and caused aggregation of the PGLM part. Glycol groups in the core were used for complex formation with ferric ions and consequently magnetite formation.

3.3.2 Grafting-to method

Grafting-from polymerization can be carried out in two ways, conventional and living radical polymerization. Both polymerizations require an initiation site on the surface of core particles. Particles having hydroxyl groups on their surface can be used for conventional radical polymerization because the surface offers radicals when ceric ions are added and constructs redox systems with hydroxyl methylene groups [10]. Such core particles are prepared by soap-free emulsion copolymerization of styrene and glycerol methacrylate or hydroxyethyl methacrylate.

Living radical graft polymerization has some advantages compared to conventional polymerization. Living radical polymerization enables monodispersed hairy chains having desirable length to be obtained, and to design the sequence of chains,

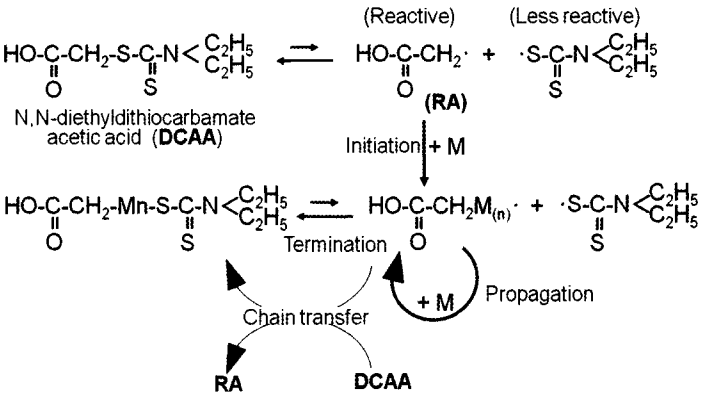

Fig. 4 Living radical polymerization using an iniferter

e.g., multi-block copolymer hairs [11]. One example of living radical graft polymerization is shown in Fig. 4.

The growth of hairs in the course of living radical polymerization is confirmed by determining the molecular weight of hairs after recovering the hairs cut from the particle. This procedure is orthodox and reasonable but troublesome. Fukuda, et al. proposed an alternative method, in which initiating species are dissolved in the living radical graft polymerization system in order to have the dissolved polymer in the water phase. The molecular weight of the polymer is regarded as that of the hairy chain because they confirmed that both polymers dissolved in water and bound to the particle surface had almost the same molecular weight [12]. More qualitatively, TEM views of hairy particles indicate the progress of living radical graft polymerization. This is shown in Fig. 5. The TEM shows (a) particles before living radical polymerization,

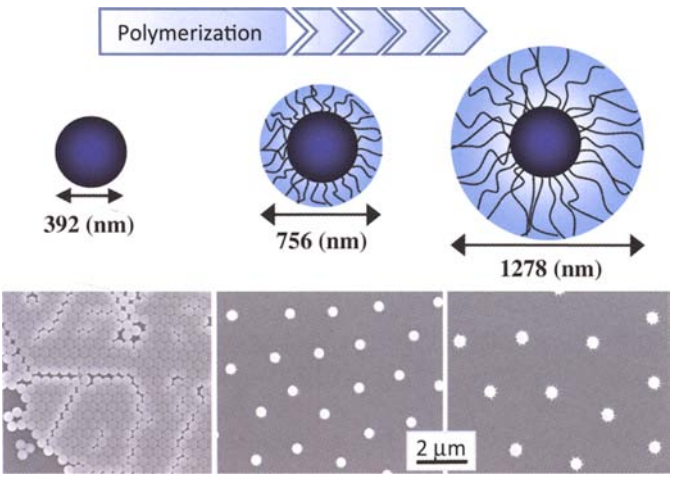

Fig. 5 TEM views of hairy particles with growing hairs

that is, particles having no hairs, (b) particles after 20 min of polymerization, and (c) particles after 40 min of polymerization.

Particles in (b) and (c) have inter-particle spaces while in (a) they are closely packed. The inter-particle spaces are attributed to exclusion volume of each particle due to the hydrated hairy shell [13].

4 Colloid chemistry of thermo-sensitive microgels

The hydrodynamic size of microgels is usually measured by dynamic light scattering. The hydrodynamic diameter of PNIPAM microgels was obtained as a function of temperature and is shown in Fig. 6. The hydrodynamic diameter drastically decreased when temperature is raised above 32°. This event means that the microgel released water molecules from the gel phase, and became hydrophobic. The difference in hydrophilicity/hydrophobicity can be estimated by the absorption peak shift of 8-anilino-naphthalene-1-sulfonic acid (ANS) when it is mixed with microgel dispersion [14]. At low temperature, the absorption peak of ANS was 515 nm whereas, above LCST, it was 500 nm. It was known that the ANS peak at 500nm in the spectrum appears in ethanol. That is, the hydrophilicity of PNIPAM microgels corresponds to that of ethanol. Shrinkage of microgels at high temperature should bring about an increase in apparent surface charge density when warmed up. This was assessed by measuring the electrophoretic mobility of microgels (Fig. 6) [15]. The sulfate groups originating from the persulfate initiator were distributed evenly in the particle after

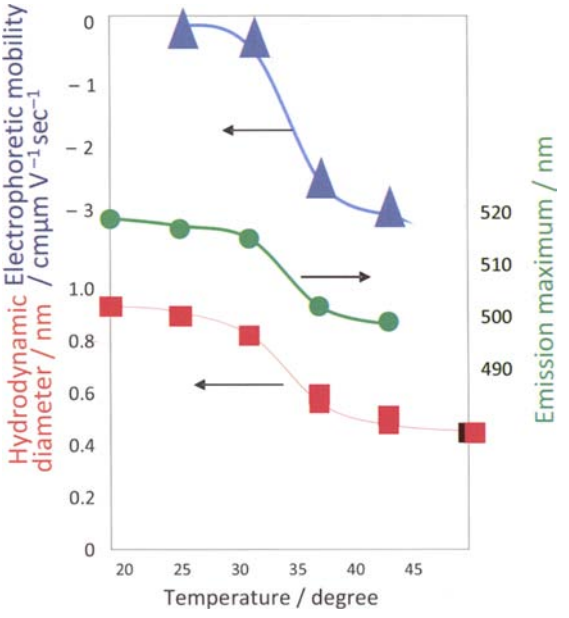

Fig. 6 Temperature dependence of colloidal properties of PNIPAM particles

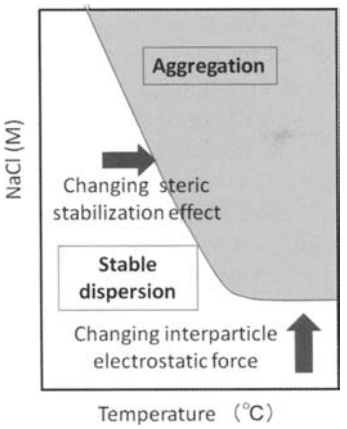

Fig. 7 Phase diagram of the dispersion of themosensitive and charged particles

polymerization. Only a limited number of sulfate groups, which locate to the surface layer of particles contributed to the electrophoretic mobility of microgels. As a result, such microgels behaved as non-charged particle. When the dispersion is warmed up above transition temperature, the microgels shrank and had a condensed number of charges, and moved with high speed in electrophoretic mobility measurement. The stability of microgel dispersion is regulated by static stabilization factors and electric repulsive forces between neighboring microgels. Titration of salt to microgel dispersion causes coagulation because electric double layers become thinner during the course of titration. Also, an increase in temperature causes coagulation because of loss of steric stabilization above LCST. An expected phase diagram of PNIPAM microgel dispersion is presented in Fig. 7 which shows the conditions needed to stably disperse the microgel and those needed to coagulate them for their quick recovery [16].

PNIPAM microgels, including gel-shell particles and hairy particles, possess moderate amphiphilicity in water at room temperature. The amphiphilicity was confirmed by surface tension measurement. Thus, the amphiphilic property of PNIPAM microgels enabled formation of a two-dimensional self-assembling layer at the surface of the droplet on a substrate. The self-assembling layer was settled on the substrate when the droplet was dried and a two-dimensional colloidal crystal was finally obtained [11]. PNIPAM microgels in selected solvents also construct Pickering emulsion [17, 18]. The condition of Pickering emulsion could be controlled by temperature and solvent. Stable Pickering emulsion in hexane at room temperature lost its stability when it was warmed above the LCST of PNIPAM.

5 Products of living radical graft polymerization

Well-designed thermosensitive hairy particles were obtained by living radical polymerization using a photosensitive Iniferter. Growth of hair during graft polymerization

could be observed with transmission electron micrographs (TEM) as already presented (Fig. 3). PNIPAM hairy particles exhibited sharper response to temperature change compared with gel-shell particles. When a small amount acrylic acid (AAc) was copolymerized with NIPAM, the resulting copolymer hairy particles showed different hydrodynamic size even if the molecular weight of the hair did not change. The hydrodynamic diameter of the NIPAM-AAc copolymer hairy particle was fairly large and the transition temperature was higher than those of the homo-PNIPAM hairy particle.

One of the merits of living radical graft polymerization is the ability to prepare block copolymer hairy particles. PNIPAM-block-poly(NIPAM-co-AAc) hairy particles were prepared and their response to temperature change was examined [9]. The result is shown in Fig. 8. In ion exchanged water, the hair behaved as poly(NIPAM-co-AAc), that is, it did not shrink at 32°, but at 38°. This was attributed to the strong repulsion between anionic groups in the outer part of the hair and in the core of the particle. The strong repulsion did not allow the inner part of the hair to shrink at its transition temperature (32°). As a result, all the hair shrank suddenly at 38°. In contrast, at pH 3.0 ([HCl] = 10^{-3} M), the poly(NIPAM-co-AAc) block with no dissociation

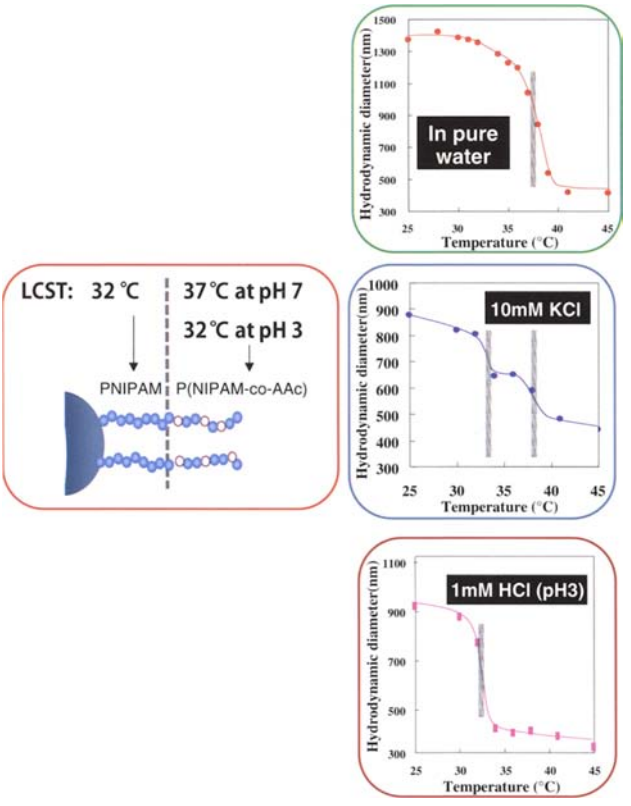

Fig. 8 Magical behavior of hairy particles with thermosensitive block copolymer hairs

of carboxyl group had almost the same transition temperature as PNIPAM block and shrank at 32°. At moderate [NaCl], each block of hair exhibited its own transition temperature respectively, and two steps change in hydrodynamic diameter could be observed. Thus, designed hair-carrying particles showed magical performance.

6 Smart composite microgels

Some functional materials were added into or onto thermo-sensitive particles, after which, function was modulated or switched by thermo-sensitiveness. The functional materials employed in this study were enzyme and magnetite, gold and titania nanoparticles.

6.1 Chymotrypsin-carrying thermo-sensitive microgels [19]

The first example of thermosensitive composite microgels were PNIPAM hairy particles which had hairs carrying enzyme at some of the chain ends. First, PNIPAM with amine function at the chain end was prepared by solution polymerization of NIPAM using chain transfer reagent with amine functions. These polymer chains were immobilized onto core particle having carboxyl groups. Among the hairs there are some chains whose free chain ends possessed amine function, to which chymotrypsin was attached. Free ended PNIPAM hair on particles showed a transition temperature of 31° whereas chymotrypsin-carrying PNIPAM hair showed a transition temperature of 38°. This architecture enabled control of enzymatic activity by temperature, that is, relative enzymatic activity was low below 31° and increased with increasing temperature. Below 31°, the enzyme was embedded in the atmosphere of swollen PNIPAM and found difficulty in encountering the substrate. This resulted in low enzyme activity (Fig. 9). Above 31°, free ended PNIPAM hair shrank and chymotrypsin-carrying hair was exposed to the medium enabling the enzyme to encounter the substrate. Therefore, the activity of the enzyme increased above 31°. It is worth mentioning that this was the case for the reaction of high molecular weight substrates, e.g., α-casein. When small molecules, e.g., BANA (N-α-benzoyl-D,L-arginine-2-naphthylamide), were used as a substrate for this enzymatic reaction system, no temperature dependence of enzymatic activity was observed. This is obvious from the difference in the rate of diffusion between small and large molecules through swollen PNIPAM hairy shells.

6.2 Magnetite nanoparticle-carrying thermo-sensitive particles

Magnetic polymer particles have attracted much attention targeting biomedical and informative applications [20, 21]. Thermosensitive magnetic particles are expected to find more sophisticated applications [22]. They were prepared here through in situ formation of magnetite nanoparticles in template particles. Template particles used for magnetite immobilization were poly(NIPAM-co-glycidyl methacrylate (GMA)) copolymer microgels which were prepared by soap-free emulsion polymerization of NIPAM, GMA and a small amount of crosslinker in water at 70 °C [9]. GMA units

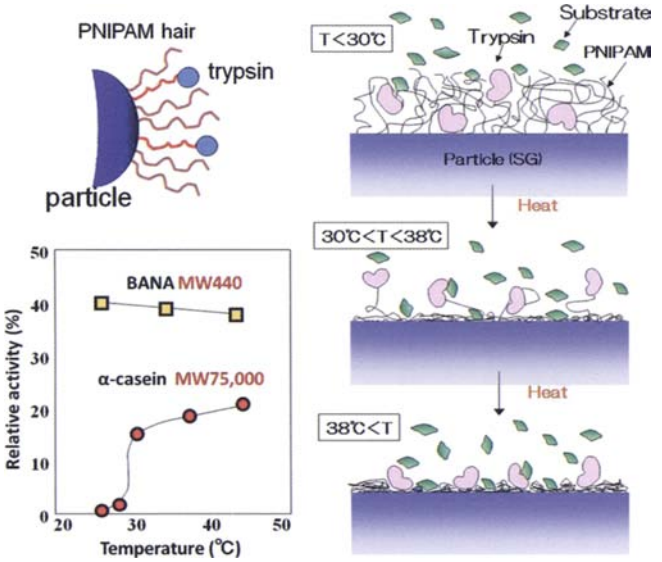

Fig. 9 Thermosensitive activity of enzyme bound to hair chain ends

were prone in locating more in the core part of microgels because of their lower water solubility and higher reactivity compared with those of NIPAM as mentioned previously. Epoxy functions in GMA units were converted to sulfonic acid functions by reaction with 3-Mercapto-1-propane sulfonic acid sodium salt (Fig. 10). The resulting anionic microgels were able to attract ferric ions from the solution due to electrostatic interaction. After removing free ferric ions, $NaNO_2$ was added to the dispersion of microgels and, after 15 min, ammonia solution was injected for in situ

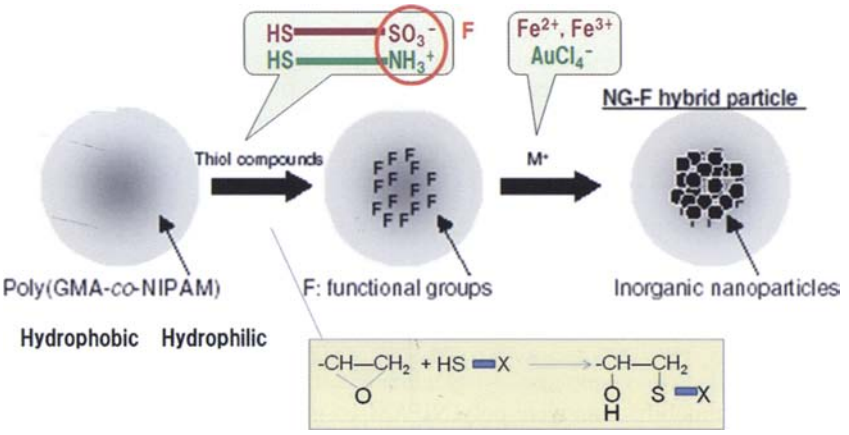

Fig. 10 In situ formation of metal or metal oxide nanoparticles in microgels

synthesis of magnetite nanoparticles. The hybrid particles were characterized directly by transmission electron microscopy. The electron micrographs revealed that microgels containing more GMA could carry magnetite nanoparticles in a more condensed manner inside the microgels. When GMA units were concentrated tightly in the core of microgels which included the largest amount of GMA, less ferric ions could reach such a hydrophobic zone. As a result, rather small amounts of magnetite nanoparticles were formed in the microgels. The obtained composite microgels dispersed stably in water even under magnetic force. This was the case for 25°. At 40°, microgels shrank and had a more hydrophobic nature. The microgels formed small aggregates and these did not sediment by themselves but were collected with a magnet and separated from the medium. This means that the magnet-mediated microgel collection was controlled by temperature.

6.3 Gold nanoparticle-carrying thermo-sensitive particles [23, 24]

Thermosensitive microgels containing gold (Au) nanoparticles are also very attractive materials due to their potential applications. Au was introduced into microgels through the following procedure. First, poly(NIPAM-co-glycidyl methacrylate (GMA)) copolymer particles were prepared by precipitation polymerization. The ratio of GMA to NIPAM was 0.01 in weight basis. Epoxy functions in GMA units were reacted with ethylenediamine to form amine functions dispersed through the microgels. Then precursor ions ($AuCl_4^-$) were introduced into aminated microgels and were converted to nanoparticles via in situ reduction reaction.

The dispersion of Au nanoparticle/PNIPAM composite microgels had color, originating from surface plasmon resonance of Au nanoparticles. When the temperature of composite microgel dispersion was raised, the color of the dispersion was reversibly changed from pink to violet (Fig. 11). The color change was attributed to the change in Au particles from being dispersed to aggregated caused by shrinkage of the microgel. Au nanoparticles seeds were grown by successive reduction of additional Au and Ag in the microgel. The enlarged Au nanoparticles and Au/Ag hybrid nanoparticles thus obtained also gave different colors tunable with temperature.

6.4 Titania nanoparticle-carrying thermo-sensitive particles [25]

Precipitation polymerization of NIPAM with AAc gave carboxylated thermo-sensitive microgels. The microgel was treated with ammonia to introduce titania into the microgels [26]. Then titanium tetraisopropoxide (TTIP) was added to the dispersion of microgels to prepare titania-carrying microgels. It is well known that titania has catalytic properties and can decompose organic compounds via a radical mechanism. The catalytic ability of titania-carrying microgels was assessed by the degree of fading of methylene blue (MB) when the mixture of microgels and MB was irradiated with UV. The more carboxyl groups there are in the microgel, the more titania was immobilized and the more MB was decomposed. TTIP was converted to titania nanoparticles in the absence of microgel as a reference. The reference titania (bare titania) was not stably dispersed in water and aggregated titania showed less relative activity to

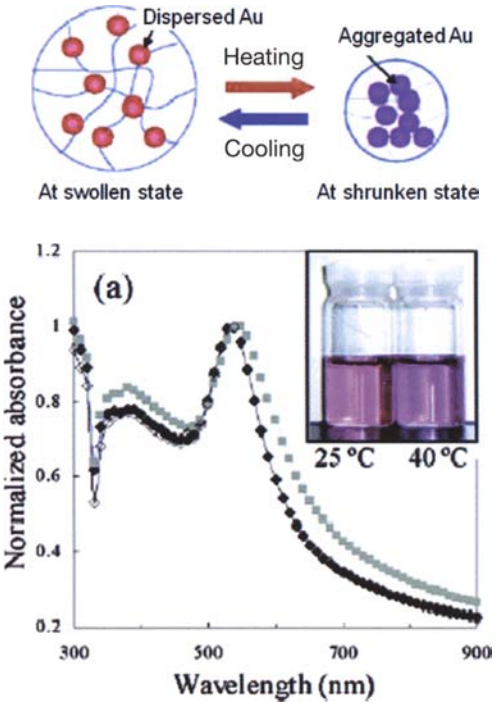

Fig. 11 Temperature dependent color change of gold nanoparticle-carrying thermosensitive microgel dispersion (Reprinted with permission from [24]. Copyright 2006 American Chemical Society)

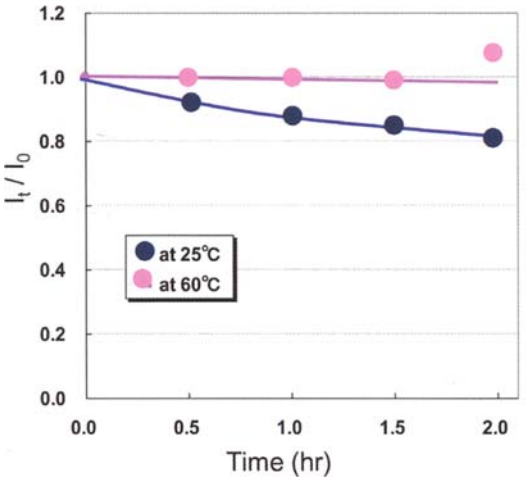

Fig. 12 Photocatalytic activity of titania-carrying PNIPAM microgels

decompose MB. Interestingly, decomposition of MB was regulated by temperature (Fig. 12). The decomposition proceeded appreciably at room temperature but almost ceased at 70°. This perhaps resulted from the shield effect by shrunken, turbid PNIPAM microgels against UV, that is, UV does not reach the inside of the particle where titania nanoparticles exist.

7 Conclusions

Several types of PNIPAM microgels were prepared. They exhibited not only volume phase transition but also changes in some physical properties as a function of temperature. Several thermo-sensitive composite microgels were prepared to create novel microgels whose functions are collaboratively regulated. The functional materials to be incorporated were enzyme, magnetite, Au, and titania. Their functions were tuned by reversible volume phase transition of microgels as a function of temperature. The methodology would not be limited to thermosensitivity but could to be developed to other stimuli such as biospecific changes.

References

[1] Schild HG (1992) Poly(N-isopropylacrylamide): Experiment, theory and application. Prog Polym Sci 17:163–249

[2] Heskins M, Guillet JE, James E (1968) Solution properties of poly(N-isopropylacrylamide). J Macromol Sci Chem A2:1441–1455

[3] Ito S (1987) Thermally reversible hydrophilic-hydrophobic polymer. Kobunshi Ronbunshu 46:437–441

[4] Pelton RH, Chibante P (1986) Preparation of aqueous latexes with N-isopropylacrylamide. Colloids Surfaces 20:247–256

[5] Tanaka T, Fillmore DJ (1979) Kinetics of swelling of gels. J Chem Phys 70:1214–18

[6] Jones CD, Lyon LA (2003) Shell-Restricted Swelling and Core Compression in Poly(N-isopropylacrylamide) Core-Shell Microgels. Macromolecules 36:1988–1993

[7] Jones CD, McGrath JG, Lyon LA (2004) Characterization of Cyanine Dye-Labeled Poly(N-isopropylacrylamide) Core/Shell Microgels Using Fluorescence Resonance Energy Transfer. J Phys Chem B 108:12652–12657

[8] Suzuki D, Kawaguchi H (2006) Stimuli-sensitive core/shell template particles for immobilizing inorganic nanoparticles in the core. Colloid Polym Sci 284:1443–1451

[9] Sato T, Tsuji S, Kawaguchi H (2008) Preparation of functional nanoparticles by assembling block copolymers formed by living radical polymerization. Ind Eng Chem Res 47:6358–6361

[10] Matsuoka H, Fujimoto K, Kawaguchi H (1998) Monodisperse microspheres exhibiting discontinuous response to temperature change. Polym Gels Networks 6: 319–332

[11] Tsuji S, Kawaguchi H (2005) Colored thin films prepared from hydrogel microspheres. Langmuir 21:8439–8442

[12] Goto A, Sato K, Tsujii Y, Fukuda T, Moad G, Rizzardo E, Thang SH (2001) Mechanism and kinetics of RAFT-based living radical polymerizations of styrene and methyl methacrylate. Macromolecules 34:402–408

[13] Tsuji S, Kawaguchi H (2006) Effect of graft length and structure design on temperature-sensitive hairy particles. Macromolecules 39:4338–4344
[14] Fujimoto K, Nakajima Y, Kashiwabara M, Kawaguchi H (1993) Fluorescence analysis for thermo-sensitive hydrogel microspheres. Polym Intl 30:237–241
[15] Ohshima H, Makino K, Kato K, Kondo T, Kawaguchi H (1993) Electrophoretic mobility of latex particles covered with temperature-sensitive hydrogel layers. J Colloid Interface Sci 159:512–514
[16] Hoshino F, Fujimoto T, Kawaguchi H, Ohtsuka Y (1987) N-substituted acrylamide-styrene copolymer lattices II. Polymerization behavior and thermosensitive stability of lattices. Polym J 19:241–247
[17] Tsuji S, Kawaguchi H (2004) Hairy particles settled on asubstrate keeping constant interparticle distance. Langmuir, 20, 2449–2455
[18] Tsuji S, Kawaguchi H (2005) Self-assembly of poly(N-isopropylacrylamide)-carrying microspheres into two-dimensional colloidal arrays. Langmuir 21:2434–2437
[19] Yasui M, Shiroya T, Fujimoto K, Kawaguchi H (1997) Activity of enzymes immobilized on microspheres with thermosensitive hairs. Colloid Surfaces 8:311–319
[20] Ramirez LP, Landfester K (2003) Magnetic polystyrene nanoparticles with a high magnetite content obtained by miniemulsion processes. Macromol Chem Phys 204: 22–31
[21] Yamagata M, Abe M, Handa H, Kawaguchi H (2006) Magnetite/polymer composite particles prepared by molecular assembling followed by in-situ magnetite formation. Macromol Symp 245/246:363–370
[22] Kondo A; Kamura H. Higashitani K (1994) Development and application of thermosensitive magnetic immunomicrospheres for antibody purification. Appl Microbiol Biotech 41:99–105
[23] Suzuki D, Kawaguchi H (2005) Modification of gold nanoparticle composite nanostructures using thermosensitive core-shell particles as a template. Langmuir 21: 8175–8179
[24] Suzuki D, Kawaguchi H (2006) Hybrid microgels with reversibly changeable multiple brilliant color. Langmuir 22:3816–3822
[25] Kawaguchi H, Suzuki D, Kaneshima D (2008) Syntheses and applications of polymeric microspheres containing inorganic nanospheres. Trans Mat Soc Jpn 33:205–208

Novel pH/Temperature-Sensitive Hydrogels Based on Poly(β-Amino Ester) for Controlled Protein Delivery

Dai Phu Huynh, Chaoliang He and Doo Sung Lee

Abstract. The concept of this research was to use poly(β-amino ester) (PAE) as a bifunctional group for synthesis of the novel stimuli-sensitive injectable hydrogels for controlled drug/protein delivery. Firstly, PAE was used as a pH-sensitive moiety to conjugate with the temperature-sensitive biodegradable triblock copolymer of poly(ethylene glycol)-poly(ε-caprolactone) (PCL-PEG-PCL) or poly(ethylene glycol)-poly(ε-caprolactone-co-D,L-lactide) (PACL-PEG-PCLA). Secondly, the cationic nature of PAE was used as the second function to make ionic complexes with anionic biomolecules loaded onto the hydrogel such as insulin. As a result, the release of the drug/protein from the hydrogel device can be controlled by the degradation of the copolymer.

1 Introduction

In recent years, controlled drug/protein delivery systems using novel carrier materials for revolutionizing the treatment of disease has become one of the most challenging achievements in the medical science field [1]. Biodegradable hydrogels [2–7] have been developed as novel drug/protein delivery systems because they have many advantages such as biocompatibility and high responsibility for specific factors. The interesting advantage of this system is that the release of drug from the hydrogel can be controlled by several elements, for instance: pore size of hydrogels, hydrophobicity, the presence of some specific functions that lead to a particular interaction between the matrix and drug, and the controlling of their degradation and biodegradability. The advantage of the copolymer hydrogel carrier for drug/protein delivery is that they can be fabricated with special properties, which apply for a correlative drug/protein. Among them, stimuli-sensitive polymer hydrogels, especially thermoreversible gels and pH-reversible gels, have been developed for polymeric drug carriers, implantation, and other medical devices over the past few years [3,8,9]. The term stimuli-sensitive hydrogels indicates that they can change their structure in response to environmental stimuli. Various stimuli such as pH [10], temperature [11–13], electric field [14, 15] and various others have been studied experimentally and theoretically

Barbucci R. (Ed): Hydrogels. Biological Properties and Applications.

[16, 17]. Injectable thermoreversible hydrogels [8, 18–20] have been developed as carriers of some biomacromolecules. However, these hydrogels have several unresolved drawbacks that limit their application in injectable drug delivery systems. When temperature-sensitive hydrogels are injected into the body via a syringe, they tend to form a gel as the needle is warmed by the body. This makes injection difficult. For this reason, pH/temperature sensitive hydrogels [21, 22] have been designed to solve the injection problem. In these studies, Lee and coworkers coupled the sulfamethazine oligomer (OSM) as a pH sensitive moiety with PCLA-PEG-PCLA or PCGA-PEG-PCGA as temperature sensitive blocks to form a pH/temperature-sensitive block copolymer. These block copolymer solutions showed a reversible sol-gel transition in response to a small pH change from 7.4 to 8.0 or to a temperature change to that of body temperature. Although these materials have some advantages in application as drug/protein delivery systems, such as, controllability of sol-gel phase transition diagram, and no clogging problem during injection into body, there are some disadvantages when using the same materials as drug/protein delivery systems in certain cases. Because OSM has an acid sensitive moiety, it is very difficult to use it as a carrier system for anionic drugs/proteins which cannot be encapsulated into the material because they have the same type of electric charge. The challenge is to use a functional group, which could form a strong reversible linkage with the anionic drug/protein to allow predictable and customizable loading and release.

The ionization/deionization transition of the pH-responsive PAE block [23-28] due to pH change around its pK_b [28]directly affects the solubility of the copolymer. In addition, the positive charges of protonated amino groups in this polymer may form electrostatic linkages with the negative charges in anionic drugs or proteins. Based on the above properties, poly(β-amino ester) is used to prepare the novel pH/temperature-sensitive injectable hydrogel for drug/protein delivery as a new concept using PAE as a bi-functional group. Firstly, PAE is used as a pH-sensitive block and introduced to the amphiphilic poly(ethylene glycol)-poly(ε-caprolactone) temperature-sensitive triblock copolymer to fabricate an injectable pH/temperature-sensitive hydrogel. Secondly, the cationic nature of the polymer is found to endow the gel with unique properties for drug loading through charge complexation as well as a sustained release profile by decomplexation through continuous matrix degradation. Therefore, the release of biomacromolecules from this hydrogel is controlled by a combination of both chemically and diffusion-controlled mechanisms due to the degradation of copolymer hydrogel.

Here we present novel pH/temperature-sensitive pentablock copolymer hydrogels based on the ABA type temperature-sensitive triblock copolymer and the pH-sensitive block poly(β-amino ester). PCL-PEG-PCL and PCLA-PEG-PCLA were synthesized from ring-opening polymerization of ε-caprolactone, D,L-lactide and polyethylene glycol. The triblock copolymers were acrylated by acryloyl chloride, and then the pentablock copolymers (PAE-PCL-PEG-PCL-PAE and PAE-PCLA-PEG-PCLA-PAE) were synthesized by addition polymerization of acrylated triblock copolymer, 1,4-butanediol diacrylate, and 4,4'-trimethylene dipiperazin to form pH/temperature-sensitive block copolymers. The aim of this research was to study the sol-gel phase transition of these pH/temperature-sensitive pentablock hydrogels, and to study the

degradation of these block copolymers caused by the degradation of the PCL and PCLA polyester blocks. In addition, the mechanisms of drug/protein loading and release from these copolymers were also investigated, and the release of insulin from the complex mixture of PAE-PCL-PEG-PCL-PAE and insulin on SD rats was investigated to study the effects of ionic linkages on the insulin release profile.

2 Experimental details

2.1 Materials

Poly(ethylene glycol)s (PEG) were purchased from Sigma-Aldrich Co. (St. Louis, MO) (Mn = 1500) and ID Biochem, Inc. (Seoul, Korea) (Mn = 1650). Those PEGs were recrystallized in n-hexane and dried in a vacuum for 3 days prior to use. D,L-lactide (LA) supplied from Polyscience Biohringer Ingellheim, was purified by recrystallization in ethyl acetate. ε-Caprolactone (CL) and phosphate buffered saline (PBS) were obtained from Sigma-Aldrich Co. Stannous octoate [$Sn(Oct)_2$] was obtained from Sigma-Aldrich Co. and dried for 24 hr under vacuum at ambient temperature prior to use. Acryloyl chloride, triethylamine (TEA), 1, 4-butanediol diacrylate (BDA), 4, 4'-trimethylene dipiperidin (TMDP), 2,3-bis(2-methoxy-4-nitro-5-susfophenyl)-2H-tetrazolium-5-carboxanilide (XTT) assay, dulbecco's modified Eagle's medium, fetal bovine serum, glucose, L-glutamine, sodium pyruvate, and sodium bicarbonate for cytotoxicity were purchased from Aldrich Chemical Co., and the NIH 3T3 fibroblast cell line was purchased from American Type Culture Collection. 37% HCl, sodium chloride, chloroform, dichloromethane (DCM), and diethyl ether were all obtained from Samchun. All other reagents were of analytical grade and used without further purification.

Insulin was obtained from Sigma-Aldrich Co. Male Sprague-Dawley (SD) rats were supplied from Hanlim Experimental Animal Laboratory, Seoul, Korea.

2.2 Synthesis of copolymers

2.2.1 Synthesis of temperature sensitive PCL-PEG-PCL triblock copolymers

PCL-PEG-PCL triblock copolymer was synthesized from ε-caprolactone and PEG by ring opening polymerization using stannous octoate as a catalyst. The representative synthesis process of triblock copolymer (PEG 1500, PCL/PEG ~ 1.8) was as follows: 4 g PEG (Mn 1500) and 0.04 g stannous octoate in a dry two-neck round-bottom flask were dried at 110 °C for 2 hr under vacuum. After cooling to 60 °C, 7.6 g of CL was added under a dry nitrogen atmosphere. The reaction mixture was dried for 1 hr under vacuum at 60 °C, and then the temperature was increased slowly to 130 °C (30 minutes). After an 18 hr reaction, the temperature was decreased to room temperature, and chloroform was added to dissolve the reactant. The precipitated product, which was obtained from cleaning the reactant in excess diethyl ether, was

dried under vacuum at ambient temperature for 48 hr. The overall yield of this triblock copolymer was over 85% after drying.

The synthesis of PCLA-PEG-PCLA triblock copolymers was under the same process as PCL-PEG-PCL. In this study, PEG 1500 was used and the weight ratio of PCLA /PEG was 2.5/1.0, the molar ratio of CL/LA was fixed at 2.0/1.0.

2.2.2 Synthesis of acrylated triblock copolymers

Triethylamine was used as a catalyst to conjugate acrylate groups to the triblock copolymer through the reaction between hydroxyl groups at the end of PCL-PEG-PCL (or PCLA-PEG-PCLA) and acryloyl chloride. Every triblock was acrylated with the same reaction ratio.

$$\text{Triblock/acryloyl chloride/TEA} = 1/3.2/2 \text{ (molar ratio)}. \quad (1)$$

Based on equation 1, the quantity of the reactants, which were used for acrylation of the triblock copolymer (PEG 1500, PCL/PEG $\sim$ 1.8), were 4 g of PCL-PEG-PCL, 0.26 ml of triethylamine and 0.25 ml of acryloyl chloride (96%). The process to acrylate this triblock was as follows. PCL-PEG-PCL was dried for 2 hr under vacuum at 80 °C in a dry two-neck round-bottom flask. Dry nitrogen was added, and then anhydrous chloroform was supplied to dissolve the triblock at ambient temperature to obtain a solution at 20 wt%. The acrylation reaction was carried out at 10 °C for 48 hr after adding TEA and acryloyl chloride to the flask. Chloroform was removed by a rotary evaporator at ambient temperature to obtain the dry reactant. The precipitated product, after cleaning the dry reactant with excess diethyl ether, was dried under vacuum at room temperature for 48 hr.

2.2.3 Synthesis of pH/temperature-sensitive pentablock copolymers

PAE was conjugated to PCL-PEG-PCL (or PCLA-PEG-PCLA) by addition polymerization between the vinyl group at the end of the acrylated triblock copolymer and 1, 4-butanediol diacrylate (BDA) and vivacious hydrogen at the amine groups of 4, 4'-trimethylene dipiperidine (TMDP). The molar ratio of BDA/TMDP was kept at 1/1. The molecular weight of the pH/temperature sensitive moiety, i.e. PAE, which was introduced into triblock acrylated by addition polymerization, could be controlled by varying the quantity of BDA and TMDP.

The reactants for synthesizing PAE-PCL-PEG-PCL-PAE (PEG 1500, PCL/PEG $\sim$ 1.8, and fixed PAE molecular weight at 2000) included 4 g acrylated triblock, 1.89 ml BDA and 1.96 g TMDP. The process to synthesize pentablock copolymer is described below: acrylated PCL-PEG-PCL, BDA and TMDP were dissolved with 40 ml of DCM in a one-neck round-bottom flask at ambient temperature. The additional reaction was carried out for 48 hr at 50 °C with a condenser connected to the neck of the flask. The DCM solvent of the reactant was removed by a rotary evaporator at 40 °C, and then the dry reactant was dissolved in THF. Thereafter, the solution of pentablock copolymer was filtered with filter paper (5C 100 circles – Toyo

Roshi Kaisha). An evaporator was used to remove the THF solvent from the polymer solution at 50 °C; for the last step, the dry copolymers were purified by excess diethyl ether. The purifying process and re-dissolving in THF were carried out several times. The precipitated product was dried under vacuum at room temperature for 48 hr. The overall yield of the pentablock copolymer was over 72% after drying. The complete synthetic routes are shown in Fig. 1 and 2.

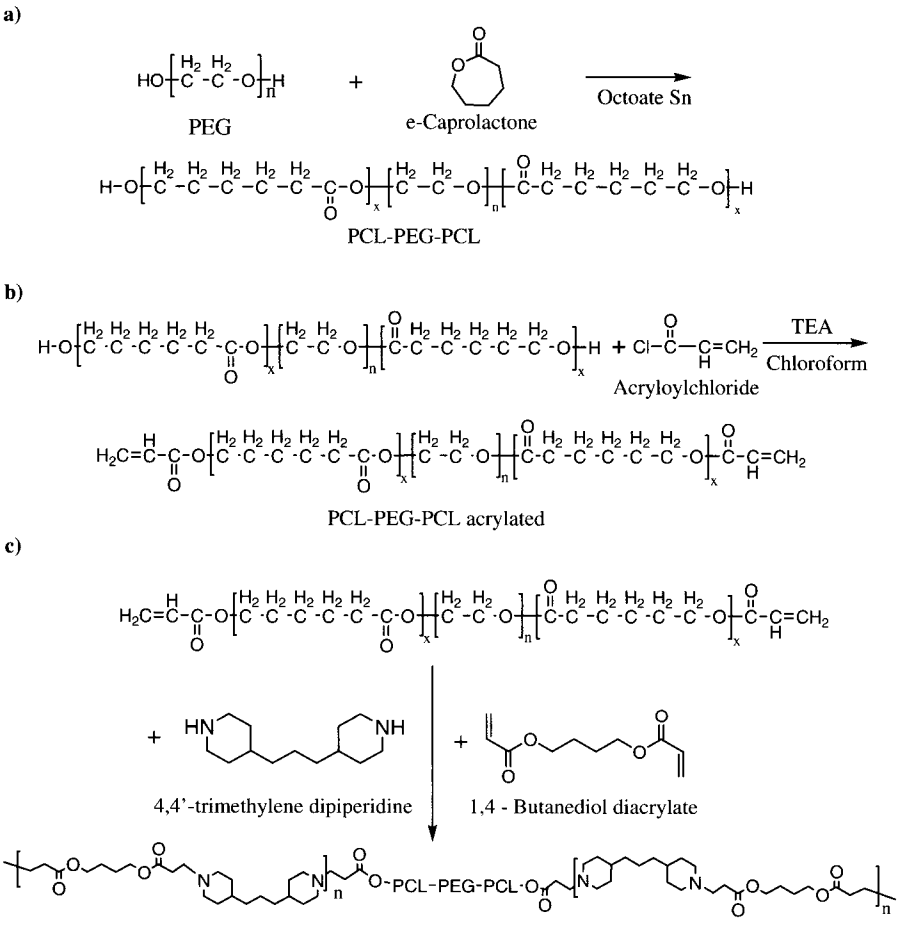

Fig. 1 Synthesis of the PAE-PCL-PEG-PCL-PAE block copolymers. **a** Synthesis of PCL-PEG-PCL triblock copolymer; **b** Synthesis of acrylated triblock copolymer; **c** Synthesis of PAE-PCL-PEG-PCL-PAE pentablock copolymers (reproduced from [32], Copyright Elsevier Limited. Reproduced with permission)

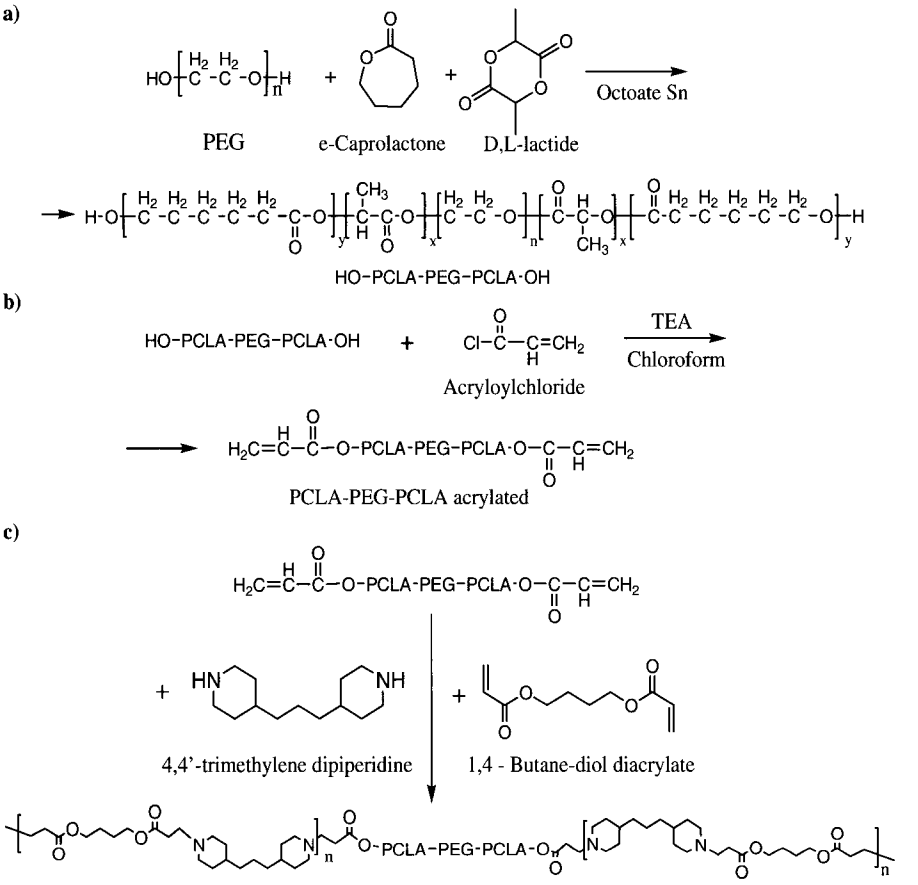

Fig. 2 Synthesis of the PAE-PCLA-PEG-PCLA-PAE block copolymers. **a** Synthesis of PCLA-PEG-PCLA triblock copolymers; **b** Synthesis of acrylated triblock copolymer; **c** Synthesis of PAE-PCLA-PEG-PCLA-PAE pentablock copolymer

2.3 Characterization

2.3.1 Polymer characterization

Molecular structure and composition of copolymers were determined by ^{1}H-NMR (Varian-Unity Inova 500NB operated at 500 MHz. Chloroform was used as a solvent, which contained 0.03 v/v% tetramethylsilane). The composition of each block was calculated on the basis of the typical proton peak integration of PEG, CL and CLA from ^{1}H-NMR spectra [29, 30]. Molecular weight and molecular weight distribution of copolymers were measured by gel permeation chromatography (GPC) (Waters Model 410) with 4 μm-two styragel columns from 500 to 10 Å in series. Poly(ethylene glycol)s (Waters Co.) with molecular weights ranging from 420 to 22,100 were used as calibration. The flow rate of eluent (tetrahydrofuran) was 1 ml/min with a refractive-index detector (Shodex, RI-101), and the retention volume was measured at 45 min.

2.3.2 Sol-gel phase transition measurement

The sol (flowing) to gel (non-flowing) phase transition behavior of the triblock copolymers in aqueous media was determined using the inverting test method with a 4 ml (10 mm diameter) vial test tube at a temperature interval of 1 °C. The block copolymers were dissolved in buffer solution at a given concentration for 2–4 days at 0 °C. The pH of these samples was adjusted with sodium hydroxide (5 M) and the solutions were maintained at 0 °C for 1–2 days. The sol-gel transition at each temperature was determined by angling the vial horizontally after keeping it at a constant temperature for 10 min [21, 22].

2.3.3 Cytotoxicity evaluation of pentablock copolymer

Cytotoxicity of the materials was characterized as a decrease in metabolic rate measured using the XTT assay [31]. The cytotoxicity of some pentablock copolymers (PEG 1750; PCLA/PEG ~ 2.0/1.0; PAE-1.3k) was compared with that of poly(ethylene imide) (PEI). NIH 3T3 fibroblast cells were plated in 96-well plates at an initial density of 10,000 cells/well in 100 μl of growth medium (90% Dulbecco's modified Eagle's medium, 10% fetal bovine serum, 4500 mg/l glucose, L-glutamine, 110 mg/l sodium pyruvate and sodium bicarbonate). The cells were grown for 24 hr, after which the growth medium was removed and replaced with fresh, serum-free medium containing polymer. Cells were incubated with polymer for 4 hrs at 37 °C, and the medium was then replaced with complete growth medium for 24 hr. XTT labeling mixture was prepared by mixing XTT labeling agent (50 μl) and electron coupling agent (1 μl) for each well and 50 μl XTT labeling mixture was then added to each well. The samples were incubated for 4 hr at 37 °C with 5% CO_2, and absorbance was read between 492 nm and 690 nm.

2.3.4 Insulin loading process

Copolymer solutions were prepared by dissolving triblock or pentablock copolymers in PBS (containing 2 v% of HCl 37%) at 2 °C, and the pH of these solutions was adjusted with NaOH 5M and HCl 5M.

Insulin was loaded into the matrix by in situ method: firstly, copolymer solution was prepared, and then the pH of this solution was adjusted to 3.0–4.0; secondly, at 2 °C insulin was encapsulated into copolymers to form complex mixtures by mixing insulin powder with copolymer solution using a magnetic bar. The pH of these mixtures was adjusted using NaOH 5M and HCl 5M at 2 °C before using.

2.3.5 Degradability evaluation of block copolymers and complex gel in vitro

The degradability of the block copolymers was evaluated by monitoring molecular weight changes with time. Degradation of triblock, pentablock gel and complex gel in vitro: 0.5 mg of copolymer solutions (20 wt%, pH 7.4) or complex gel (20 wt%, 5 mg insulin per ml copolymer solution at pH 7.4) in 4 ml vials was incubated at 37 °C to

form a gel. Then, 3 ml of PBS at 37 °C and pH 7.4 was added. At a given time, the sample vial was removed and then freeze-dried to obtain a solid. It was then dissolved in tetrahydrofuran and filtered [21]. The degradation of the polymers was investigated by GPC (Waters Model 410, equipped with 4 mm styragel columns from 500 to 10 Å in series, at a flow rate of 1.0 ml/min (eluent: THF, 36 °C, PEG as standard)).

2.3.6 Insulin release in vitro

To certify the mechanism of insulin loading and releasing, the release of insulin in vitro was carried out by two sampling methods. 0.5 g of the complex gel (5 $mg.ml^{-1}$ insulin in PAE-PCL-PEG-PCL-PAE (20 wt%)) at pH 7.4 was placed in a 6 ml vial. The solution in the vials changed to gel state after incubation at 37 °C for 30 min (step 1). Fresh serum (2.4 wt% Tween 80, 4 wt% Cremophor EL in PBS buffer at pH 7.4) [21]at 37 °C was added to the vial samples; thereafter, insulin was released from the complex gel to the serum.

Sampling method 1

The amount of initial fresh serum was 3 ml (step 2). At a given time, 1.5 ml of the serum in vials (releasing sample) was extracted from the sample vials, and 1.5 ml of fresh serum was supplemented (step 3).

Sampling method 2

The amount of initial serum was 6 ml. Releasing sample is 3 ml, and supplementary fresh serum is 3 ml.

The release of insulin from PCL-PEG-PCL gel in vitro: 0.5 g of the mixture (5 $mg.ml^{-1}$ insulin in PCL-PEG-PCL solution (20 wt%)) at pH 7.4 was placed in a 6 ml vial, the solution changed to gel state after incubation at 37 °C for 30 min. The releasing samples were taken by sampling method 1.

The insulin concentration in releasing samples was determined by HPLC. The release samples were filtered by 0.2 μm PTFE filter (Toyo Rosho Kaisha, Ltd. Japan). Insulin in releasing samples was determined by HPLC (Column: C18, 250 - 4.0 mm, 5.0 μm; mobile phase: ACN/H2O = 28/72, 0.15%v/v of tetraflouro acetic acid; flow rate: 0.5 ml/min; detector: UV at 214 nm).

2.3.7 Insulin release *in vivo* in SD rats

Insuline release in vivo experiments were carried out with male Sprague-Dawley (SD) rats (Hanlim Exeprimental Animal Laboratory, Seoul, Korea). The SD rats (5–6 weeks old, average body weight 200 g) were cared for according to the National Institute of Health (NIH) guidelines for the care and use of laboratory animals (NIH publication 85-23, revised 1985). Before the experiment, the rats were acclimatized for 1 week with free access to water and food in the animal facility (12 hr dark/bright cycle). Then, the SD rats were divided into 3 groups (n = 5 in each group). One group was treated

with the insulin solution. In this group, 200 µl of solution (0.25 mg.ml^{-1} insulin in PBS buffer pH 7.4) was administered by intraperitoneal injection (0.05 mg insulin/rat). The other two groups were treated with insulin loaded hydrogels made from PCL-PEG-PCL and PAE-PCL-PEG-PCL-PAE, respectively. The 25 wt% aqueous solution (pH 7.0) of above triblock and pentablock copolymer containing insulin (5 mg.ml^{-1}) were subcutaneously injected into the back side of the SD rats at 10 °C (200 µl or 1 mg insulin for each rat).

300 µl of blood samples were then taken from the rat tail vein and kept in poly(propylene) tubes in which 3 µl of heparin plasma was present. Serum and heparin plasma samples were centrifuged at 13,000 rpm for 5 min to obtain plasma samples. All samples were stored at –10 °C until analysis.

Insulin concentration in plasma samples was analyzed by Mercodia Insulin ELISA (Mercodia AB, Sweden).

3 Results and discussion

3.1 Polymer characterization

The molecular structure and molecular weight of PCL-PEG-PCL/PAE-PCL-PEG-PCL-PAE and PCLA-PEG-PCLA/PAE-PCLA-PEG-PCLA-PAE were further characterized using ^{1}H-NMR, the compositions obtained by calculation of the corresponding peak areas [29,30]. Moreover, their molecular weight and molecular distribution (PDI) were measured by gel permeation chromatography. The composition of PCL-PEG-PCL and PCLA-PEG-PCLA was 1584-1650-1584 and 1885-1500-1885, the composition and PDI of PAE-PCL-PEG-PCL-PAE and PAE-PCLA-PEG-PCLA-PAE were 1258-1584-1650-1584-1258 and 1.45, 1340-1885-1500-1885-1340 and 1.44, respectively.

3.2 Sol-gel transition of block copolymer solutions

To specify the pH-sensitive function of PAE-PCL-PEG-PCL-PAE, the sol-gel phase transitions of the aqueous solutions of the pentablock copolymer and the triblock copolymer precursor were tested and compared. In Fig. 3a and b, the sol-gel transition of PCL-PEG-PCL/PCLA-PEG-PCLA triblock copolymers in aqueous solution only depended on the temperature change. There were three temperature zones corresponding to different states of this material: the sol state below 34/28 °C, gel region between 34/28 °C and 54/27 °C, and the sol (sedimentation) area at temperatures above 54/47 °C, respectively. In contrast, PAE-PCL-PEG-PCL-PAE/PAE-PCLA-PEG-PCLA-PAE pentablock copolymers showed a sol-gel transition responding to both temperature and pH [32]. Four states of sol–gel of the pentablock copolymers, which depend on temperature and pH, are shown in Fig. 3. At low temperature and pH, PAE was ionized and played the role of hydrophilic block [28], and the hydrophobicity of PCL was weak. As a result, PCL-PAE became a hydrophilic block and the amount of micelle, which was made by the pentablock copolymer,

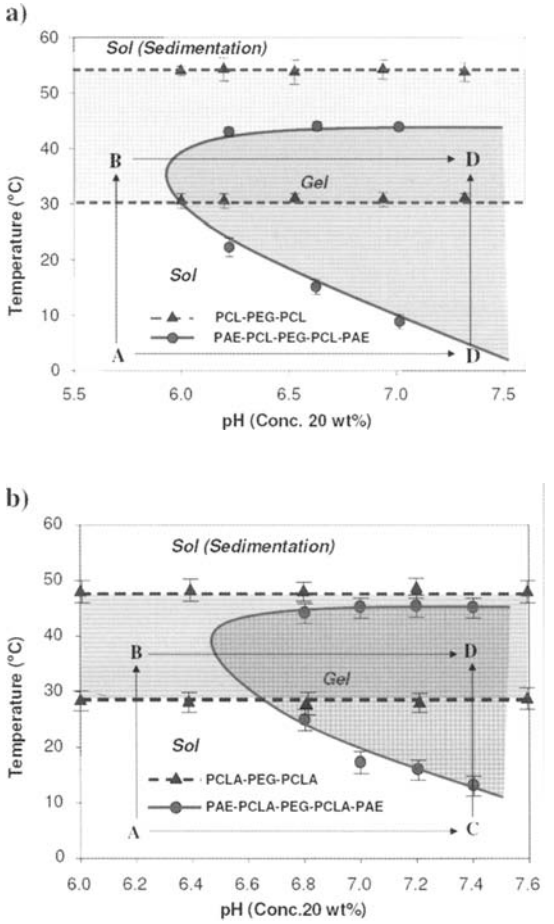

Fig. 3 Sol-gel phase transition diagram of triblock and pentablock copolymer solutions at 20 wt%. **a** PCL-PEG-PCL and PAE-PCL-PEG-PCL-PAE; **b** PCLA-PEG-PCLA and PAE-PCLA-PEG-PCLA-PAE (a reproduced from [32], Copyright Elsevier Limited. Reproduced with permission)

was very small and the copolymer solution stayed at a sol state (A). Although the temperature increased and PCL/PCLA became hydrophobic, the solution could not become a gel because of the hydrophilic effect of the ionized PAE block at low pH (B). If the temperature increase was great, the copolymer aggregated as a result of hydrophobic interaction between PCL/PCLA. When the copolymer solution changed from A to C, PAE became hydrophobic block because of de-ionization due to an increase of pH to 7.4. However, PCL/PCLA was a weakly hydrophobic block at low temperature, and the amount of hydrophobic link as a bridge between micelles was not enough to form a gel. In case D (37 °C and pH 7.4), PAE became a hydrophobic block because of de-ionization. In addition, the hydrophobicity of

PCL/PCLA was increased due to the increase in temperature. They strongly induced the hydrophobicity of PCL-PAE/PCLA-PAE. Consequently, at a high concentration of copolymer, many bridges between micelles were formed by hydrophobic interaction between PCL-PAE/PCLA-PAE blocks, and pentablock copolymer solutions underwent "micellar-interconnecting gelation". The sol-gel phase transition diagram of pH/temperature-sensitive copolymers shows a critical gel pH (CGpH) and two critical gel temperatures (CGT) can be obtained from the curve (the lower CGT corresponds to the sol-to-gel transition at a lower temperature, while the upper CGT to the gel-to-sol transition at a higher temperature) (Fig. 3a and b).

3.3 Cytotoxicity evaluation of pentablock copolymers

Langer noted that PAE was a non-toxic material [24, 33]. In this study, the cytotoxicity of pentablock copolymers was investigated by direct contact method. Polyethyleneimine (PEI) was used as a positive control and cells incubated without polymer were used as negative control [31]. Fig. 4 shows the cytotoxicity determination of PAE-PCL-PEG-PCL-PAE (PCL/PEG ~ 1.5/1, and PAE ~ 1.25-1.3 k) with different PEG molecular weights and PAE-PCLA-PEG-PCLA-PAE (PEG1750, PCLA/PEG ~ 2.0/1.0, PAE ~ 1.3 k). It is found that at the PEI concentration of 20 $\mu g.ml^{-1}$, NIH 3T3 cell viability is about 40%, and at higher concentration, as few as 10% of cells treated with PEI are viable. However, cell viability remains around 100% with all pentablock copolymers (95%, 105%, and 98% for PEG 1500, 1650, and 1750 in the case of PAE-PCL-PEG-PCL-PAE and 98% in the case of PAE-PCLA-PEG-PCLA-PAE) even when the concentration of copolymer increased up to 100 $\mu g.ml^{-1}$. The results indicate that these copolymers can be used as a biomaterial for drug delivery.

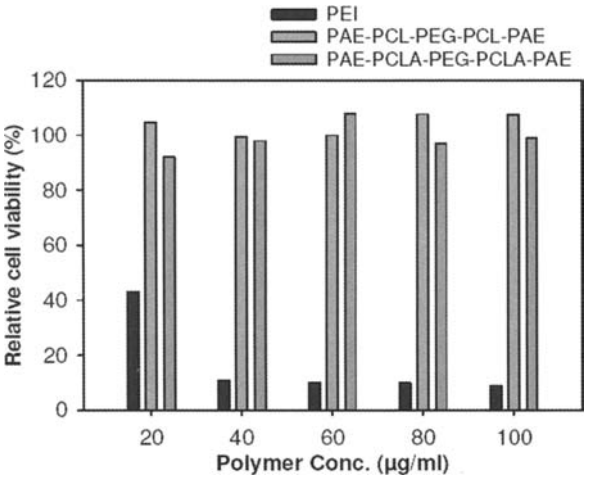

Fig. 4 Cytotoxicity evaluation of pentablock copolymers

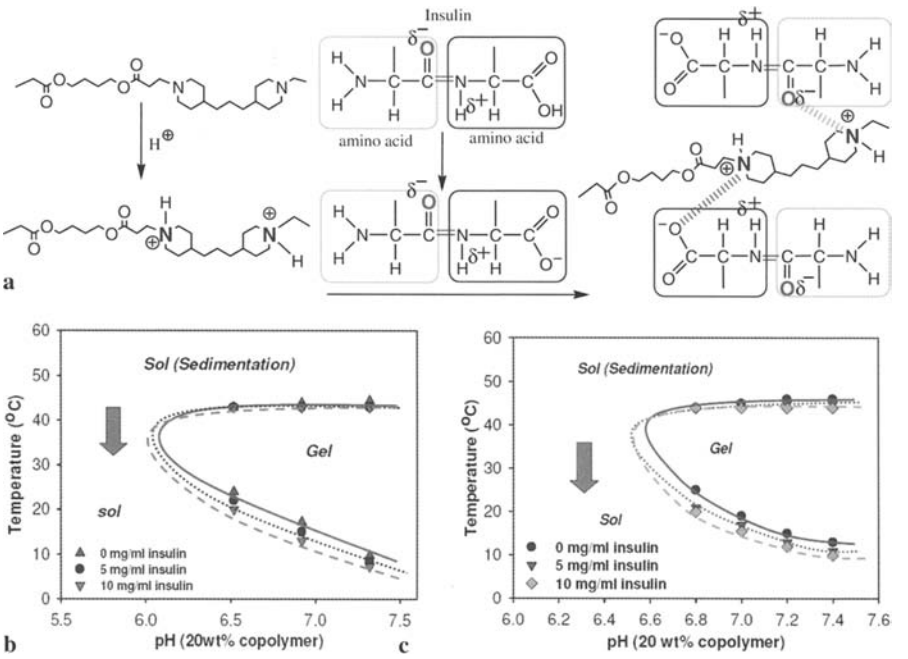

Fig. 5 Effect of ionic complexes on sol-gel phase transition diagrams of PAE-PCL-PEG-PCL-PAE solution. **a** Schematic illustration of ionic complexes between ionized PAE block and amino acids of insulin; **b** Sol-gel phase transition of complex solution with different insulin formulation. PAE-PCL-PEG-PCL-PAE (PEG 1.65k; PCL/PEG~1.8/1; PAE~1.25k) copolymer solution (20%); **c** Sol-gel phase transition of complex solution with different insulin formulation. PAE-PCLA-PEG-PCLA-PAE (PEG 1500; PCLA/PEG~2.5/1.0; PAE~1.3k) copolymer solution 20 wt% (a and b reproduced from [32], Copyright Elsevier Limited. Reproduced with permission)

3.4 Insulin loading and release in vitro

3.4.1 Effect of insulin on sol-gel transition diagram of pentablock copolymer

The second function of PAE block copolymer is simulated in Fig. 5a. At pH 3.0–4.0, H^+ ions in buffer solution combined with nitrogen from amino groups in PAE to form positively charged nitrogen. The ionic linkages between the positive charges in ionized PAE and negative charges of the amino acids in insulin [32] formed the complex ionic unit. As a result, the viscosity of the mixture increased, and the links made the mixture change easily into a complex gel as compared with copolymer solution only. Fig. 5b and c show the comparison between the sol-gel transition of PAE-PCL-PEG-PCL-PAE (or PAE-PCLA-PEG-PCLA-PAE) solution and that of the mixture of copolymer and insulin. As can be seen in this figure, the lower CGT's, which were shown in the sol-gel transition phase diagram, decreased with increasing insulin concentration, while the upper CGT's and CGpH's did not change.

3.4.2 Mechanism of insulin loading and release

The mechanism of insulin loading into PAE-PCL-PEG-PCL-PAE and release from the hydrogel is explained in Fig. 6. When insulin was added to pentablock copolymer solutions at low pH, most of the biomolecules connected with the PAE blocks by ionic linkages between the positive charges and negative charges of the amino acids of insulin as discussed above (Fig. 6a). A small amount of PAE plays the role of hydrophobic block because it is not ionized. This made PAE-PCL/PAE-PCLA hydrophobic and thus the pentablock copolymer could form minor micelles. Pentablock copolymers formed the gel structure as discussed previously, when pH and temperature increased to 7.4 and 37 °C, respectively. Furthermore, the PAE-insulin unit was not broken down because of the sufficiently strong linkage. Consequently, a part of the mixture of pentablock copolymers and insulin composed a complex gel by ionic linkages (Fig. 6b). The two steps of pharmacokinetic release of insulin from the complex gels could be described as chemically controlled and Fick Kian diffusion-controlled

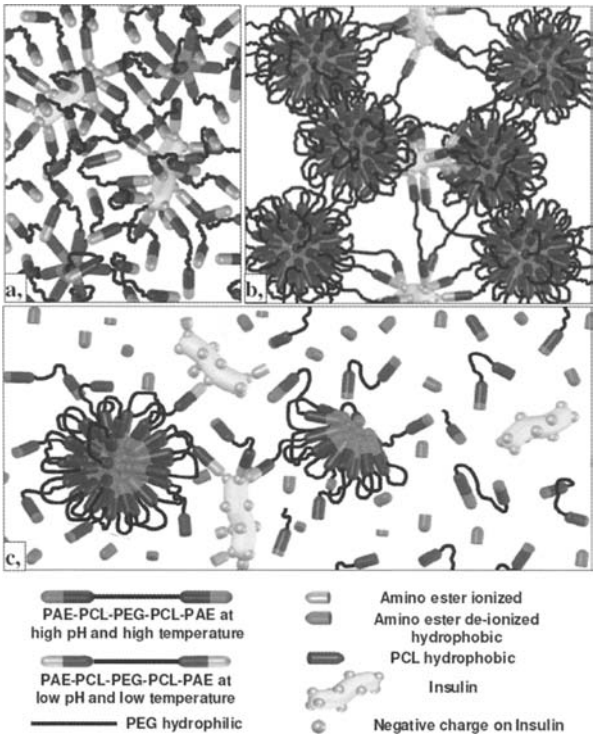

Fig. 6 Mechanism of insulin loading and release. **a** The polymer solution is sol state at 10 °C and pH 7.0 with the ionic complex between insulin and pentablock copolymers; **b** Gel formed by insulin free pentablock copolymer after injection into the human body (37 °C and pH 7.4); **c** Insulin release from the gel by polymer degradation (reproduced from [32], Copyright Elsevier Limited. Reproduced with permission)

by the degradation of the copolymer. Firstly, β-amino ester-insulin units were liberated because of PAE degradation. The second step was the release of insulin under the influence of an insulin concentration gradient (ICG) between the inside of the complex gel and outside serum as a diffusion-controlled process (Fig. 6c).

The mechanism was demonstrated by in vitro pharmacodynamic results, as shown in Fig. 7 and 8. With the same amount of insulin loading and different amount of releasing media and sampling methods, the insulin concentration (IC) in the serum which was sampled by method 1, was higher than that sampled by method 2 (Fig. 7). This suggested that the gradients of IC between the inside of the hydrogel and outside

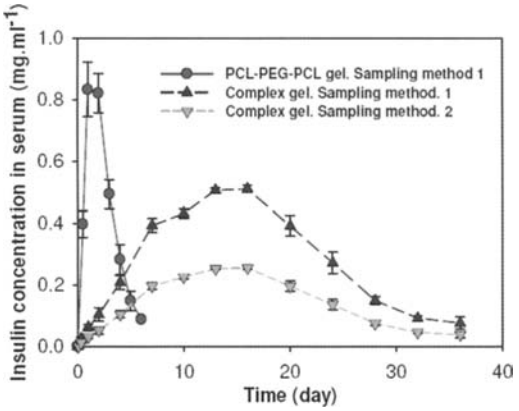

Fig. 7 Insulin release in vitro (PAE-PCL-PEG-PCL-PAE (PEG 1.65k; PCL/PEG~1.8/1; PAE~1.25k)) – Serum insulin concentration ($mg.ml^{-1}$). Error bars represent the standard deviations (n = 4) (reproduced from [32], Copyright Elsevier Limited. Reproduced with permission)

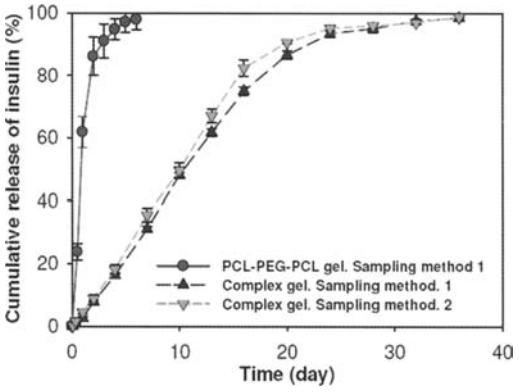

Fig. 8 Insulin release in vitro (PAE-PCL-PEG-PCL-PAE (PEG 1.65k; PCL/PEG~1.8/1; PAE~1.25k)) – Cumulative release of insulin (%). Error bars represent the standard deviations (n = 4) (reproduced from [32], Copyright Elsevier Limited. Reproduced with permission)

serum were different. However, the cumulative release profiles of insulin by the two sampling approaches were almost same (Fig. 8). This demonstrated that the liberation of insulin from the complex gel depended only on the degradation of copolymer and was not influenced by the gradient of IC. The effect of charge complex on insulin release from PCL-PEG-PCL and complex gel is also shown in Fig. 7 and 8. It should be noted that there was no initial burst of insulin from the complex gel formulation. The complex gel played an important role in long-term sustained release of insulin. The ionic complexation between insulin and the PAE segments of the polymer stabilized the insulin physically and chemically, and prevented an initial burst release. The release of complex gel showed more or less constant release kinetics over the duration of 36 days. Without ionic complexation, the release profile of PCL-PEG-PCL exhibited a higher burst effect and shorter duration.

3.5 Comparison between PAE-PCL-PEG-PCL-PAE and PAE-PCLA-PEG-PCLA-PAE

3.5.1 Degradability evaluation of block copolymer and complex gel in vitro

Fig. 9 shows the in vitro degradation of triblocks, pentablock copolymers and complex gels. The data in this figure proclaimed that there were two steps in the degradation curve of pentablock copolymers. First, PAE disintegrated very fast, and then the triblock copolymer degraded slowly. However, when insulin was encapsulated in the pentablock, the hydrolysis of PAE became slow because of the ionic linkage between insulin and PAE. As a result, the decomposition of PAE in complex gel was behindhand.

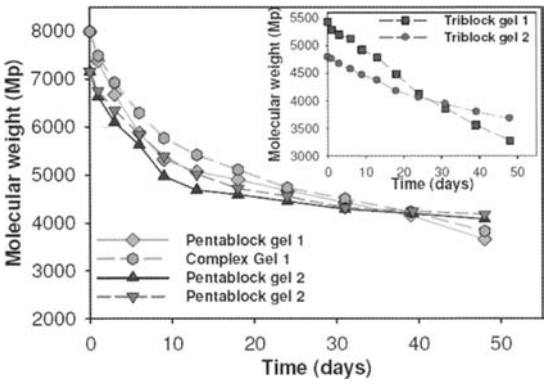

Fig. 9 Change of molecular weights of PAE-PCL-PEG-PCL-PAE and PAE-PCLA-PEG-PCLA-PAE due to degradation in vitro. (Group triblock, pentablock and complex gel 1: PEG 1.5k; PCLA/PEG~2.5/1.0;PEA~1.3k. Group triblock, pentablock and complex gel 1: PEG 1.65k; PCL/PEG~1.8/1.0;PEA~1.25k; 5 mg/ml insulin in copolymer solution 20 wt%)

This figure also shows a comparison between the degradation of PAE-PCLA-PEG-PCLA-PAE (group 1) and PAE-PCL-PEG-PCL-PAE (group 2). Triblock copolymers consist of PEG and biodegradable hydrophobic block. The ester group density, which was located in PCLA of triblock 1, was higher than that in PCL of triblock 2. As shown in this figure, the slope of the degradation curve of triblock 1 was higher than that of triblock 2. This suggested a quicker decomposition of PCLA due to ester hydrolysis. As a result, PCLA-PEG-PCLA degraded faster than PCL-PEG-PCL. In conclusion, this caused group 1 to be more easily degraded as compare with group 2.

3.5.2 Effect of the copolymer's degradation on the release of insulin

Fig. 10 shows the cumulative release of insulin from different complex gels. In this figure, at the same insulin formulation and sampling method, more than 90% of insulin was released from complex gel 1 within 16 days, whereas it took 22 days in the case of complex gel 2. It should be noted that there was some relation between the data in section 3.5.1 and 3.5.2 and the data of insulin release, as shown in Fig. 10. That relation indicated that the cumulative release of insulin from those complex gels increased directly with the degradation of the complex gels as discussed in section 3.4. Consequently, the cumulative release of insulin from the complex gel of cationic pH/temperature-sensitive hydrogel based on the bi-functional PAE block can be controlled by decomposition of the copolymer.

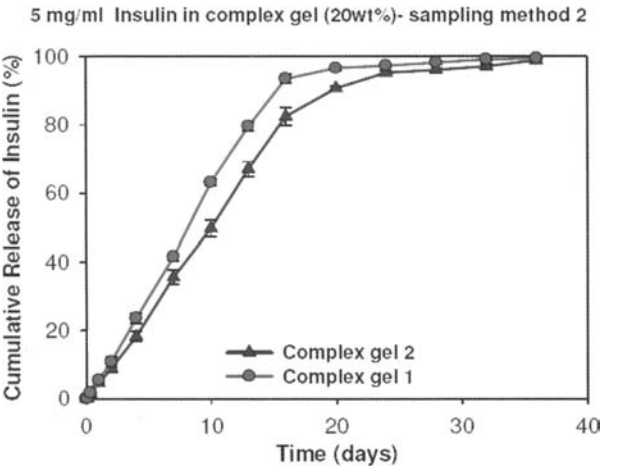

Fig. 10 Cumulative release of insulin with time from complex gel by the degradation of copolymer. Experiment in vitro, error bars represent the standard deviation (n = 4). Complex gel 1: 5 mg/ml insulin loaded in copolymer (20 wt%) of PAE-PCLA-PEG-PCLA-PAE (PEG 1.5k; PCLA/PEG~2.5/1.0;PEA~1.3k); complex gel 2: 5 mg/ml insulin loaded in copolymer (20 wt%) of PAE-PCL-PEG-PCL-PAE (PEG 1.65k; PCL/PEG~1.8/1.0;PEA~1.25k); Sampling method 1

3.6 Insulin release from triblock and complex gel in SD rats

In order to investigate the effect of charge complex on insulin release, an animal study using male Sprague-Dawley rats was performed with an insulin-loaded complex hydrogel. Fig. 11 shows the concentrations of plasma insulin of the insulin-only, insulin-triblock gel and complex gel formulation in SD rats. For the insuline-only group, there was a higher initial burst release within 1 hr. In the case of the insulin-triblock gel group, without ionic complexation, the release profile of insulin exhibited a higher burst effect and shorter duration 3 hr post-injection as a diffusion-controlled release (most insulin in this group was released in 4 days). The insulin level of complex gel formulation was almost constant for 15 days and dropped at 19 days because of chemical and diffusion – controlled release as discussed before. Thus, in vivo insulin release from the insulin-loaded complex hydrogel was constant for 15 days following subcutaneous injection [32].

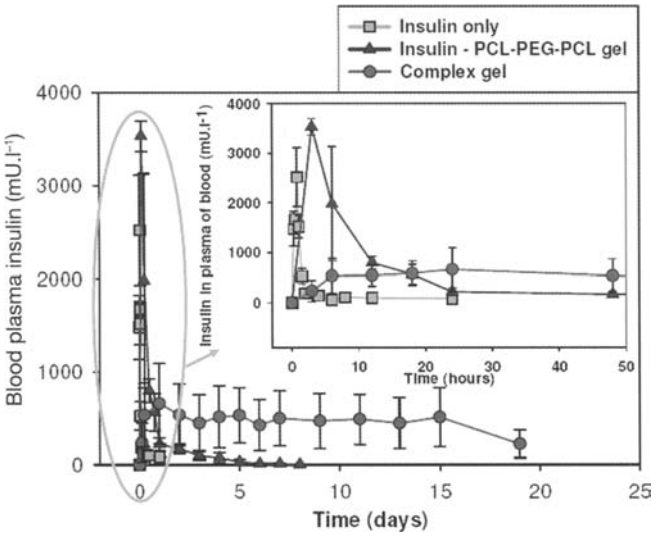

Fig. 11 Insulin release experiment in vivo. For the insulin only group, 200 μl of insulin solution 0.25 mg.ml^{-1} (in PBS buffer (pH 7.4) was administered by intraperitoneal injection (0.05mg insulin for each rat). For the insulin –PCL-PEG-PCL (PEG 1.65k; PCL/PEG~1.8/1.0) gel group, 200 μl of solution (5 mg.ml^{-1} insulin in PCL-PEG-PCL solutions 25 wt%) at pH 7.0 and 10 °C was subcutaneously injected into the back side (1 mg insulin for each rat). For the complex gel group, 200 μl of complexation insulin solution (5 mg.ml^{-1} in PAE-PCL-PEG-PCL-PAE (PEG 1.65k; PCL/PEG~1.8/1.0;PEA~1.25k) solutions 25 wt%) at pH 7.0 and 10 °C is subcutaneously injected into the back side (1 mg insulin for each rat). (Female SD rats, Error bars represent the standard deviations (n = 5) (reproduced from [32], Copyright Elsevier Limited. Reproduced with permission)

3.7 Storage stability of pentablock copolymers

Fig. 12 shows the degradation of the pentablock copolymers under two conditions. The results in this figure showed that the degradation of pentablock solution at pH 6.6 was faster if compared with that of pentablock powder. After storage in a refrigerator at 0 °C for 6 months, the molecular weight of PAE-PCL-PEG-PCL-PAE and PAE-PCL-PEG-PCL-PAE powder decreased from 6732 to 6593 and from 7950 to 7887. Molecular weights reduced from 6732 to 5376 and from 7950 to 7032 respectively, when stored as a solution at pH 6.6. It was believed that the molecular weight of PAE-PCL-PEG-PCL-PAE remained constant over a 6 month-period when in a powder state at 0 °C.

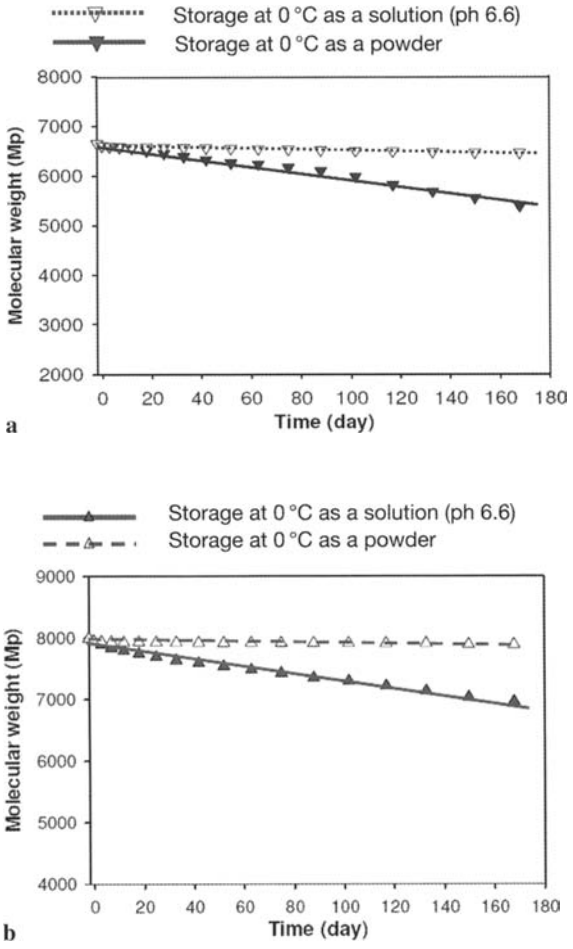

Fig. 12 Molecular weight change with time. **a** PAE-PCL-PEG-PCL-PAEs (PEG 1.5k; PCL/PEG~1.8/1; PAE~1.25k); **b** PAE-PCLA-PEG-PCLA-PAEs (PEG 1.5k; PCLA/PEG~2.5/1; PAE~1.3k)

4 Conclusions

We report a functionalized injectable hydrogel, which can be used for controlled release of protein drugs such as insulin by subcutaneous injection. The sol-gel phase transition of aqueous media of the copolymers was investigated. They changed from a sol phase to a gel phase with increasing temperature and pH. A typical phase diagram exhibited CGC, CGpH and two CGT curves. The results of in vitro cytotoxicity experiments indicated that the copolymer could be used as a biomaterial. In addition, the copolymer solution (20 wt% concentration at 10 °C and pH below 7.0) can form a gel within minutes after being injected into the animal. Moreover, degradation experiments of PAE-PCLA-PEG-PCLA-PAE and PAE-PCL-PEG-PCL-PAE showed that the decomposition of pH/temperature-sensitive biodegradable hydrogel, which was based on the bi-functional group of PAE, was controllable. In conclusion, the release of anionic drug/protein such as insulin from this material can be controlled by adjusting the degradation of copolymers.

The results of in vivo insulin release in SD rats showed that the ionic linkage between insulin and PAE lead to sustained release in this system. The materials have various advantages as drug/protein delivery systems, including direct injection without any surgical procedure, no clogging during injection, straightforward drug loading into the polymer solution, dry powder form, easy to dissolve, easy to sterilize by UV, simple dose adjustment, system biocompatibility with no inflammatory reaction, as well as no requirement of organic solvents during fabrication.

Acknowledgment. This work was supported by the Korea Research Foundation Grant KRF-2006-005-J04602.

References

[1] Tyagi P (2002) Insulin delivery systems : present trends and the future direction. Indian J Pharmacol 34:379–389

[2] Qiao M, Chen D, Ma X, Liu Y (2005) Injectable biodegradable temperature-responsive PLGA–PEG–PLGA copolymers: synthesis and effect of copolymer composition on the drug release from the copolymer-based hydrogels. Int J Pharm 294:103–112

[3] Hoffman AS (2002) Hydrogels for biomedical applications. Adv Drug Deliver Rev 53:3–12

[4] Cohn D, Stern S, González MF, Epstein J (2002) Biodegradable poly(ethylene oxide)/poly(ε-caprolactone) multiblock copolymer. J Biomed Mater Res 59:273–281

[5] Zhao SP, Zhang LM, Ma D (2006) Supramolecular hydrogels induced rapidly by inclusion complexation of Poly(ε-caprolactone)-poly(ethylene glycol)-poly(ε-caprolactone) block copolymers with α-cyclodextrin in aqueous solutions. J Phys Chem B 110:12225–12229

[6] Huang X, Lowe TL (2005) Biodegradable thermoresponsive hydrogels for aqueous encapsulation and controlled release of hydrophilic model drugs. Biomacromolecules 6:2131–2139

[7] Yang YW, Yang Z, Zhou ZK, Attwood D, Booth C (1996) Association of triblock copolymers of ethylene oxide and butylene oxide in aqueous solution: A study of $B_nE_mB_n$ copolymers. Macromolecules 29:670–680

[8] Choi SW, Choi SY, Jeong BS, Kim W, Lee D S (1999) Thermoreversible gelation of poly(ethylene oxide) biodegradable polyester block copolymer. J Polym Sci Part A: Poly Chem 37:2207–2218
[9] Jeong B, Kim SW, Bae YH (2002) Thermosensitive sol-gel reversible hydrogels. Adv Drug Deliver Rev 54:37–51
[10] Tanaka T, Fillmore DS, Sun T, Nishio I, Swislow G, Shah A (1980) Phase transitions in ionic gels. Phys Rev Lett 45:1636–1639
[11] Amiya T, Hirokawa T, Hirose Y, Li Y, Tanaka, T (1987) Reentrant phase transition of N-isopropylacrylamide gels in mixed solvent. J Chem Phys 86:2375–2379
[12] Chen G, Hoffman AS (1995) Graft copolymers that exhibit temperature-induced phase transition over a wide range of pH. Nature 373:49–52
[13] Yoshida R, Uchida K, Taneko T, Sakai K, Kikuchi A, Sakurai Y, Okano T (1995) Comp-type grafted hydrogels with rapid de-swelling response to temperature range. Nature 374:240–242
[14] Tanaka T, Nishio I, Sun ST, Nishio SU (1982) Collapse of gels in an electric field. Science 218:467–469
[15] Osada Y, Okuzaki H, Hori H (1992) A polymer gel with electrically driven motility. Nature 355:242–244
[16] Irie M (1993) Stimuli-responsive poly(*N*-isopropylacrylamide) Photo- and chemical-induced phase transitions. Adv Polym Sci 110:49–65
[17] Suzuki A, Tanaka T (1990) Phase transition in polymer gel induced by visible light. Nature 346:345–347
[18] Qiu Y, Park K (2001) Environment-sensitive hydrogels for drug delivery. Adv Drug Delivery Rev 53:321–339
[19] Jeong B, Bae YH, Lee DS, Kim SW (1997) Biodegradable block copolymers as injectable drug-delivery systems. Nature 388:860–862
[20] Shim MS, Lee HT, Shim WS, Park I, Lee H, Chang TS, Kim W, Lee DS (2002) Poly(D,L-lactic acid-co-glycolic acid)-b-poly(ethylene glycol)-b-poly (D,L-lactic acid-co-glycolic acid) triblock copolymer and thermoreversible phase transition in water. J Biomed Mater Res 61:188
[21] Huynh DP, Shim WS, Kim JH, Lee DS (2006) pH/temperature sensitive poly(ethylene glycol)-based biodegradable polyester block copolymer hydrogels. Polymer 47:7918–7926
[22] Shim WS, Yoo JS, Bae YH, Lee DS (2005) Novel Injectable pH and Temperature Sensitive Block Copolymer Hydrogel. Biomacromolecules 6:2930–2934
[23] Akinc A, Anderson DG, Lynn DM, Langer R (2003) Synthesis of Poly(β-amino ester)s optimized for highly effective gene delivery. Bioconjugate Chem 14:979–988
[24] Potineni A, Lynn DM, Langer R, Amiji MM (2003) Poly(ethylene oxide)-Modified Poly(β-amino ester) Nanoparticles: A Long-Circulating pH-Sensitive Biodegradable System for Paclitaxel Delivery. J Control Release 86:223–234
[25] Berry D, Lynn DM, Sasisekharan R, Langer R (2004) Internalized heparin using poly(b-amino ester)s promote cellular uptake of heparin and cancer cell death. Chem Biology 11:487–798
[26] Little SR, Lynn DM, Ge Q, Anderson DG, Puram SV, Chen J, Eisen H, Langer R (2004) Poly(β-amino ester-containing microparticles enhance the activity of nonviral genetic vaccines. Proc Natl Acad Sci USA 101:9534–9539
[27] Ferruti P, Bianchi S, Ranucci E, Chiellini F, Caruso V (2005) Novel poly(amido amine)-based hydrogels as scaffolds for tissue engineering. Macromol Biosci 5:613–622
[28] Kim MS, Lee DS, Choi EK, Park HJ, Kim JS (2005) Modulation of poly(β-amino ester) pH-sensitive polymers by molecular weight control. Macromol Res 13:147–151

[29] Jeong BM, Lee DS, Shon, J, Bae YH, Kim SW (1999) Thermorevirsible gelation of poly(ethylene oxide) biodegradable polyester block copolymer II. J Polym Sci Part A 37:751–760

[30] Jeong BM, Bae YH, Kim SW (1999) Thermoreversible gelation of PEG-PLGA-PEG triblock copolymer aqueous solution. Macromolecules 32:7064–7069

[31] Stevens MG, Olsen S (1993) Comparative analysis of using MTT and XTT in colorimetric assays for quantitating bovine neutrophil bactericidal activity. J Immunol Methods 157:225–231

[32] Huynh DP, Nguyen MK, Pi BS, Kim MS, Chae SY, Lee KC, Kim BS, Lee SW, Lee DS (2008) Functionalized injectable hydrogels for controlled insulin release. Biomaterials 29:2527–2534

[33] Anderson DG, Lynn DM, Langer R (2003) Semi-automated synthesis and screening of a large library of degradable cationic polymers for gene delivery. Angrew Chem Int Ed 42:3153–3158

On-Off Switching Properties of ultra thin Intelligent Temperature-Responsive Polymer Modified Surface

Yoshikatsu Akiyama and Teruo Okano

Abstract. Intelligent temperature-responsive polymers are currently utilized in a variety of fields within engineering and medicine. Particularly, special attention has been paid to the temperature-responsive polymer, poly(*N*-isopropylacrylamide) (PIPAAm). We have investigated properties of PIAAm grafted surfaces and applied the surfaces to novel chromatography matrix and novel cell culture surfaces. In this chapter, we describe the features of PIPAAm grafted surfaces in response to external temperature stimuli. We discuss the features in terms of the degree of the mobility of the grafted polymer chains as well as hydration and dehydration of the chains by temperature change. For culturing cells on PIPAAm grafted surfaces, nanometer-thickness of the grafted PIPAAm layer plays a crucial role in cell adhesion/attachment behavior. Furthermore, we introduce a new concept for tissue engineering, utilizing temperature-responsive polymer grafted tissue culture dishes, and summarize the development of advanced temperature-responsive cell culture surfaces.

1 Introduction

Poly(*N*-isopropylacrylamide) (PIPAAm) shows a lower critical solution temperature of around 32 °C in water [1]. PIPAAm is hydrated and soluble in water below LCST, while, above LCST, precipitation of the polymer and solution turbility is observed due to dehydration of PIPAAm. Owing to hydration and dehydration characteristic of the PIPAAm chains, the PIPAAm graft surfaces exhibit hydrophilic/hydrophobic alternation accompanying temperature change. We have been carrying out the preparation of temperature-responsive polymer-modified surfaces with designated molecular configuration at the interfaces [2, 3]. These surfaces are utilized to propose new chromatographic separation methods for a variety of types of bioactive and organic compounds in a sole aqueous mobile phase. [4–9] We further applied the temperature-responsive surfaces to thermally regulated cell adhesion and detachment [10,11] and successfully recovered the cultured cells as a single contiguous cell sheet with deposited extracellular matrix (ECM) [12, 13]. We propose a new concept, cell sheet engineering, applying the cell sheets to tissue engineering [14, 15].

In this chapter, we describe an effect of the degree of the mobility of the grafted PIPAAm chains on resulting surface wettability, and applied the surfaces to chro-

Barbucci R. (Ed): Hydrogels. Biological Properties and Applications.

matography media and temperature-responsive cell culture. Thermal separation of the organic and bioactive compounds by the novel chromatography and thermal regulation of cell adhesion and detachment behavior by the novel cell culture surface is discussed in terms of the molecular mobility of the grafted PIPAAm chains. Furthermore, we summarize the development of the advanced temperature-responsive cell culture surfaces.

2 Poly(N-isopropylacrylamide) grafted surfaces

The PIPAAm chain grafted surfaces exhibit hydrophilic/hydrophobic alternation in response to temperature. Below LCST, the polymer grafted surfaces exhibit hydrophilic property due to hydration of the polymer chains, while dehydration of the polymer chains produces hydrophobic surfaces above LCTS [2, 3]. Graft polymer chain conformation significantly affects wettability of resulting surfaces. Takei et al investigated temperature dependence for dynamic contact angle changes on terminally PIPAAm grafted and multipoint PIPAAm grafted surfaces by Wilhelmy plate techniques [2]. These surfaces were prepared by introduction of end-carboxyl PIPAAm and poly(*N*-isopropylacrylamide-*co*-acrylic acid) (P(IPAAm-*co*-AAc)) onto cover glass coated with poly(styrene-*co*-aminomethylstyrene) [2]. Although these surfaces exhibit contact angle change by temperature change, terminally PIPAAm grafted surfaces showed significantly larger and rapid contact angle change than multipoint PIPAAm rafted surfaces around 24 °C. Transition temperature of the polymer grafted surfaces lower than that of PIPAAm solution (32 °C) was likely to be due to the influence of basal polystyrene composition. Multipoint graft conformation constrains the dehydration of the polymer chains and prevents aggregation of the dehydrated polymers. In contrast, terminally grafted PIPAAm chains respond rapidly and show drastic and discontinuous contact angle change due to their highly mobile nature.

An influence of graft polymer chain conformation on contact angle change was further investigated using four model surfaces, (a) terminally PIPAAm graft, (b) multipoint PIPAAm graft, (c) terminally PIPAAm grafted onto multipoint PIPAAm and (d) thin PIPAAm hydrogel surfaces (Fig. 1) [3, 4]. Temperature-dependent wettability of multipoint PIPAAm graft surfaces is influenced by the dynamic motion of the modified PIPAAm chains. In good solvent such as 1, 4-dioxane, PIPAAm chains exist in relatively expanded conformation, and react with the surfaces maintaining this expanded conformation. The dynamic motion of the grafted polymer chains is restricted, resulting in smaller and linear contact angle change with increasing in temperature. By contrast, in poor solvent such as 1,4-dioxane/toluene, the polymer chains exist in relatively globular conformation. This globular conformation produced looped chain configuration retaining larger mobility and larger dynamic motion of the surfaces. The surfaces showed discontinuous and larger contact angle change in response to temperature. Aminated glass cover slip was employed as basal substrate for grafting PIPAAm. Graft density of PIPAAm of these four surfaces was larger than Takei et al [2].

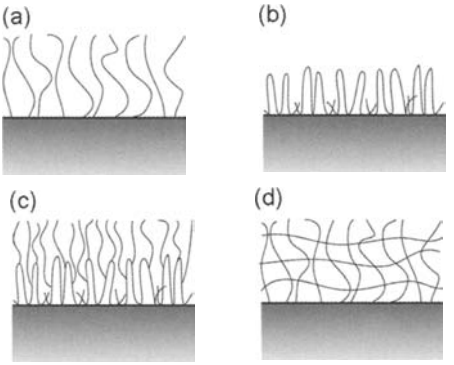

Fig. 1 Schematic overview of four types of PIPAAm modified surfaces with different molecular architecture. **a** Terminal PIPAAm graft (surface A), **b** Multipoint PIPAAm graft (surface B), **c** Terminal PIPAAm grafted onto multipoint PIPAAm (surface C) and **d** Thin PIPAAm hydrogel surfaces (surface D)

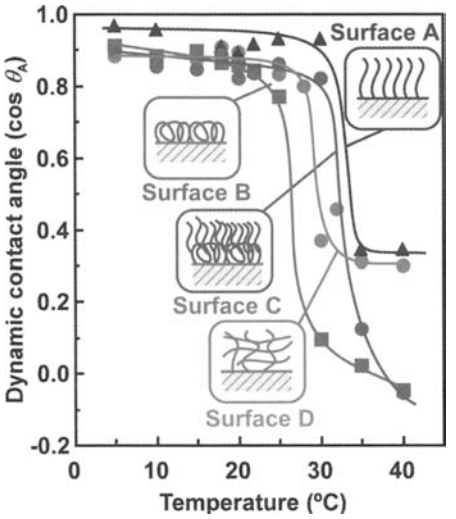

Fig. 2 Temperature-dependent water contact angle changes for four types of PIPAA-grafted surfaces with different architecture represented in Fig. 1 (Reprinted from [18], with permission from Elsevier)

Temperature-dependent contact angle change of these four surfaces is shown in Fig. 2 using Wilhelmy plate technique [12]. AFM measurement of these surfaces revealed that the effect of roughness on contact angle is negligible. All four surfaces showed larger $\cos\theta$ values at lower temperature and lower $\cos\theta$ values at higher temperature, indicating alternation of hydrophilic/hydrophobic surfaces. For surfaces A and C, discontinuous surface wettability change was observed near 32 °C corresponding to LCST of PIPAAm in aqueous solution due to terminal PIPAAm chains with

free mobility. In contrast, for surface B, the multipoint graft configuration restricting the polymer chains' mobility at lower temperature where surface wettability change occurs (ca. 27 °C). Surface C, obtained by grafting free end PIPAAm onto looped chains (surface B), has a larger amount of the grafted PIPAAm than surface A, clearly indicating that larger amounts of the polymer make larger changes in contact angle. PIPAAm hydrogel grafted surface (surface D) exhibits smaller change in contact angle due to restriction of the chain mobility caused by the crosslinked structure. These results demonstrate that conformation of the graft chain has a significant influence on the property of the graft polymer surface as well as their chain mobility. We modulated the interaction of the PIPAAm modified surfaces with biomolecules and cells, utilizing features of the chain conformation, as described below.

3 Green chromatography utilizing PIPAAm modified surfaces

PIPAAm modified glass beads were applied to gel permeation chromatograph by Gewehr et al [16]. Hosoya et al also reported a surface-selective modification procedure for the incorporation of PIPAAm into porous polymer beads [17]. They performed size exclusion chromatography of dextran with water as a mobile phase. This matrix utilized coli-globule transition of modified PIPAAm to control the pore size of the glass and porous beads. On the other hand, we utilized hydrophilic/hydrophobic alternation of PIAAm modified surfaces to separate hydrophobic biomolecules into the aqueous mobile phase.

Kanazawa et al successfully separated five steroids and benzene, employing PIPAAm end grafted silica beads as chromatography matrix [4]. The matrix was prepared as follows; PIPAAm with carboxyl terminal groups was synthesized by radical telomerizaition reaction in the presence of 3-mercpropropionic acid as telogen. The end carboxyl group of the resultant polymer was activated with hydroxysuccimide followed by reaction with aminopropylsilica beads. Chromatograms of a mixture of five steroids and benzene were obtained at different temperatures. Below LCST (5 °C), four of the steroids were not separated. With an increase in temperature, retention time of each steroid was retarded. Above LCST (35 °C and 50 °C), four steroids were fully separated. Unmodified silica beads did not separate these compounds at any temperature. The order of the eluted steroids is in agreement with the order of partition coefficient (log P value) of the steroids. The van't Hoff plots for five steroids on a PIPAAm-grafted silica packed column clearly indicates discontinuities in the plots at the temperature around the PIPAAm phase transition, suggesting hydration/dehydration of the grafted PIPAAm chains. [4] Namely, these results indicate that the steroid compounds hydrophobically interact with the grafted polymer.

In order to enhance the selectivity and retention time for the solutes, hydrophobic moieties such as *n*-butylmethacrylate (BMA) were incorporated into semitelechelic PIPAAm through telomerization and the resulting copolymers were introduced onto aminopropylsilica beads as stationary phase [5]. LCST of the copolymers were lower than that of PIPAAm, decreasing with increasing BMA content of the copolymer. Since hydrophobic BMA moieties strongly interacts with the hydrophobic steroid,

retention time of the steroids increased with an increase in BMA content of the copolymer even below LCST of the grafted copolymer. For example, for silica beads modified with P(PIPAAm-co-BMA) of 3.2 mol% BMA content, peaks of each steroid were observed at 5 °C, although silica beads modified with PIPAAm showed insufficient separation of each steroid.

For the silica beads modified with the copolymer, successful separation of hydrophobic compounds was achieved at 30 °C where sufficient separation was not observed for the PIPAAm silica beads. Although total elution time of five steroids from the copolymer column was much longer, step temperature gradient successfully shortens the retention time. This is due to features of reversible hydrophilic and hydrophobic alternation of the modified polymer. Namely, after steroids with lower log P values are eluted from silica beads modified with P(IPAAm-co-BMA) (BMA content = 3.2 mol%) at 30 °C, decreasing the temperature to 5 °C shortened the retention time of steroids with larger log P values with sharper peaks. This result indicates that interaction of the surfaces with the steroid as well as hydrophilic and hydrophobic properties of the surfaces can be controlled by temperature.

The copolymer column could be applied to separate of peptides such as the insulin A chain, β-endorphin and insulin chain B [6]. A mixture of these peptides was not sufficiently separated, however, at 30 °C, successful separation was obtained with an elution order of insulin chain A < β-endorphin fragment < insulin chain B in 0.5 M NaCl solution (pH 2.1). The order of elution is consistent with that of the hydrophobicity (Zf) of the peptides (insulin chain A < β-endorphin fragment < insulin chain B). This result also indicates that such hydrophobic peptides are separated through hydrophobic interaction with the modified polymer and eluted in the order of lower hydrophobicity of the peptides. The copolymer column is also applicable to the separation and analysis of the phenylthiohydantoin-amino acid (PTH-amino acid) and endocrine disrupter bisphenol A using water solution [7–9].

As described above, graft conformation of surface PIPAAm has a significant influence on wettability of the surfaces. Thus, one can expect that different graft conformation also shows different elution behavior for steroids. We prepared silica beads modified with graft conformation of different PIPAAm (surfaces B, C and D) as chromatography media and examined silica beads for temperature-dependent elution behavior of steroids at 5 °C and 45 °C (Fig. 3) [4, 18]. Since the graft density of PIPAAm chains is higher than free mobile PIPAAm chains (surface A), partition of steroid molecules within PIPAAm layers should influence retention time and peak broadening of the eluted steroids. Longer retention time was observed for silica beads with PIPAAm chain loops followed by modification with free mobile PIPAAm chains (surface C) compared to those seen for PIPAAm chain loops (surface B). In contrast, PIPAAm thin hydrogel grafted silica bead surfaces exhibit significant broadening peak and retention time of the steroids. Partition of steroid molecules into the PIPAAm layer should be affected by the three-dimensional cross-linked structure of the grafted PIPAAm hydrogel (surface D). In addition, restricted mobility of the PIPAAm chains duet to the three-dimensional cross-linked structure influences not only peak broadening but also extension of elution time of the steroids.

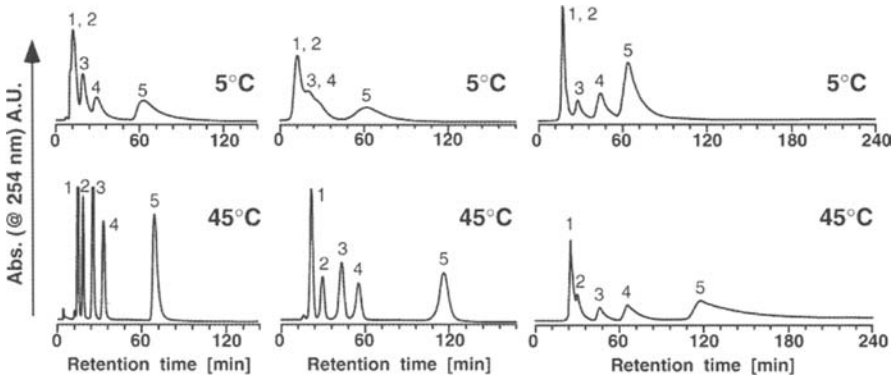

Fig. 3 Chromatograms of steroids from PIPAAm-modified surfaces at 5 °C and 45 °C. Left multipoint PIPAAm graft (surface B), center terminal PIPAAm grafted onto multipoint PIPAAm (surface C) and right thin PIPAAm hydrogel surfaces (surface D) (Reprinted from [18], with permission from Elsevier)

As results showed above, separation and analysis carried out in aqueous conditions without organic solvent is a feature of green chromatography. Thus, such a chromatography system not only reduces cost for analysis and waste of the mobile phase but is also kind to the environment.

4 Modulation of cell adhesion and detachment properties using intelligent temperature-responsive surfaces

It is well known that cells adhere and proliferate on hydrophobic surfaces rather than hydrophilic ones, and tend to adhere to the surface with appropriate hydrophobicity [19]. As a first contact between cells and material surfaces, cells physicochemically adhere to the hydrophobic surfaces (passive adhesion). The adherent cells remain intact and are readily detached from the surfaces. After contact, adherent cells change their morphology and spread, accompanied metabolic process using ATP. This process is categorized as active adhesion [17, 20, 21]. In general, enzymes such as trypsin are employed for digestion of extracellular matrix proteins in order to detach cells from the surfaces. However, treatment with these enzymes degrades cell-surface molecules, including growth factor receptors and ion channels, and disrupts cell-cell junction proteins that are vital for the differentiated functions of many cell types (Fig. 4 upper).

In 1990, we reported the successful modulation of cell attachment and detachment behavior, utilizing features of hydrophobic and hydrophilic alternation of PIPAAm grafted tissue culture polystyrene (PIPAAm-TCPS) by reducing temperature to below 32 °C (Fig. 4 bottom) [10]. Such cell adhesion-detachment modulation is a novel concept, because no enzymatic treatment is required. PIPAAm was modified with TCPS surfaces by utilizing electron beam irradiation. In brief, appropriate amounts of 2-propanol solutions of IPAAm monomer were spread uniformly

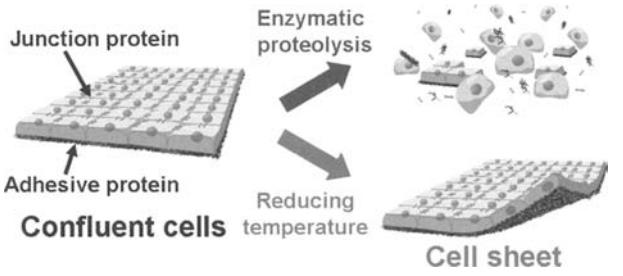

Fig. 4 Schematic drawing of recovery of confluent cells from (upper) commercially available tissue culture polystyrene by enzymatic proteolysis, (bottom) temperature-responsive cell culture surface by reducing temperature

over TCPS surfaces, followed by electron beam irradiation. During this procedure, IPAAm monomer is both polymerized and simultaneously grafted covalently onto the TCPS surfaces. PIPAAm-TCPS exhibited hydrophobic properties at 37 °C, allowing for cell attachment and adhesion (passive and active adhesion). In contrast, cells adherent to PIPAAm-TCPS were spontaneously detached from the surfaces by reducing temperature to below 32 °C. Given mild temperature changes and no requirement for enzymatic treatment, cells are not subjected to damage such as destruction of cell-cell junctions and cell membrane proteins during the recovery process. Thus, the recovered cell sheet maintains deposited extracellular matrix (ECM) at the basal surface and cell-cell junctions (Fig. 4 bottom). The deposited ECM allows easy adhesion of the recovered cell sheet to various surfaces such as the culture dish, other cells sheets, and the host tissue. Optimal temperature conditions for efficient cell recovery is different among different types of cultured cells (20 °C for cultured endothelial cells and 10 °C for hepatocytes). The cellular detachment process involves intracellular signal transduction and reorganization of the cytoskeleton, accompanied by the consumption of ATP molecules. In order to recover and manipulate the cell sheet, supporting membranes composed of poly(ethylene terephthalate), poly(vinylidene-difluoride), chitin, or parchment paper sheets were used [22–24]. This membrane allows the direct transfer of cell sheets onto native tissue or other cell sheets. In addition to these membranes, we developed a new polyion complex gel as a novel support, by mixing poly(*N*,*N*-dimethylacrylamide-*co*-2-acrylamido-2-methylpropane sulfonic acid) as anionic water-soluble polymers and poly(*N*,*N*-dimethylacrylamide-*co*-2-acryloxyethyltrimethylammonium chloride) as cationic water-soluble polymers [25]. We term this new cell manipulation technology "cell sheet engineering" and have utilized the technique to prepare a variety of cell sheets. In addition, many types of tissues have been successfully reconstructed using cell sheet engineering technology, including skin, corneal epithelium and bladder and cardiac tissue [23–26].

Various kinds of cells adhered and proliferated on PIPAAm-TCPS surfaces under normal conditions at 37 °C with 5 % CO_2 [11–13, 22–30]. Cell adhesion and proliferation behavior was comparable to commercially available TCPS. Cellular interaction with PIPAAm-TCPS surface and surface wettability measured by the captive bubble

Table 1 Properties of 1.4PIPAAm-TCPS, 2.9PIPAAm-TCPS and 5000PIPAAm

	1.4PIPAAm-TCPS	2.9PIPAAm-TCPS	5000PIPAAm[a]
Density of grafted PIPAAm ($\mu g/cm^2$)	1.4 ± 0.1	2.9 ± 0.1	1,080
Contact angle ($\cos\theta$)			
(37 °C)	0.20	0.35	0.65 (40 °C)
(20 °C)	0.42	0.50	0.98 (10 °C)
Thickness of the grafted PIPAAm (nm)	15.5 ± 7.2	29.3 ± 8.4	5,000
Cells attachment/detachment properties			
(37 °C)	Yes	No adhesion	No adhesion
(20 °C)	Yes	–	–
An amount of adsorbed FN (ng/cm^2)			
(37 °C)	150 ± 50	UD	UD
(20 °C)	UD	UD	UD

UD : Undetectable

a) Glass coverslips were used as base substrate of 5000IPAAm. Density and thickness of the grafted PIPAAm were measured in a dry state.

method are significantly influenced by polymer graft density and/or thickness of the PIPAAm layer (Table 1) [31]. Cells were adhered to and proliferated on PIPAAm-TCPS surfaces with polymer graft density ranging from 1.4 $\mu g/cm^2$ to 2.0 $\mu g/cm^2$, and were recovered from the surfaces by reducing temperature (PIPAAm-TCPS with 1.4 $\mu g/cm^2$ of the grafted PIPAAm was abbreviated as 1.4PIPAAm-TCPS). For polymer density lower than 1.4 $\mu g/cm^2$, cells adhered to and proliferated on the PIPAAm-TCPS surfaces, but they did not detach even below LCST. In contrast, cells were not adhered to PIPAAm-TCPS with a graft density of more than 2.0 $\mu g/cm^2$ or with a graft thickness of more than 30 nm. Thus, 2.9PIPAAm-TCPS exhibited cell repellent surfaces. Such cell adhesion behavior was correlated with their surface wettability and protein adsorption of ECM proteins such as fibronectin. These surfaces are fully covered with a PIPAAm layer as determined by angular-dependent X-ray photoelectron spectroscopy (XPS) analyses [32, 33]. Thus, retention of cell adhesion on the PIPAAm-TCPS with a lower polymer density below 32 °C is not due to exposure of hydrophobic basal TCPS surfaces. Namely, the grafted PIPAAm chains dominantly interact with cells and/or adsorbed proteins.

As described above, mobility of the grafted PIPAAm chains affects surface wettability. Swelling ratio for single side fixed PIPAAm hydrogel is much less than that of non-fixed PIPAAm hydrogel. In addition, the swelling ratio for single sided fixed PIPAAm hydrogel with 0.5 mm thickness of the PIPAAm (Table 1, 5000PIPAAm) was less than half of that for fixed hydrogel with 1.0 mm thickness of the PIPAAm. This difference is due to the different molecular mobility of the polymer chains in

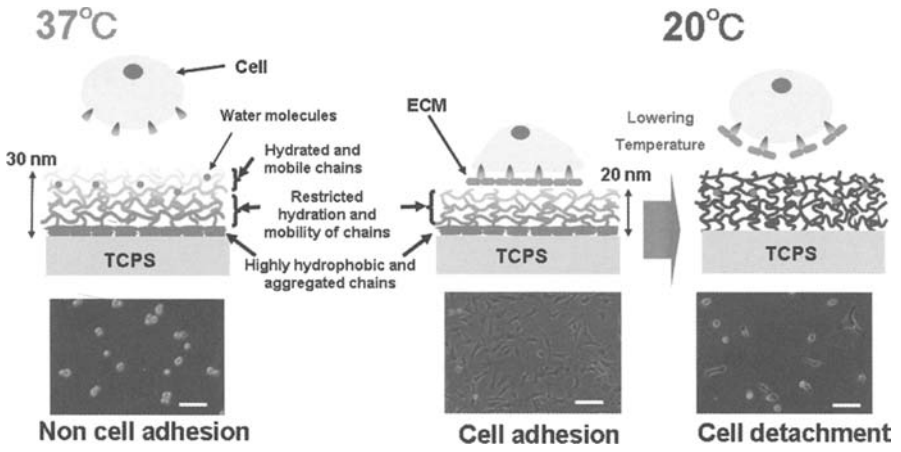

Fig. 5 Schematic drawings of the influence of molecular motion of grafted PIPAAm chains on hydration of the polymer chains, when the grafted PPAAm layers are thin (right) and thick (left) at and 37 °C and/or 20 °C. Hydrophobic TCPS interfaces promoting aggregation and dehydration are represented as a black region in TCPS. Molecular motion of the grafted polymer chains becomes larger according to the distance away from TCPS interfaces

each hydyrogel system [31]. Fixation of the polymer gel on glass surfaces restricts molecular mobility of the PIPAAm chains in the vicinity of the basal glass surfaces, causing extensive hydrophobic aggregation and limited hydration of the chains. Such restriction of the polymer chain mobility hinders the general network response of the PIPAAm chains in the hydrogel. Thus, PIPAAm chains at the outermost region are more mobile, more hydrated and more rapid respond to stimuli compared to those within fixed and cross-linked PIPAAm hydrogel. This consideration should be extended to the PIPAAm-TCPS system with ultra thin PIPAAm thickness. Fig. 5 illustrates a schematic drawing of possible causes for different chain mobility of the grafted chains of PIPAAm layers. In the case of the ultra chin PIPAAm gel layers on TCPS, hydrophobic interaction at TCPS interfaces also promotes aggregation and enhanced dehydration of the grafted PIPAAm chains. The hydrophobic and immobile TCPS interfaces restrict molecular motion of the PIPAAm grafted chains. Such restriction of chain mobility and dehydration of the grafted PIPAAm chains should be progressively extended to outermost regions of the grafted PIPAAm chains. Thus, PIPAAm-TCPS with thinner PIPAAm layer (20 nm PIPAAm thickness) exhibited more hydrophobicity than that with thicker PIPAAm layers (30 nm PIPAAm thickness). For thicker PIPAAm layers, more polymer chains at the outermost regions are hydrated than those of thinner PIPAAm layers. Consequently, PIPAAm-TCPS with thinner PIPAAm layers showed cell adhesive surfaces, while that with thicker PIPAAm layers showed repellence one, even above LCST.

The grafted PIPAAm thickness-dependency on cell adhesion property was also investigated in detail using PIPAAm grafted glass coverslips with different thicknesses and amounts of the grafted PIPAAm [34]. PIPAAm was covalently grafted onto glass

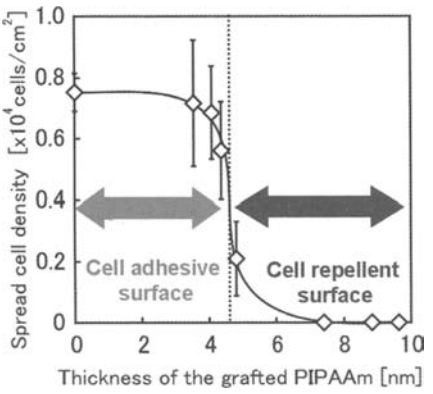

Fig. 6 Cell adhesive properties dependent on the thickness of the grafted PIPAAm for the PIPAAm grafted glass coverslip system

coverslips by EB irradiation. The thickness and amount of the grafted polymer, as well as the surface wettability, increased with the initial monomer concentration. When the monomer concentration was 5 wt%, the grafted polymer density and polymer thickness was 0.84 μg/cm^2 and 3.5 ± 0.2 nm respectively (PIPAAm grafted glass coverslips with 0.84 μg/cm^2 PIPAAm density are abbreviated as 0.84PIPAAm-CS), and cells adhered and spread on the surface at 37 °C, but detached at 20 °C. In contrast, when the monomer concentration was 35 wt%, the polymer density and the thickness was 1.28 μg/cm2 and 7.4 ± 0.3 nm respectively and the surfaces were cell repellent even at 37 °C. The correlation between cell adhesion behavior and thickness of the grafted PIPAAm shown in Fig. 6, evidently indicating the thickness-dependency. The thickness of the border dominating following cell adhesion behavior is approximately 4.5 nm. Both the graft polymer density and thickness suggested that the estimated PIPAAm density of PIPAAm-CSs is larger than those of PIPAAm-TCPS (ca. 1.0 g/cm^3) and typical synthetic polymers (ca. 1.0 g/cm^3). The results also strongly suggest that nanometer thickness of the grafted PIPAAm is a key factor for following thermal modulation of cell adhesion and detachment. Taken together, the grafted PIPAAm chains of 0.84PIPAAm-CS are extremely compacted. These results show a remarkable contrast to those obtained from PIPAAm-TCPS, since various types of cells showed temperature-dependent cell adhesion/detachment when the grafted density was around 2 μg/cm^2 on these surfaces. As a plausible explanation, remaining hydrophilic silanol groups do not promote dehydration of the grafted PIPAAm chains at the interfaces with glass, as hydrophobic basal TCPS promotes. To compensate for this drawback, for 0.84PIPAAm-CS, a more dense, thinner layer of the grafted PIPAAm may be necessary to promote the restriction of molecular motion of the grafted PIPAAm chains and to exhibit cell attachment/detachment properties in response to a change in temperature. We assume that the boundary line of the PIPAAm-CSs system being lower than that of the PIPAAm-TCPS system is attributable to the remaining silanol groups and the greater density of the grafted PIPAAm layer.

5 Accelerated cell sheet recovery from various types of PIPAAm grafted surfaces

Fabrication of functional tissue constructs from designed three-dimensional structure of cells using the layered method of cultured cell sheet is an attractive approach to tissue engineering. Rapid detachment of cultured cell sheets is important to maintain the biological function and viability of the recovered cell sheets as well as for practical assembly. In addition, for the application of cell sheets to the clinical area, rapid recovery reduces patients' and operator's burden during the operation. However, cell sheet detachment from PIPAAm-TCPS surfaces is slow, occurring gradually from the sheet periphery toward the interior [35, 36]. The rate limiting step of cell sheet recovery is the hydration of the underlying PIPAAm-TCPS surfaces. That is to say, water molecules required to hydrate PIPAAm chains at lower temperature penetrate the culture matrix from only the periphery of each cell to the interface between the cell and grafted PIPAAm chains. To accelerate the hydration of the grafted PIPAAm chains and achieve rapid cell sheet recovery, we developed the following two methodologies.

5.1 PIPAAm grafted porous membrane for rapid cell sheet recovery

Poly(ethylene terephthalate) (PET) porous membrane was exploited as a substrate for efficient supply of water molecules to the underlying PIPAAm grafted surfaces and promote the hydration of the grafted PIPAAm chains by lowering temperature [35]. PIPAAm was grafted onto the porous membrane (PIPAAm-PM) using EB irradiation. Successful graft of the PIPAAm was confirmed by FT-IR /ATR and XPS analysis. AFM images elucidated that PIPAAm-PM exhibited smoother surfaces than ungrafted membrane while maintaining the porous structure. The root mean square values of PIPAAm-PM and ungrafted membrane surfaces were mutually equivalent, suggesting that the graft of PIPAAm does not significantly affect the roughness of the surfaces. PIPAAm-TCPSs were compared with PIPAAm-PM in cell spreading assays. Cell

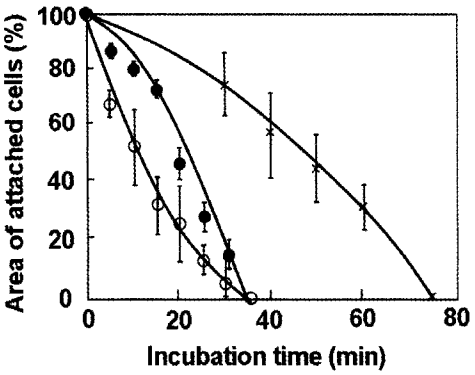

Fig. 7 Area of attached cells on PIPAAm-TCPS (×), PIPAAm-PM (•) and PIPAAm (PEG0.5 %)-PM (○) surfaces at 20 °C

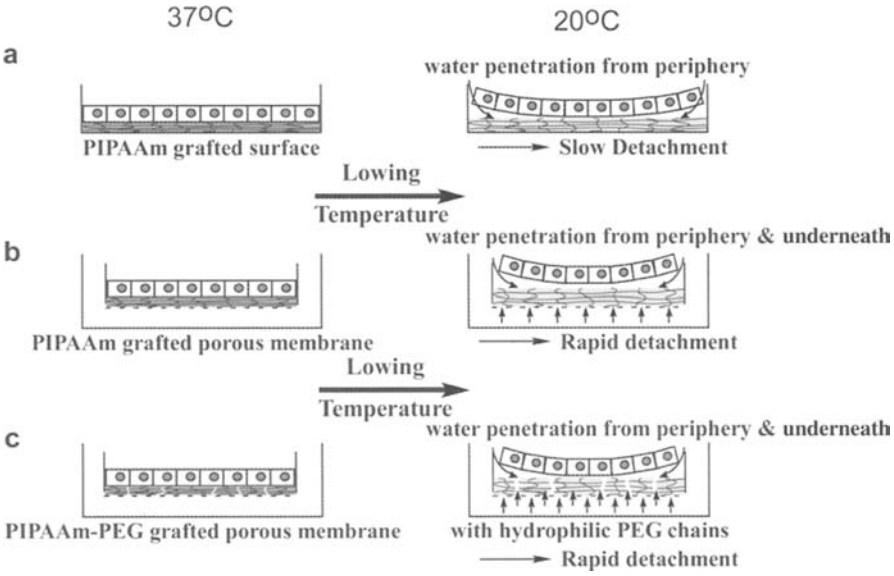

Fig. 8 Schematic drawing of cell sheet detachment through different types of water supply to: **a** PIPAAm-TCPS, **b** PIPAAm-PM and **c** P(IPAAm-*co*-PEG)-PM surfaces

adhesion and growth were highly suppressed on the membrane with pore diameters of more than 5μm, because cells cannot readily bridge over large pore sizes. Cells cannot sense distance longer than the average length of a pseudopodium [37]. In contrast, cells are adhered to and proliferated onto PIPAAm grafted porous membrane with 0.45 μm pore size in diameter as well as PIPAAm-TCPS surfaces. In cell sheet detachment experiments, approximately 75 min was required to completely detach cell sheets from PIPAAm-TCPS compared to only 30 min to detach cell sheets from PIPAAm grafted porous membrane (Fig. 7). For porous membranes, the water molecules access the PIPAAm-grafted surface from underneath and peripheral to the attached cell sheet, resulting in rapid hydration of grafted PIPAAm molecules and detachment of the cell sheet (Fig. 8 middle). By contrast, for PIPAAm-TCPS surfaces, water molecules are supplied from only the periphery of a cell sheet, showing a slower detachment process (Fig. 8 upper).

5.2 Further rapid cell sheet recovery utilizing hydrophilic unit

PIPAAm hydrogel containing poly(ethylene glycol) (PEG) introduced as graft chains exhibited rapid swelling and deswelling behavior in comparison with conventional PIPAAm hydrogel [38]. This is due to the formation of water release channels within the hydrogel by the grafted PEG chains. Thus, we expect that the introduction of the PEG chains into the PIPAAm grafted layer could lead to more rapid hydration of the cell culture surfaces and accelerate recovery of the cell sheets [36].

Reaction solution containing IPAAm monomer and PEG methacrylate macromonoer spread over PM surfaces was subjected to EB irradiation and P(IPAAm-*co*-PEG) was grafted (P(IPAAm-*co*-PEG)-PM). For comparison, PIPAAm-PM was prepared in the same way. Both of the surfaces exhibited hydrophilic/hydrophobic alternation in response to temperature change. At 37 °C, contact angles of P(IPAAm-*co*-PEG)-PM obtained from IPAAm and 0.1 mol% PEG in feed (P(IPAAm-*co*-PEG0.1)-PM) and 0.5 mol% PEG in feed (P(IPAAm-*co*-PEG0.5)-PM) were almost equivalent to that of PIPAAm-PM. In contrast, contact angles of P(IPAAm-*co*-PEG)-PMs decreased with an increase in initial concentration of PEG at 20 °C. These results suggest that grafted PEG chains scarcely exist in the outermost area of the membrane surface due to hydrophobically contracted PIPAAm chains at 37 °C. By lowering temperature below LCST, embedded PEG chains interior to the dehydrated PIPAAm network with limited mobility are more mobile through hydration of the PIPAAm chains, leading to rearrangement of PEG chains. Cells adhered and grew to confluence on a P(IPAAm-*co*-PEG)-PM as well as on a PIPAAm-PM at 37 °C. However, cells did not proliferate to confluency on (P(IPAAm-*co*-PEG1.0) surfaces because of the more hydrophilic property of the surfaces by incorporation of a larger amount of PEG. After cells become confluent, by reducing the temperature to 20 °C, cell sheets detached from the P(IPAAm-co-PEG0.1)-PM more quickly than the PIPAAm-TCPS and the PIPAA-PM (Fig. 7). These results suggest that introduction of a limited amount of PEG chains into the PIPAAm grafted layer allows rapid access and diffusion of water molecules from beneath as well as from the periphery of the cultured cell sheets, facilitating rapid hydration of grafted PIPAAm chains and cell sheet detachment (Fig. 8 bottom).

Instead of PEG chains, either 2-carboxylisopropylacrylamide (CIPAAm) or acrylic acid (AAc) was copolymerized with IPAAm monomer and each of the copolymers was grafted onto TCPS surfaces using EB irradiation. Cell adhesion and detachment properties were investigated using the copolymer grafted TCPS surfaces [39]. Cells adhered to and proliferated to confluency on p(IPAAm-co-CIPAAm) grafted TCPS as well as PIPAAm-TCPS surfaces, while cells were not adhered to P(IPAAm-co-AAc) grafted TCPS surfaces due to excess hydration. Cell detachment was accelerated on P(IPAAm-co-CIPAAm) grafted TCPS surfaces compared to PIPAAm-TCPS. These results suggest that hydrophilic carboxyl group microenviroment in the monomer and polymer is important to accelerate hydration of the grafted PIPAAm chains below LCST, resulting in rapid cell detachment. Relatively hydrophilic CIPAAm carboxylate anion at pH 7.4 is likely to induce the rapid hydration of the grafted PIPAAm chains.

6 Functionalization of temperature-responsive cell culture surfaces

6.1 Thermal control of cell adhesion and detachment using temperature-responsive copolymer grafted surfaces

It is known that LCST of PIPAAm dissolved in aqueous solution is elaborately modulated by copolymerization of IPAAm with hydrophilic and hydrophobic monomers

in previous reports [40, 41]. In order to regulate cell adhesion and detachment from temperature-responsive cell culture surfaces at controlled temperature, we further applied this copolymerization technique to the cell culture surfaces. The hydrophobic monomer, *n*-butyl methacrylate (BMA) was incorporated into PIPAAm to lower PIPAAm phase transition temperatures for the regulation of cell adhesion and detachment [42]. Poly(IPAAm-co-BMA)-grafted TCPS surfaces were prepared by EB irradiation, changing initial BMA content in the feed. Copolymer-grafted surfaces decreased grafted polymer transition temperatures with increasing BMA content as shown by water wettabilities compared to PIPAAm-TCPS surfaces. Bovine endothelial cells readily adhered and proliferated on poly(IPAAm-co-BMA) grafted TCPS as well as PIPAAm-TCPS at 37 °C, finally reaching confluence. Cell sheet detachment behavior from copolymer grafted surfaces depended on the culture temperature and BMA content. At 28 °C, detachment of cell monolayers was observed from only PIPAAm-TCPS and P(IPAAm-*co*-BMA) grafted TCPS with 1 mol% BMA content (P(IPAAm-*co*-1.0BMA) grafted TCPS), while no cell monolayer detached from either P(IPAAm-*co*-3.0BMA) grafted TCPS or P(IPAAm-*co*-5.0BMA) grafted TCPS surfaces. P(IPAAm-*co*-3.0BMA) grafted TCPS and P(IPAAm-*co*-5.0BMA) surfaces remained hydrophobic at this temperature due to the reduction in the transition temperature of the surface by the incorporation of a hydrophobic BMA moiety. In sharp contrast, complete recovery of the cell sheet from P(IPAAm-*co*-3.0BMA) grafted TCPS and P(IPAAm-*co*-5.0BMA) grafted TCPS surfaces was observed at 25 °C and 20 °C, although a longer time was required for complete cell sheet detachment. These results demonstrate that cell attachment/detachment can be controlled by an arbitrary temperature by varying the content of hydrophobic monomer incorporated into PIPAAm grafted to culture surfaces.

6.2 Patterned dual temperature-responsive surfaces for recovery of continuous co-cultured cell sheets

Heterotypic cell-to-cell interactions are crucial to achieve and maintain specific functions in many tissues and organs. To mimic such heterotypic cellular interactions in vitro, co-culture of different cell types has been carried out on various types of patterned surfaces [43]. We developed a patterned surface modification technique to enable the co-culture of heterotypic cells and endothelial cells, and the recovery of patterned co-cultured cell sheets for application in tissue engineering. Poly(*n*-butyl methacrylate) (PBMA) was introduced into limited surface areas of PIPAAm-TCPS by utilizing EB irradiation through a metal mask with 1 mm holes (Fig. 9a) [44]. The resulting surface consists of a PIPAAm-grafted and P(IPAAm–BMA) co-grafted domain, exhibiting patterned dual thermoresponsive properties. Angle resolved XPS analyses of the P(IPAAm-*co*-BMA) co-grafted surfaces revealed that PIPAAm sequences were distributed to the air side, while BMA sequences were buried nearer underlying polystyrene surfaces. Thus, the co-grafted domains maintain their thermoresponsive wettability changes. However, the original PIPAAm chain hydration and mobility was somehow restricted by the co-grafted BMA sequences, decreasing the transition temperature of the co-grafted domains. On patterned sur-

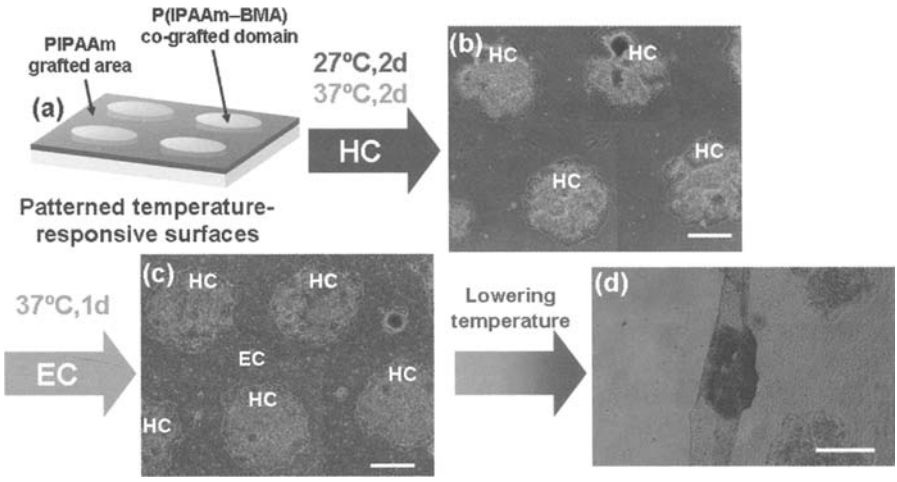

Fig. 9 Patterned co-culture of rat primary hepatocytes (HCs) and bovine carotid artery endothelial cells (ECs): **a** Illustration of patterned dual temperature-responsive P(IPAAm-BMA) co-grafted surfaces. **b** Selective adhesion of rat primary HCs onto P(IPAAm-BMA) co-grafted domains cultured at 27 °C for 2 days and then at 37 °C for an additional 2 days. **c** Sequentially seeded ECs adhere to hydrophobic PIPAAm regions and co-culture with pre-seeded HCs at 37 °C into organized patterns. **d** Reducing culture temperature to 20 °C induces spontaneous detachment of the patterned co-cultured cell monolayer. Scale bars: **b**, **c** and **d**: 0.5 mm (Reprinted from [44], with permission from Elsevier)

faces, domain-selective adhesion and growth of rat primary hepatocytes (HCs) and bovine carotid endothelial cells (ECs) allowed patterned co-culture, exploiting hydrophobic/hydrophilic surface chemistry in response to the sole variable of culture temperature. At 27 °C, seeded HCs adhered selectively onto hydrophobic, dehydrated P(IPAAm-co-BMA) domains with a size of 1 mm in diameter, but not onto neighboring hydrated PIPAAm domains (Fig. 9b). Sequentially seeded ECs then adhered exclusively to hydrophobic PIPAAm domains with increasing culture temperature to 37 °C, achieving patterned co-cultures (Fig. 9c). At the interfacial boundary zones between these two cell types in planar co-culture, phenotypic hepatocyte functions, albumin secretion and urea synthesis by ammonium metabolism, were increased compared to homotypic cultures [44]. Such metabolic functions could also be increased with decreasing patterned domain sizes without changing the ratios of the two cultured cell types. By lowering the temperature to 20 °C, alternation of polymer-grafted domains to hydrophilic property allows the release of co-cultured, patterned cell monolayers as continuous cell sheets maintaining heterotypic cell interactions (Fig. 9d).

6.3 Affinity control between cell integrins and RGDS ligands immobilized onto temperature-responsive cell culture surfaces

Acrylic acid (AAc) has been utilized to introduce reactive carboxyl groups to a temperature-responsive polymer, PIPAAm. However, AAc introduction highers the

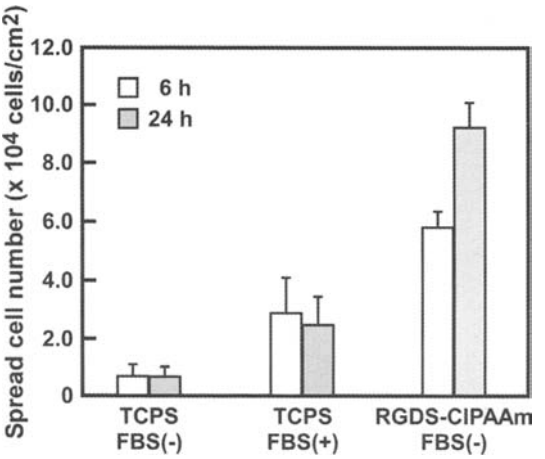

Fig. 10 HUVEC spreading on TCPS and P(IPAAm-co-CIPAAm) surfaces modified with RDGS after 6h and 24h culture with or without serum at 37 °C. Cells were cultured onto TCPS with/without serum (TCPS FBS (+) and TCPS (–)), P(IPAAm-co-CIPAAm) modified with RDGS without serum (RDGS-CIPAAm FBS (+))

copolymer phase transition temperatures and dampens the steep homopolymer phase transition with increasing AAc content [45]. We previously synthesized CIPAAm having both a similar side chain structure to IPAAm and a functional carboxylate group in order to overcome these shortcomings [46, 47]. Actually, p(IPAAm-*co*-CIPAAm) solution exhibits very sensitive phase transition in response to temperature changes with phase transition temperatures nearly the same as those of PIPAAm [46]. Utilizing the features of the CIPAAm monomer, RGDS peptides, found in fibronectin, type I collagen and other ECM proteins, were immobilized onto P(IPAAm-co-CIPAAm) copolymer grafted TCPS surfaces [48]. These surfaces facilitate the spreading of human umbilical vein endothelial cells (HUVECs) without serum, depending on RGDS surface content at 37 °C (above the lower critical solution temperature, LCST, of the copolymer), although addition of dilute serum facilitates HUVEC spreading on TCPS (Fig. 10). Moreover, cells spread on the surfaces immobilized with RGDS peptides at 37 °C, detach spontaneously by lowering culture temperature below the LCST as hydrated grafted copolymer chains dissociate immobilized RGDS from cell integrins. These cell lifting behaviors upon hydration are similar to results using soluble RGDS in culture as a competitive substitution for immobilized ligands. Binding of cell integrins to immobilized RGDS on cell culture substrates can be reversed spontaneously using mild environmental stimulation, such as temperature, without enzymatic or chemical treatment. These findings are important for control of specific interactions between proteins and cells, and subsequent "on-off" regulation of their function. Furthermore, the method allows serum-free cell culture and trypsin-free cell harvest, essentially removing mammalian-sourced components from the culture process.

7 Conclusions

In this chapter, we described the features of PIPAAm grafted surfaces and their application to novel separation and the cell culture system. Successful modulation of interaction between PIPAAm grafted surfaces and samples or cultured cells was apparent with alternation of surface property through temperature control. Cell sheet engineering by utilizing temperature-responsive cell culture surfaces is available for fabrication and recovery of functional tissue. These features should be feasible to develop a green chromatography system and an advanced cell culture system for tissue engineering.

References

[1] Schild HG (1992) Poly(*N*-isopropylacrylamide): experiment, theory and application. Prog Polym Sci 17:163–249

[2] Takei YG, Aoki T et al (1994) Dynamic contact angle measurement of temperature-responsive surface properties for poly(*N*-isopropylacrylamide) grafted surfaces. Macromolecules 27:6163–6166

[3] Yakushiji T, Sakai K et al (1998) Graft architecture effects on thermoresponsive wettability changes of poly(*N*-isopropylacrylamide) surfaces. Langmuir 14:4657–4662

[4] Kanazawa H, Yamamoto K et al (1996) Temperature-responsive chromatography using poly(*N*-isopropylacrylamide)-modified silica. Anal Chem 68:100–105

[5] Kanazawa H, Kashiwase Y et al (1997) Temperature-responsive liquid chromatography. 2. effects of hydrophobic groups in *N*-isopropylacrylamide copolymer-modified silica. Anal Chem 69:823–830

[6] Kanazawa H, Sunamoto T et al (2000) Temperature-responsive chromatographic separation of amino acid phenylthiohydantoins using aqueous media as the mobile phase. Anal Chem 72:5961–5966

[7] Kanazawa H, Kashiwase Y et al (1997) Analysis of peptides and proteins by temperature-responsive chromatographic system using *N*-isopropylacrylamide polymer-modified column. J Pharm Biomed Anal 15:1545–1550

[8] Yamamoto K, Kanazawa H et al (2000) Temperature-responsive chromatographic separation of bisphenol A with water as a sole mobile phase. Environ Sci 7:47–56

[9] Kanazawa H (2000) Thermally responsive chromatographic materials using functional polymers. J Sep Sci 30:1646–1656

[10] Yamada N, Okano T et al (1990) Thermo-responsive polymeric surfaces; control of attachment and detachment of cultured cells. Makromol Chem Rapid Commun 11:571–576

[11] Okano T, Yamada N et al (1993) A novel recovery system for cultured cells using plasma-treated polystyrene dishes grafted with poly(*N*-isopropylacrylamide). J Biomed Mater Res 27:1243–1251

[12] Kushida A, Yamato M et al (1999) Decrease in culture temperature releases monolayer endothelial cell sheets together with deposited fibronectin matrix from temperature-responsive culture surfaces. J Biomed Mater Res 45:355–362

[13] Yamato M, Konno C et al (2000) Release of adsorbed fibronectin from temperature-responsive culture surfaces requires cellular activity. Biomaterials 21:981–986

[14] Shimizu T, Yamato M et al (2003) Cell sheet engineering for myocardial tissue reconstruction. Biomaterials 24:2309–2316

[15] Yang J, Yamato M et al (2006) Corneal epithelial stem cell delivery using cell sheet engineering: not lost in transplantation. J Drug Target 14:471–482

[16] Geweher M, Nakamyra K et al (1992) Gel permutation chromatography using porous glass beads modified with temperature-rsponsive polymers. Makromol Chem 193:249–256

[17] Hosoya K, Sawada E et al (1995) Temperature-controlled high-performance liquid chromatography using a uniformly sized temperature-responsive polymer-based packing material. Anal Chem 67:1907–1911

[18] Kikuchi A, Okano T (2002) Intelligent thermoresponsive polymeric stationary phases for aqueous chromatography of biological compounds. Progress in Polymer Science 27:1165–1193

[19] Tamada Y, Ikada Y (1994) Fibroblast growth on polymer surfaces and biosynthesis of collagen. J Biomed Mater Res 28:783–789

[20] Okano T, Yamada N et al (1995) Mechanism of cell detachment from temperature-modulated hydrophilic–hydrophobic polymer surfaces. Biomaterials 16: 297–303

[21] Kikuchi A, Okano T (2005) Nanostructured designs of biomedical materials: applications of cell sheet engineering to functional regenerative tissues and organs. J Control Release 101(1-3):69–84

[22] Kikuchi A, Okuhara M et al (1998) Two-dimensional manipulation of confluently cultured vascular endothelial cells using temperature-responsive poly(*N*-isopropylacrylamide)-grafted surfaces. J Biomater Sci Polym Ed 9:1331–1348

[23] Kushida A, Yamato M et al (1999) Decrease in culture temperature releases monolayer endothelial cell sheets together with deposited fibronectin matrix from temperature-responsive culture surfaces. J Biomed Mater Res 45:355–362

[24] Hirose M, Kwon OH et al (2000) Creation of designed shape cell sheets that are noninvasively harvested and moved onto another surface. Biomacromolecules 1:377–381

[25] Tang Z, Kikuchi A et al (2007) Novel cell sheet carriers using polyion complex gel modified membranes for tissue engineering technology for cell sheet manipulation and transplantation. React Func Polym 67:1388–1397

[26] Yamato M, Utsumi M et al (2001) Thermo-responsive culture dishes allow the intact harvest of multilayered keratinocyte sheets without dispase by reducing temperature. Tissue Eng 7:473–480

[27] Nishida K, Yamato M et al (2004) Corneal ceconstruction with tissue-engineered cell sheets composed of autologous oral mucosal epithelium. N Engl J Med 351:1187–1196

[28] Shiroyanagi Y, Yamato M et al (2004) Urothelium regeneration using viable cultured urothelial cell sheets grafted on demucosalized gastric flaps. BJU Int 93:1069–1075

[29] Shimizu T, Yamato M et al (2002) Fabrication of pulsatile cardiac tissue grafts using a novel 3-dimensional cell sheet manipulation technique and temperature-responsive cell culture surfaces. Circ Res 90:e40–e48

[30] Nandkumar MA, Yamato M et al (2002) Two-dimensional cell sheet manipulation of heterotypically co-cultured lung cells utilizing temperature-responsive culture dishes results in long-term maintenance of differentiated epithelial cell functions. Biomaterials 23:1121–1130

[31] Akiyama Y, Kikuchi A, M et al (2004) Ultra thin poly(*N*-isopropylacrylamide) grafted layer on poly(styrene) surfaces for cell adhesion/detachment control. Langmuir 20:5506–5511

[32] Uchida K, Sakai K et al (2000) Temperature-dependent modulation of blood platelet movement and morphology on poly(N-isopropylacrylamide)-grafted surfaces. Biomaterials 21:923–929

[33] Akiyama Y, Kushida A et al (2007) Surface characterization of poly(*N*-isopropylacrylamide) grafted tissue culture polystyrene by electron beam irradiation, using atomic force microscopy, and x-ray photoelectron spectroscopy. J Nanosci Nanotechn 7:796–802

[34] Fukumori K, Akiyama Y et al (2008) Temperature-responsive glass coverslips with an ultrathin poly(*N*-isopropylacrylamide) layer. Acta Biomaterialia doi: 10.1016/j.actbio.2008.06.018

[35] Kwon OH, Kikuchi A et al (2000) Rapid cell sheet detachment from poly(*N*-isopropylacrylamide)-grafted porous cell culture membranes. J Biomed Mater Res 50:82–89

[36] Kwon OH, Kikuchi A et al (2003) Accelerated cell sheet recovery by co-grafting of PEG with PIPAAm onto porous cell culture membranes. Biomaterials 24:1223–1232

[37] Lee JH, Lee SJ et al (1999) Interaction of fibroblasts on polycarbonate membrane surfaces with different micropore size and hydrophilicity. J Biomater Sci Polym 10:283–294

[38] Kaneko Y, Nakamura S et al (1998) Rapid deswelling response of poly(*N*-isopropylacrylamide) hydrogels by the formation of water release channels using poly(ethylene oxide) graft chains. Macromolecules 31:6099–6105

[39] Ebara M, Yamato M et al (2003) Copolymerization of 2-carboxyisopropylacrylamide with N-isopropylacrylamide accelerates cell detachment from grafted surfaces by reducing temperature. Biomacromolecules 4:344–349

[40] Bae YH, Okano T et al (1990) Temperature dependence of swelling of crosslinked poly(N,N-alkyl substituted acrylamides) in water. J Polym Sci Part B Polym Phys 28:923–936

[41] Feil H, Bae YH et al (1993) Effect of comonomer hydrophilicity and ionization on the lower critical solution temperature of *N*-isopropylacrylamide copolymers. Macromolecules 26:2496–2500

[42] Tsuda Y, Kikuchi A et al (2004) Control of cell adhesion and detachment using temperature and thermoresponsive copolymer grafted culture surfaces. J Biomed Mater Res 69A:70–78

[43] Bhatia S, Yarmush M et al (1997) Controlling cell interactions by micropatterning in co-cultures: hepatocytes and 3T3 fibroblasts. J Biomed Mater Res 34:189–99

[44] Tsuda Y, Kikuchi A et al (2005) The use of patterned dual thermoresponsive surfaces for collective recovery as co-cultured cell sheets. Biomaterials 26:1885–1893

[45] Chen G, Hoffman AS (1995) Graft copolymers that exhibit temperature-induced phase transitions over a wide range of pH. Nature 373:49–52

[46] Aoyagi T, Ebara M et al (2000) Novel bifunctional polymer with reactivity and temperature sensitivity. J Biomater Sci Polym Edn 11:101–110

[47] Ebara M, Aoyagi T et al (2000) Introducing reactive carboxyl side chains retains phase transition temperature sensitivity in *N*-isopropylacrylamide copolymer gels. Macromolecules 33:8312–8316

[48] Ebara M, Yamato M et al (2004) Temperature-responsive cell culture surfaces enable "on-off" affinity control between cell integrins and RGDS ligands. Biomacromolecules 5:505–510